PhD Thesis

Hybrid multi-curve models with stochastic basis

Vytautas Savickas

A dissertation submitted in partial fulfillment

of the requirements for the degree of

Doctor of Philosophy

of

University College London.

Department of Mechanical Engineering

Financial Computing and Analytics Group

University College London

November 6, 2017

Declaration

I, Vytautas Savickas, confirm that the work presented in this thesis is my own. Where information has been derived from other sources, I confirm that this has been indicated in the work.

Abstract

The financial markets have changed radically since the start of the 2007 credit crisis. Following the bankruptcies of large financial institutions as well as bailouts of multiple banks and asset management institutions like Bear Sterns, Lehman Brothers, and AIG, the market participants recognised the serious credit and liquidity risks present in the widely traded interest rate derivatives. The effect of rising credit and liquidity risks was observed by the spike in the spreads between nearly risk-free OIS rates used for collateral and risky unsecured LIBOR loan rates. Most of the classical interest rate models used by mentioned market participants relied on the assumption that there exists a risk-free and unique LIBOR lending rate, which is no longer true. This has opened new ground for complex, hybrid models for interest rate derivatives.

This PhD thesis presents my work on developing novel interest rate models which are mathematically and historically sound and can be used for pricing interest rate derivatives including stochastic basis spreads between unsecured LIBOR and OIS rates. This work is split into two problems: first we analyse the discrepancies between forward-LIBOR lending rates and their classic replication strategy with spot-LIBOR rates. For this problem, we propose an extension of a known LIBOR Panel Model, which enables us to jointly model OIS and spot- and forward-LIBOR rates with an error within the quoted bid-ask spreads.

The second part of this thesis looks into the problem of pricing non-linear derivatives like caps linked to rates on multiple LIBOR tenors. We propose a novel hybrid credit-interest rate model, which allows to jointly model OIS and multi-tenor LIBOR rates and to price multi-tenor caps. The proposed hybrid short-rate model is intuitive, semi-analytically tractable and can be calibrated using liquid, available market data. We compare the market data fit with a benchmark model using fixed LIBOR-OIS spread assumption. The last chapter shows the impact of this model on credit value adjustments for interest rate trades.

Acknowledgements

This thesis discusses the results of more than three years of PhD research at University College London. I would like to thank some of the people that contributed their expertise to this research project.

First of all, I would like to thank Prof. Ian Eames for his guidance during the research and for the fruitful discussions that we held during this time. It has been a great pleasure to learn from his experience.

I would like to thank Dr Veronica Malafaia, Dr Drona Kandhai and Dr Artem Tsvetkov from ING Bank for enabling this PhD research project as a cooperation between the university and banking industry. Their constructive criticism and market-participant view on my proposed approaches have been highly appreciated.

I would like to express my gratitude to all my colleagues at the Fluid Dynamics group and the Doctoral Training Centre in Financial Computing at UCL. It was a great experience working with you.

The greatest thanks go to my wife Andrada, who has supported me throughout all these years, proof-read my writing, helped prepare for each of my public presentations.

Contents

List of Figures

List of Tables

Nomenclature

Symbol	Description
$\mathbb{E}(\cdot)$	Expectation operator.
$\mathbb{E}^{Q}$	Expectation operator with respect to probability measure Q.
$\mathbb{E}^{\mathbb{Q}_{\mathrm{T}}}$	Expectation operator with respect to OIS-T Forward measure.
$r(t)$	Instantaneous short-term interest rate at time t.
bp	Basis point, equal to 0.01%, used for small interest rate measurement.
$B(t)$	Money-savings account at time t.
t	Calendar time.
T	Maturity time (final trading date).
τ	Tenor (difference between rate fixing and payout dates).
K	Strike price.
$P(t,T)$	Zero-coupon bond paying 1 at time T, priced at time t.
$F_M(t,T,S)$	A market forward rate between time T and S, valued at time t.
$R(t,\mathcal{T},N,K)$	A market swap rate valued at time t with coupon schedule $\mathcal{T}$, notional N and strike K.
CDS	Credit default swap. A contract exchanging fixed fee for protection against a default of some company or government entity.
DTCC	Depository trust and clearing corporation. It is a global repository that records all the details of CDS trades in the global markets.
LIBOR	The London interbank offer rate. Rate at which large banks are willing to lend to other premium banks in unsecured fashion.
EURIBOR	The Euro interbank offer rate. Similar to LIBOR, but set by a larger European panel of banks.

EONIA	Euro over-night index average. An effective overnight interest rate computed as a weighted average of all over-night unsecured lending transactions in the market.
OIS	Overnight indexed swap. A swap that is indexed to daily values of either EONIA or FED funds rates. The swap exchanges a fixed interest rate versus the dynamic daily index.
LOIS	LIBOR-OIS spread.
CSA	Collateral support annex. A document specifying how two counterparties will post collateral for the underlying contract.
CVA	Counterparty valuation adjustment.
DVA	Debt value adjustment.
FRA	A forward rate agreement.
IRS	Interest rate swap, a contract usually swapping fixed interest rate for floating LIBOR-linked payments.
Swaption	An option allowing the bearer to enter into and IRS at the expiry of the option.
Bootstrapping	Refers to a method for constructing a yield curve from the prices of coupon-bearing products, e.g. bonds or swaps.
HW	Hull-White model.
DD	Displaced-diffusion model.
HW1F	One factor Hull-White model.
HW2F	Two factor Hull-White model.
CIR	Cox-Ingersoll-Ross model.
HCIR	Hybrid Hull-White and Cox-Ingersoll-Ross model introduced in this thesis.
LMM	LIBOR market model.
GBM	Geometric Brownian motion.
PDF	Probability density function.
CDF	Cumulative density function.
VaR	Value at risk. A commonly used measure of risk.
SDE	Stochastic differential equation.
ZCB	Zero coupon bond.

Chapter 1

Introduction: Basis Risk

1.1 Introduction

At the core of modern financial markets there are four main traded asset classes:

- equity (stocks),
- debt (bonds, loans),
- commodities (oil, gas),
- and foreign exchange.

The debt markets are probably the most diverse regarding complexity and structure of the products traded. These can be split into more fine-grained categories, such as:

1. retail lending,
2. commercial and governmental debt (usually in the form of bonds),
3. structured products (asset-backed securities),
4. and interest rate derivatives (swaps, caps, etc.).

The main interest of this thesis is looking into how the above instruments are priced. To issue the most elementary loan for some fixed period, the issuer (e.g. a bank) needs to set the effective interest rate for this loan. In a classic textbook approach, one would take the so-called "risk-free" rate and add an estimated credit and liquidity premium to it, obtaining the final interest rate of the loan.

In practice, the risk-free rate does not exist. However, there are liquid assets and contracts which are nearly risk-free and are excellent proxies of the real riskless interest rate. The classic examples of close-to-riskless rates are given by the US Treasury bonds and notes, OIS (overnight indexed swap) rates and up until the credit crisis of 2007-2008,

the LIBOR and EURIBOR rates.

The risk-less rate is the most important concept in modern finance. It is used at the very core of finance, discounting (potential) future cash flows to obtain their present value. The modern financial pricing theory relies on having a unique, risk-free rate as it is used in the pricing of bonds, equity forwards, derivatives (options), futures, etc.

The most commonly used risk-free rate proxies were LIBOR and Euribor rates. They are publicly quoted indices. LIBOR, for example, is the "London Inter-Bank Offer Rate". It is computed as a trimmed average of quotes submitted by a panel of banks. Each of these banks must quote the borrowing rate at which a prime London bank can get an unsecured short-term loan. The LIBOR rate is used as a benchmark for interbank borrowing and pricing various derivatives.

Before the 2007-08 credit crisis, market participants assumed the LIBOR-based lending to be risk-free. This led to widespread use of few fundamental relations between risk-free loans, which were not entirely true. One of them, which we shall discuss extensively in this thesis is the ability to replicate a future-dated loan with two other loans starting immediately. The replication strategy is very simple:

1. A forward-loan is issued starting from time T to time S at a forward-LIBOR rate.
2. To finance the loan, we borrow at the LIBOR rate for S years,
3. The money is lent out for the first T years as we don't need it until then.

The above strategy works if we can borrow at the LIBOR rate and also if there is no credit-liquidity risk in either of related parties or embedded in the LIBOR rates themselves. If any of our assumptions does not hold, we may get a gap in the replication strategy, often named "a basis", which is one of the few problems that broke the standard financial models during and after the credit crunch.

1.2 Problem Statement

Basis risk and stochastic basis modelling have become an important subject in mathematical finance since the beginning of the credit crisis in 2007. Standard textbooks refer to basis spreads when describing the spread between the prices or levels of two nearly identical assets, e.g. they refer to the same cash flows in the future, or they are highly correlated (Gupta, 2005). Basis risk comes into place when this spread is non-deterministic and hedg-

ing movements of one asset, using another, can result in a loss. There are multiple classical examples of basis risk, such as the difference between an index and its future contract.

A modern and highly relevant example of a basis spread is the gap between OIS and the LIBOR rates, otherwise known as the LIBOR-OIS spread. The larger of the two rates is the LIBOR. LIBOR refers to unsecured short-to-mid term lending rates between panels of banks. These rates were conventionally thought to be risk-free and were nearly identical to the OIS rates, which refer to a stream of overnight loans that can be interrupted if there are any concerns about credit risk or liquidity. These rates started diverging since the beginning of the credit crisis in September 2007, as market participants realised that LIBOR contracts carry significant counterparty credit risk, as opposed to still nearly risk-free OIS rates (Bianchetti, 2012). This was followed up by a sharp decrease in LIBOR lending, which further increased the LIBOR-OIS spread.

Now, LIBOR-based lending is negligible, as the market moved to collateralized, OIS-based, lending, but LIBOR reference rates are still used in various long-term interest rate swaps, caps and other derivatives. To avoid potentially massive losses, every interest rates derivatives trading desk must have a consistent pricing and hedging model for LIBOR-based derivatives. Additionally, every risk-management desk must have a model to assess the Value-At-Risk of their LIBOR-linked portfolios as well as their credit risk and CVA charges as these are required by the regulatory authorities after passing the Basel III regulations (BIS, 2010). An important additional requirement by BIS is to account for the wrong-way risk in the CVA for the interest rate portfolios. This wrong-way risk is observed as a correlation between interest rates and a higher probability of counterparty default, which would lead to increased losses in case of defaults.

1.3 Research Questions

At the moment, there is no market-wide consensus about which models to use in pricing and risk management of interest rates with stochastic basis. Lack of consensus yields many problems in determining the present value of future cash flows, the risk that the trades carry and more. Disagreements on the latter can lead to a lack of trading with certain counterparties, even lawsuits regarding existing contracts if they involve clauses, like collateral margins, as parties may not agree on how much collateral must be posted.

While multiple models have been proposed, we have identified two subject areas in the literature that were not well explored. First, there are multiple works with econometric analysis on the LIBOR-OIS basis spreads, but very few try to incorporate these econometric facts into derivatives pricing models. Additionally, many of the new proposed models are over-parametrised versions of classical models which are hard to calibrate and interpret. We reviewed multiple interest rate models and their extensions to the multi-curve derivatives pricing setting in detail in Chapter 2.2.

In this thesis, we will propose solutions to two main objectives of post-crisis interest rate modelling:

1. First, we investigate whether we can jointly model risk-free OIS rates together with directly observable spot-LIBOR rates and forward-LIBOR rates, visible via traded derivative contracts.
2. Then, we look into joint modeling of the forward-LIBOR rates, which now depend on the LIBOR-tenor. We investigate whether we can design a model which would allow pricing volatility-dependent derivatives like caps and floors consistently in the multi-curve setting?

Secondary objectives of this thesis are to find out if:

- Is it possible to include historically observed stylistic facts about the risk-free, LIBOR rates as well as credit and liquidity impact on them?
- Can we design the models to be analytically or semi-analytically tractable and easy to calibrate to liquid, available market data?
- How do the proposed models compare to benchmarks, if any?
- Can they be used for CVA assessment and what is the impact?

1.4 Contributions

In this thesis we have made a number of contributions:

- In-depth analysis of the LIBOR panel model on different data sets and discussion of its limitations.
- Introduction of the implied-volatility framework for the panel podel, which yields a brand new look at the data. Using global optimisation techniques for the implied volatilities we were able to find the best possible fit of the panel model when re-

pricing liquidly traded market FRAs.

- Extension of the LIBOR panel model using uncertain volatility parameters. The resulting model allows for re-pricing of market data within bid-ask spreads. The follow-up parameter study of the extended model shows how one can identify major events of the credit crisis simply from the dynamics of implied volatility parameters. (*Quantitative Methods in Finance, 2013.*)
- Definition of a novel hybrid short rate model, mixing two well-known Hull-White and CIR short-rate models. This model, by construction, allows calibrating to single-tenor interest rate options and re-pricing illiquid multi-tenor options by using information from basis spreads. We derive analytical and semi-analytical pricing formulas for bond and options pricing (presented in Savickas (2015)).
- Analysis of market data fit of our model and comparison with available benchmark models.
- Guide for pricing counterparty valuation adjustments with the hybrid model and the inclusion of wrong-way risk. The latter analysis includes comparison with a chosen benchmark model.

1.5 Thesis Structure

We start this thesis by introducing the basic formulas for pricing interest rate derivatives in Chapter 2. In Chapter 2.2 we discuss the related articles and approaches for modelling basis spreads in the literature and introduce the most known stochastic basis models in section 2.3. In Chapter 3 we will provide an in-depth study of a LIBOR panel model. We show the mechanics and the assumptions of the model, analyse its limits and propose an extension to achieve a possible fit to market data with errors close to the bid-ask spread. We conclude this chapter with an intermediate summary of achievements and a discussion of the panel model limitations. Chapter 4 discusses a novel hybrid short-rate model, which can be calibrated to liquid market data, like swaps and single tenor caps and then used to price illiquid off-market caps and supply missing volatility information for risk management measures like CVA. In this chapter, we demonstrate the semi-analytic calibration techniques for the model as well as pricing formulas for interest rate derivatives and benchmark the model performance against a popular displaced diffusion-type model. The following Chapter 5 is

a study of the application of the latter model to credit valuation adjustments. We analyse the model performance in CVA assessment in multiple scenarios and compare it to a benchmark model. Finally, general conclusions of this work are made in Chapter 6 along with a description of ways to take this work forward in the future.

Chapter 2

Background

In this chapter, we give the basic definitions of interest rates and interest rate derivatives and introduce the notation and terminology which will be used throughout this thesis.

2.1 Definitions

2.1.1 Fundamental Theorem of Asset Pricing

The concept of no-arbitrage says, in principle, that it is impossible to make money out of nothing. Therefore, to make a return larger than some risk-free rate, one has to take on some risk.

This concept will be used throughout this thesis, as we will price derivatives under the so-called 'risk-neutral' measure. It stems from the fundamental theorem of asset pricing. It states that a bounded process $S = (S_t)_{0 \geq t \geq T}$ admits no-arbitrage if and only if there is a probability measure $\mathbb{Q}$ equivalent to $\mathbb{P}$ (real measure) such that S is a martingale under $\mathbb{Q}$. For more details about arbitrage-free pricing, we refer the reader to the book by Brigo and Mercurio (2006). The definitions and models in this thesis were constructed with the arbitrage-free assumption in mind.

2.1.2 Interest Rates and Discount Factors

The most important quantities that we will consider in this thesis are the discounting factors and zero-coupon bonds. In the following we give the textbook (Brigo and Mercurio, 2006), definitions of the most important concepts, such as different types of interest rates, like the collateral rates, interbank rates and government rates, which shall be used throughout this work.

Definition 2.1 (Bank Account). *We define $B(t)$ to the value of a bank account at time $t \geq 0$. We shall assume that $B(0) = 1$ and that it evolves according to the differential equation*

$$dB(t) = r(t)B(t)dt,\ B(0) = 1, \tag{2.1}$$

where $r(t)$ is a function of time. The solution to $B(t)$ is

$$B(t) = \exp\left(\int_0^t r(s)ds\right). \tag{2.2}$$

The rate $r(s)$ is also called the short rate. It is an instantaneous interest rate valid in the period $(s, s + ds)$, where ds in an infinitesimally small increment.

Definition 2.2 (Stochastic Discount Factor). *The (stochastic) discount factor $D(t, T)$ between times t and T, $t \leq T$ is the amount we need to invest at time t to obtain exactly one unit of the currency at time T. The discount factor is given by*

$$D(t,T) = \frac{B(t)}{B(T)} = \exp\left(-\int_t^T r(s)ds\right). \tag{2.3}$$

Here the time T is in the future, hence if the short-rate $r(s)$ is stochastic the discount factor $D(t, T)$ is as well.

Definition 2.3 (Discount Bond or Zero-Coupon Bond (ZCB)). *A zero-coupon bond (or pure discount bond) is a contract that pays one unit of currency at maturity time T with no intermediate coupon payments. The value of a ZCB (related to the short rate r) at time $t < T$ is obtained under risk-neutral numeraire $\mathbb{Q}$ as*

$$P(t,T) = \mathbb{E}^{\mathbb{Q}}\left[D(t,T)\right] = \mathbb{E}^{\mathbb{Q}}\left[\exp\left(-\int_0^t r(s)ds\right)\right]. \tag{2.4}$$

If the short rate process $r(s)$ is deterministic, then $P(t,T) = D(t,T)$, otherwise the $P(t,T)$ is the expectation of the stochastic discount factor (w.r.t. risk-neutral measure Q) and the $D(t,T)$ is a random variable depending on the future evolution of the short rate.

The discount factors are usually derived from the LIBOR and Euribor rates, or the collateral rates.

Definition 2.4 (Collateralized Zero-Coupon Bond). *A collateralized zero-coupon bond is nearly equivalent to a ZCB, but here the interest rate matches the collateral rate and this bond is secured from default risk by collateral. The collateralized zero-coupon bond price can be calculated as*

$$P_c(t,T) = \mathbb{E}^{\mathbb{Q}}\left[D_c(t,T)\right] = \mathbb{E}^{\mathbb{Q}}\left[\exp\left(-\int_t^T c(s)ds\right)\right]. \tag{2.5}$$

In this dissertation, we will mostly refer to this as the discounting factor, or the OIS discounting factor if we have in mind the collateral rate $c(s)$. It is market-wide practice do pay EONIA or OIS rate for posted collateral. Hence, the collateralized discount rate and OIS-discount rate coincide.

Definition 2.5 (OIS T-Forward Pricing Measure). *We define a new measure, the OIS T-Forward pricing measure $\mathbb{Q}^{c,T}$ by means of a Radon-Nikodym derivative (Brigo and Mercurio, 2006):*

$$\frac{d\mathbb{Q}^{c,T}}{d\mathbb{Q}}\Big|_t := \frac{\mathbb{E}_t[D_c(0,T)]}{P_c(0,T)} = \frac{D_c(0,t)P_c(t,T)}{P_c(0,T)}, \tag{2.6}$$

which is a $\mathbb{Q}$-martingale and we use it normalized, e.g.

$$\forall T\ \frac{d\mathbb{Q}^{c,T}}{d\mathbb{Q}}\Big|_0 = 1. \tag{2.7}$$

Definition 2.6 (Year Fraction, Day-Count Convention). *We denote by $\tau(t,T)$ the chosen time measure between t and T. Since most of the interest rates are publicly reported in an annualised form, $\tau(t,T)$ will be equal to the distance between t and T in years. There are many day-count conventions that can be used, but in this thesis, we choose Actual/365, where the year is 365 days long and the year fraction between the two dates is the actual number of days between them divided by 365.*

Definition 2.7 (**Simply-Compounded Spot Interest Rate**). *The simply-compounded spot interest rate at time t with maturity T is denoted by L(t,T) and is the constant rate at which $P(t,T)$ units of currency have to be invested at time t to produce one unit of currency at maturity. Its relation with the discount bonds can be expressed as*

$$L(t,T) = \frac{1 - P(t,T)}{\tau(t,T)P(t,T)}. \tag{2.8}$$

The market quoted LIBOR, EURIBOR and collateral rates are simply-compounded rates. Using the latter definition we can express the zero-coupon bond price as

$$P(t,T) = \frac{1}{1 + L(t,T)\tau(t,T)}. \tag{2.9}$$

Definition 2.8 (**Annually-Compounded Spot Interest Rate**). *The annually-compounding spot interest rate at time t with maturity T is denoted by $Y(t,T)$ and is the constant interest rate at which one must invest $P(t,T)$ units of currency at time t, reinvest the obtained amounts once a year and finally obtain unit at time T*

$$Y(t,T) = \frac{1}{[P(t,T)]^{1/\tau(t,T)}} - 1, \tag{2.10}$$

$$P(t,T) = \frac{1}{(1 + Y(t,T))^{\tau(t,T)}}. \tag{2.11}$$

Definition 2.9 (**Continuously-Compounded Spot Interest Rate**). *The continuously compounding spot interest rate at time t for the maturity T is denoted*

$$R(t,T) = -\frac{\ln P(t,T)}{\tau(t,T)}. \tag{2.12}$$

$R(t,T)$ is the constant rate at which continuously reinvesting $P(t,T)$ units of some currency yields a return of one unit at maturity time T. In particular

$$P(t,T)e^{R(t,T)\tau(t,T)} = 1, \tag{2.13}$$

$$P(t,T) = e^{-R(t,T)\tau(t,T)}. \tag{2.14}$$

Definition 2.10 (**Yield Curve**). *The yield curve is the graph of the function*

$$T \to \begin{cases} L(t,T),\ t < T \leq t+1 \\ Y(t,T),\ T > t+1 \end{cases} \tag{2.15}$$

The yield-curve is often referred to when talking about the term-structure of interest rates at time t. Up to one year from valuation date t, this is equal to the simply compounded rate, but after one year this becomes an annually compounded rate. A flat yield curve would show that the interest rates for an investment of any maturity is the same. This is usually not the case and the yield curve shows this so-called term-structure, as illustrated in Figure 2.1.

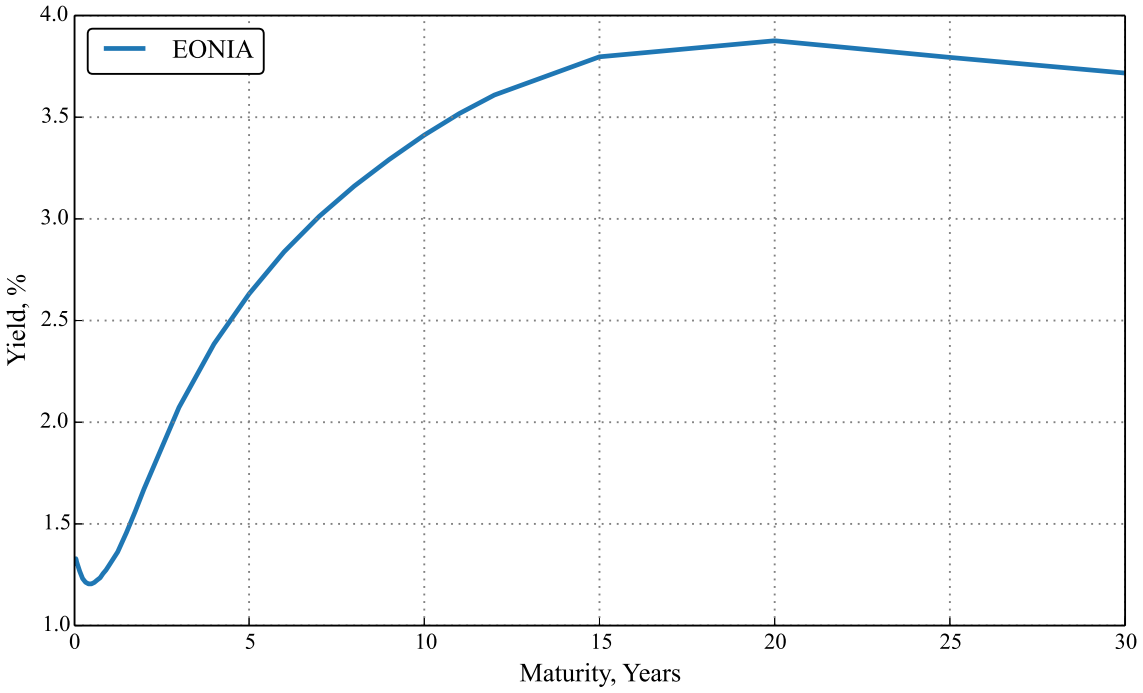

Figure 2.1: Yield curve representing the interest rate derived from the EUR OIS (EONIA) swaps. Data taken from Reuters, 2009-01-26.

Definition 2.11 (Forward Rates). *The simply-compounded forward interest rate measured at time t, expiring at time $T > t$ and maturing at $S > T$ is denoted by $F(t;T,S)$ and defined by*

$$F(t;T,S) = \frac{1}{\tau(T,S)}\left(\frac{P(t,T)}{P(t,S)} - 1\right). \tag{2.16}$$

The forward rate gives the borrowing cost or the lending rate for a loan starting at future time T and maturing at S, but measured at current time t.

2.1.3 Linear Interest Rate Derivatives

The first class of interest rate derivatives that we will use extensively throughout the thesis is the linear derivatives. The value of these contracts depends linearly on the reference

interest rates.

Definition 2.12 (**Forward Rate Agreement**). *A forward rate agreement (FRA) is a contract where one party agrees to pay floating (LIBOR, EURIBOR) rate in exchange for a fixed rate K payment for the same period in the future $[T, S]$. The market price of this contract $F_M$is the discounted expected payoff under the risk-neutral measure, in formulas:*

$$F_M(t, T, S, N, K) = N\tau(T, S)\mathbb{E}^{\mathbb{Q}}[D(t, S)(K - L(T, S))], \tag{2.17}$$

where N is the notional of the contract, $D(t, S)$ is the discounting factor (can be based on LIBOR or collateral rates) and $L(T, S)$ is the simply-compounded LIBOR rate, fixed at future time T and maturing at time S. Since we do not know the future LIBOR fixing, the value of a FRA is an expectation under risk-neutral measure.

Definition 2.13 (**Interest Rate Swap (IRS)**). *Interest rate swap valued at time t, starting at time T_0 and maturing at time T_M is a contract specifying a series of exchanges of fixed and floating cashflows an a set of pre-determined dates $\mathcal{T} = \{T_1, ..., T_M\}$. Just like a FRA 2.12, the floating side of the cashflows is usually indexed with LIBOR or EURIBOR interest rates, but the fixed rate K is fixed at time t and remains the same until maturity of the swap. In formulas:*

$$R(t, \mathcal{T}, N, K) = \sum_{i=1}^{M} F_M(t, T_{i-1}, T_i, N, K). \tag{2.18}$$

In the market the FRAs and IRS's are quoted using fair rates. A fair rate is such a fixed rate K, which renders the value of the contract zero. It is convenient to look at fair swap rates, because these are independent on the notional of the contract. A FRA contract becomes zero if we set the fixed rate to be the expected LIBOR rate $K = \mathbb{E}^{\mathbb{Q}}[L(T, S)]$.
The fair rate of an interest rate swap (or the par rate) is be computed as:

$$S_{\mathcal{T}}(t) = \frac{\sum_{i=1}^{M} \tau(T_{i-1}, T_i)\mathbb{E}^{\mathbb{Q}}[D(t, T_i)(L(T_{i-1}, T_i))]}{\sum_{i=1}^{M} \tau(T_{i-1}, T_i)\mathbb{E}^{\mathbb{Q}}[D(t, T_i)]}. \tag{2.19}$$

Definition 2.14 (Overnight Indexed Swap (OIS)). *An overnight indexed swap is a contract which exchanges the fixed coupon against the daily-compounded overnight (ON) lending rate once every year until maturity T_N. The overnight rates are currency dependent, i.e. Euro has the EONIA rate, US dollar has the Fed funds effective rate and GBP has the SONIA rate. The (fair) OIS rate is determined as*

$$S_N = \frac{P_c(t,T_0) - P_c(t,T_N)}{\sum_{i=1}^{N} \delta_i P_c(t,T_i)}, \tag{2.20}$$

where δ_i is the year fraction between times T_{i-1} and T_i.

This swap rate is quoted in the market for different maturities T_N. One can use the OIS swaps to determine the collateralized zero-coupon-bond prices P_c (2.5). This is why the discount curves based on the collateral (instead of risk-free) rate are often called "OIS discount curves".

Definition 2.15 (Basis Swap or Tenor Swap). *A basis swap is a contract where two parties exchange floating payments, but indexed to different reference interest rates. One of the parties also pays a 'basis spread' to compensate for the expected differences in the interest rate levels. A basis swap is priced by finding such b_N that the following holds:*

$$\sum_{n=1}^{N} \tau_n (\mathbb{E}^{\mathbb{Q}}[L(T_{n-1},T_n) + b_N) D(t,T_n)] = \sum_{m=1}^{M} \tau_m (\mathbb{E}^{\mathbb{Q}}[L(T_{m-1},T_m)) D(t,T_m)], \tag{2.21}$$

where τ_n and τ_m indicate different year fractions.

Common basis swap example is the exchange floating 3-month and 6-month LIBOR payments within same currency, e.g. EUR.

2.1.4 Non-Linear Interest Rate Derivatives

Another class of interest rate derivatives are the non-linear contracts. The payoff and value of these contracts do depend non-linearly on the underlying interest rates. While there is a large variety of non-linear derivatives in general, we will only consider the vanilla derivatives: caps and floors in this thesis.

Most of the standard models for valuing the non-linear derivatives include the use of geometric Brownian motion:

Definition 2.16 (**Geometric Brownian Motion (GBM)**). *A geometric Brownian motion is a continuous-time stochastic process satisfying the following stochastic differential equation (SDE):*

$$dS(t) = \mu S(t)dt + \sigma S(t)dW(t). \tag{2.22}$$

Given initial value S_0, the GBM SDE has an analytic solution:

$$S(t) = S_0 \exp\left(\left(\mu - \frac{\sigma^2}{2}\right)t + \sigma W(t)\right). \tag{2.23}$$

The latter solution is a log-normally distributed random variable with:

$$\mathbb{E}[S(t)] = S_0 e^{\mu t} \tag{2.24}$$

$$\mathbb{V}[S(t)] = S_0^2 e^{2\mu t}\left(e^{\sigma^2 t} - 1\right). \tag{2.25}$$

The GBM is used in quantitative finance to price derivatives using the Black-Scholes model.

Definition 2.17 (**Black-Scholes Equation**). *Let S be the current level of an interest rate. Then, we can determine the price of a European call option under the Black-Scholes model C_{BS} with strike K, annualized drift rate μ, σ - the volatility of the rate and T - the time to expiry of the option with the following formula:*

$$C_{BS}(S, K, \sigma, \mu, T) = \mathcal{N}(d_1)S - \mathcal{N}(d_2)Ke^{-\mu T}, \tag{2.26}$$

$$d_1 = \frac{1}{\sigma\sqrt{T}}\left[\ln\left(\frac{S}{K} + (\mu + \frac{\sigma^2}{2})T\right)\right], \tag{2.27}$$

$$d_2 = d_1 - \sigma\sqrt{T}, \tag{2.28}$$

with $\mathcal{N}$ being the cumulative normal distribution function.

Definition 2.18 (**Bachelier Normal-Volatility Option Price**). *The Bachelier model assumes standard (non-geometric) Brownian motion as the driver of the underlying rates.*

$$dS = \mu dt + \sigma dW_t, \tag{2.29}$$

which implies that the rate $S(t)$ is normally distributed with mean $\mu(t)$ and volatility σ^2. Like in Black-Scholes framework with GBM driver for the rates we can price an European

call option with maturity T, discounting rate r and strike K (Dawson et al., 2007) as:

$$C = e^{-rT}\mathcal{N}(d)\left(S + \sigma\sqrt{T}\frac{\mathcal{N}(d)}{\mathcal{N}'(d)} - K\right), \tag{2.30}$$

$$d = \frac{S-K}{\sigma\sqrt{(T)}}, \tag{2.31}$$

where $\mathcal{N}$ is the cumulative distribution function and $\mathcal{N}'$ is the density function of the normal distribution.

Definition 2.19 (Caps and Floors). *A cap is a contract similar to a payer IRS, but here the payment is made only if its value is positive. The discounted payoff of a cap can be written as:*

$$N\sum_{i=1}^{M}\mathbb{E}^{\mathbb{Q}}\left[D(t,T_i)(T_i - T_{i-1})(L(T_{i-1},T_i) - K)^+\right], \tag{2.32}$$

where $L(T_{i-1},T_i)$ is the LIBOR fixing and K is pre-arranged fixed rate (strike). A floor is an inversely constructed contract on a receiver IRS:

$$N\sum_{i=1}^{M}\mathbb{E}^{\mathbb{Q}}\left[D(t,T_i)(T_i - T_{i-1})(K - L(T_{i-1},T_i))^+\right]. \tag{2.33}$$

In this thesis, we will be also pricing caplets and floorlets. The latter names refer to single-piece caps and floors with $M = 1$.

Definition 2.20 (Swaption). *A swaption is an option to engage in an interest rate swap. An European payer swaption gives the holder the right (not an obligation) to enter into payer IRS at the time of expiry of the swaption. The European swaption value can be computed as follows:*

$$\mathbb{E}^{\mathbb{Q}}\left[D(t,T_1)(R(t,\mathcal{T},N,K))^+\right] = \mathbb{E}^{\mathbb{Q}}\left[D(t,T_1)\left(\sum_{i=1}^{M}(L(T_{i-1},T_i) - K)\right)\right], \tag{2.34}$$

where K is the swaption strike and T_1 is the expiry. The receiver swaption, equivalently, gives holder the right to enter a receiver IRS at the time of expiry.

2.1.5 Risk Management Measures

In the last chapter of this thesis, we will assess the model impact on risk-management measures. The primary measure of interest we want to test is the credit value adjustment

which estimates the expected loss of the underlying contract due to a potential default of the counterparty.

Definition 2.21 (**Credit Value Adjustment (CVA)**). *Credit value adjustment is the difference between a risk-free portfolio value P and a portfolio including the risk of a counterparty default. Unilateral CVA is given by risk-neutral expectation of the discounted losses on the portfolio exposed to counterparty default risk.*

$$CVA = (1 - R) \int_t^T \mathbb{E}^{\mathbb{Q}} \left[D(t, s)(P(s))^+ d\lambda(s) \right], \tag{2.35}$$

where R is the portfolio fraction available for recovery and $\lambda(s)$ is the instantaneous probability of counterparty default.

The recovery fraction R is commonly assumed as constant, even though there is some research done on stochastic recovery, as shown by Kitwiwattanachai (2012). The default process $\lambda(s)$ can be either treated as a deterministic, time-dependent function or a separate stochastic process. In this thesis, we shall look into both setups of the hazard rate: when it is deterministic and when stochastic, driven by a uniformly distributed random variable with some given mean.

In post-crisis banking, CVA is used as an additional charge for over-the-counter transactions, which do not get cleared via an exchange and do not have collateral posted to counteract the effects of counterparty default.

2.2 Literature Overview

In this section, we review the recent literature on the stochastic interest rate spreads. We introduce the two basis spreads that we have analysed in this thesis. Then, we discuss the empirical studies of the stochastic basis spreads and their implications and review the existing stochastic models for interest rates that incorporate the stochastic basis spreads. The third part of the literature review is split into two parts: the first one discusses the post-crisis changes in the interest rate modelling environment and how the pre-crisis standard interest rate models were adapted, and in the second part we present new non-standard models which have particularly interesting properties for derivatives pricing and risk measurement.

2.2.1 Basis Spreads

In this thesis, we are focusing on two connected aspects of the stochastic basis problem. The first one is the already-mentioned LIBOR-OIS spread, yielding the difference between collateral (secured lending) and unsecured LIBOR lending rates. This spread is fundamentally linked to credit and liquidity risks in the inter-bank lending system. The second interest rate spread that we will discuss and later analyse in depth is the LIBOR-FRA gap. In the following, we briefly introduce the background behind both of them.

LIBOR-OIS Basis

LIBOR refers to "London interbank offer rate". It represents the rate at which large, LIBOR-panel, banks give unsecured loans. Before the 2007-2008 crisis, LIBOR loans were treated as risk-free. Since there was plenty of lending and borrowing in the system, there was hardly any concern regarding the liquidity of the banks (Bianchetti, 2012).

Since the credit crisis, the market participants have realised that banks can default and that liquid, unsecured lending can dry out. The impact of credit and liquidity risks can be observed in the LIBOR-OIS spread. OIS swaps are indexed to the overnight lending rates and are a good proxy of the interest rate one can earn by lending day-by-day overnight. Such style of lending minimises both default and liquidity risk and, currently, is the closest proxy to the real risk-free rate (Bianchetti, 2012). Figure 2.2 shows the historical LIBOR and OIS rates from 2007 to 2014 as well as the LIBOR-OIS spread. This demonstrates that the gap between 3-months LIBOR rates and OIS rates has widened significantly since the 2008 crisis started.

Our interest in LIBOR-OIS basis sparks not only because this spread is a good indicator of credit and liquidity risk in the financial markets, but also because the OIS rates are now used nearly in all derivatives trades as the discounting rates. Because of this, it is crucial to understand the relationship between LIBOR and OIS, and how to price derivatives when using LIBOR as the reference rate and the OIS as the discounting rate.

LIBOR-FRA Basis

A related basis spread is the LIBOR-FRA basis. In short, a FRA contract on 3-month LIBOR lets you exchange the future time-T 3-month LIBOR rate with a rate K fixed at the inception of the contract.

Before the credit crisis, one could replicate, or perfectly structure a mimicking payoff of the FRA rates using the spot-LIBOR rates $L(t,T)$ as:

$$F_M(t,T,S) = \frac{1}{(S-T)}\left(\frac{1+S\cdot L(t,S)}{1+T\cdot L(t,T)} - 1\right). \tag{2.36}$$

In practice replication of a $F_M(t,T,S)$ could be done by:

1. Borrowing money at LIBOR rate $L(t,S)$ until time S.
2. Lend the same amount at $L(t,T)$ until time $T < S$.

This replication was fundamentally important for the hedging strategies of market FRA, IRS contracts and even more complicated derivative products like caps, floors and swaptions.

The FRA rate and its standard replication rate used to be identical, as they both referred to the same unsecured loans, but since September 2007 this is no longer true. Due to increased credit risk, the banks stopped lending under unsecured terms, and all borrowing is done on collateral basis making FRA replication in practice is a difficult task, as unsecured borrowing at LIBOR rates is no longer a common practice. Additionally, the FRA contracts are collateralized which makes them nearly credit-risk free, yielding a fundamental difference between FRA and its spot-LIBOR replica. Nevertheless, the FRA payouts are still indexed to the daily-published, unsecured LIBOR rates. Therefore FRA and LIBOR values are fundamentally connected.

Figure 2.3 shows the market-traded FRA's and synthetic forwards from spot LIBOR and OIS curves. We can observe that the OIS-forward rates are the lowest as the rates are nearly riskless. Then we have the market FRAs, which are collateralized, but still LIBOR-linked. Finally, spot-LIBOR forward rate carries the largest risk premium as this type of loan does not offer any default protection.

Discussion

As a result of the aforementioned basis spreads nearly all market participants have moved to the so-called multi-curve pricing framework (Mercurio, 2009). All future cash flows are discounted with OIS rates, if the derivative is collateralized, or using the Bank's internal unsecured funding curve. Then, the LIBOR-linked cash flows (FRAs and IRS) are indexed to tenor-dependent LIBOR curves. These are bootstrapped from corresponding (6-month

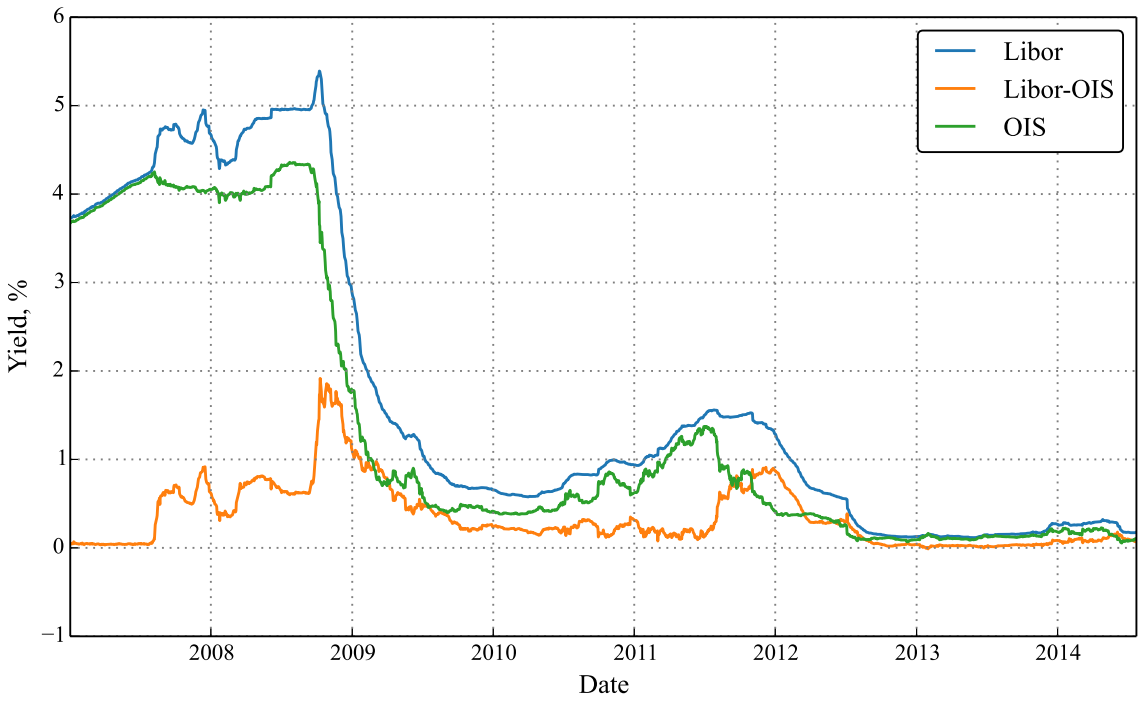

Figure 2.2: Comparison of historical 3-month LIBOR, 3-month OIS rates and the size of LIBOR-OIS spread. The LIBOR-OIS spread was negligible, few basis points, before September 2007, but increased dramatically up to 200 bp and remained stochastic and volatile throughout the full period of our analysis. Data from Reuters Eikon.

and 3-month LIBOR) IRS, FRA and even Futures contract rates. Constructing a consistent set of interest rates for every tenor as well as assessing the volatility of each rate has many issues. Not all-tenor swaps are liquidly traded, and the prices of non-liquid swaps are 'synthetically' obtained using basis swaps with payments of a different tenor. Cap and floor pricing is also complicated as volatility data is only available for one or two tenors (e.g. 3 and 6-months) and strikes. We have included flow-charts of before/after-crisis pricing frameworks in Appendix B.

In the end, this affects risk-management measures, like CVA, as to compute the risk profile of every swap, one needs to know the volatility of underlying rates, which are often not available. Therefore we seek to investigate several interest-rate models that jointly reprice the market FRA's, IRS's and caps. Additionally, we look for models that explicitly model the stochastic basis in a historically-sound way. Last, we are looking for models that can relate the stochastic basis to the liquidity and credit risk. Empirical evidence suggests that the latter are closely connected (Filipovic and Trolle, 2013) which has adamant

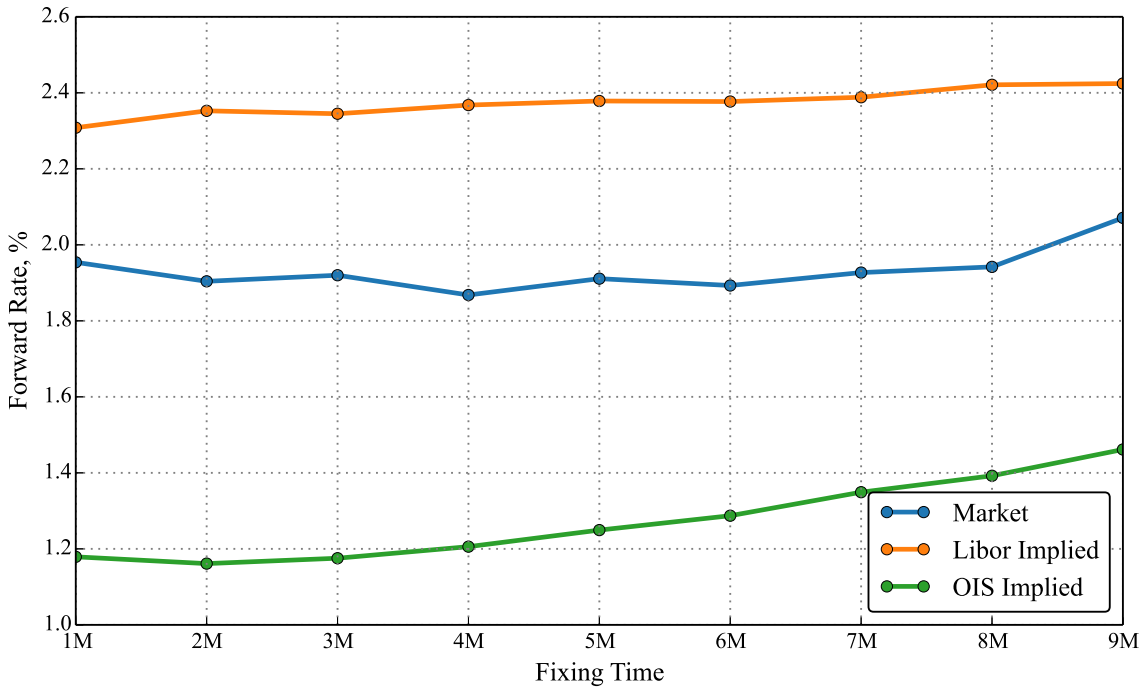

Figure 2.3: Comparison of 3-month LIBOR, 3-month OIS and market-traded 3-month forwards with forward-starting times from 1-month till 9-months. Forward rates were obtained using standard replication of LIBOR Rates, OIS Rates and FRA rates were taken directly from the market. Data from Reuters Eikon, 2009-01-26.

implications for credit risk assessments and CVA charges.

2.2.2 Empirical Review of Stochastic Basis Spreads

Before looking for a suitable model for the basis spreads, it is important to understand their structure and potential drivers. Several studies were done in this area, most with overlapping results and running into the same problems.

For example, Filipovic analysed the historical term-structures of the USD and EUR LIBOR-OIS spreads (Filipović et al., 2012). Their in-depth study reveals that there is a distinct term-structure in the LIBOR-OIS spreads with the spread or 'interbank risk' increasing with maturity. In this study, they have constructed a credit proxy from LIBOR panel CDS spreads and a liquidity proxy from the average daily trading volume as reported by the DTCC . Using the latter proxies they decomposed the LIBOR-OIS spread into credit and non-credit components. This decomposition showed that the short-end of the spread term structure is driven by liquidity (non-credit) risk and the long end is driven by the credit risk. The constructed CDS proxy was also used as the explanatory variable for the credit

component of the LIBOR-OIS spread, and the remaining factor was called non-credit, as only 53% and 65% of (USD and EUR markets respectively) could be explained by their liquidity proxy.

A similar empirical study on the 3-Month USD LIBOR-OIS spread was published by Poskitt and Waller (2011). The LIBOR-OIS spread was decomposed into credit and non-credit parts using JP Morgan CDS index as the credit proxy. The authors emphasised on the problem of finding a good proxy for liquidity and constructed several proxies from off-shore USD money markets, which only partially explained the non-credit part of the LIBOR-OIS spread. Nevertheless, this study showed that the credit impact is smaller than the non-credit (liquidity) on the LIBOR-OIS spread. It also confirmed that finding a reliable proxy for liquidity is a difficult task as there is no traded asset class related to the liquidity of the lending markets.

Michaud and Upper (2008), Heider et al. (2009), Eisenschmidt and Tapking (2009) identify several causes of the LIBOR-OIS spread, in particular, the roles of credit and liquidity factors. When finding explanatory data sets becomes very difficult, the next step is attempting to construct a logically and mathematically sound non-linear model to explain the LIBOR-OIS disparity. An innovative idea was demonstrated by Crépey and Douady (2012). The authors showed an economically-sound model, where the size of the LIBOR-OIS spread is be influenced by the trading dynamics of overnight and long-term unsecured funding. The proposed model assumes that the rise of collateralization and the use of OIS-type lending since the start of the credit crisis impacted the LIBOR-OIS spread. The proposed equilibrium model for OIS and LIBOR lending, which yields a tractable solution for the LIBOR-OIS spread:

$$L(T) - \text{OIS}(T) = \alpha + \beta\sqrt{T} \tag{2.37}$$

where α is the interbank credit skew and β stands for liquidity cost of capital. The authors have performed an empirical analysis of this model, by looking into the differences in LIBOR-OIS spreads in different tenors (3-month, 6-month, 9-month LIBOR curves and OIS). It shows that after fitting the model to market data for every tenor the resulting credit component is shared between all tenors, but liquidity parameters are different. Nevertheless, the size of liquidity components forms a clear structure, where liquidity components for longer tenors (6,9 months) are larger than for short tenors (3 months). Therefore this con-

firms that the mathematically and empirically sound model for LIBOR-OIS spread should be based on credit and liquidity effects and also demonstrates that every tenor loan carries an individual level of liquidity risk, forming a term-structure.

A recent study by Cui et al. (2016) looked into the drivers of LIBOR-OIS spreads in five major currencies (USD,EUR,GBP,CHF and JPY). This study provided evidence that systemic risk, market volatility, liquidity and counterparty risk were the primary drivers of the LIBOR-OIS spreads during the crisis. What is more, it showed that the relevance of these determinants was not constant and changed in different periods of the crisis, and few other factors, such as secondary market liquidity and banks risk tolerance levels were significant drivers of the USD spreads.

While various works discuss the existence and empirical facts of the LIBOR-OIS spread, very few look into the follow-up problem of forward LIBOR and FRA basis spread. A very important study was done by Morini (2009). The author examined the discrepancies between the standard LIBOR replication of a forward and the market-quoted forward rates. In particular, this paper analysed the spreads between different tenor forward LIBOR curves (obtained from market FRA contracts). One of the main contributions in the paper is proof that the spreads between FRA contract rates can be perfectly replicated using traded basis swap contracts. Additionally, he introduced a stochastic model based on LIBOR panel dynamics. Using this model he showed that the gap between standard FRA replication (2.16) and market FRA quotes could be bridged using iTraxx CDS index at-the-money options volatility, covering above $\approx 85\%$ of the gap. The author concluded that this replication model can still be improved by adding liquidity next to credit as an influencing factor.

2.2.3 Derivatives Pricing with Stochastic Basis

To mitigate the rising credit risk, CSA agreements became widely adopted between large market participants. CSA, as expected, did reduce the counterparty-related credit and liquidity risk involved in financial contracts. Unfortunately, this did not affect the default and liquidity risk component implicitly carried by the LIBOR rate. Inherently, the interest rate swaps under CSA agreements are still not counterparty risk-free. This can be observed in the market-quoted basis swap (2.21) spreads, which are both collateralized and far from zero at the same time (Bianchetti, 2012).

As a result of widespread CSA agreements, modern-derivatives pricing works in a so-called "multi-curve framework" (Kenyon, 2010). The discount curves must be computed using the OIS curve or the bank's internal funding curve, depending if there is a CSA agreement between the two counterparties. Then, the FRA rates with different tenors must be computed from multiple tenor-dependent yield curves. Moreover, if the derivative in question is non-linear, e.g. caplet or swaption - tenor and maturity dependent volatilities are needed for their pricing. For more information on the move from single-curve to the multi-curve framework, we have included flow-carts in the Appendix B.

The latter move from single-curve to multi-curve pricing framework and added complexity comes at a high cost as it requires highly heterogeneous market data, which might be illiquid or even absent. Additionally, the involvement of multiple curves in the valuation exposes simple swap portfolios to multiple delta sensitivities (multiple basis risks), making the hedging of plain, vanilla derivatives a complex task.

Modelling the Basis with Pre-Crisis Models

Since the LIBOR rates and the discounting (OIS) rates became separated, the classical interest rate derivatives pricing framework with a single curve was no longer valid, as the risk-free discounting curve no longer matched the LIBOR-payout curve. Several studies were published on the topic of the two-curve and multi-curve pricing framework. The vast majority of the proposed models were standard interest rate models adapted to the multi-curve environment, often under the assumptions of LIBOR-OIS independence.

The early works concentrated on pricing derivatives in a two-curve framework, one curve for discounting and one curve for the forward rates, treating the two curves as entirely independent of each other. One of the first studies introducing a two-curve pricing framework was done by Chibane and Sheldon (2009). The paper outlined pricing formulas and a full calibration procedure for consistent construction of the discounting and forward curves in a multi-currency setting using linear interest rate derivatives, like interest rate swaps, basis swaps and cross-currency swaps. Several more elaborate works on the pricing of more non-linear derivatives in the two-curve framework were done by Mercurio (2009). He obtained arbitrage-free pricing of the forward rate agreements and interest rate swaps in a two-curve environment matching previous works. Moreover, he showed that the

classic Black's formula for option pricing can be extended to price caplets and swaptions in the two-curve environment under log-normal models for FRA and swap rate evolutions (Brigo and Mercurio, 2006). Another contribution of this work was the derivation of Black-like caplet and swaption pricing formulas under extended LIBOR market model (LMM), where he modelled the spot LIBOR and FRA rates separately for each tenor. The drawback of this model is that we have to solve a system of 15 or more SDEs, which is a significant computational burden.

In 2010 few more elaborate models were proposed for derivatives pricing, including models with term-structure and volatility smile. Pallavicini and Tarenghi (2010) discussed the market evidence that led to the market-wide switch to the multi-curve pricing of interest rate derivatives. They also define a Heath, Jarrow, Merton (HJM) model framework based on multi-curve approach presenting a bootstrap algorithm to strip curves off the IRS and FRA data. Following that, they showed how to price more complicated derivatives like the Constant-Maturity-Swaps (CMS) and CMS spread options using their model.

A follow-up work by Moreni and Pallavicini (2014) discusses extending the HJM framework and analytical swaption pricing in multi-curve framework using an approximated formula. Work also includes calibration examples to real market data and comparison with few other benchmark models for swaptions pricing. An extensive analysis and impact assessment of using this HJM framework for pricing derivatives, CVA with wrong-way risk as well as gap risk was recently accomplished by Bormetti et al. (2015).

A more recent work by Mercurio (2010) on the two-curve pricing problem looked into explicitly modelling the spread between the OIS discounting curve and the FRA rates for each tenor. The LIBOR rate was decomposed into OIS rate and basis so that the stochastic basis spread could be viewed as a factor driving the evolution of the forward LIBOR rates. In this framework, the FRA and IRS pricing formulas remained unchanged, but the Caplet formula became more involved. The author also investigated in detail the Stochastic-Alpha-Beta-Rho (SABR) stochastic volatility extension for the basis spread and derived and a semi-analytic solution for pricing of caplets.

The most recent works on the topic of modelling LIBOR-OIS spreads includes an introduction of a multiple curve framework with affine LIBOR models (Grbac et al., 2015), which allows for semi-analytic pricing of caps, swaptions and basis swaptions, when the

rates are positive and hints towards a model extension for negative rates as well. Another recent article by Hull and White (2016) shows how to jointly model LIBOR and OIS rates using a three-dimensional tree. The latter work shows how well-established techniques can be extended to the new multi-curve framework and shows how to value spread options and Bermudan swaptions.

Advanced Models for Stochastic Basis

Several later mathematical works explicitly address the post-crisis interest rate modelling problems other than the existence of the LIBOR-OIS spread and multi-curve framework. We find these works exceptionally interesting and useful in modern derivatives pricing and CVA calculation.

We have already discussed the work of Morini (2009) in the section 2.2.2 together with empirical analysis papers. The LIBOR panel model is one of the models we shall pursue to extend as it allows for joint pricing of spot-LIBOR, OIS and FRA rates and yields an explicit link with credit risk in the market. The original the panel model and its extension are explored in detail in Chapter 3.

A Levy-process based model for default-free OIS rates and 'defaultable' LIBOR rates was demonstrated by Crepey et al. (2013). The authors showed calibration and fit results for the model when pricing FRA, IRS and even non-linear derivatives as caps and swaptions. In their framework, the authors demonstrated the ability of the model to reproduce the market FRA rate levels during the peak of the credit crisis. Moreover, as this was a follow up of their earlier works, they extended their framework for credit valuation adjustment pricing as their original model already included default component in the LIBOR rates.
A more recent work by Li and Mercurio (2016) looks into modelling the LIBOR-OIS basis as a simple Poisson jump process with applications to gap risk and CVA pricing.

Another post-crisis problem, which was not well explored is the pricing of non-standard tenor options, like caps and swaptions. The most liquid USD and EUR caps are based on, respectively, 3-month and 6-month LIBOR rates. Because of the switch to the multi-curve framework, to price an illiquid cap on a 9-month LIBOR rate one needs a 9-month LIBOR volatility rate, which can no longer be directly implied from 3 or 6-month Caps. This problem of extrapolating caplet and swaption volatilities to non-standard tenors,

given quotes for standard tenors, was revisited by Kienitz (2013). The author proposed an arbitrage-free model with displaced diffusion for the forward rates and standard lognormal diffusion for the OIS rates. With this setup, the author showed how to calibrate the model to given ATM caplets and extrapolate the obtained volatilities to a different tenor. What is more, he showed that it is possible to fit a stochastic alpha-beta-rho (SABR) model to a single-tenor volatility curve and shift the volatilities to another tenor while preserving the same SABR volatility smile.

A more recent work by Morino and Ruggaldier (2014) discussed a low-parameter short rate setup for two-curve modelling with an affine three-factor model. The authors presented a clean-valuation framework for FRAs and caps (linear and non-linear derivatives) with the main goal of their model exhibiting an adjustment factor when passing from the single-curve to two-curve setting. We believe that their additive short-rate factor construction framework can be extended to solve multi-curve derivative pricing problems, like pricing of illiquid-tenor caps as well as price CVA on illiquid-tenor FRA and IRS contracts. We shall discuss our proposed mixed short-rate model in Chapter 4.

Few novel articles discuss issues with multi-curve modelling and stochastic basis that go beyond this thesis. The topics include pricing of cross-currency trades with multiple currency collateral available (Moreni and Pallavicini, 2015), which adds additional complexity levels for consistently bootstrapping the interest rate curves from OIS (and equivalent) rates, single currency swaps, basis swaps, and cross-currency basis swaps. Furthermore, Brigo and Pallavicini (2013) look into other details affecting multi-curve pricing of trades, including collateral, clearing, funding, netting, re-hypothecation and closeout issues.

2.3 Basis Spread Models

In this section, we introduce the core models used for derivatives pricing with stochastic basis, as discussed in recent literature. Our goal is to familiarise the reader with the different model constructions and features as well as with the immediate results of these models, such as pricing simple derivatives like the IRS, caps and swaptions analytically. Moreover, we discuss the ease of obtaining risk-measurements like VaR and CVA when using these models.

2.3.1 Short Rate Models

The original theory of interest-rate modelling was based on the assumption that a specific one-dimensional instantaneous spot-rate process r was driving all the observable interest rate quantities.

Modelling the short-rate process is convenient as all the observable interest rates, bond prices and other derivatives are readily defined, using no-arbitrage arguments, as the risk-neutral expectation of payoff $H(T)$ discounted with the short rate (Brigo and Mercurio, 2006):

$$H(t) = \mathbb{E}_t \left[D(t,T) H(T) | \mathcal{F}_t \right] = \mathbb{E} \left[e^{-\int_t^T r(s) ds} H(T) \right] \tag{2.38}$$

It should be clear that whenever we can clearly define the dynamics of $r(s)$, we can find the above expectation and price simple zero-coupon bonds.

There are many choices for $r(s)$ dynamics. A very popular class of models is the affine short-rate models. They are called 'affine' as the solution for zero-coupon bond price is of the form:

$$P(t,T) = A(t,T) e^{B(t,T) r(t)}, \tag{2.39}$$

where $A(t,T)$ and $B(t,T)$ are deterministic functions of time. For example, we can model the OIS rates as one factor Hull-White process:

$$r(t) = \theta(t) + y(t), \tag{2.40}$$

$$dy(t) = -k y(t) dt + \sigma(t) dW(t), \; y(0) = 0, \tag{2.41}$$

where $k > 0$ and $\sigma(t), \theta(t)$ are deterministic functions of time and $dW(t)$ is a standard Brownian motion increment (2.16).

There are different variants of the short-rate dynamics specifications: it can include two correlated Brownian motions dW_1, dW_2, it can have a square-root diffusion term $\sigma(t)\sqrt{r(t)} dW(t)$, etc. Nevertheless, as we shall show in later chapters that it is convenient to use short-rate models as many of their variants do have analytic solutions for ZCB, cap and swaptions prices. This feature allows for easy calibration to available market data. Additionally, short-rate models normally have up to 3 driving stochastic factors (Brownian motions). Therefore risk-assessments like VaR or CVA include only a simulation of a 3+1 (credit risk factor) SDE system.

To model stochastic basis, we would need a multi-dimensional system to model the OIS rates and each of the forward-LIBOR curves. This can be done in several ways:

- Short rate model for OIS and another for x-LIBOR curve
- Short rate model for OIS and another for x LIBOR-OIS spread
- Short rate model for x-LIBOR curve and another for x LIBOR-OIS spread.

In each of the setups, we would obtain short-rate systems that (ideally) can analytically price ZCB and analytically or semi-analytically price non-linear derivatives such as caps and swaptions.

2.3.2 LIBOR-Market Model Approach

Another very popular class of interest rate models is the market models. The main reason for their popularity is in the agreement between the well-established market formulas for basic derivative products, like caps. The lognormal forward-LIBOR model (LFM) prices caps with Black's formula (Brigo and Mercurio, 2006), which is a classic standard for options valuation. Then, the lognormal forward-swap model (LSM) prices swaptions with again the simple Black's formula. Under the LFM, we model every forward-LIBOR payment $F_k^x = F(T_k, T_{k+1}), x = T_{k+1} - T_k$ as a stochastic asset:

$$dF_k^x(t) = \sigma_k^x F_k(t) dZ_k^x(t), \tag{2.42}$$

$$\tag{2.43}$$

where F_k^x is the x-tenor forward rate, maturing at time T_k, σ_k^x is the k- LIBOR forward rate volatility and dZ_k^x is the standard Brownian motion.

The main drawback of the LFM model is its large number of degrees of freedom, as each forward on every single curve is modelled separately. This produces a large computational burden for VaR and CVA assessments. Additionally, the large set of parameters must be calibrated to a large number of market-traded FRAs, caps, and other derivatives, which in some markets are not available. We shall address the problem of forward-rate volatility estimation when relevant caps are not traded in later chapters.

2.3.3 Generalized Approach

Mercurio showed that there is an easy way to use the additive stochastic basis with existing LIBOR market models for interest rates (Mercurio, 2010). We say that our forward-LIBOR

rate is the sum of OIS-forward and the basis

$$L_k^x(t) = F_k^x(t) + S_k^x(t)$$

where $L_k^x(t) = \mathbb{E}^{\mathbb{Q}}\left[L(T_k, T_{k+1})|\mathcal{F}_t\right], F_k^x(t) = \mathbb{E}^{\mathbb{Q}}\left[F(T_k, T_{k+1})|\mathcal{F}_t\right]$. In a very general way, we define the basis as:

$$d\chi_k^x(t) = \chi_k^x(t)[\sigma_{k,1}^x(t)dZ_1(t) + \sigma_{k,2}^x dZ_2(t)], \tag{2.44}$$

$$S_k^x(t) = S_k^x(0) + \alpha_k^x[F_k^x(t) - F_k^x(0)] + \beta_k^x[\chi_k^x(t) - \chi_k^x(0)],\ \chi_k^x(0) = 1, \tag{2.45}$$

where $\sigma_{k,i}^x, \alpha_k^x, \beta_k^x$ are constant parameters chosen to fit our basis dynamics, $dZ_i, i \in 1, 2$ are independent Brownian motions, α_k^x controls the correlation between the spreads and OIS rates, β_k^x defines the volatility of the spreads, and the stochastic basis factors χ_k^x may be different for tenors x and maturities k.

As a result of this formulation, the LIBOR rates can be explicitly written as:

$$L_k^x(t) = L_k^x(0) + (1 + \alpha_k^x)[F_k^x(t) - F_k^x(0)] + \beta_k^x[\chi_k^x - \chi_k^x(0)]. \tag{2.46}$$

Note: It may be practical to assume independence of OIS rates and basis spreads S, which can be simply done by setting $\alpha_k^x = 0$. The OIS forward rates are explicitly given by:

$$F_k^x(t) = [A(t, T_{k-1}^x, T_k^x)e^{-B(t,T_{k-1}^x,T_k^x)y(t)} - 1]/\tau_k^x, \tag{2.47}$$

where A, B are deterministic.

The basis factors χ we model with GBM:

$$\chi_k^x(t) = \chi^x(t),\ \forall k, \tag{2.48}$$

$$d\chi^x = \eta^x(t)\chi^x(t)dZ^x(t),\ \chi^x(0) = 1, \tag{2.49}$$

where η^x is deterministic, and Z^x is independent of OIS rates. This choice of a joint model for OIS rates and the spreads gives:

1. Caplets and swaptions can be valued as 2-dimensional integrals.
2. Conditioned on OIS rates model, LIBOR and swap rates are affine functions of χ
3. The integration can be made semi-analytic, by evaluating the inner integral as a modified Black formula.

2.3.4 LIBOR Panel Model

We took the liberty of naming the "LIBOR as an Option" (Morini, 2009) approach to modelling of 'risky' LIBOR rates and future FRA payoffs, as the LIBOR panel model. The underlying idea behind this model is that LIBOR is a trimmed average rate from submissions made by an approved panel of banks. This average works as a lending rate of a 'prime' bank in the panel. We can assume that a bank matching the rate of the prime bank is indeed in the panel. Therefore, every day at the LIBOR rate fixing time, one of the panel banks stands as the 'prime' bank in the panel. If the credit rating of the current prime bank does not change much with respect to the rest of the panel it remains the prime bank, but if it significantly worsens it loses the prime bank status and another bank steps in.

In the following, we introduce the mathematical formulation of the model in question. We start by separating the (future) LIBOR rate into the risk-free interest rate component and a credit-liquidity spread

$$L(T,S) = L^{rf}(T,S) + S(T,S). \tag{2.50}$$

We denote the rate of the bank, denoted as 'prime' at time zero by L^{X_0} and its credit-liquidity spread as S^{X_0} as in the following equation

$$L^{X_0}(T,S) = L^{rf}(T,S) + S^{X_0}(T,S). \tag{2.51}$$

The forward credit-liquidity spread for this counterparty can be rewritten in terms of zero-coupon bonds as:

$$\mathbb{E}^{\mathbb{Q}}[S^{X_0}(T,S)|\mathcal{F}_t] \approx S^{X_0}(t,T,S) = \frac{1}{T}\left(\frac{P^{rf}(t,T)}{P^{rf}(t,S)} - \frac{P^{X_0}(t,T)}{P^{X_0}(t,S)}\right). \tag{2.52}$$

This spread, despite a small convexity adjustment (< 2 basis points) (Morini, 2009), is the expectation of the future spread of our 'prime' counterparty. As we have mentioned, the prime counterparty may change, therefore our real credit-liquidity spread must include conditions for a potential refreshment of the counterparty. Hence, the realised prime counterparty at future time T remains the same as the starting one if S^{X_0} does not exceed pre-

defined panel exit level S^{Exit}, otherwise gets replaced by substitute counterparty as:

$$S(T,S) = \begin{cases} S^{X_0}(T,S) & \text{if } S^{X_0}(T,S) \leq S^{\text{Exit}}, \\ S^{\text{Subst}} & \text{if } S^{X_0}(T,S) > S^{\text{Exit}}. \end{cases} \tag{2.53}$$

To simplify the counterparty refreshment scheme above, as in the original formulation (Morini, 2009), we assume a 'mirrored' evolution of future spreads for LIBOR counterparties: for every positive deviation of the expectation, there exists a counterparty with equivalent negative deviation e.g. if the spread of X_0 bank increased by 1%, another bank X_1 steps in with its spread improved by the same 1%.

This leads to the future spread over risk free rate as the sum of forward spread of the initial counterparty and the realised change in this spread, which is now the spread of the substitute prime bank

$$S^{\text{Subst}} = S^{X_0}(0;T,S) + (S^{X_0}(0;T,S) - S^{X_0}(T,S)). \tag{2.54}$$

We can now rewrite the equation (2.50) in terms of the forward spread of initial prime bank:

$$L(T,S) \;\; = \;\; L^{X_0}(T,S) - 2\max\left(S^{X_0}(T;T,S) - S^{X_0}(0;T,S), 0\right), \tag{2.55}$$

the above future LIBOR fixing is unknown at current time zero, but we can take its expectation under the risk-free measure. The expectation of a forward-LIBOR for prime bank X_0 is equal to the standard replication of the forward $F_{Std}(0;T,S) = \mathbb{E}^{rf}[L^{X_0}(T,S)]$. Overall, the expectation of future LIBOR fixing, including the counterparty substitution property can be simplified as

$$\mathbb{E}^{\mathbb{Q}}[L(T,S)] = F_{\text{Std}}(0;T,S) - 2\mathbb{E}^{\mathbb{Q}}\left[\left(S^{X0}(T;T,S) - S^{X0}(0;T,S)\right)^{+}\right]. \tag{2.56}$$

If we assume that the credit-liquidity spread for any bank evolves as driftless GBM (2.16):

$$dS^{X0}(t,T,S) = S^{X0}(t,T,S)\sigma dW(t), \tag{2.57}$$

we obtain a simple formula for the future LIBOR as an ATM option:

$$\mathbb{E}^{\mathbb{Q}}[L(T,S)] = F_{\text{Std}}(0;T,S) - 2C_{BS}\left(S^{X0}(0;T,S), S^{X0}(0;T,S), \sigma, \mu = 0, T\right), \tag{2.58}$$

$C_{BS}(\cdot)$ denotes a driftless ATM Black call (2.26) with volatility σ, current spread level and ATM strike $S^{X0}(0;T,S)$ and expiration T.

The latter time-zero risk-neutral expectation is a traded market product - the forward rate agreement $F_M(t,T,S) = \mathbb{E}^{\mathbb{Q}}[L(T,S)]$. Therefore, the gap between the market-traded FRAs and the standard forward replica is equal to the option value on the credit-liquidity spread of the prime bank. To compute the value of this option we need to know the σ parameter - the average volatility of credit-liquidity spreads of the LIBOR panel banks.

2.4 Research Gaps and Conclusion

The divergence of LIBOR and risk-free lending rates has caused turmoil in lending markets, as well as rendered the current interest rate models no longer useful. Several adaptations of classic stochastic models and few new ones were proposed for pricing derivatives in the setting of multiple LIBOR and risk-free rates, most of these fall into the categories of short-rate and LIBOR-market models.

The short-rate models are attractive for their simplicity but do not always have enough degrees of freedom to fit the curve and volatility data within the bid-ask spreads. The current multi-curve short rate proposals in the literature have adapted a 'curve-per-tenor' approach, where each LIBOR tenor (1M,3M,6M,12M) has a separate model, with imposed correlation between the drivers. These approaches have the benefit of fitting each curve perfectly to market data, but the principle itself has little to do with the common empirical drivers of all the curves (credit and liquidity). What is more, calibrating four completely separate models is challenging if volatility-dependent derivatives, like caps or swaptions, are not liquid for every single tenor.

The generalised LIBOR-Market models have a few more degrees of freedom, but are hard to calibrate due to lack of liquid data for volatilities and correlations as well as the proposed short-rate models. Their main benefit is the freedom of choice of the volatility structure.

Very few of the published variants of these models explicitly refer to the link between LIBOR-OIS spreads and credit-liquidity risk in the interbank lending market. In the following sections, we shall introduce possible model constructions that have either implicit or explicit link with the risks mentioned above. The model that is explicitly approaching

the linking problem is the Panel Model (Morini, 2009), but as we shall show, more analysis needs to be done on its applicability in practice.

Chapter 3

LIBOR Panel Model for Forward Rate Replication

3.1 Introduction

The existence of the stochastic basis spread causes multiple problems. The forward rates replication (as we have introduced it in section 2.2.1) is a widely-discussed issue impacting many derivatives pricing models. Nevertheless, the majority of articles (2.2.3) show how to price derivatives in the new setting, by taking the LIBOR-FRA disparity as already given in the initial setup. There is a gap in the literature and a need for a model which would explain the relation between the current spot-LIBOR rates curve and the market-traded FRA rates. There is vast econometric evidence (Section 2.2.2) on the relation between the basis spreads and credit and liquidity risks. For instance, the LIBOR-panel mechanics based model (Morini, 2009) assumes an explicit relation between credit risk and LIBOR-OIS basis spreads. Using this relationship, we can price market-traded FRA contracts using information from the spot-LIBOR curve and LIBOR panel bank credit risk indices. Explicit relation of LIBOR-OIS spread and credit risk in this model can have tremendous implications for risk management practices such as VaR and CVA (2.35) computation (Kenyon and Stamm, 2012).

The goal of this chapter is to verify and follow-up the LIBOR panel model (Morini, 2009). We start this chapter by introducing the forward rate replication problem. Following that, we introduce the concept and mechanics behind the LIBOR panel model and validate the results obtained by Morini (2009) (using iTraxx volatility proxy, as in the original pa-

per). We complement the analysis by moving from a single FRA contract to replication of full series of market-traded FRAs and introduce a FRA-implied volatility framework capable of additionally reducing FRA replication errors. Using the latter results, we discuss the remaining data replication errors and limitations of the default panel model formulation.

In the second part of this chapter, we extend the model using our observations from the error analysis of the original model. We propose the use of uncertain volatility model (Alexander, 2004) and demonstrate that it reduces the replication error by nearly an order of magnitude and the decreased error remains within the bid-ask spread over 95% of the time. We conclude this chapter with a discussion on historical implied parameter dynamics in the extended model and its overall usefulness in derivatives pricing area.

3.2 Standard Model Forward Rate Replication

Construction of the forward LIBOR rate is a vital principle in modern interest rate derivatives pricing. Before the credit crisis, a forward starting LIBOR-linked loan was constructed using two spot-LIBOR loans as shown in (2.17).

Since mid-2008, the interest rate market has moved from single-curve to multi-curve pricing framework, which means that now we have a discounting curve for every tenor of the loan e.g. if we construct a future loan for a 3-month period, we have to use the 3-month curve, for a 9-month loan and the corresponding 9-month curve. An example market yield curve snapshot is shown in Figure 3.1.

Despite the added complexity of discounting loans on different curves, we also learned that the standard replication formula (2.11) is no longer valid, as the market-traded FRA rates no longer match their standard-replication counterparts. This introduces the separation between the spot-LIBOR curve and the forwarding curves, which is counter-intuitive, as all the LIBOR-linked derivative payouts are indexed on the spot-LIBOR curve and not the forward curves.

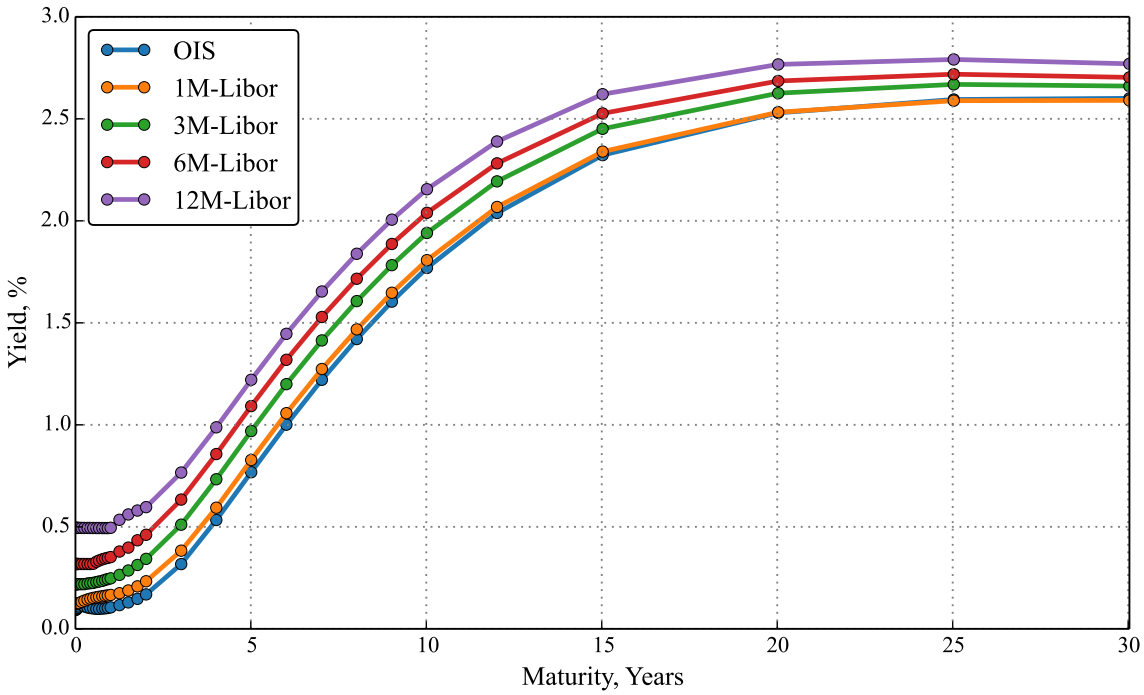

Figure 3.1: Plot of multi-tenor discounting curves. The curves were bootstrapped from OIS swaps as well as 1,3,6,12-month FRA and IRS linear derivatives. In the multi-curve discounting environment, cashflows with different payment frequencies are discounted with corresponding yield curves.

Figure 3.2 compares the 3-month LIBOR, OIS and market-traded FRA rates with forward-starting times from 1-month till 9-months. It shows that the market-traded FRA rates are substantially different from the replicated forward rates using the unsecured LIBOR or even the OIS rates. Therefore, to correctly price a FRA one has to take into account the credit and liquidity premiums embedded in the LIBOR, as well as the fact that the FRA contracts are collateralized and nearly risk-free by themselves. Moreover, from the figures 3.2a and 3.2b we can see that the forward LIBOR-OIS term structure gap is dynamic and changes over time. Therefore a static, constant spread model for LIBOR-FRA spread would incorrectly represent its dynamics.

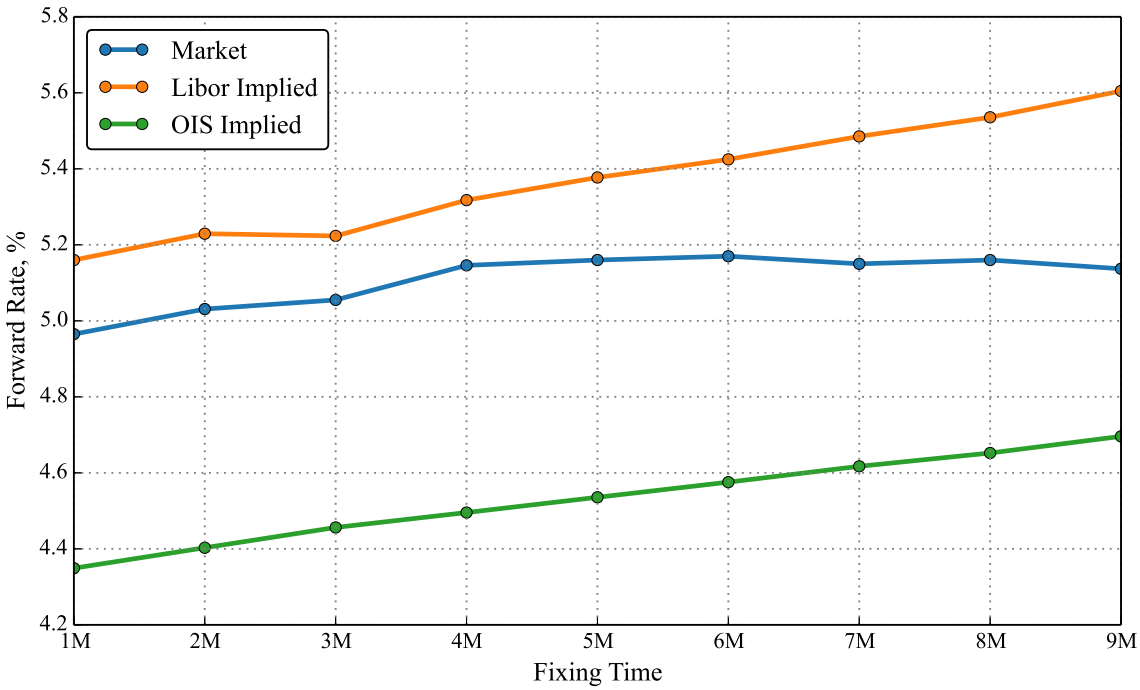

(a) Data from 2008-06-26.

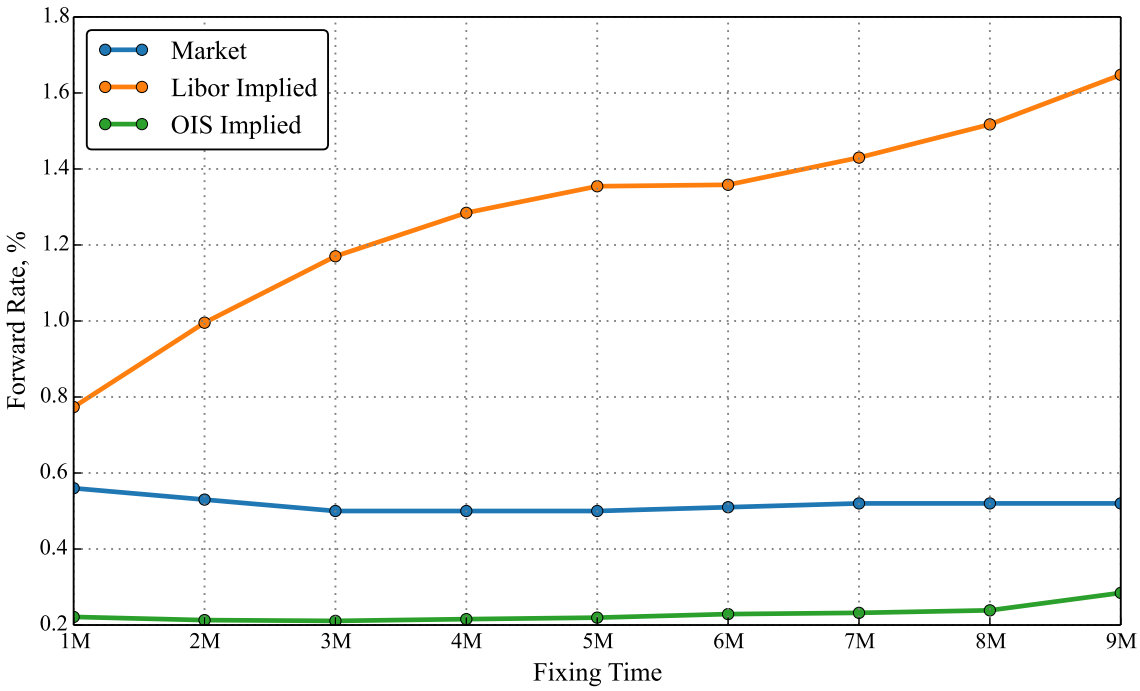

(b) Data from 2012-06-26.

Figure 3.2: Comparison 3-month LIBOR, OIS and market-traded forwards with forward-starting times from 1-month till 9-months. Data was taken from Reuters Eikon from different dates. The figures show that term-structure of market-traded FRAs changes in time: it was closer to the LIBOR-implied ones in mid-2008, but already by mid-2012 the market FRAs were more aligned to OIS-implied forward rate levels.

3.3 LIBOR Panel Model for FRA Pricing

The main problem that is in question when using the LIBOR panel model is how to bridge the gap between the market-traded FRA rates and the rates obtained via standard LIBOR replication (2.16). We start this section by demonstrating the main replication results of the LIBOR panel model for a 6 to 12-month FRA contract. We are using EUR interest rate data, and as a proxy for the credit-liquidity spread volatility we use i-Traxx CDS index 6-month options volatility and obtain equivalent results to (Morini, 2009). Then we extend the analysis to multiple FRA contracts, as well as multiple tenors, investigating both 3-month and 6-month tenor FRAs. Ideally, we would like to see a similar performance of their replication quality over time as both contracts are close to each other by construction. We also apply the model beyond EUR market to USD and GBP forward-rate markets and compare the model fits for all three currencies as well as look into the overlapping periods of large fitting errors.

Moreover, we demonstrate an alternative approach to obtaining the volatility parameter for the credit-liquidity spreads of LIBOR-panel banks. Our approach removes the need for external volatility proxy, which is hard to get and can still be unreliable. We propose the use of FRA-implied volatility, which can be obtained by solving the equation (2.58) for σ, as we have the spot-LIBOR curve available for current prime bank and a set of data for market-traded FRAs. The latter concept is widely used in derivatives pricing, e.g. when the 'implied' volatility for a stock price is obtained from the traded European option price. This implied volatility shows the market expectations of the volatility of the underlying until the maturity of the option.

The obtained implied-volatility gives almost perfect data fits when fitting the model to a single-contract and low-error fits when fitting full series of FRA contracts (e.g. 3-month FRAs starting in $\{1, 2, 3, ..., 9\}$-months. We analyse resulting model errors and show that, while this basic model has the potential to explain the standard replication gap, it is not flexible enough to minimise all the replication errors, especially during the peak of the credit crisis. In section 3.3.5 we conclude with discussion of the results and the motivation for our model extension in the following section 3.5.

3.3.1 Basic Replication and Analysis

In this section, we compare the historical FRA rates for multiple traded FRA contracts with classical standard replication formula (3.3.1) as well as panel model (2.58) to replicate the historical FRA rates.

In figure 3.3 we show the performance of historical FRA (6x12-month contract) replication with the two models. Simple visual analysis of the figure indicates that the use of standard replication leads to large, up to 200 bp pricing errors throughout the historical period. The resulting FRA values from the panel model are much closer to the market 6×12 FRA rates, with maximal errors not exceeding 50 bp.

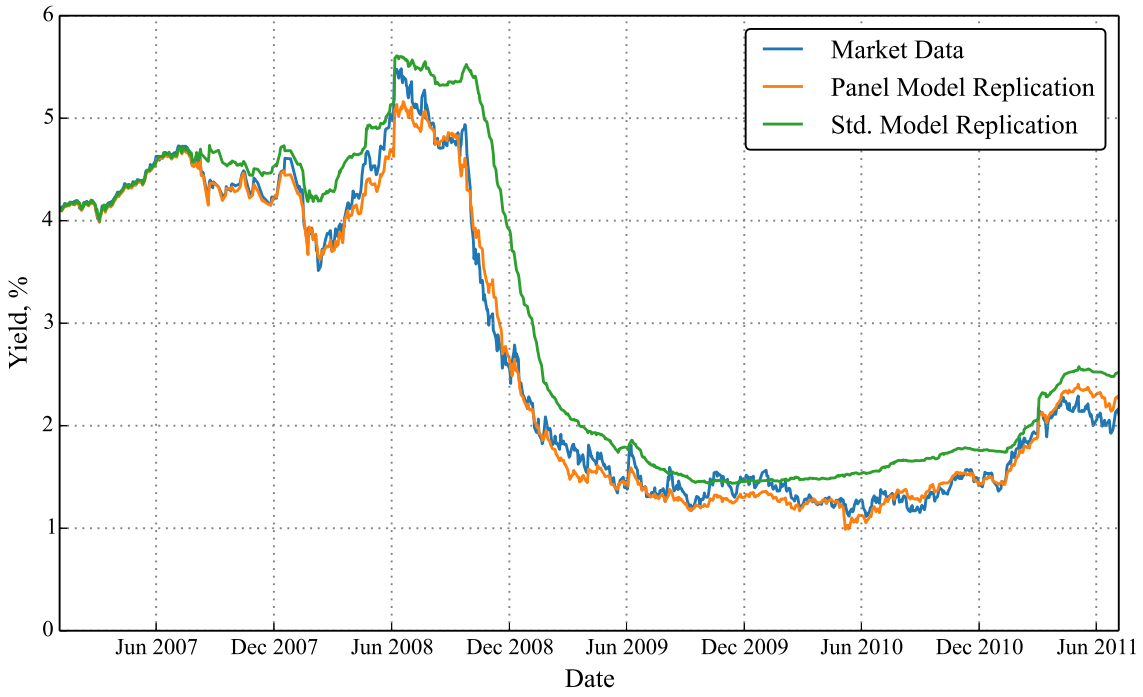

Figure 3.3: Historical replication of 6×12 FRA rate. The figure shows comparison of market-traded FRA rates and forward rates implied by the standard replication model and the panel model. The result is trimmed to June-2011 due to limitations of our iTraxx implied volatility dataset.

To obtain an aggregated look at the replication errors over all the contracts at our disposal we fitted the model to series of FRA prices, with different volatility σ_i parameters and computed model-introduced replication errors:

$$\mathrm{E}_{\sigma_i}(t_i, S_j, \tau) = F_M(t_i, S_j, \tau) - F_{\sigma_i}(t_i, S_i, \tau, \sigma_i), \tag{3.1}$$

for every day t_i, for all maturities $S_j \in \{1, 2, 3, ...9M\}$ and both tenors of interest $\tau \in \{3M, 6M\}$. Then, we took the mean, minimum and maximum errors for all maturities S_j on each day t_i. This way we visualise the 'worst-replicated' contracts from all the FRAs we had data for.

In figure 3.4a we show the average, minimum and maximum of the errors of classic standard replication model for series of 6-month FRA contracts. The error, when using the standard model nearly reaches 200 basis points (2%), as it happened during the peak of the 2007-2009 financial crisis. In the periods before the peak of the credit crisis and after it the replication error stays within 50 bp error margin. Additionally, in figure 3.4b we show the errors of standard replication for series of 3-month FRA contracts, here the error spikes slightly above 200 bp and stays higher during the leftover periods 50 to 100 bp.

The panel model, using the iTraxx volatility, is performing better than the standard replications as shown in Figures 3.5a and 3.5b. The average error of the panel model stays within 20-30 basis points when replicating all the FRA contracts, and reaches 60 basis points during the peak of the crisis. This holds for both, 3-month and 6-month FRA contracts.

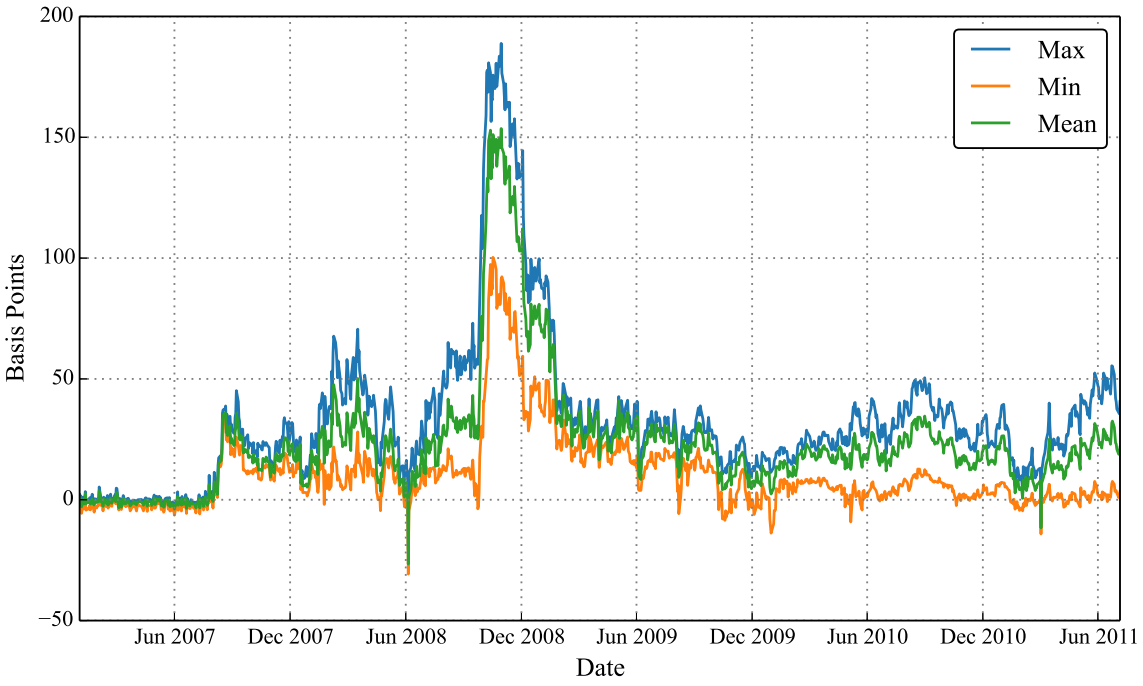

(a) Min, mean, max replication errors for 6-month EUR FRAs.

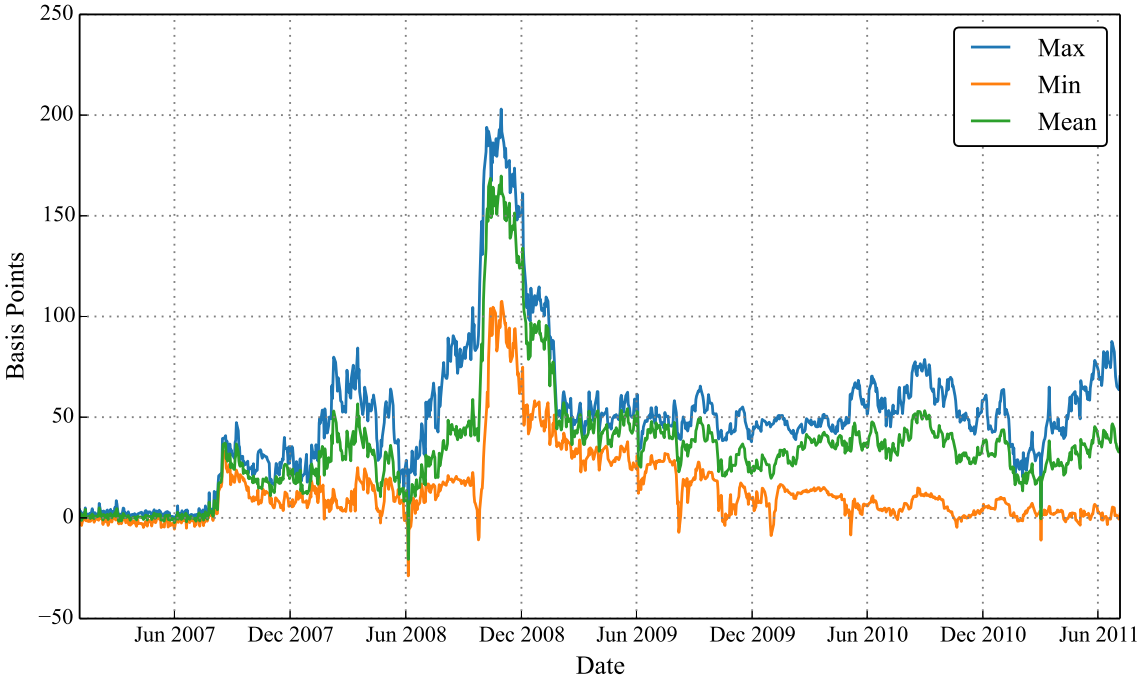

(b) Min, mean, max replication errors for 3-month EUR FRAs.

Figure 3.4: Historical min, mean, max replication errors for EUR FRAs. The figures show the replication error ranges for groups of, respectively, nine 3-month and six 6-month FRAs when using the standard replication model.

(a) 6-month FRA replication error with panel model using iTraxx implied volatility.

(b) 3-month FRA replication error with panel model using iTraxx implied volatility.

Figure 3.5: Historical min, mean, max replication errors for EUR FRAs. The figures show the replication error ranges for groups of, respectively, nine 3-month and six 6-month FRAs when using the panel model.

3.3.2 Extension to Multiple Currencies

An important part of our experiment is to extend the use of this model from EUR to other currencies, such as the US Dollar and the Great Britain Pound. In the following, we provide the results and a short discussion of using the panel model with the Euro iTraxx implied volatility.

At the time of writing, there were no liquid CDS options traded in USD and GBP markets, like the Euro iTraxx ATM Options. We argue, that because the LIBOR-panel banks in EUR, USD and GBP panels are overlapping (Intercontinental Exchange, 2014) and all three markets are highly inter-connected (Bhar and Nikolova, 2013) the credit-liquidity volatility behaviour should be similar across all three markets. Therefore, to investigate the potential of the panel model in USD and GBP FRA rates - we fitted the model to their respective spot LIBOR curves and used the Euro iTraxx volatility index for the σ parameter. In Figures (3.6a, 3.6b) we show the replication errors for 3-month FRAs in USD and GBP currencies. Our results show that:

1. Replication errors for USD FRAs stay mostly within ± 40 bp range but reach 60 bp during the peak of the crisis at the end of 2008 and the first half of 2009.
2. Replication errors for GBP stay most of the time within ± 50 bp range but spike to over 120 bp at the end of 2008. Additionally, we can observe a trend of increasing error in the second half of our data sample, which shows that out EUR iTraxx proxy for volatility is insufficient to jointly replicate the series of GBP FRAs.

Overall, the FRA replication using the panel mode and iTraxx options-implied volatility is a major improvement when compared with the standard replication approach. The panel model, as expected, works best for EUR market.

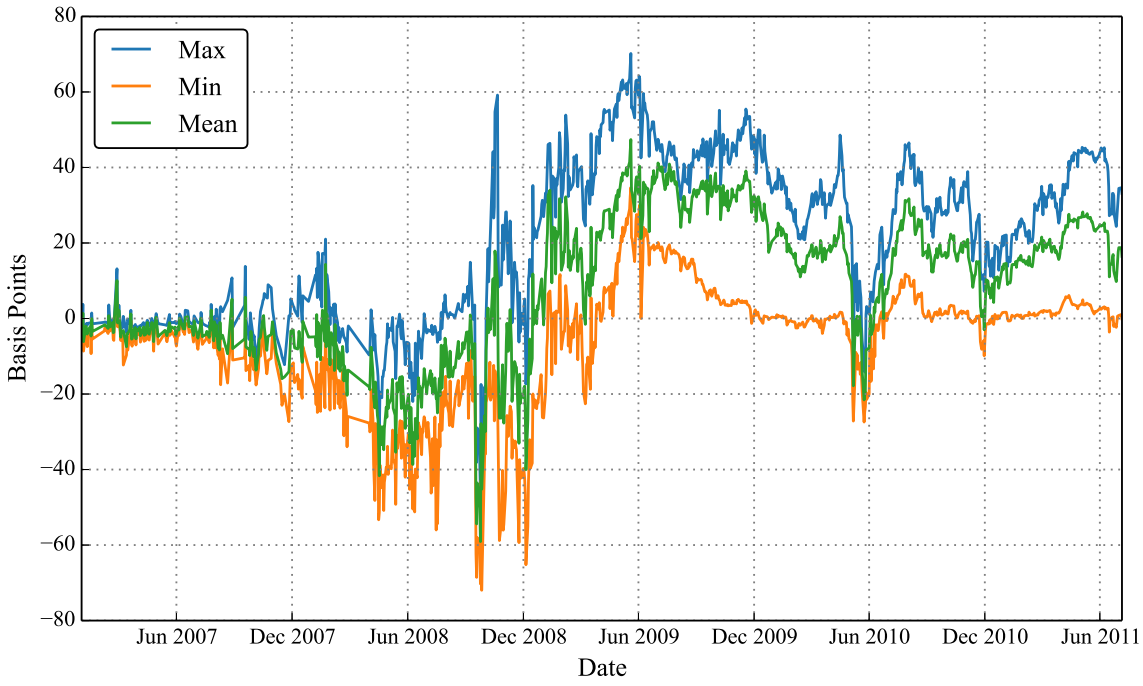

(a) 3-month USD FRAs replication with LIBOR panel model errors.

(b) 3-month GBP FRAs replication with LIBOR panel model errors.

Figure 3.6: Historical min, mean, max replication errors for USD and GBP FRAs. The figures show the replication error ranges for group of nine 3-month USD and GBP FRAs when using the panel model.

3.3.3 FRA-Implied Volatility

The LIBOR panel model for FRA replication requires an input for the volatility σ as given in equation (2.58). This parameter should reflect the volatility of the CDS spread of the 'prime' bank in the LIBOR panel. No derivative instrument is available that could provide such information directly, but we can use a close proxy, such as the iTraxx index ATM 6-month implied option volatility values, which were also used by Morini and Brigo (2008). This underlying iTraxx index shows the CDS levels of the biggest and most liquid European stocks. While the option volatility on this index is not what is truly needed for this model - this is the most liquid and reliable proxy. In general, finding CDS-index option implied volatilities is a hard task, as these are not very liquid. Additionally, the CDS indices that we are traded do not completely reflect the LIBOR-panel composition (Morini and Brigo, 2008).

Hence, we took an alternative view by reversing the problem: instead of replicating the FRA levels with given volatility, we calculated the "FRA-implied" volatility which gives the match between historical FRA levels and the LIBOR panel model. The implied volatility over multiple contracts should reflect the true volatility of the credit-liquidity premiums in the LIBOR-panel. In the following Figure 3.7) show the FRA-implied volatility from Euro 3-month FRA data. The time-series values were obtained by solving

$$\sigma_{i,j}^{IV} = \min_{\sigma}(E(t_i, S_j, \tau, \sigma))^2 \tag{3.2}$$

$$E(t_i, S_j, \tau, \sigma_i^j) = F_M(t_i, S_j, \tau) - F_P(t_i, S_j, \tau, \sigma_i^j) \tag{3.3}$$

using a numerical solver (Brent, 1971), where i is the date (in the time series), t_i is the valuation date and S_j are the maturities. The σ_i^j is the panel model volatility for t_i date and S_j maturity and the LIBOR panel model for FRA price $F_P(\cdot)$ is given in (2.58).

We have plotted the resulting historical implied-volatilities, per-contract, in Figure 3.7. The implied volatilities were not relevant before September 2007, as the basis spreads were close to zero and the resulting volatilities as shown in Figure 3.7 are full of fitting noise. Nevertheless, since September 2007, the implied volatilities do move in a synchronised fashion, which shows a strong relation to the different contracts. This observation confirms our intuition as these contracts, even if they have different maturities, they do rely on the

same tenor LIBOR rates, and, inherently, carry the same embedded credit-liquidity risk.

What is more, the implied volatilities from the set of contracts follow a clear structure: the FRA contracts with longer maturities, such as $6 \times 9M, 7 \times 10M, 8 \times 11M$ have lower volatilities than the short-end ones. This effect is often observed in the market traded caps and floors - their forward volatility often decreases with maturity (Brigo and Mercurio, 2006). Finally, the distance between individual volatilities is not constant, which can be a sign of a badly-specified model (e.g. insufficient degrees of freedom).

The Figure 3.7 also shows some of the volatility extremes fitted by the model. The implied-volatility gets negative when the resolved option value in the model is negative, or FRA rate is less than the standard replication. This may happen due to illiquid FRA quotes or simply because in our dataset we use mid-prices for the FRAs, but the difference between the FRA rate and standard replication price was within the Bid-Ask spread. Moreover, when the implied-volatility of the LIBOR-OIS spread is above 100%, it means that the value of embedded option in the FRA contract is much larger than the LIBOR-OIS spread itself.

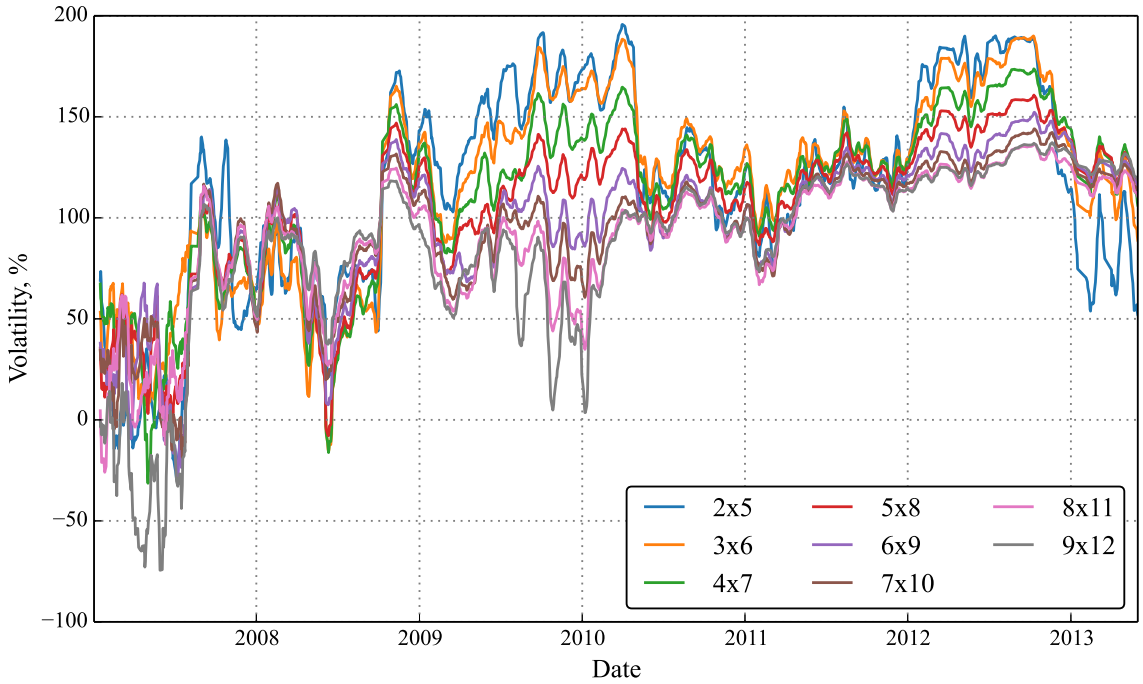

Figure 3.7: Historical FRA implied-volatility (IV) for EUR 3-month FRA contracts. We compare the historical implied Panel-model volatility for every 3-month FRA contract we analysed. The per-contract IV follow each other with distinct periods of high and low dispersion. The volatilities follow a term-structure, where with increasing starting time, the FRA-IV decreases. This result is often found in other interest rate derivatives, like caps.

3.3.4 Global Implied Volatility

As we have shown in the previous section, different FRA contracts, even if they are indexed to the same LIBOR tenor, yield different implied volatilities in the panel model. To clarify the results of the previous section we set up the following experiment. We want to test the limits of the LIBOR panel model, as is, and to see if we can produce a single implied-volatility, fitted across full series of FRAs, which allows us to price any FRA within the bid-ask spread.

We note that the historical bid-ask spreads for 6-month FRAs were usually 4-5 bp in some cases 8-10 bp with some recorded jumps to 20, while the market FRA levels were between 100 and 600bp. The 3-month FRAs were usually traded within 3-5 bp spread, in some cases 8 bp.

In the following analyse the replication quality of FRAs when applying global calibration. In both cases (3-month and 6-month) we calibrated a the daily optimal volatility level for full series of respective contracts

$$E(t_i, S_j, \tau, \sigma) = F_M(t_i, S_j, \tau) - F_P(t_i, S_j, \tau, \sigma), \tag{3.4}$$

$$\sigma_i^{GL} = \min_{\sigma_i} \sum_{j=0}^{M} (E(t_i, S_j, \tau, \sigma_i))^2, \tag{3.5}$$

and measured the maximum, mean and minimal errors in replication quality across all contracts

In figure 3.8a we show that using globally-fitted implied volatility, we can replicate the 3-month FRAs with errors bounded by 20 bp in most cases, with some spikes up to 40 bp. The 6-month FRAs, as shown in figure 3.8b are better replicated when using the global-IV, here the replication error is as low as 10 bp in most cases, but peaks are still at $\pm$ 40 bp.

(a) Historical replication errors of 3-month FRA with globally fitted 3-month IV

(b) Historical replication errors of 6-month FRA with globally fitted 6-month IV

Figure 3.8: Max, min, mean errors in historical replication of the 3-month and 6-month FRA groups, when the panel model volatilities were globally fitted to, respectively, 3-month FRA and 6-month FRAs. The result is a strong improvement over errors of standard replication model in both cases, but we still have two distinct periods where the error in panel model is above 20 basis points.

We performed the global volatility calibration on both, series of 3-month FRAs and 6-month FRAs. This allows us to compare the implied volatility data tenor-by-tenor. As shown in Figure 3.9, before mid-2007 the implied volatilities are full of noise as the basis spreads are close to zero. Later, from 2007 till 2009 the 3-month and 6-month volatility levels closely follow each other and at the end of the period bifurcate into two distinct, but correlated levels. The Figure 3.9 shows several significant events: when the market realised about the hidden risks of LIBOR trading the standard replication broke down and the panel model implied volatilities spiked up to 200% in September 2007, but the forwards of the 3-month and 6-month tenors were traded nearly identically, carrying similar quantities of volatility. Later, around the end of 2008, the market bifurcated and started trading the two tenor FRAs as different products, most likely differentiating by the liquidity differences in 3-month and 6-month loans. A similar observation was also made by Crépey and Douady (2013), where they concluded that in this model for the LIBOR-OIS spreads, each tenor carries different liquidity components to account for the difference between the LIBOR forward and OIS curves.

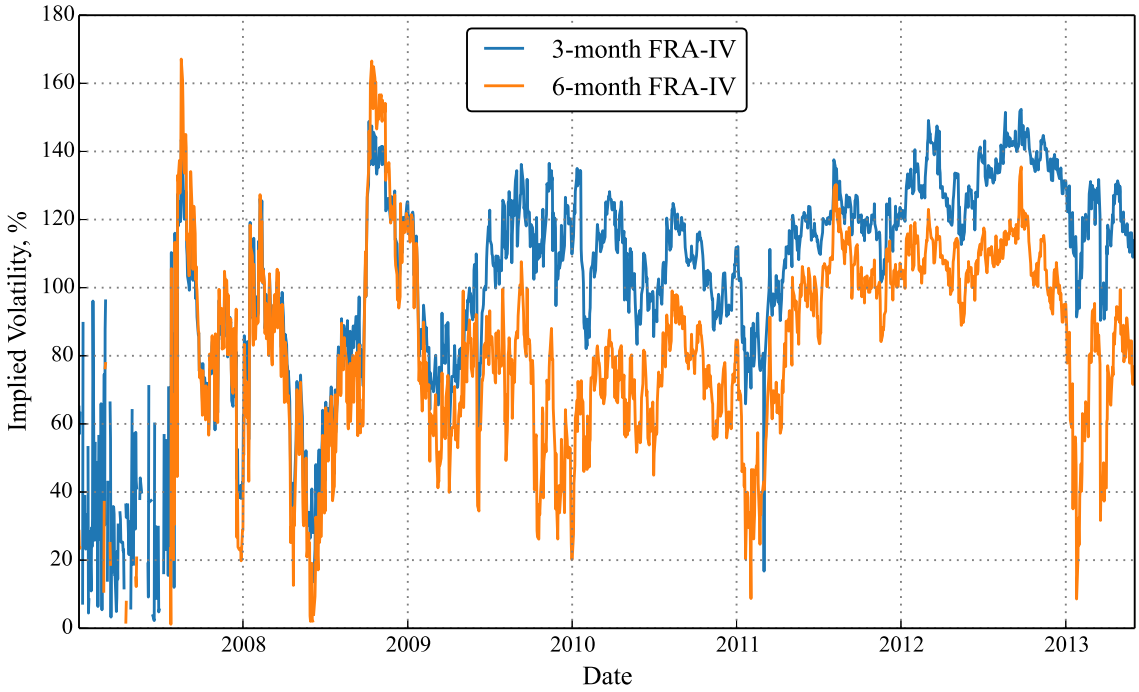

Figure 3.9: Historical EUR FRA-implied volatility for 3-months and 6-month fixings. The global implied volatilities for both 3-month and 6-month FRA groups closely followed each other until Q2 2009 and then bifurcated into two distinct but highly correlated levels.

3.3.5 Discussion

The panel model offers a large improvement for FRA replication over the standard replication model, but it is not perfect. First of all, the lack of LIBOR-panel credit-liquidity volatility proxy is an issue, but not impossible to overcome. It is a wide market practice to imply option volatilities from traded contract prices, which is performed in equities, interest rates, foreign-exchange and the credit market. Therefore, we can use market traded FRA quotes to imply the missing volatilities. The resulting implied volatilities yield a volatility term structure, similar to cases in interest rate caplets (Brigo and Mercurio, 2006), where the volatility decreases with increasing maturity of the option.

Afterwards, we have tested the replication limits of this model, by jointly fitting full series of single-tenor FRAs. In theory, if the model is well specified, a single volatility estimate should yield a good market fit of all involved FRA contracts. We found that this is not always the case and errors often reach 20 and 40 basis points in the historical period that we analysed.

Therefore, in the following section, we shall look into potential ways of modifying the panel model, to allow for a few extra degrees of freedom and decrease the joint-replication error. Ideally, we want to the error to stay below the bid-ask spread level over 95% of the time in the historical series.

Method	Average Error	Maximum Error
Standard Replication	50 bp	up to 200 bp
Panel Model with iTraxx IV	25 bp	up to 60-80 bp
Panel Model with globally-fitted IV	10-20 bp	up to 40 bp

Table 3.1: Table summarizing FRA replication errors from different models. The standard replication model does not perform well since mid-2007 and introduces and average error of 50 bp (up to 200bp) in replication. The panel model greatly improves upon the standard model and with iTraxx implied-volatility input reduces the replication error and performs even better when using globally-fitted FRA-IV. Nevertheless, the errors are still above 5 basis points, which is a common bid-ask spread level for FRAs in the market.

3.4 Empirical Assessment of Model Assumptions

So far we have shown that the LIBOR panel model is a major improvement over the standard replication and has the potential for joint modelling of all FRAs in our FRA-implied volatility framework. Nevertheless, the residual error in standard panel model specification

is non-negligible. In this section, we demonstrate our attempts to find the source of the error coming from the LIBOR panel model. We have looked into three possible issues:

1. First, we looked if the market FRA bid-ask spreads correspond to same periods of large model errors, indicating that FRA liquidity issue causes the bad fits in the model.
2. Second, we looked if the periods with large replication errors correspond to large dispersion of individual FRA implied volatilities as in Figure (3.7). This would indicate a missing maturity-dependent skew in the volatilities.
3. Last, as the panel model assumes the normal distribution for the credit spread (2.58), we checked if the underlying assumption is valid. To do this we compared the historical forward LIBOR - OIS spread dynamics with GBM 2.16 model dynamics.

3.4.1 Liquidity

To investigate if our errors in the model were affected by the lack of liquidity in the market during the credit crisis we have compared the errors from:

1. Standard replication model for FRA
2. Panel model with iTraxx implied volatility
3. Panel model with globally calibrated implied volatility.

We measured and plotted the error resulting from the replication of EUR 6x12M FRA in all three cases as together with the 6x12M FRA bid-ask spreads, one of a few available proxies of trading liquidity, to see if low trading liquidity correlated with large model errors.

Figure 3.10 shows that the errors in the three cases have strongly overlapping periods of large replication errors, but the actual bid-ask spread of the FRA remains small, mostly within 5-10 bp. Additionally, the correlation between bid-ask spreads and errors is small, as the spreads stay mostly constant and both, increase and decrease in spread levels happen whenever the replication errors are large. Therefore, using bid-ask spread as a liquidity proxy does not help explain any of the errors as after 2007.

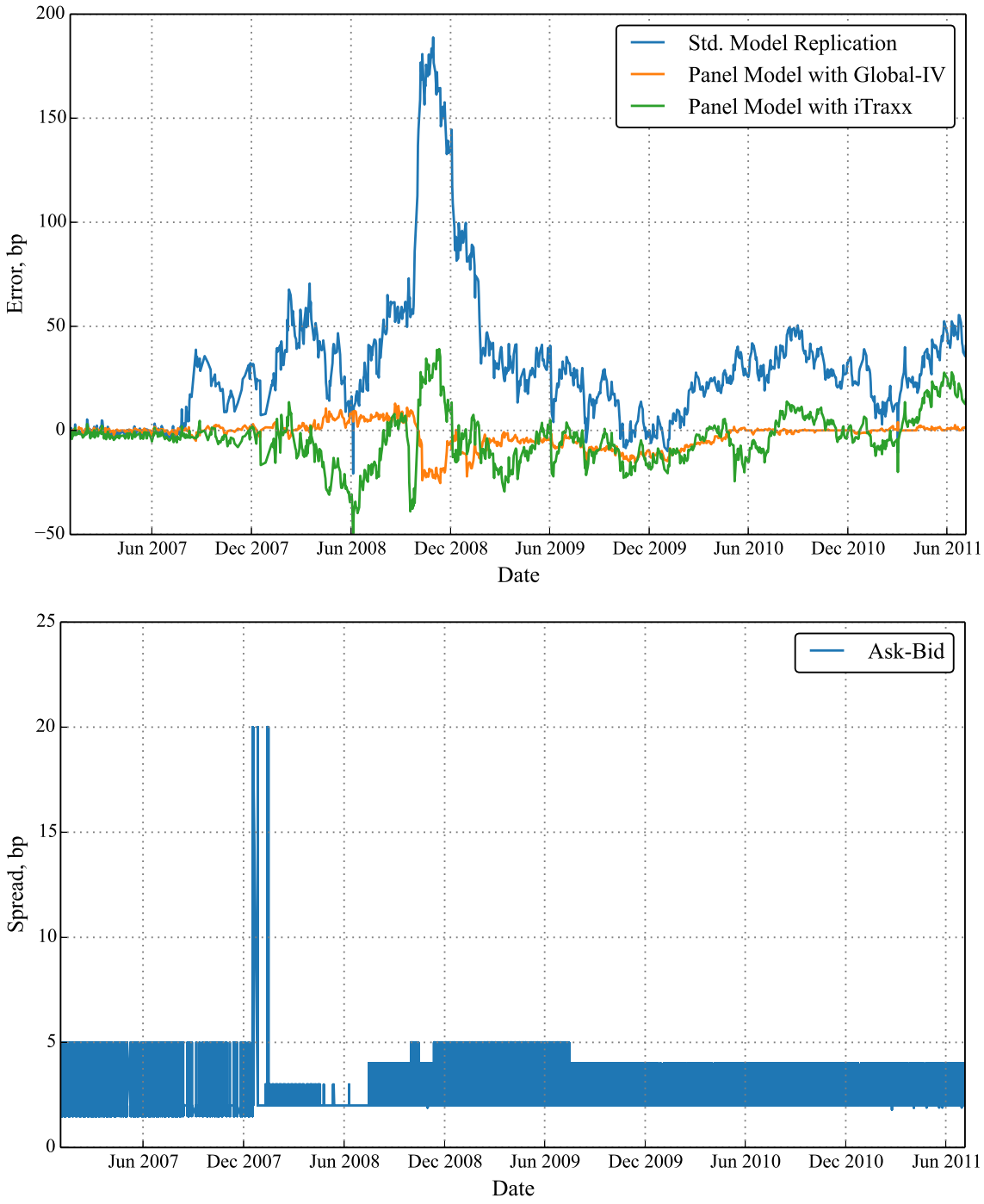

Figure 3.10: Historical error of 3 FRA replication models for 6x12 EUR FRA. We investigated if there are periods of large model error overlapping with periods with high bid-ask spread. A correlation of the two would indicate impact of FRA liquidity on the replication quality. This effect is not visible as the FRA trading spreads were contained below 5 bp during most of the period with few jumps up to 20 bp.

3.4.2 Degrees of Freedom

Our globally calibrated volatility erroneously reproduces the market FRAs, because the individual implied volatility of each of the FRA differs, as we have shown in Figure 3.7. To see if periods of large dispersion of the implied volatilities affects the overall error of replication, we compare the standard deviation of the IV

$$\Sigma_i = \sqrt{\frac{1}{M}\sum_{j=0}^{M}(\sigma_i^j - \mu)^2} \tag{3.6}$$

$$\mu = \frac{1}{M}\sum_{j=0}^{M}\sigma_i^j \tag{3.7}$$

and the absolute FRA replication errors. We performed the latter test for multiple FRAs and chose to demonstrate 6x12M FRA as an example. As we can see from the figure 3.11, the larger dispersion is followed by a large FRA replication error, but this relationship is far from perfect. For example, high-dispersion in beginning of 2008 overlaps with small replication errors, also large dispersion in end of 2012 corresponds to a period of low-replication error. This test remains inconclusive but does give us a hint that solving the IV-dispersion problem could lead to a better overall fit.

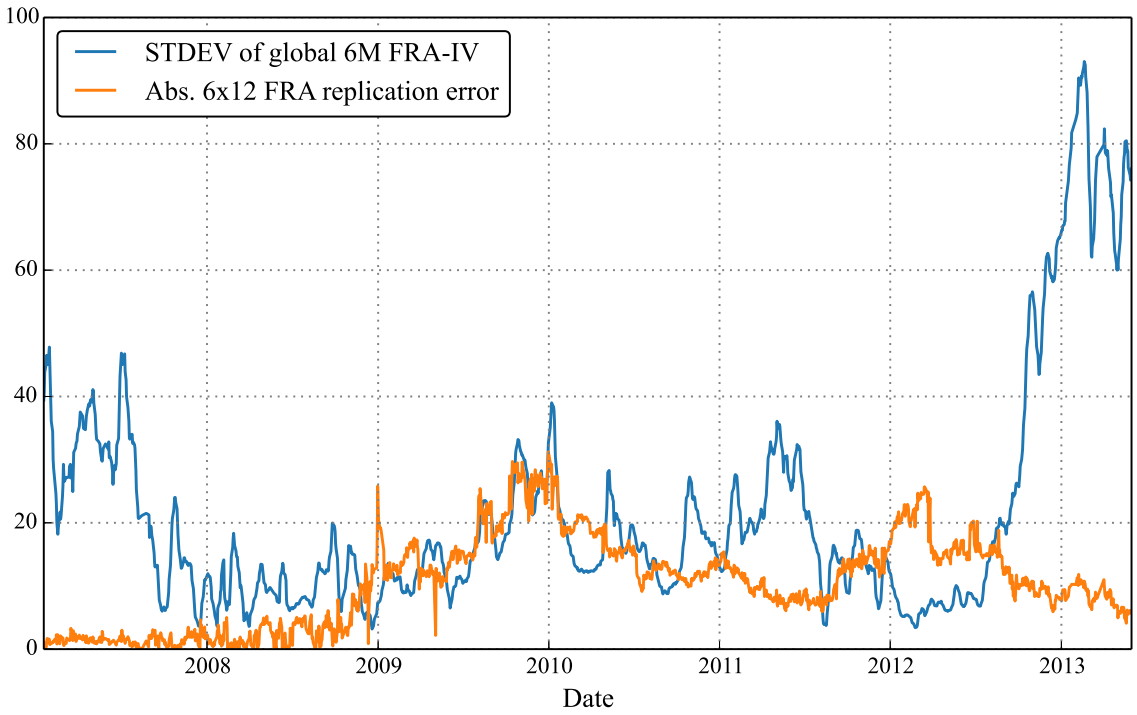

Figure 3.11: Historical error of 6x12M FRA replication using global-IV, compared to the dispersion of the 6-month globally calibrated FRA implied volatilities. The relation between large model error and dispersion of implied volatilities is not perfect, but the long period from mid-2008 up to mid-2012 of large model error and IV-dispersion hint at the main problem in our replication exercise.

3.4.3 Specification of Diffusion Dynamics

One of the major assumptions in the LIBOR panel model is that the LIBOR-OIS spread of the prime bank is log-normally distributed. This assumption is implicitly given, as we model the spread as geometric Brownian motion. To test this assumption we compared the daily log-returns of the forward LIBOR with the forward EONIA spread obtained using the historical spot rates. By the GBM model the spread S should satisfy:

$$\ln \frac{S(t_i)}{S(t_{i-1})} = \sigma \cdot dW(t_i), dW(t_i)\, \mathcal{N}(0, t_i) \tag{3.8}$$

therefore by taking the log returns of the spread series, we obtain the empirical distribution of dW. Our goal is to check if it is a normal distribution.

In the figure 3.12 we have plotted the histogram of historical spread return and fitted (normal, log-normal, Student-T) distributions to the data. Then, we performed Kolmogorov-Smirnoff test (Massey, 1951) with null-hypothesis that our sample belongs

to one of these distributions. The test strongly rejected ($p <<< 1\%$) the hypothesis that sample comes from normal or log-normal distributions. Student-T distribution was confirmed to give a more appropriate fit with $p = 80\%$.

The Student-T distribution is rather inconvenient to use in option pricing (Cassidy et al., 2010), due to the infinite variance properties of the Student-T distribution. An alternative route, taken in quantitative finance (Brigo and Mercurio, 2002), is to use a pair of normally-distributed random variables as the drivers for the LIBOR-OIS log-returns.

In the figure 3.12 we show that we can obtain a good fit of the historical histogram by using a mixture of two normals. When compared to the normal distribution, the mixture captures the peak and heavy tails better.

The appropriate AIC (Bozdogan, 1987) criteria results are: -3849 for normal distribution, -4569 for a mixture of two Gaussians, -4565 for a mixture of three Gaussians and -4922 for Student-T distribution. Therefore, using a mixture of two Gaussians instead of a single normal distribution yields a vast improvement in the historical log-returns fit. On the other hand, using three Gaussians would not yield a significantly better fit of the historical log-returns. In the end, Student-T gives the best fit, but we exclude this model from our analysis due to analytical tractability difficulties as mentioned before.

Moreover, as shown in Figure 3.13 the two fitted components are clearly distinct: the first component is low-volatility fitting the central peak and middle sections of the historical distribution. The second component has large volatility and therefore gives a good fit to the far tails of the empirical distribution. We acknowledge that even better fit could be obtained with three or even four components, but their function would be less easy to distinguish. We shall elaborate on the latter in the later chapters.

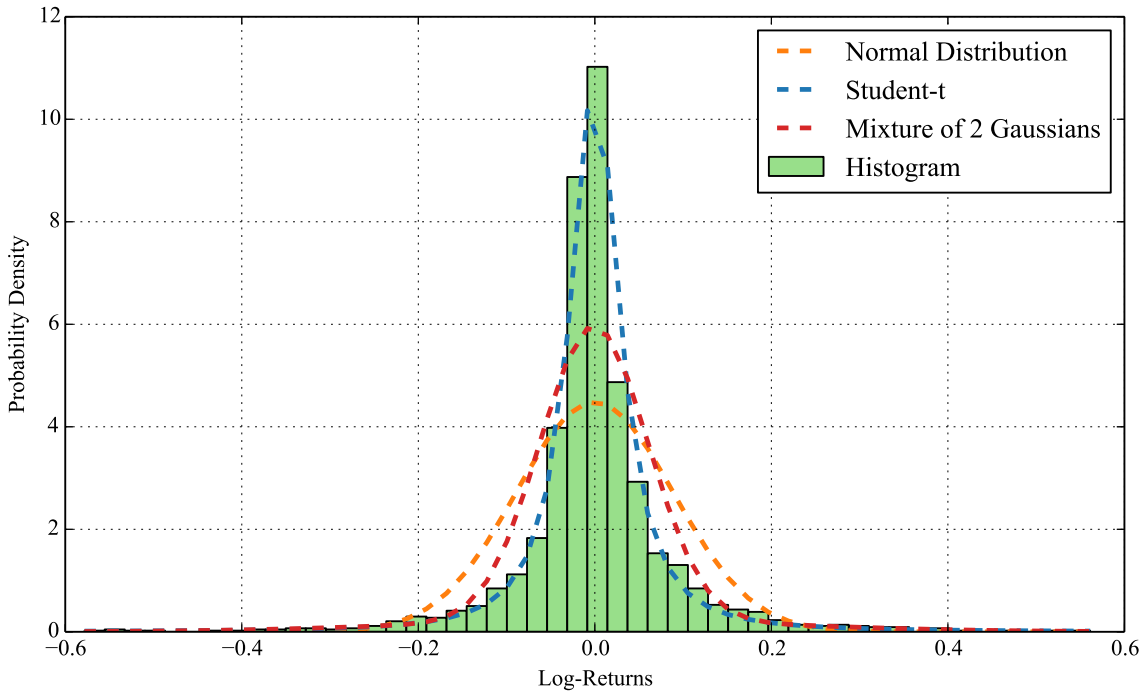

Figure 3.12: Histogram of 3-month EUR LIBOR-OIS spread log-returns and selected probability density fits. The obtained log-returns series does not follow a normal distribution, the best fit is obtained using heavy-tailed Student-T probability density function. A mixture of two Gaussians provides and intermediate fit.

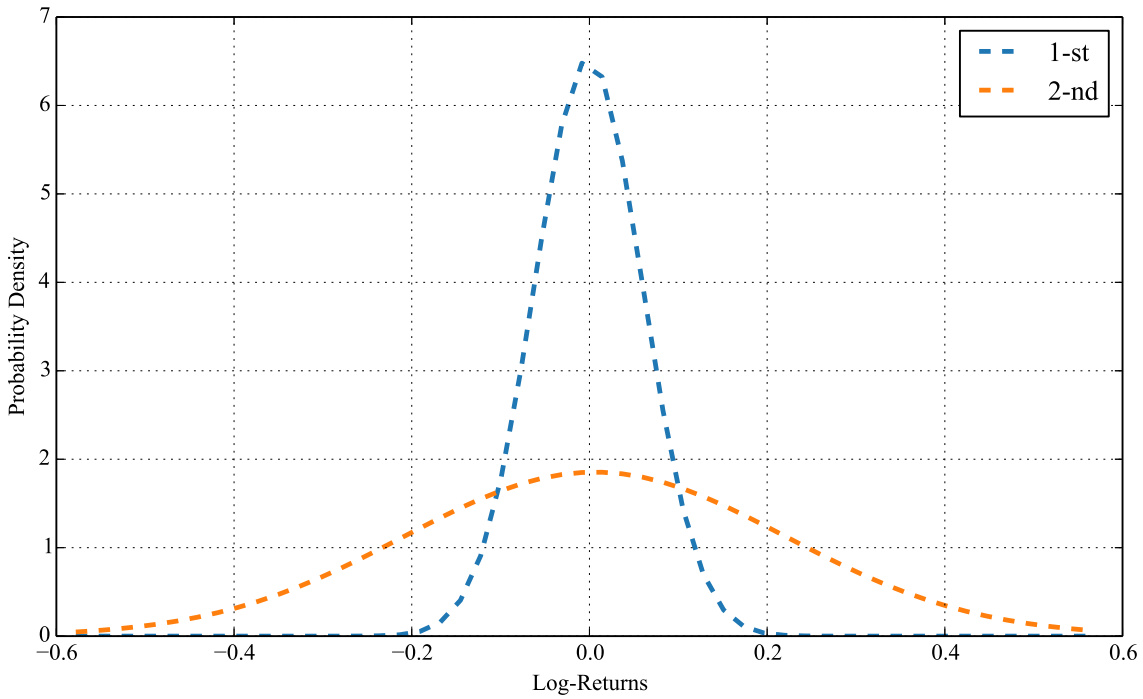

Figure 3.13: Probability density fits for the mixture components of the 3-month EUR LIBOR-OIS spread log-returns. The two components are clearly distinct - one corresponding to the high peak and the second one with the heavy tails of the dataset.

3.4.4 Summary

Our brief empirical model assumption analysis shows that as there was no visible correspondence between the bid-ask spreads and replication errors, the liquidity of data used is not the main cause of replication errors. We have observed that the dispersion of implied volatilities does correspond to dates with increased error of replication. Hence, the panel model is too constrained and needs a few more degrees of freedom to be able to fit multiple FRA contracts simultaneously. On the other hand, we have also shown that the log-normal Brownian motion assumption in the panel model is not correct, as the actual historical dynamics of the LIBOR-OIS spread are much closer to Student-T distribution or a mixture of two Gaussians. We note that pricing options using a Student-T distribution not practical and a similar effect can be achieved with the mixture model.

3.5 Extended LIBOR Panel Model

Using our observations in previous section, we introduce an extension of the panel model using a mixture model. In this model we assume that our credit-liquidity spread is driven by

a single Brownian motion (2.22), but with uncertain volatility. This way we obtain so-called uncertain parameter model (Alexander, 2004):

$$dS(t) = S(t)\sigma_Z dW(t) \tag{3.9}$$

where Z is a discrete random variable, independent of W, taking values in set $\{1, ..., m\}$ with probabilities $\lambda_i > 0$. In this formulation, the log-return distribution of the spread becomes a mixture of m Gaussian components. Additionally, this under this model, the European call option price can be written as a weighted sum of Black-Scholes call options:

$$C_{Mix}(S, K, t, T) = \sum_{i=1}^{N} \lambda_i C_{BS}(S, K, t, T, \sigma_i), \tag{3.10}$$

where $\sum_{i=1}^{N} \lambda_i = 1$ and C_{BS} is driftless Black call option defined in (2.17). Computing the FRA value under the extended LIBOR panel model is as simple as:

$$F_P(t_i, T, S) = \mathbb{E}^{rf}[L(T, S)] = F_{\text{Std}}(t_i; T, S) - 2\sum_{i=1}^{N} \lambda_i C_{BS}(S, K, t_i, T, \sigma_i). \tag{3.11}$$

The uncertain parameter extension is the simplest model choice which preserves analytic tractability and also adds additional degrees of freedom in the model. We propose to use a two-volatility mixture model, where we have volatilities σ_1, σ_2's and weight parameter λ_1, the remaining $\lambda_2 = 1 - \lambda_1$. This choice adds two additional degrees of freedom that can be used to fit FRA data instead of a single σ as in the original model. We have looked at other alternatives, e.g. using two correlated Brownian motions or a local-volatility model like the Stochastic-Alpha-Beta-Rho (SABR (West, 2005)), but these options are over-parametrised and may unnecessarily complicate calibration procedures and our ability to interpret the results as we shall show in the following sections.

3.5.1 Model Fit in EUR Market

In this section, we show the performance of the mixture model for the problem of FRA replication. We will show the remaining errors for replicating series of FRAs as well as compare the model with its predecessor, namely the normal LIBOR panel model. To demonstrate the results we fit the mixture model to series of 3-month and 6-month EUR FRA contracts for every trading day in our dataset. Then, we show the mean,min and

max errors of the replication exercise and also compare the performance of normal (single-driver) and mixture (two-component) models by assessing theirs total replication errors:

$$\mathrm{E}_{\text{Normal}}(\tau, t_i) = \sum_{j=0}^{M} |F_M(t_i, S_j, \tau) - F_{\text{Normal}}(t_i, S_j, \tau, \sigma_i)|, \tag{3.12}$$

$$\mathrm{E}_{\text{Mix}}(\tau, t_i) = \sum_{j=0}^{M} |F_M(t_i, S_j, \tau) - F_{\text{Mix}}(t_i, S_j, \tau, \sigma_i^1, \sigma_i^2, \lambda_i)|. \tag{3.13}$$

which helps to simplify the picture when comparing the performance of the two models.

Below, Figure 3.14 shows that in the mixture model the absolute maximal errors, per contract, shrank to less than 10 basis points in most cases and even go under the 5 bp limit. In turn, this makes the mixture model useful in FRA trading or risk-management, as we can jointly price series of FRAs with error close to the bid-ask spreads.

Moreover, Figure 3.15a shows that the mixture model outperforms the normal model by up to an order of magnitude. This effect is sustained throughout 3 and 6-month tenors as shown in Figure 3.15b. The mixture model outperforms the normal model in periods of excessive stress when the normal model fails to correctly replicate FRA rates, e.g. between September-2008 and June 2010, and January 2012 to Jan 2013. During other periods, when the normal model performs well, the mixture model offers modest improvement.

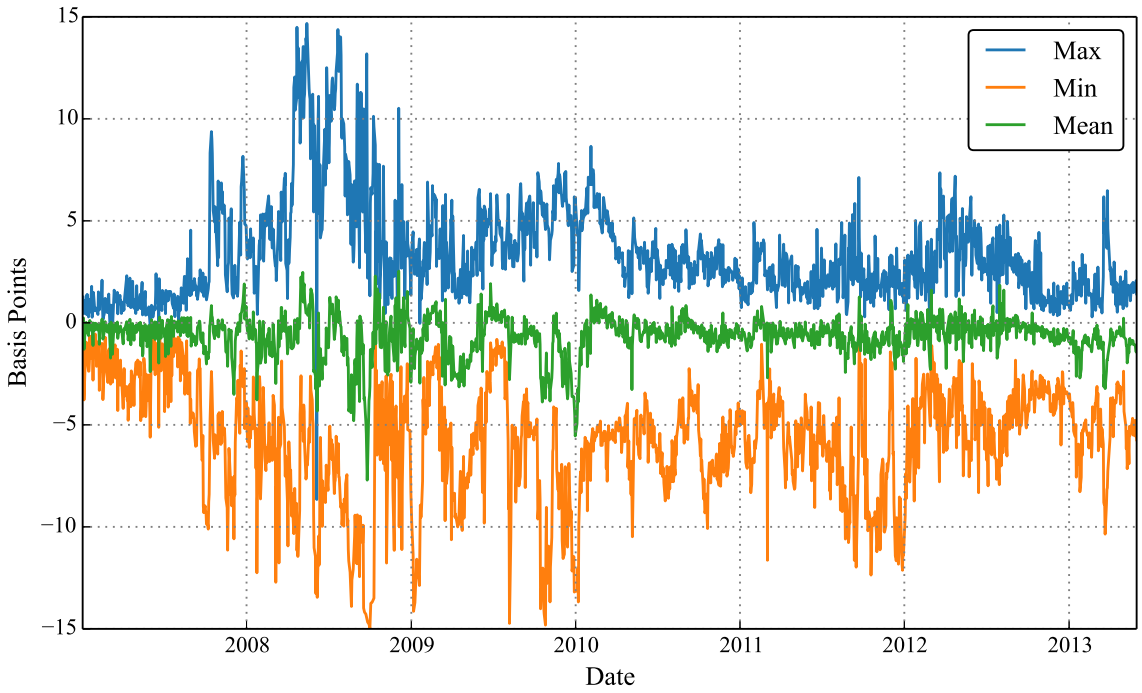

(a) Historical replication errors of 3-month FRAs with the Extended Panel Model

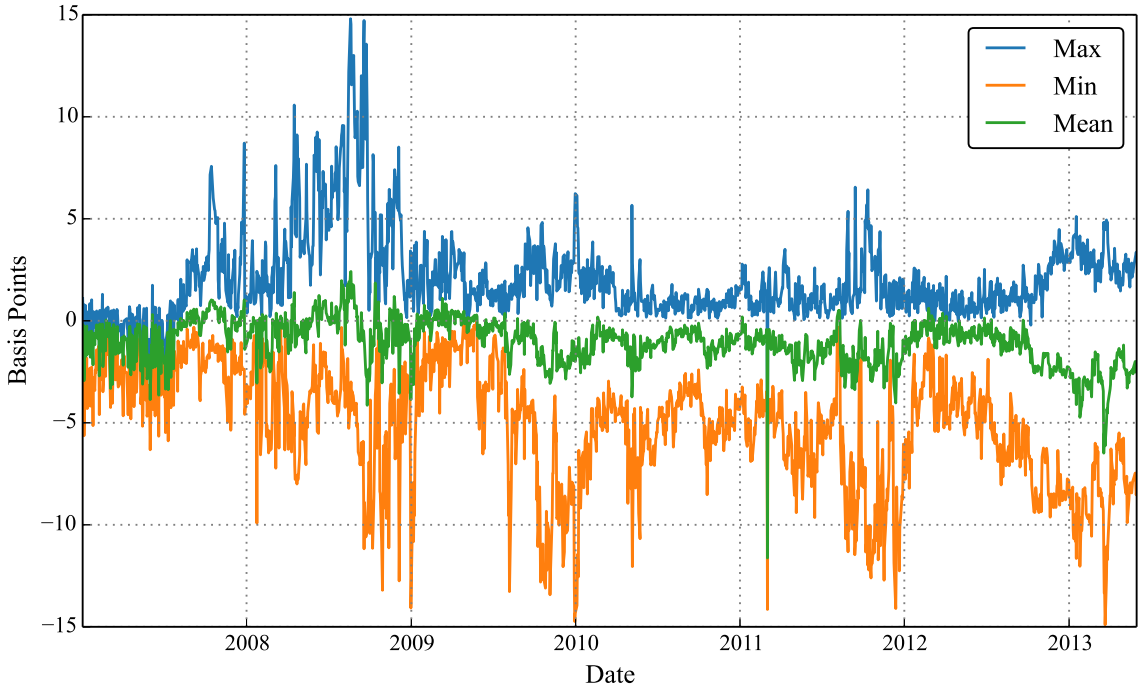

(b) Historical replication errors of 6-month FRAs with the extended panel model

Figure 3.14: Max, min, mean errors in historical replication of the 3-month and 6-month FRA groups using the globally-fitted extended panel model. The figures show that by using the extended model we can replicate series of FRAs within 5 basis points error margin in 95% of cases in the historical dataset.

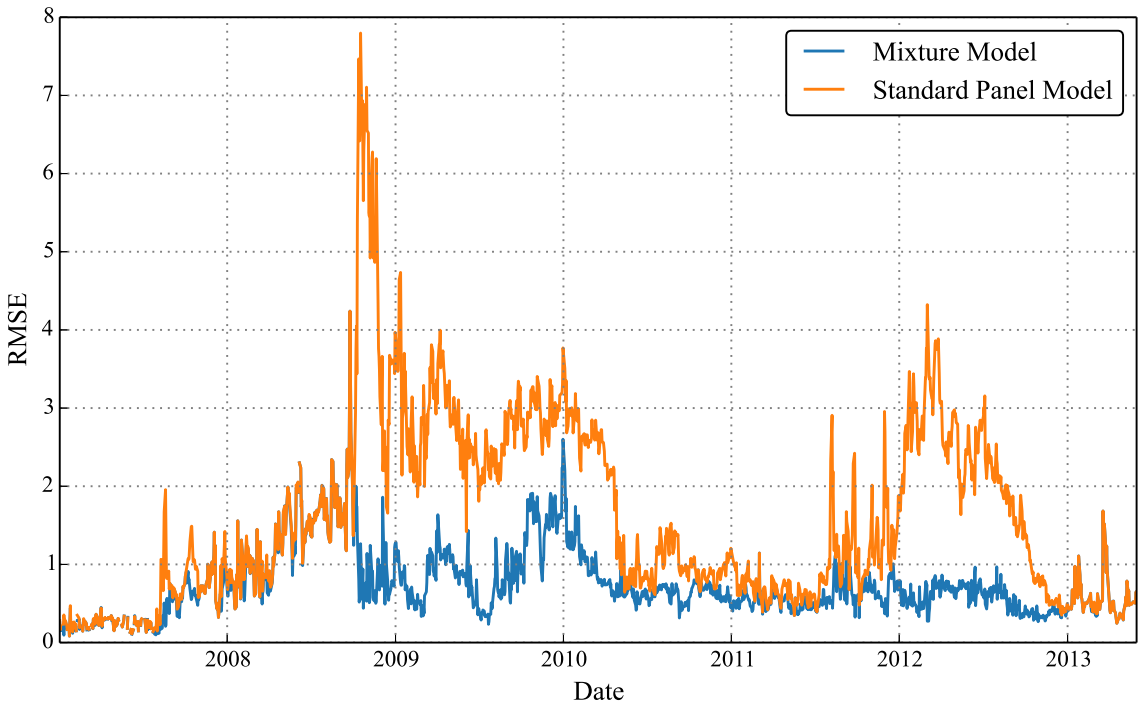

(a) 3-month EUR FRAs. Mixture model vs normal model error comparison.

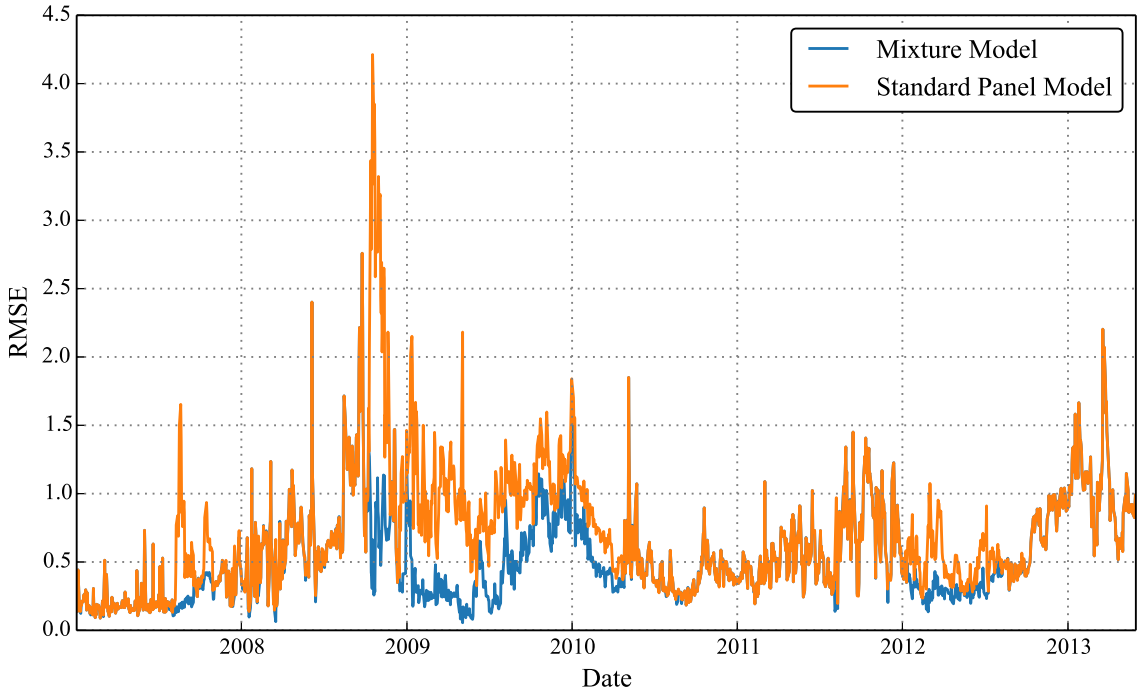

(b) 6-month EUR FRAs. Mixture model vs normal model error comparison.

Figure 3.15: Comparison of total absolute errors for replicating groups of 3-month and 6-month FRAs between the panel model and the extended panel model. The extended model improves the replication error by and order of magnitude and works especially well in periods of high market volatility.

3.5.2 Mixture Model in USD and GBP Markets

We have extended our analysis and model comparison to USD and GBP markets. The order-of-magnitude out-performance of the mixture model is sustained in these markets as well. As shown in Figures 3.16, 3.18, the mixture model performs well in peak times of crisis, when the normal model encounters large replication errors. The remaining FRA errors are contained in a tighter region than EUR FRAs as before, mostly within 5-10 bp range. We do have singular spikes in error, resulting from separate FRA quotes, which may have been mispriced in an increasingly low-liquidity market, but as the official bid-ask spreads were still within 5 bp it is hard to prove that there was a clear issue of liquidity for the FRA quotes.

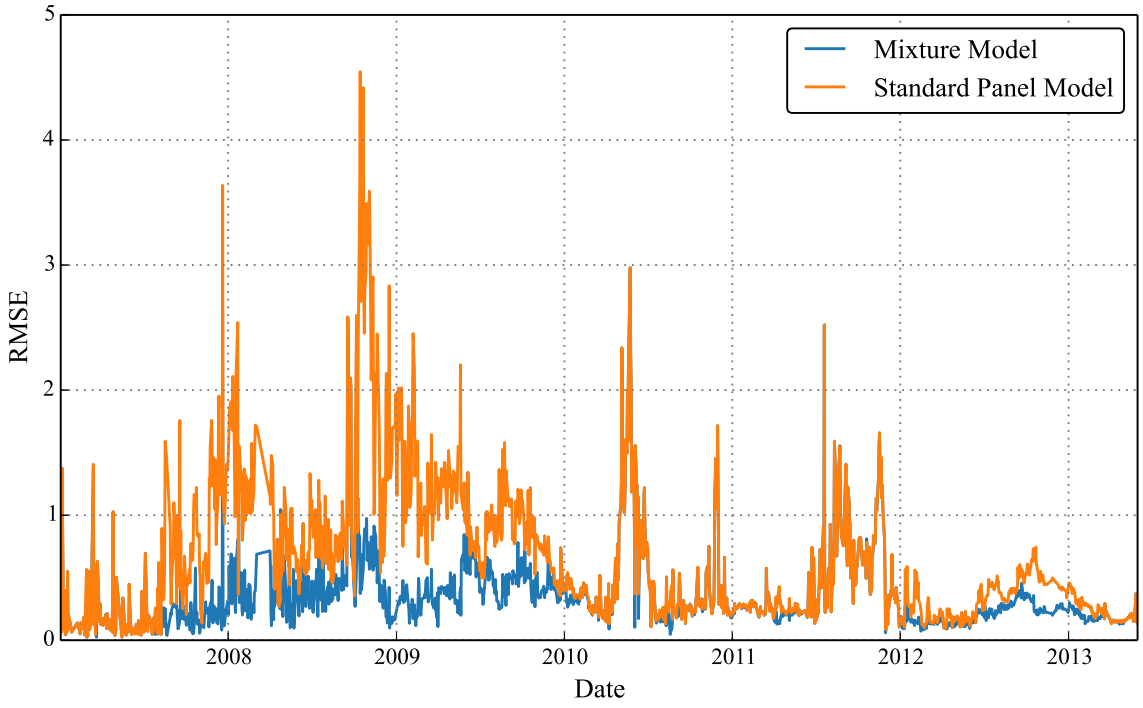

Figure 3.16: 6-month USD FRAs. Mixture vs normal model error comparison. The extended model improves the replication error of USD FRAs nearly by an order of magnitude, just like in the EUR market.

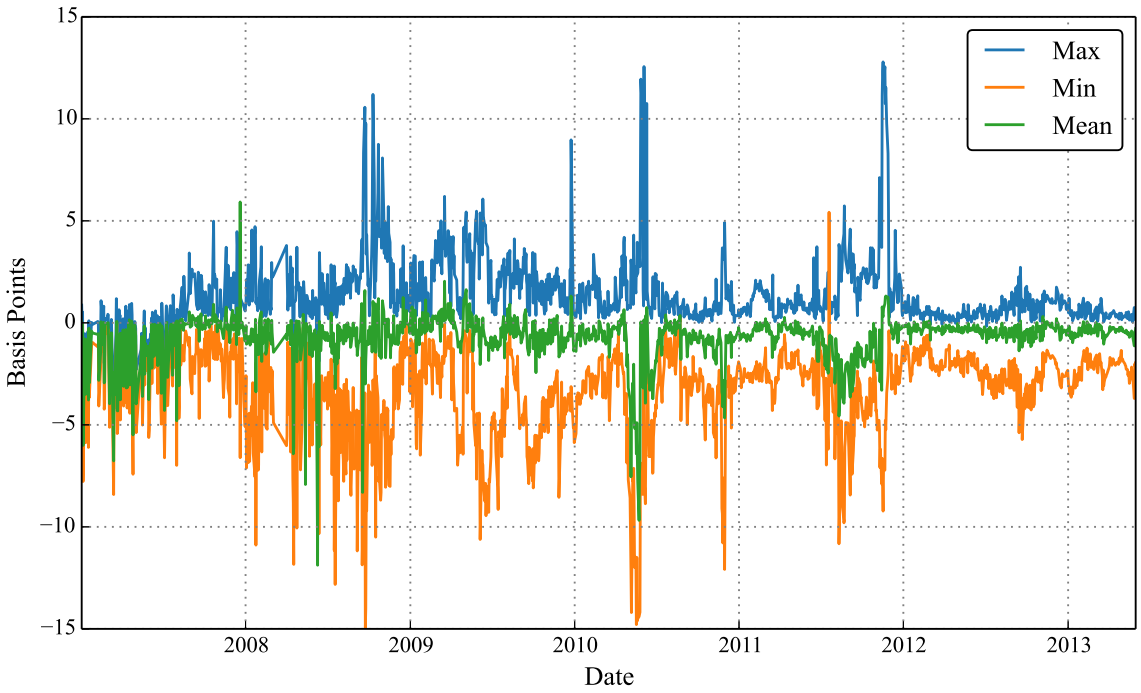

Figure 3.17: 6-month USD FRAs. Mean, min, max errors of the extended LIBOR panel model. The replication error stays within the 5bp margin in 95% of cases.

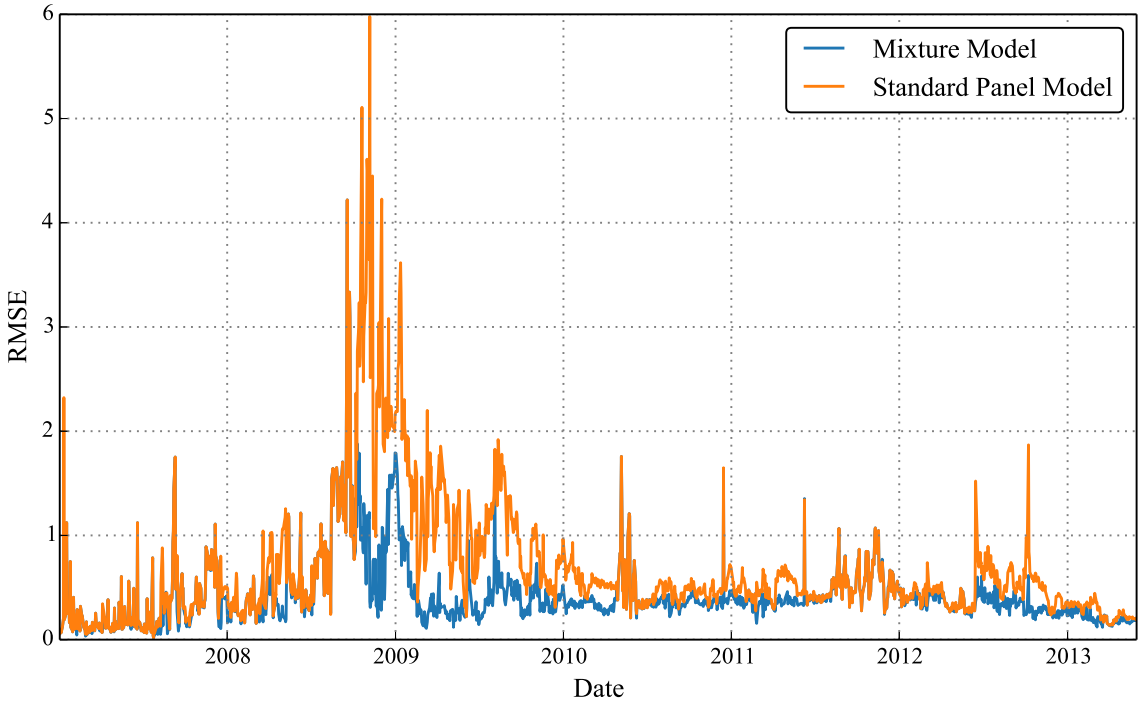

Figure 3.18: 6-month GBP FRAs. Extended vs standard LIBOR panel model error comparison. The extended model improves the replication error of GBP FRAs nearly by an order of magnitude, just like in the EUR market.

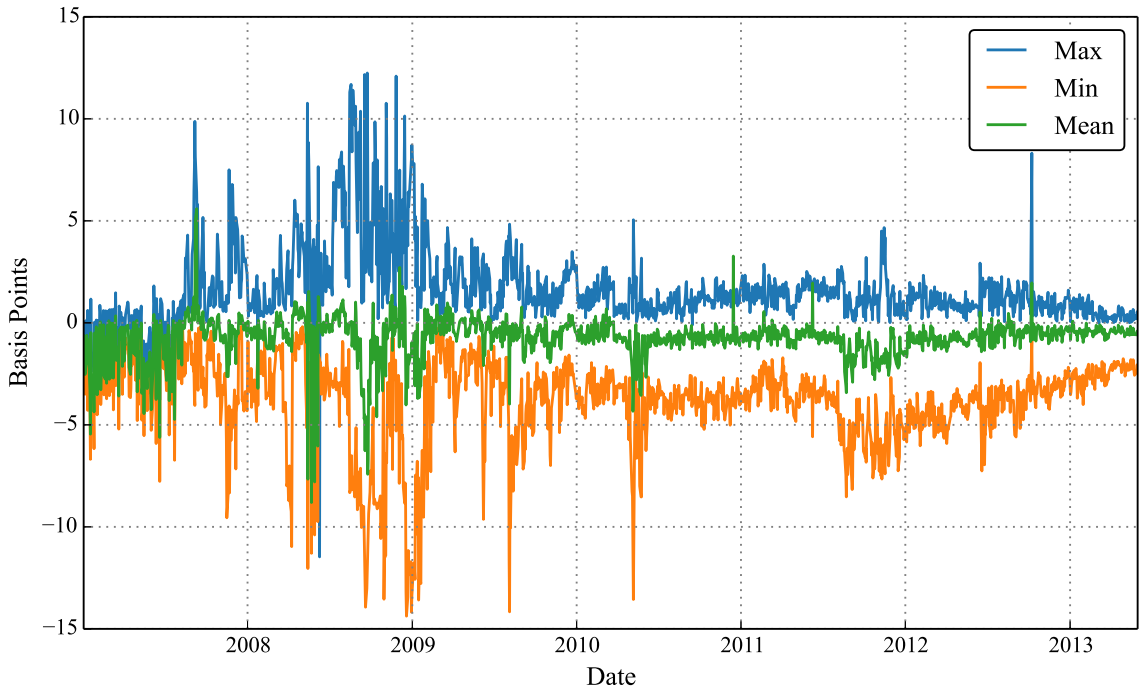

Figure 3.19: 6-month GBP FRAs. Mean, min, max errors of the extended LIBOR panel model.The replication error stays within the 5bp margin in 95% of cases.

3.6 Analysis of Parameter Dynamics

In our last section on the extended LIBOR panel model, we analyse the historical dynamics of the fitted model parameters. Our set of parameters $\sigma_1, \sigma_2, \lambda_1$ was calibrated to a set of FRA rates available every trading day in our historical dataset. We plotted the resulting parameters to investigate the significance of changes in their levels. The Figure 3.20 shows the obtained parameter results for EUR and GBP 6-month FRAs.

We would like to emphasise on several points. First, it is clear that the levels of implied volatilities is not constant and undergo volatile changes throughout the historical dataset. A small part of the volatile and sharp-edged behaviour of the parameters may be caused by overfitting in the calibration exercise. Nevertheless, the two mixture model components are defined by very different volatility levels:

- The low-volatility first component, has $\sigma \in \{0\% - 120\%\}$
- The high-volatility second component, has $\sigma \in \{150\% - 1500\%\}$

In our dataset, the first component in the model was the main driver of the mixture (had the largest weight λ_1) most of the days. On the other hand, the second, high-volatility

component, takes part ($\lambda_2 >> 0$) during several extended historical periods. This holds for all EUR, GBP and USD markets. We investigated if this matches any of the important historical events during the credit crisis. In the Figure 3.20 we have marked several periods of interest, where the second component had a large weight. We placed 'green' markers where a period of excessive credit volatility started and 'red' where it ended.

The first period starts in August 2007 with increased market volatility and inter-bank lending liquidity shortages (Mauro F. Guillén, 2012). The approximate end of the first period is in March 2008, when ECB started offering refinancing operations with six-month maturities to support the normalisation of the functioning of the euro money market. This first period of the initial liquidity crisis is visible across all EUR, GBP and USD markets.

The second crisis period starts around September 28, 2008. This day the Washington Mutual and Wachovia banks collapsed. Also, the European banking and insurance giant Fortis was partly nationalised to ensure its survival, which marks one of the starting days of the credit crisis (Mauro F. Guillén, 2012). We find it strange that the FRA market did not react already on the 15th of September during the default of Lehman Brothers.

This period ended on May 2, 2010, when Greece received a 110 billion EUR (93 billion) bail-out from other countries using the Euro, and the IMF .

In the third period starting mid-June 2010 and ending in August 2011, there is visible turmoil in the GBP and USD FRA markets, but not the EUR zone. During this period both Ireland and Portugal receive bailout packages from the European Central Bank and second round of quantitative easing takes place in the US.

The last analysed crisis period started around January 13, 2012. This time, the Standard & Poor's credit rating agency has lowered long-term credit ratings on the eurozone countries of Cyprus, Italy, Portugal and Spain by two marks and Austria, France, Malta, Slovakia and Slovenia by one mark (Kraemer and Gill, 2012). Many financial analysts and newspapers were anticipating the collapse of China's economic bubble, which will bring the economic crisis to climax in 2012 (Elliott, 2012).

Moreover, as we have marked in Figure 3.20, the three out of four high-volatility component periods nearly completely overlap in both EUR and GBP markets. The levels of the second volatility component are similar as well. This is a good indicator showing how closely connected are the two markets. The same parameter graph for USD does not

show great similarity to EUR or GBP markets.

Therefore, the two-factor mixed panel model not only improves the FRA calibration results by order of magnitude but also allows us to identify major events in the LIBOR lending markets by showing structural change events across different FRA markets.

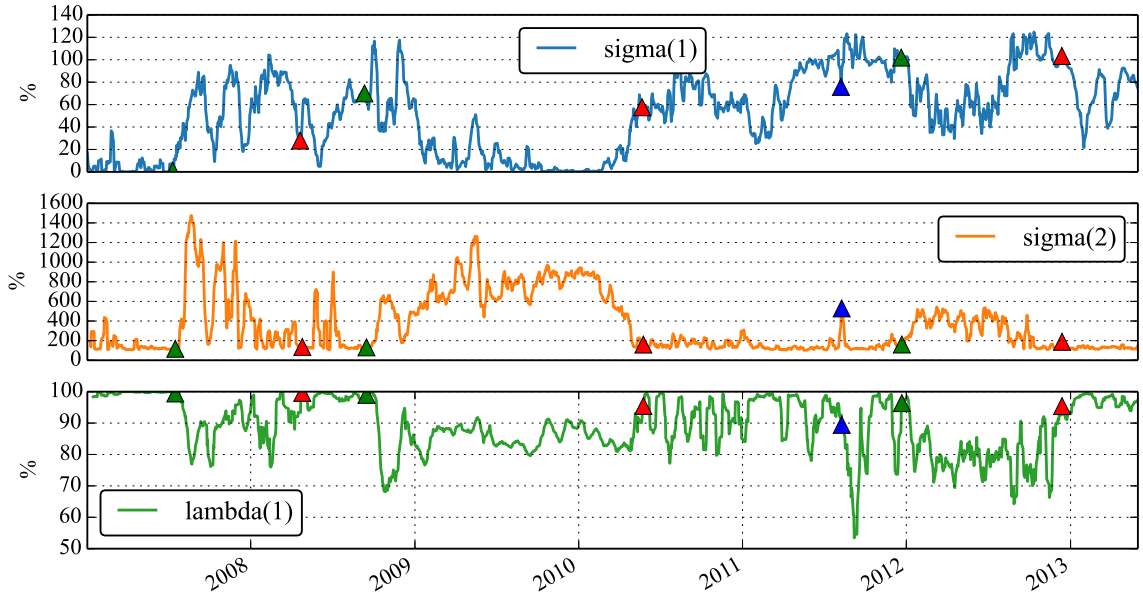

(a) Historical parameters for the mixture model. EUR 6-month FRAs

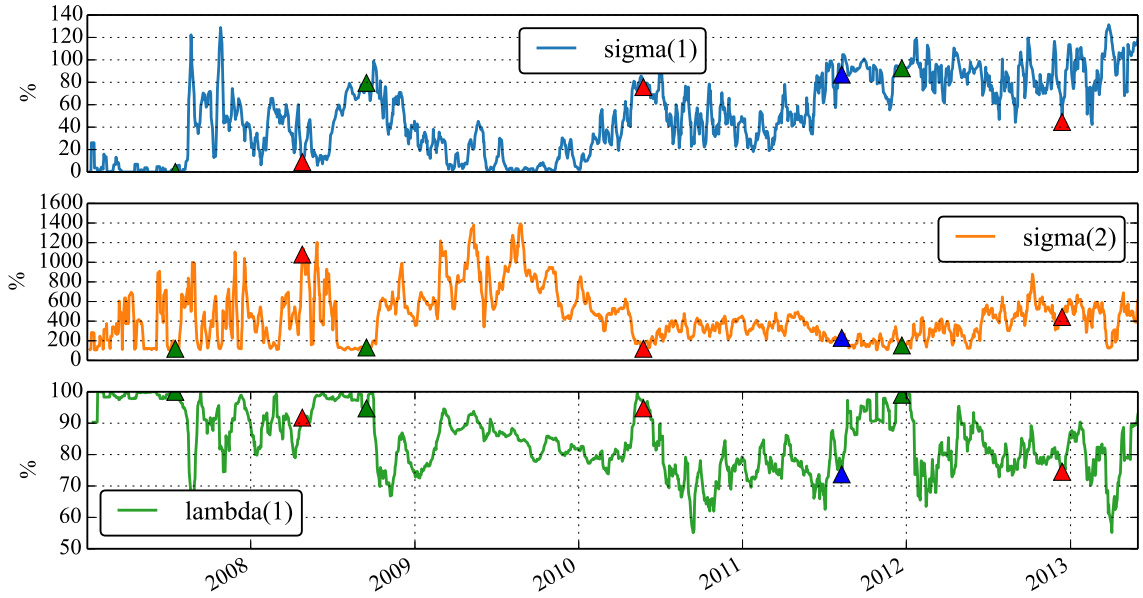

(b) Historical parameters for the mixture model. GBP 6-month FRAs

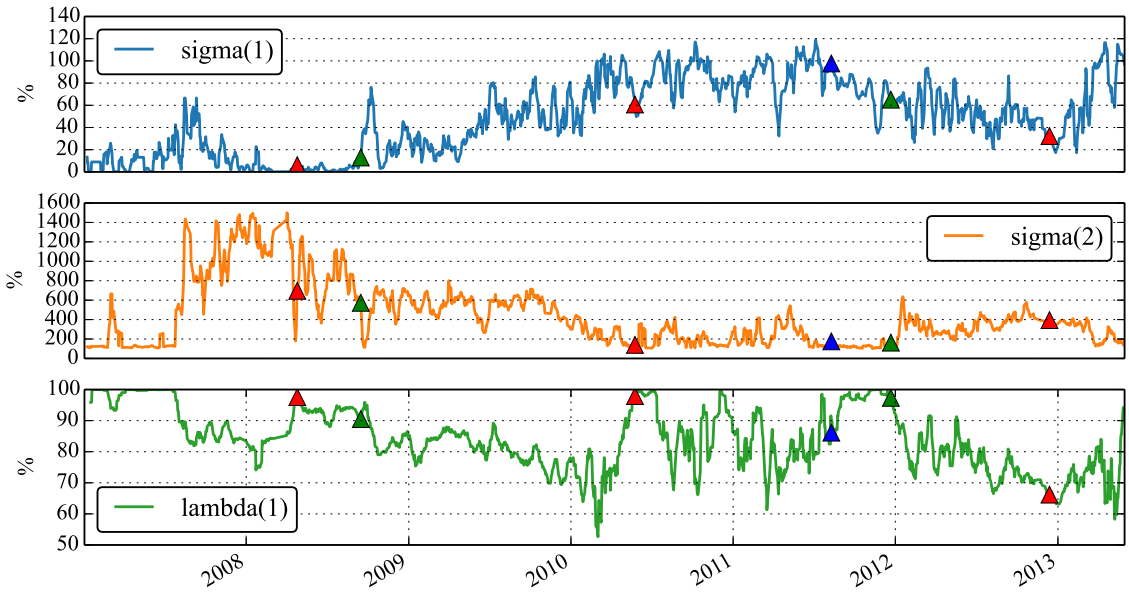

(c) Historical mixture model parameter dynamics for USD 6-month FRAs.

Figure 3.20: Historical mixture model parameter dynamics for EUR, GBP and USD 6-month FRAs. The figure shows the two-component volatility levels σ and the weight parameter for the first component. Throughout the dataset, the driving factor is the first component, but the high-volatility component gains weight in several, distinct periods. The green and red markers show the start and end points of these periods. The blue marker refers to an important event of 2011 only observed in EUR series.

3.7 Conclusion

The LIBOR panel model is not a common choice for an interest rate model in the financial literature and industrial practice. However, we chose to analyse and extend the model for its nearly-unique capability of relating OIS and LIBOR funding rates with credit-liquidity risks present in the lending markets. As we have shown, the model in its original formulation is a large improvement over the standard replication model since the start of the credit crisis but suffers from the lack of a good LIBOR-panel CDS option volatility index. To overcome the latter problem we reformulated the problem and constructed FRA-implied volatility. Using globally-calibrated implied volatility, we have shown that the panel model is a promising model for joint replication of series of market-traded FRAs. After careful analysis, we proposed an extension using an uncertain parameter model. This extension, with additional two degrees of freedom, yields excellent results in replication the market-traded FRAs - our maximal replication errors were within 5 bp error margin throughout our historical

dataset. Additionally, the analysis of historical parameter dynamics gave a unique outlook on the main structural changes in the FRA markets during the credit crisis. We found that there are concrete, extended periods when the single-volatility is under-performing, and the high-volatility component of the mixture model contributes a significant part in FRA replication. We have also shown that these high-volatility periods for EUR and GBP FRA markets are largely overlapping, which indicates strong interconnectedness of the latter two markets. Lastly, we have also identified the most likely historical events which triggered these structural changes in the FRA trading. These findings were presented in (Savickas, 2013).

3.7.1 Limitations of the Panel Model

Unfortunately, there are a few limitations of this model that do not allow us to use it for pricing of more complicated interest rate derivatives. We would like to discuss one of them, which is our main reason for looking into other low-parameter models for stochastic basis modelling as we do in the following chapter of this thesis.

The panel model relies on the availability of spot-LIBOR and OIS curves for FRA pricing under standard replication as in (2.58). Here, while OIS curve can be bootstrapped from traded OIS Swaps following guidelines made by Ametrano and Bianchetti (2013), the spot-LIBOR curve is publicly quoted up to 1-year maturity. The LIBOR curve for larger maturities was, in a classic setting without multiple curves, bootstrapped from market IRS (2.18). The problem here is that IRS is a series of FRAs, therefore using IRS to imply a spot-LIBOR curve for maturities larger than 1-year would result in LIBOR forward rates nearly matching the market FRA rates. If we do this, we can no longer imply volatilities from the same IRS and FRAs. Therefore, as long as we do not have a reliable proxy for the LIBOR-panel CDS spread volatility, the panel model can currently be used for FRAs with maturities until 1-year as the spot-LIBOR is not quoted after that.

Chapter 4

Hybrid Model for Multi-Curve Pricing

4.1 Introduction

Before the 2008 credit crisis, inter-bank lending rates with different financing frequencies, e.g. overnight or 1,3,6,9,12 - months were practically equivalent to each other, because of lack of perceived risk in the inter-bank lending market (Bianchetti, 2012). Pricing non-linear derivatives in the pre-crisis market was a relatively easy task, as the forward LIBOR curve was unique and knowing the volatility of caps based on one LIBOR-tenor would lead to implied volatility of the other rate via simple extrapolation (Kienitz, 2013). Since the crisis, significant basis appeared in between the different tenor lending rates, especially the overnight (OIS) rates (Morini, 2009). This split up of interest rates led to complications in non-linear derivatives pricing. For example, while liquid interest rate swaps in the EUR market rely on the LIBOR four tenors: 1,3,6,12-months, the non-linear derivatives like caps and floors are only traded on the 3-month and 6-month tenors. More precisely, for EUR market there are quotes for 1 to 2-year maturity caps with 3-month tenor and 2 to 30-year maturity caps with 6-month tenor for several strikes K. All the other caps are currently very illiquid and therefore hard to price as the 1 and 12-month rate volatility data is not available or at least cannot be directly implied from liquid products (Kenyon, 2010).

One of the aims of this project is to develop a multi-curve model with a stochastic basis which would allow pricing of multi-tenor derivative contracts (e.g. cap), without the need for artificial proxies and estimates for illiquid volatilities. In this chapter, we recap the definitions of Cox-Ingersoll-Ross and Hull-White short-rate models and introduce the hybrid Cox, Ingersoll and Ross (HCIR) model which approaches the multi-curve cap

pricing problem.

4.2 Theoretical Background

In this section, we introduce the Cox-Ingersoll-Ross (CIR) and the hybrid Hull-White CIR (HCIR) models that we shall use for caplet, cap and CVA pricing. We will also show the derivations for caplet prices in the HCIR model cases with 2 and 3-factors.

4.2.1 The CIR Model

The Cox-Ingersoll-Ross model (Brigo and Mercurio, 2006) is the first model to use the square-root diffusion term in the short rate diffusion SDE:

$$dc(t) = \kappa[\theta - c(t)]dt + \sigma_c\sqrt{c(t)dW(t)}, c(0) = c_0, \tag{4.1}$$

where $c_0, \kappa, \theta, \sigma_c$ are constants.

The CIR model yields non-Gaussian dynamics for the short-rate, in particular the $c(t)$ has the density of a non-central Chi-squared distribution (Brigo and Mercurio, 2006). The price at time t of a zero-coupon bond with maturity T can be obtained in an analytic, affine form, full details are given in Appendix C.1.

The CIR model is a popular stochastic spread model, especially in credit derivatives. A few more features of this model make it very attractive for the purpose of LIBOR-OIS spread modelling, namely guaranteed positivity of the spread, mean-reversion which is visible in the empirical analysis of LIBOR-OIS spreads (Filipovic and Trolle, 2013), analytic pricing of bonds and, inherently, fast calibration of model parameters to given spread curves. Due to its popularity in credit models, it is intuitive to introduce correlation between the LIBOR-OIS spread and credit-default dynamics of a LIBOR-panel bank.

4.2.2 Hybrid Hull-White and CIR Framework

We have included the definitions and derivations of bond-pricing under the 1-factor and 2-factor Hull-White models in the appendix C.2. Since the CIR model is non-Gaussian, combining the two models requires a non-standard setting. In contrast to the usual techniques in the short-rate modelling, such as assuming a correlation between the driving Brownian motions between the Hull-White and CIR processes, we shall assume the correlation to be zero, but we construct the basis spread process as an explicit sum of the Hull-White and

CIR processes.

The following setup results in a fully analytical Hull-White framework for OIS swap pricing and calibration as well as analytical pricing of the LIBOR-bonds and semi-analytical pricing of caps and floors in the hybrid model. We introduce the two potential models for the problem, the first being a mix of 1-factor Hull-White and CIR process (HW1F-CIR) and the second one including a 2-factor Hull-White and CIR processes (HW2F-CIR).

We define the short-rate process $r(t)$ to be the driver of the instantaneous OIS rates, and the process s_t the driver of the LIBOR-OIS spread as:

$$r(t) = \Psi_1(t), \tag{4.2}$$

$$s(t) = k\Psi_1(t) + \Psi_2(t), \tag{4.3}$$

where Ψ_1 is a short rate from standard Hull-White one factor (HW1F) model (Brigo and Mercurio, 2006) and Ψ_2 is the CIR short rate model as in equation 4.1 and k is the correlation-dependence level between the risk-free OIS rate and the LIBOR-OIS spread.

In this setup, the OIS rates are normally distributed and can be negative. Then, while $\Psi_2(t)$, the CIR process, is positive, due to the explicit involvement of $HW1F$ process, the spread $s(t)$ can be negative. The "explicit" LIBOR-OIS spread and OIS correlation parameter k introduces a dependence of LOIS spread on OIS rates instead of more traditional correlation of stochastic drivers. This choice was made to preserve analytic tractability of bond pricing when the correlation is non-zero. Because of this, the LOIS spread can become negative, but it is highly unlikely. From a practical point of view this may not be very realistic, but again, there is no guarantee that LIBOR rates will always be higher than the OIS rates.

Next, this additive model yields a couple of convenient results. First, the OIS zero-coupon-bond prices are determined as in standard textbook extended Hull-White model (Brigo and Mercurio, 2006)

$$P_{\text{OIS}}(t,T) = P_{\text{HW}}(t,T). \tag{4.4}$$

Then, the LIBOR zero bond is expressed as a product of k-scaled OIS bond and CIR-bond:

$$P_L(t,T) = P^k_{\text{HW}}(t,T)P_{\text{CIR}}(t,T), \tag{4.5}$$

where the analytic expression for P_{CIR} is given in Appendix C.1 and for P^k_{HW} is given in Appendix C.2.

The HCIR model is a 2/3-factor model, where one of the factors is CIR with non-central Chi-squared distributed rates. However, the separable model formulation as given in (4.2) allows us to price caplets using semi-analytic formula of the form:

$$\text{Cplt}_{\text{HCIR}}(t,T,S,K) = P_{OIS}(t,S)\mathbb{E}^{\mathbb{Q}_S}\left[\frac{1}{P_{\text{CIR}}(T,S)}\left(e^{-\mu+\frac{1}{2}\hat{V}^2}\Phi(d) - \hat{X}\Phi(d-\hat{V})\right)\middle|\mathcal{F}_t\right], \tag{4.6}$$

details for the $\mu, \hat{V}, \hat{X}$ are given in Appendix C.4. Using a semi-analytical formula instead of a two-dimensional integral improves the computation time by an order of magnitude.

To price an interest rate cap with strike K and fixing dates T_i, under HCIR model, we only need to sum the caplet values:

$$\text{Cap}(t,\{T_0,...T_N\},K) = \sum_{i=1}^{N}\text{Cplt}_{\text{HCIR}}(t,T_{i-1},T_i,K). \tag{4.7}$$

4.2.3 Benchmark Model: Displaced Diffusion

Kienitz (2013) has suggested a simple, yet innovative model to imply y-tenor volatilities from x-tenor caplet quotes. His work is based on fixed basis spread assumption and the LIBOR market model. We shall briefly introduce the concept, but if the reader would like to know full details please refer to (Kienitz, 2013). We shall use this model as a benchmark for extrapolation volatilities to different LIBOR tenors against the HCIR model.

This procedure models the forward LIBOR rates, with x as the tenors of the rate and k as the index (linked to start/end-period (T_{k-1}, T_k)):

$$dL^x_k(t) = ...dt + \sigma^x_k L^x_k dW(t). \tag{4.8}$$

The forward LIBOR rate in question is split into the OIS forward rate and a (constant) basis spread:

$$dL^x_k(t) = ...dt + \sigma^x_k(F^x_k(t) + b^x_k)dW(t). \tag{4.9}$$

In the above transformation we have a displaced diffusion (DD) model. We rename its volatility to $\sigma^{\text{DD}}_{x,k}$, and using it, we can find the log-normal model OIS $F^x_k(t)$ at-the-money (ATM) caplet volatility using a formula from Joshi and Rebonato (2003):

$$\sigma^{\text{DD}}_{x,k} = \frac{2}{\sqrt{T}}\Phi^{-1}\left[\frac{1}{\beta}\Phi\left(\frac{\sigma^{\text{DD}}_{x,k}\beta\sqrt{T}}{2}\right) - \frac{1-\beta}{2\beta}\right], \tag{4.10}$$

where the β parameter is set by the diffusion shift b^x_k and the forward rate

$$\beta = 1/(F^x_k b^x_k + 1). \tag{4.11}$$

The ATM OIS volatility (for tenor x) can be transformed to another tenor y using single curve forward rate relations as shown in the example below. Then, using y-tenor basis spreads b^y_k and forward rates F^y_k we obtain the $\sigma^{\text{DD}}_{y,k}$ and convert the black volatility back to displaced diffusion volatility:

$$\sigma^{\text{DD}}_{y,k} = \frac{2}{\beta\sqrt{T}}\Phi^{-1}\left[\beta\Phi\left(\frac{\sigma^{\text{DD}}_{y,k}\sqrt{T}}{2}\right) + \left(\frac{1+\beta}{2}\right)\right]. \tag{4.12}$$

Briefly, the full conversion scheme works as follows:

$$\sigma^x_{\text{LIBOR}} = \sigma^x_{\text{DD,OIS}} \implies \sigma^x_{\text{DD,OIS}} \implies \sigma^y_{\text{DD,OIS}} \implies \sigma^y_{\text{DD,OIS}} = \sigma^y_{\text{LIBOR}}. \tag{4.13}$$

The latter approximation can be made for time-dependent volatilities as well (Kienitz, 2013). Also, backwards procedure, where we imply shorter (1-month, 3-month) tenor volatilities from 6M volatilities can be done by assuming some term-structure of the short-term volatilities, e.g. flat, linearly increasing or some parametric form.

Moreover, the latter volatility shift procedure can be expanded to a SABR (Mercurio and Morini, 2007) stochastic volatility model by:

- Calibrating the smile with quoted caplets
- Shifting the ATM volatility as above
- Reconstructing the SABR smile by assuming same fixed parameters as before.

Example. Construction of the 6-month OIS volatilities is done using the simple single-curve framework relations of forward rates. The commonly used construction of a long, 6-month forward rate $F_{1,3}$ from two shorter, but consecutive 3-month forward rates $F_{1,2}, F_{2,3}$

is done by compounding the following interest rates:

$$\tau_{6M}F_{1,3}(t) = \tau_{3M}F_{1,2}(t)(1 + \tau_{3M}F_{2,3}(t)) + \tau_{3M}F_{2,3}(t). \tag{4.14}$$

We can relate the 6-month forward rate volatility in the LIBOR market model (Brigo and Mercurio, 2006) to the two corresponding 3-month volatilities as:

$$\sigma_{1,3}^2 = V_1(t)^2\sigma_{1,2}^2 + V_2(t)^2\sigma_{2,3}^2 + 2\rho V_1(t)\sigma_{1,2}V_2(t)\sigma_{2,3}, \tag{4.15}$$

where

$$V_j := \frac{\tau_{j,j+1}F_{j,j+1} + \tau_{j,j+1}F_{j,j+1}\tau_{j+1,j+2}F_{j+1,j+2}}{\tau_{6M}F_{1,3}(t)}. \tag{4.16}$$

4.3 Application: Pricing of Illiquid Caps

The most liquid interest rate swaps in the EUR market rely on the four tenors: 1,3,6,12-months. At the same time, the caps/floors are mostly traded on the 3-month and 6-month tenors, for EUR caps. More precisely, there are market quotes for 1,2-year caps with 3-month tenor and 2,3,...,30-year caps with 6-month tenor with multiple strikes. All the other caps are illiquid and therefore hard to price.

The HCIR model is beneficial for these situations where market liquidly trades caps on only one of the tenors. By construction, the HCIR model can be calibrated to market OIS and LIBOR forward curves and a set of single-tenor cap volatilities. Then, we can directly price any caps on the other, less liquid tenors.

In this section, we shall demonstrate the HCIR model calibration results in several market data cases and show the potential of the model for pricing illiquid caps by benchmarking the model against J. Kienitz displaced-diffusion approach and given trader quotes for the less liquid cap surfaces.

In particular, we shall fit HCIR model variants (with HW1F and HW2F drivers) to:

1. only ATM caps,
2. single 3% strike,
3. single 4% strike and chosen illiquid caps,
4. again ATM caps, but in negative interest rates dataset.

4.3.1 ATM Cap Fitting

Our initial investigation relies on ATM-cap pricing using the hybrid HCIR model. We will analyse two branches of the model where the spread CIR-model is combined with HW1F and HW2F models for the OIS base rate. We shall refer to the combination of HW1F and HW2F model with CIR, respectively, as HW1F-CIR and HW2F-CIR. We will refer to HCIR model in general when discussing both of branches at the same time.

HW1F-CIR

We have calibrated the HW1F-CIR model to available market data:

1. OIS yield curve and four (1, 3, 6, 12)-month forward rate curves
2. 6-month ATM caps with maturities from two to 30-years.

Then, we re-priced the 4-curve forward rates and 6-month ATM caps and estimated new ATM levels for 1-month, 3-month and 12-month caps from market forward rates by pricing them with the HCIR model. For comparison reasons we converted the present value of the latter caps to normal volatilities by inversely solving the Bachelier cap pricing formula (2.18) with corresponding ATM strikes for each of the caps.

We note that the CIR model parameters are dependent on the calibrated HW parameters. Both HW2F parameters σ_i, a_i, ρ_{HW} (or just σ and a for 1-factor HW.) and full CIR parameter set $\rho, \sigma_c, \theta, \kappa, c_0$ influence the resulting cap prices, hence the calibration to market data is "joint": we minimize the least-squares error of the market forwards and market caps at the same time. Therefore, the full calibration involves up to 10-parameters, when we calibrate to 6-month forwards and 6-month caps. There are multiple local minima in the solution, and the user must use a global calibration routine, e.g. basin-hopping (Wales and Doye, 1997) or differential evolution (Das and Suganthan, 2011) to avoid finding only a local minima.

Figure 4.1 shows the calibrated model results for forward rates. Additionally, we made a tenor-by-tenor comparison of the forward rates errors in Figure 4.2 between the market and model-implied ones as well as normal cap volatilities in Figure 4.3.

Several things can be noted from the obtained results:

1. The HW1F-CIR model can replicate the yield curves and market forwards with average 5bp error (relative 2% error), similar to bid-ask spreads in the ICAP broker dataset.
2. The biggest discrepancy on the forward rates is in the first few points (15bp)
3. The replication of cap volatilities with HW1F driver for OIS rates is problematic as the model cannot capture the low-volatility setting of the short end curve. Here the normal volatilities are as low as 20bp and then rise to 100 bp in the middle resulting in very low short-term cap prices. Because of this, we decided to extend the model to HW2F as shown in the next section.

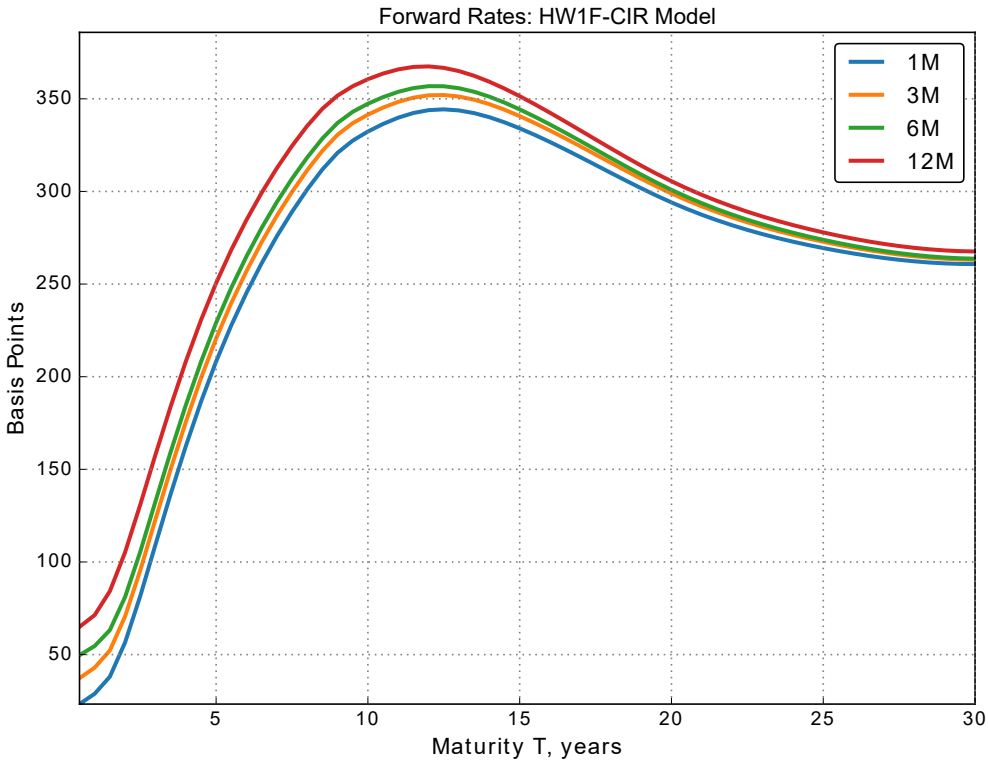

Figure 4.1: Resulting forward rates from multi-tenor LIBOR-curves under HW1F-CIR model. Market data of 22-Nov-2013.

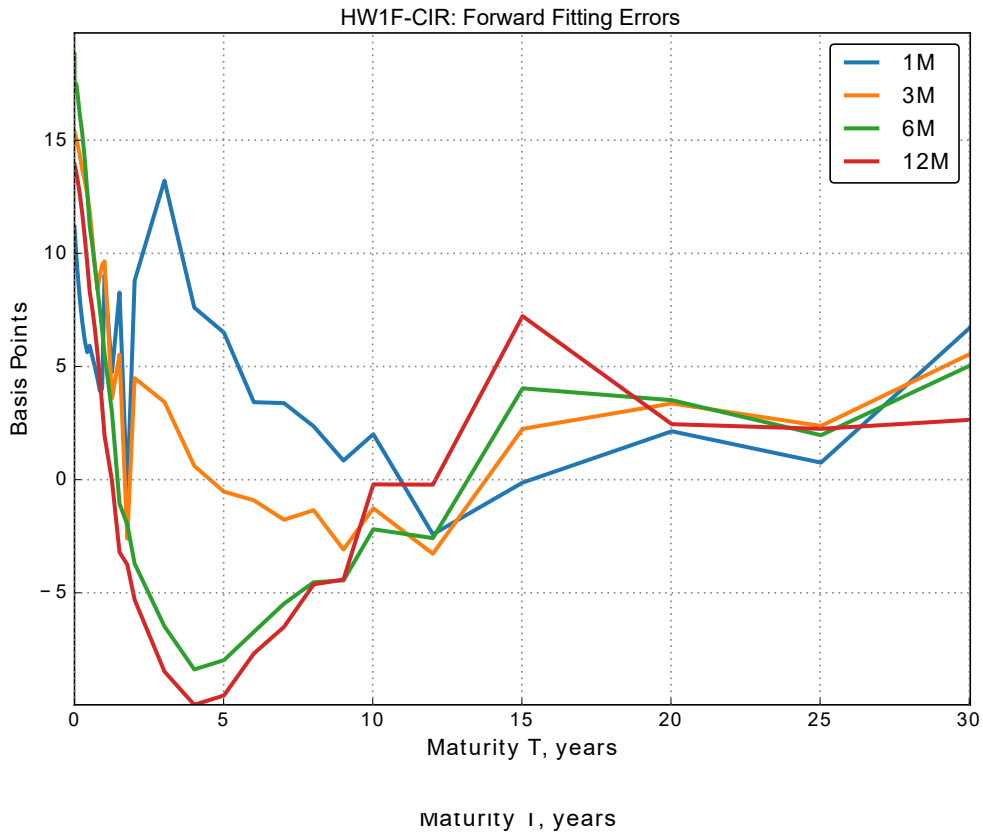

Figure 4.2: Forward replication errors, HW1F-CIR model vs market data of 22-Nov-2013.

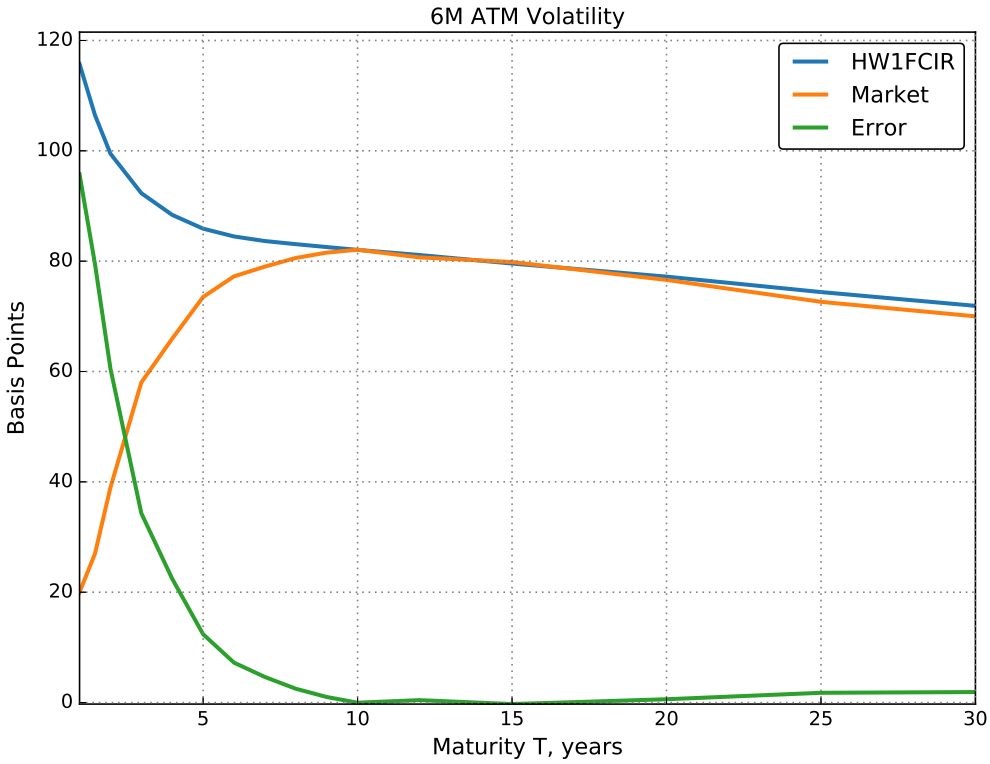

Figure 4.3: Comparison of 6-month ATM cap (normal) volatilities. HW1F-CIR Model vs market data from 22-Nov-2013.

HW2F-CIR

First, we would like to demonstrate the potential of the 2-factor Hull-White model for caps pricing. The biggest problem we have with the 1-factor Hull-White model is the steep cap price increase in the short term, which is not visible in the market data.

In the 2-factor model, the correlation ρ parameter can help control this ascent. By setting the correlation between the two Brownian motions to a negative number, we can decrease the ascent as shown in the Figure 4.4:

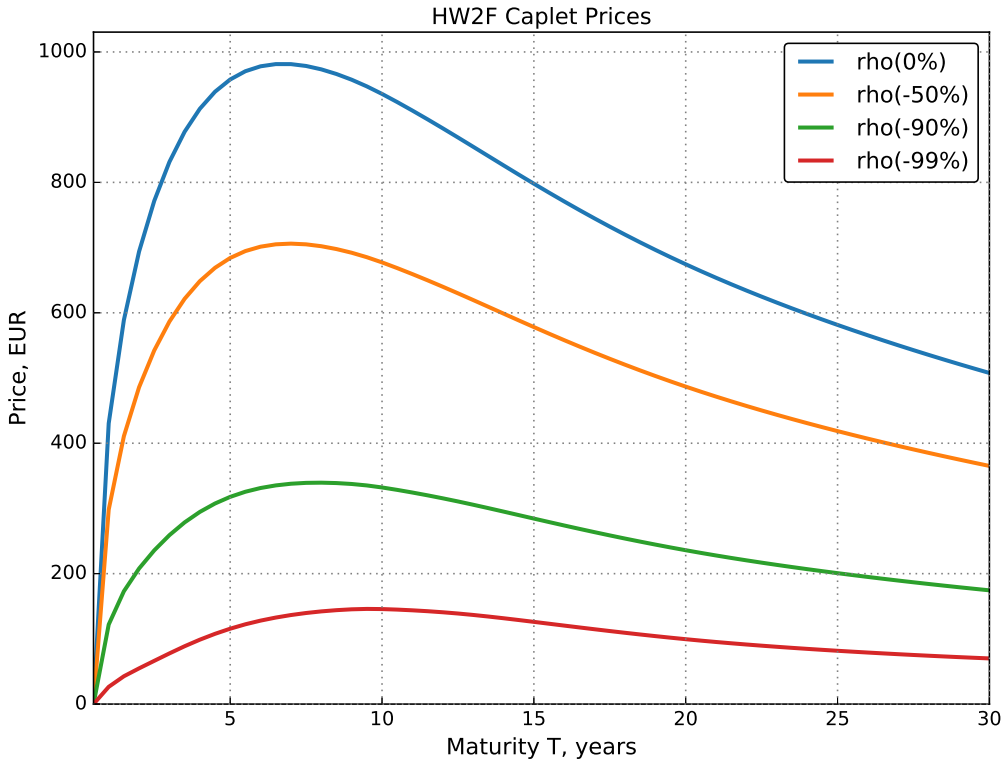

Figure 4.4: Example ATM caplet prices (notional of 1 EUR) across maturities, using the 2-factor HW model with correlation ρ values from -99% to 0%.

We calibrated the HW2F-CIR model in the same setting as in the previous section. In the following Figures 4.5 and 4.7 we show the HW2F-CIR and market multi-curve forward rate errors as well as normal cap volatilities and absolute errors. We observe that:

- The 2-factor HW model combined with CIR provides a similar fit to the market forward curve as the HW1F-CIR model.
- On the other hand, the 2-factor Hull-White model improves on the low-volatility issue in the short-end of the 6-month cap pricing curve.
- Additionally, using the HW2F/HW1F-CIR model we can immediately price illiquid caps based on 1,2,3-month tenors without any external data, as shown in Figure 4.8. This is the major innovation for a short-rate model to be able to extrapolate liquidly traded cap volatilities to illiquid ones without the need for external data proxies and adjustments.

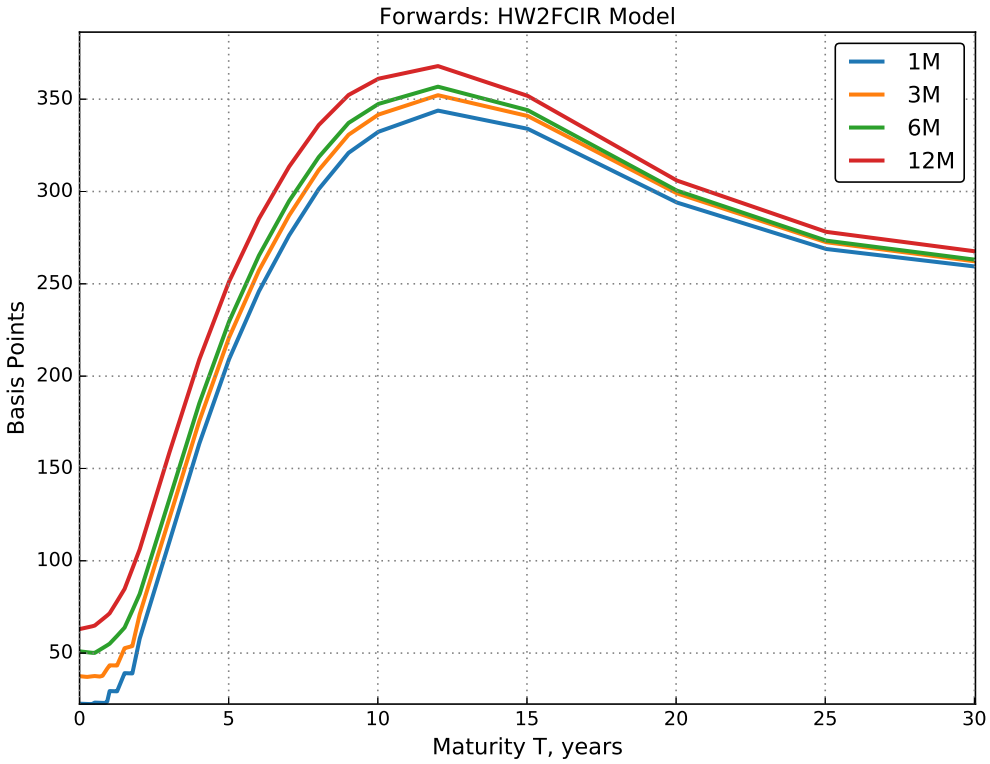

Figure 4.5: Tenor-by-tenor comparison of forward rates. HW2F-CIR model vs market

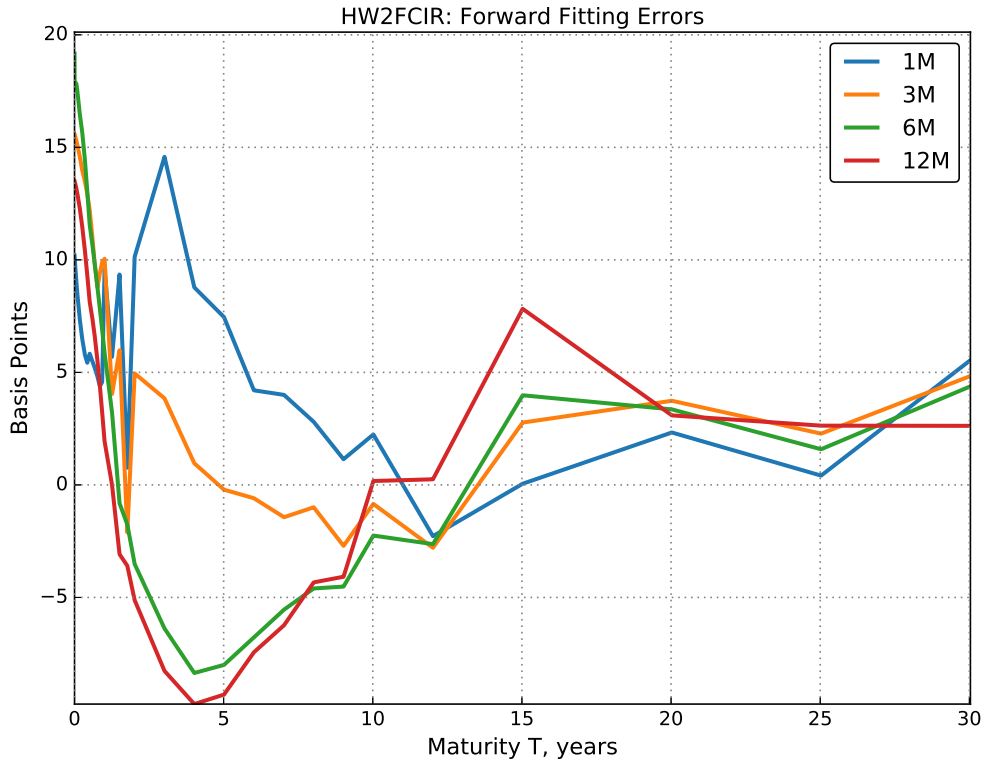

Figure 4.6: Calibration errors for market forwards - HW2F-CIR model forward rates, data from 22-Nov-2013.

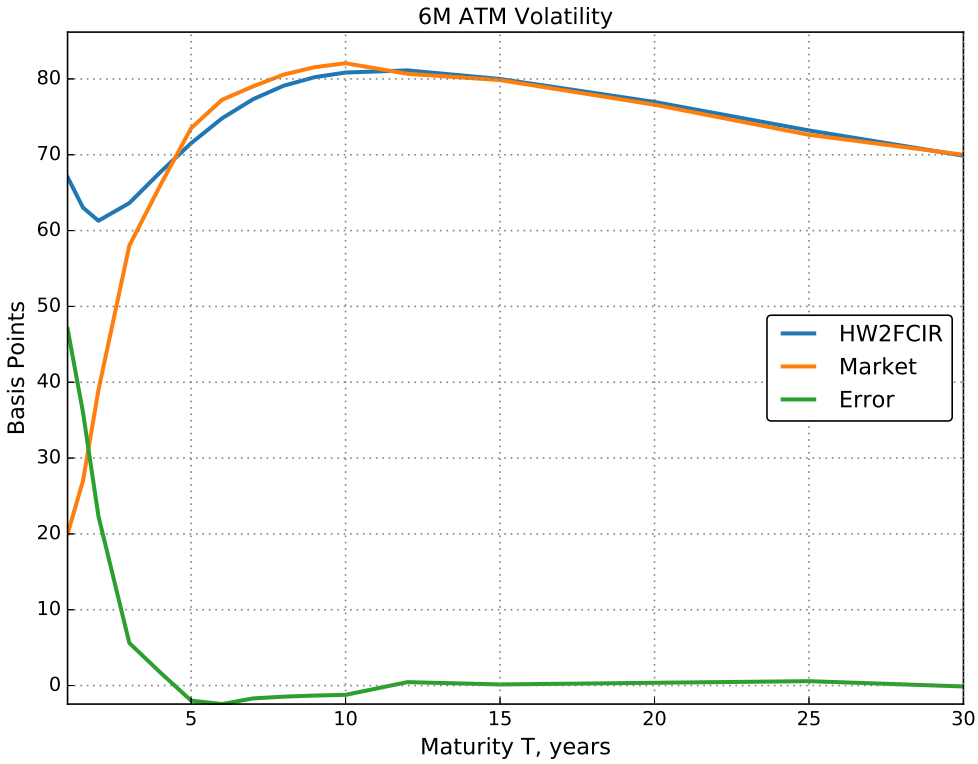

Figure 4.7: Comparison of 6-month ATM cap (normal) volatilities. HW2F-CIR model vs market data from 22-Nov-2013.

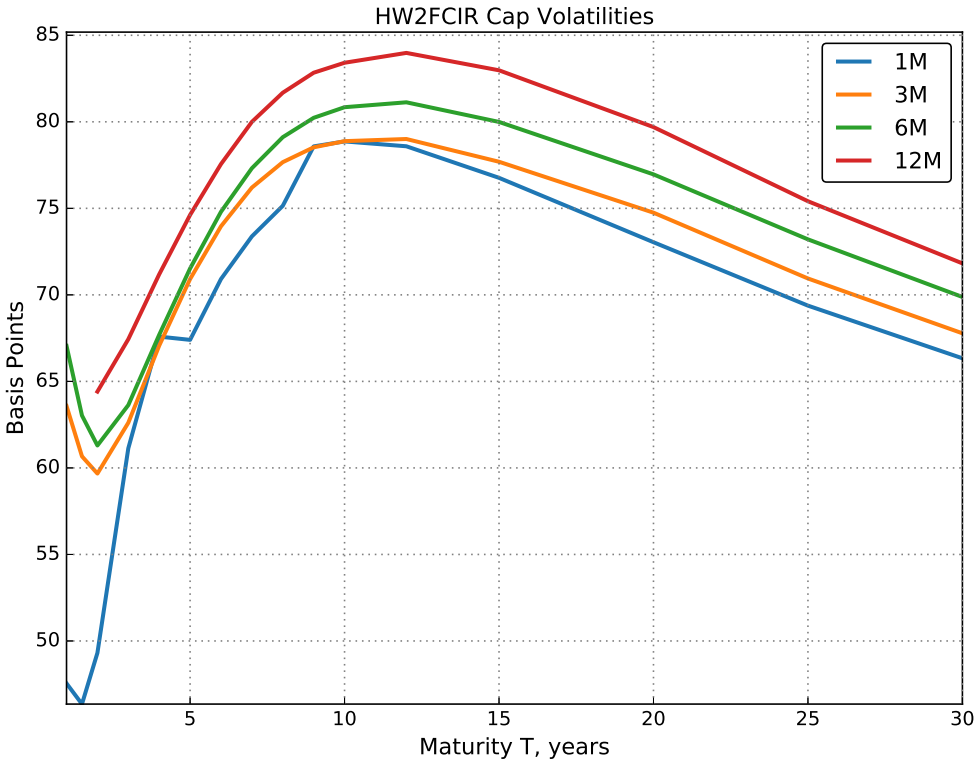

Figure 4.8: Cap volatilities for every tenor priced under HW2F-CIR model. The pricing procedure only requires liquid market data and does not need to be adjusted with any proxies. This is a novel and most important feature of the HW2F-CIR model. Data of 22-Nov-2013.

For completeness of the model comparison, we provide the calibrated model parameters in Table 4.1. The HW2F has two random drivers with two distinct mean-reversions and volatilities. The spread (CIR)-components for every curve have an explicit negative correlation to OIS movements. This correlation ρ_{CIR} is decreasing, in the absolute sense, as the tenor of the curve increases. The other parameters are entirely dependent on the term-structure of the LIBOR-OIS forward spreads.

Model	a_x	σ_x	a_y	σ_y	ρ_{HW}
HW2F-CIR	45.07%	2.07%	12.3%	2.49%	-99.6%
Model	ρ_{CIR}	σ_c	θ	k	c_0
HCIR-CIR: 1M	-4%	0.06%	1e-4	4.9%	0.13%
HCIR-CIR: 3M	-3.4%	0.3%	1e-4	6.1%	0.28%
HCIR-CIR: 6M	-2.0%	0.4%	1e-4	9.4%	0.42%
HCIR-CIR: 12M	-1.8%	0.35%	1e-4	8.0%	0.54%

Table 4.1: HW2F and CIR model parameters for LOIS spread in the 2-factor HW2F-CIR model.

Comparison with J. Kienitz Benchmark

J. Kienitz volatility extrapolation approach is rather different from HCIR model, namely:

1. It assumes LIBOR market model dynamics for LIBOR and OIS forward rates
2. But assumes that each LIBOR forward is a shifted (as in Displaced-Diffusion) OIS forward by constant spread $b_i j$.
3. The extrapolation from tenor x to y relies on:
   - differences in tenor lengths,
   - differences in basis spread sizes $b_i x$ and $b_i y$,
   - and the correlation ρ between neighbouring OIS forwards $F(T_{i-1}, T_i)$ and $F(T_i, T_{i+1})$.

To produce a simple benchmark with J. Kienitz vol extrapolation method, we used 6-month caplet volatility data, and then transformed them to 1,3,12-month cap volatilities with the procedure outlined in section 4.2.3. We chose the $\rho = 95\%$ parameter as this choice provided a close match to the HCIR model and in literature, the historically estimated values vary between 0.7 to 0.95.

In figure 4.10 we demonstrate the HCIR model and Kienitz-method extrapolated cap volatilities. The figures show that the tenor-structure of the volatilities is the same on both models, namely the volatilities of caps with larger basis spread, like the 12-month, are overall larger. The long-end volatilities in both models are within several basis points distance of each other, which shows that the HCIR model and DD model are compatible with each other, even if the DD model fit is strongly influenced by the forward-rate correlation parameter ρ, which is not present in HCIR model. On the other hand, the fits diverge for short-maturity ($\leq$ 2-years) caps, as our initial 6-month cap fit in HCIR model does not

capture very-low short-end volatilities.

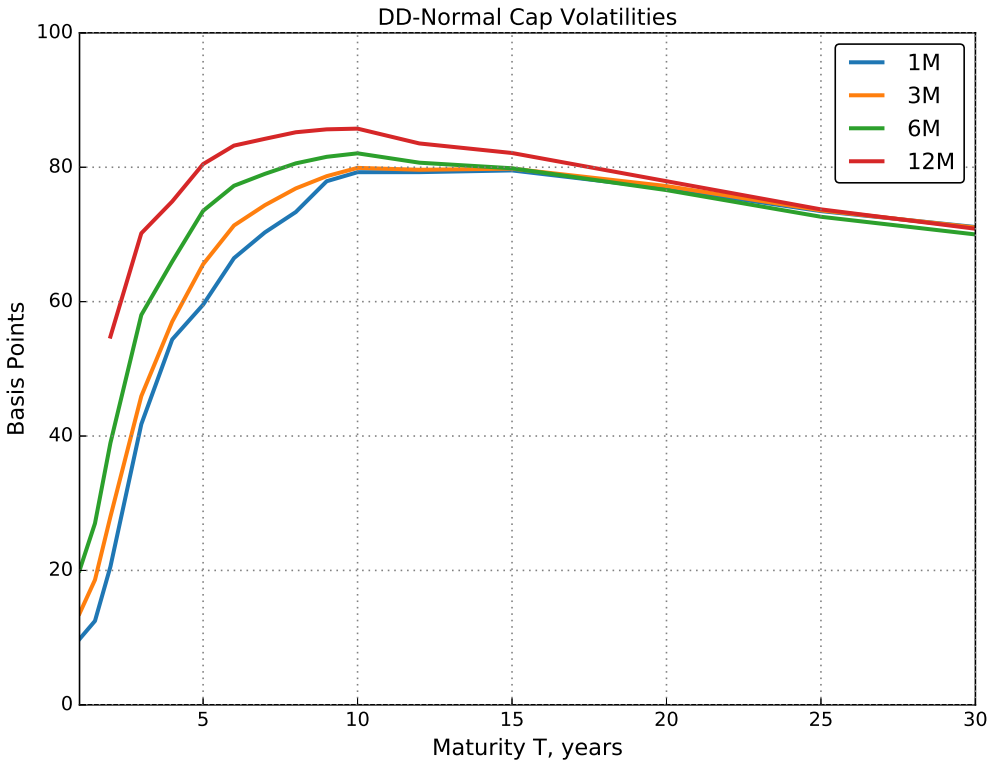

Figure 4.9: Normal ATM cap volatilities for all tenors in displaced-diffusion model.

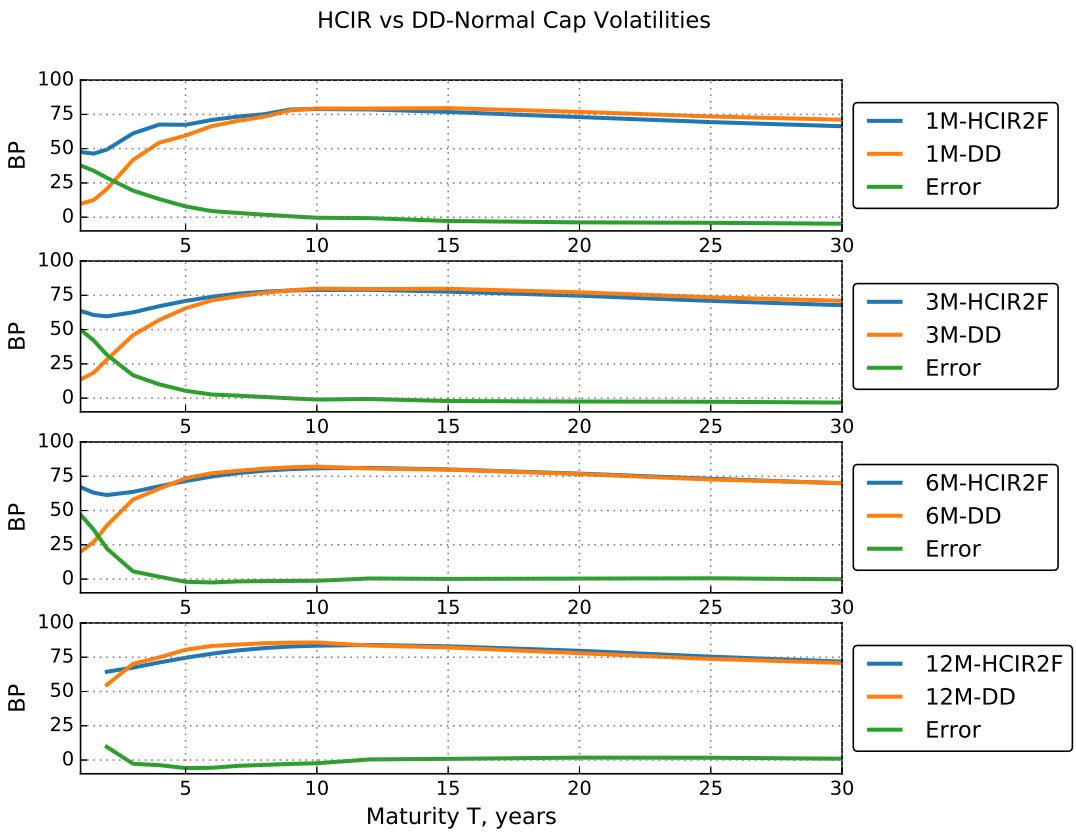

Figure 4.10: Normal ATM cap volatilities for all tenors. Comparison between the HW2F-CIR model and displaced-diffusion extrapolated normal volatilities.

4.3.2 Single Strike Non-ATM Cap Fitting

The second experiment we set up, is HCIR model fitting to non-ATM caps, where we chose a single 3% fixed strike for 6-month caps with maturities up to 30-years for model calibration. Here we evaluate the ability of the 2-factor HW combined with CIR model (HW2F-CIR) to replicate market caps on 6-month tenor as well as extrapolate and price caps on 1,3,12-month tenors.

Fitting of forward rate curves was achieved with similar accuracy as in the ATM case, hence we skip the figure showing that. The following Figure 4.11 demonstrates that for 6M caps with maturities > 7 years we can achieve fits with difference less than one bp in volatility. Caps with shorter maturities were not fitted as well, first, because we fitted the present value of the caps and they did not carry much weight, and because the HW2F-CIR model just like HW2F cannot jointly produce volatilities very low and very high in respectively, short and long-ends of the curve. This issue could be solved by using a piecewise-constant

volatility functions for the Hull-White process, but we leave this topic for further research 6.3.

For assessment of these volatility levels, we compare the obtained result with extrapolated volatilities from market data using the constant-spread approach as shown in Figure 4.13. Using displaced diffusion extrapolation with $\rho = 0.9$ we can achieve a similar picture as in HCIR case, but not a precise match, with differences of 5bp for Caps maturing after 5-years.

Figure 4.13 shows some anomalous behaviour of 6-month cap volatility across maturities in the DD-method, it is the highest from the set for maturities < 12-years and then decreases below 1-month and 3-month cap volatility levels. This effect comes from Black-to-normal volatility conversion in the caplets as shown in Figure 4.14. While in Black (log-normal) volatilities the tenor-structure of volatilities is strict, e.g. 12-month volatility is smaller than 6-month, 6-month smaller than 3-month, etc., after conversion to normal caplet volatilities, the 12-month caplets obtain very high volatility around 5-year maturity, simply from the differences in forward rate levels between the curves.

The table of calibrated model parameters for the 3% cap calibration case is given in Appendix D.

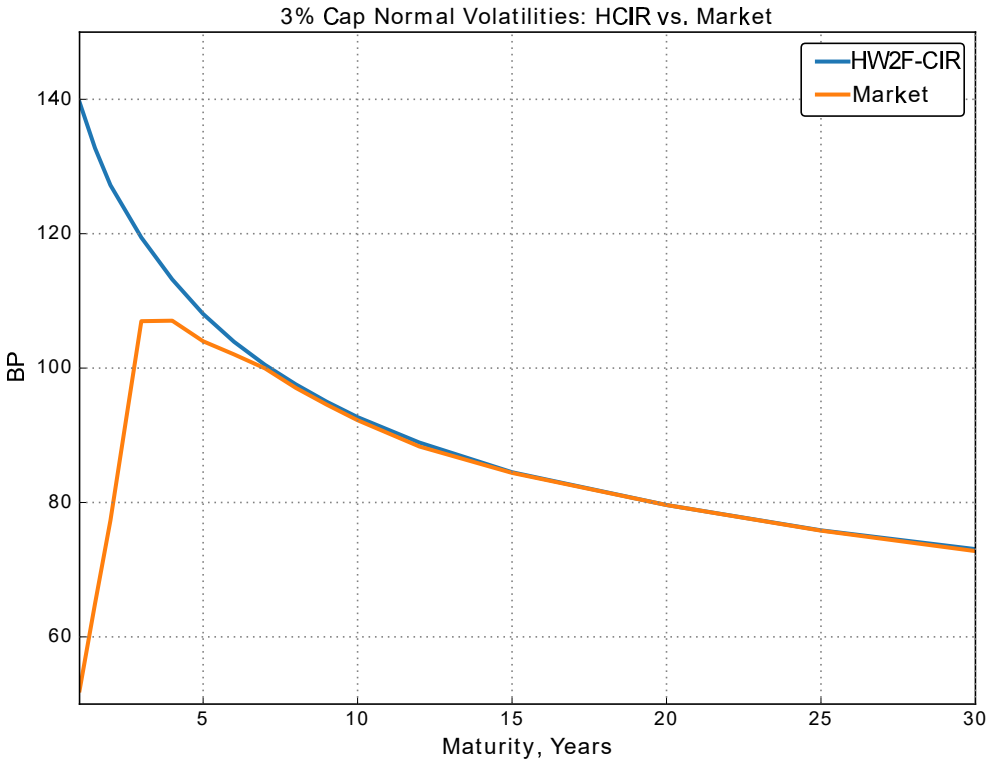

Figure 4.11: 6-month cap volatility comparison between HW2F-CIR model and market data. The model accurately calibrates to 5-year and longer maturity cap volatilties, but has difficulty fitting the short-end volatilities as they are very low.

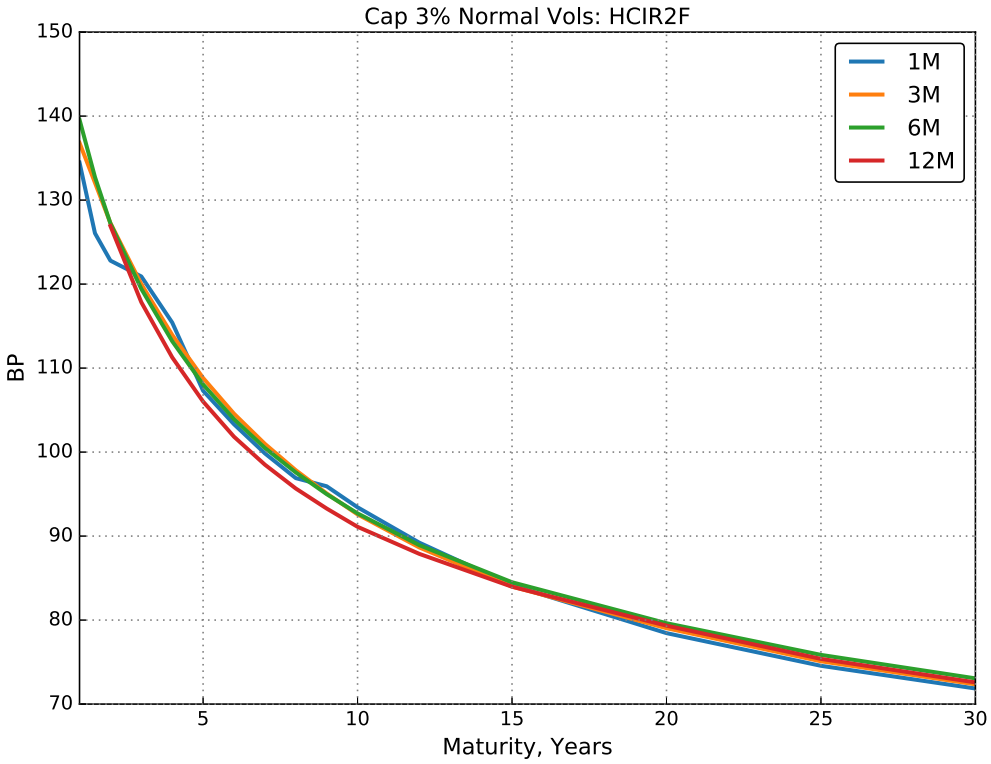

Figure 4.12: Multi-tenor cap volatilities for HW2F-CIR model. The model took market 6-month volatilities and extrapolated to other tenors.

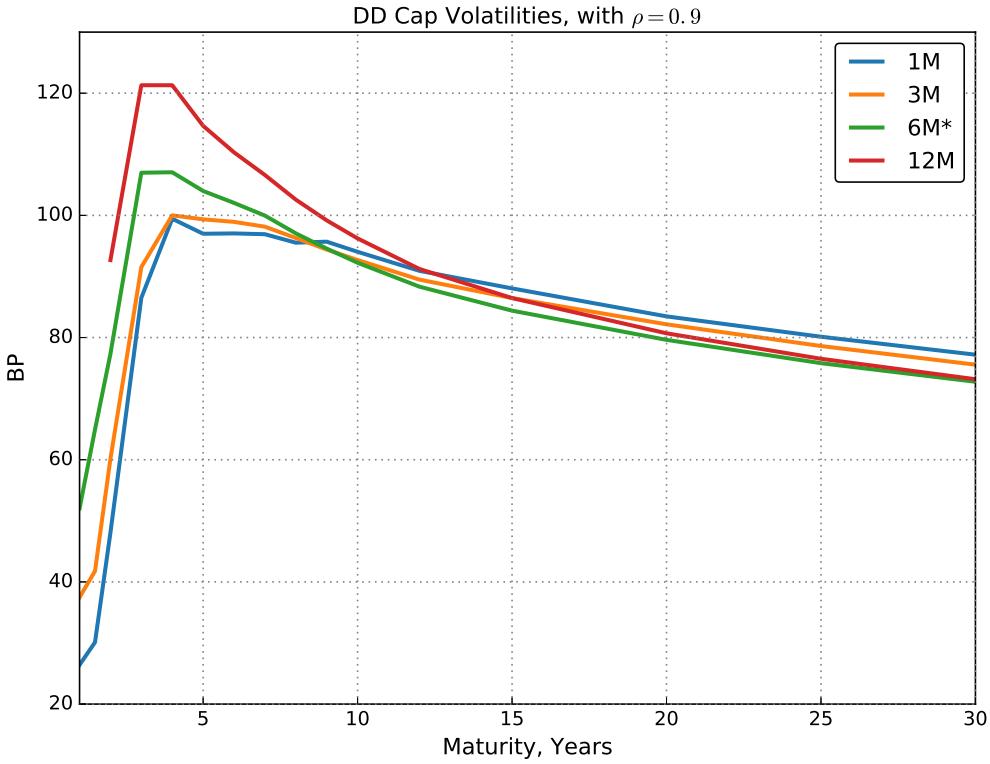

Figure 4.13: Tenor-by-tenor comparison of cap (normal) volatilities. Plots compare market 6-month 3% and DD-extrapolated cap volatilities for other tenors with $\rho = 0.9$.

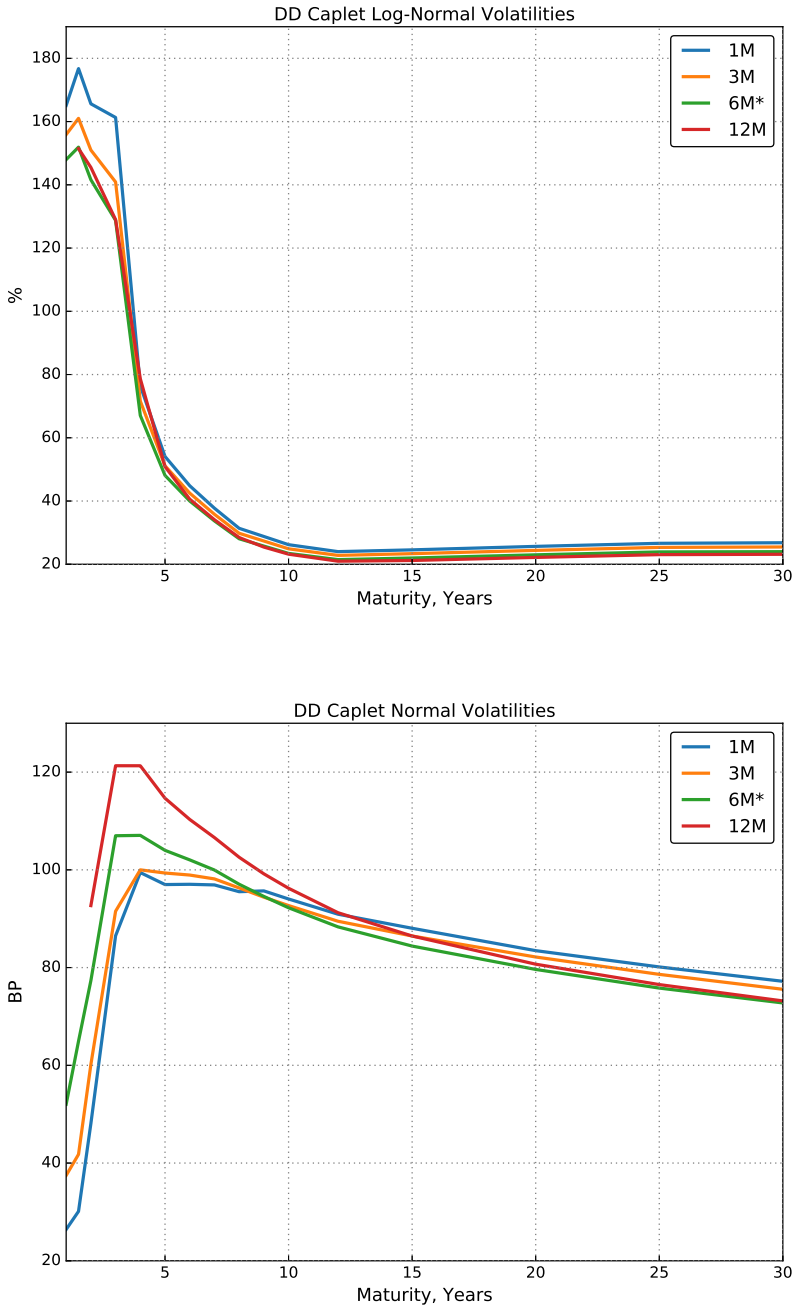

Figure 4.14: Tenor-by-tenor comparison of cap normal and log-normal volatilities. Results plotted for Kienitz-extrapolated volatilities using $\rho = 0.9$.

4.4 Multi-Strike and Cap Surface Fitting

In this section, we include the additional simulation results for the multi-tenor cap pricing problem. We show the calibration and pricing results for multi-strike caps when the calibra-

tion was performed using $3, 4, 5\%$ 6-month EUR caps and analyse the results, demonstrating that the HCIR model is not flexible enough to calibrate to the market volatility smile. Then, we also show our test cases with data from different historical dates, which demonstrate that the HCIR model cannot well fit the market forwards if the LIBOR-OIS spread term structure does not satisfy the smoothness criteria of CIR model.

To test the HCIR model ability to deal with multiple cap strikes and volatility smile, we have calibrated the HW2F-CIR model to caps on three chosen strikes: $3, 4, 5\%$. The calibration result demonstrated in Figure 4.15, shows that the HW2F-CIR model cannot replicate the market smile. The latter fact is already known for the standard HW2F model, and our hybrid version does not correct for this. The resulting calibration to three strikes ended up in an intermediate fit without any smile features, preserving 3% cap volatilities in the short end and 4% volatilities in the long-end of the curve.

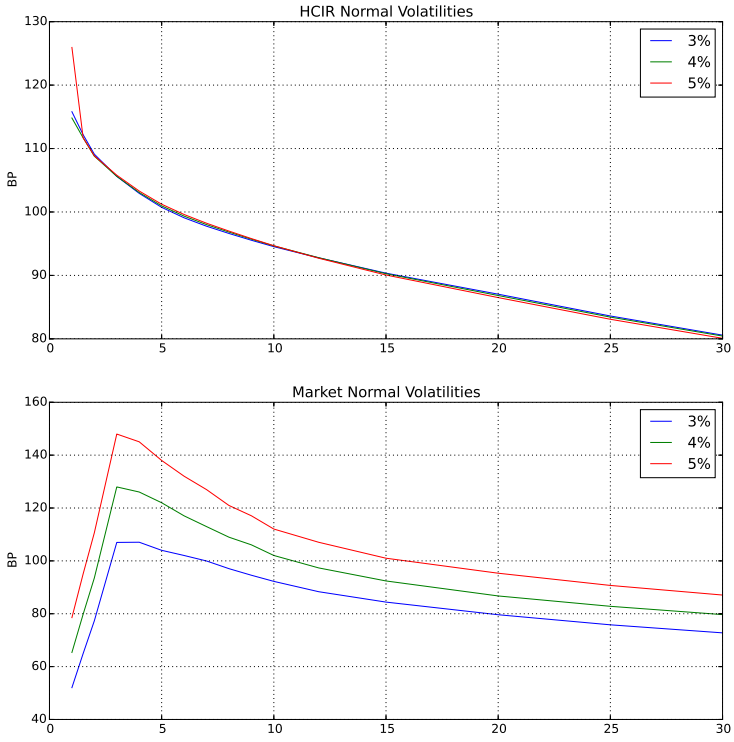

Figure 4.15: HCIR calibration result to 3,4,5% EUR 6-month caps. We re-price $3, 4, 5\%$ caps and 6-month forward rates to show the overall resulting fits. Data from 22-Nov-2013

4.4.1 The 'Tail' Problem

Our results in the previous sections show that while we can fit the HW2F-CIR model to series of multi-maturity caps on a single strike or all the ATM levels, we are not able to reproduce the full volatility surface. This problem mainly stems from the HW2F model, which does not handle smile well.

In our particular case, we are overvaluing the low-strike caps and undervaluing the high-strike caps. We show an example Figure 4.16 below.

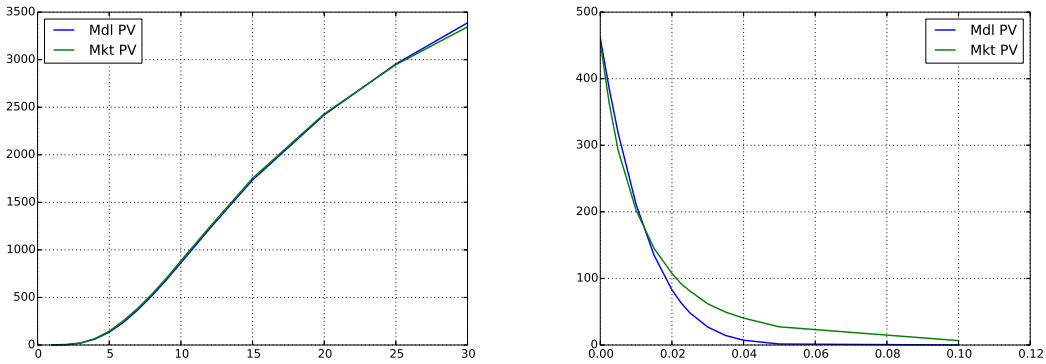

Figure 4.16: Comparison of present value for model and market caps. 6-month 1.5% caps over maturities from 1-year till 30 years (left), 5-year caps case over strikes from 0.25% to 10% (right)

Once we look at the Black volatilities - we see that while the fit over maturities is good, the volatility smile is not well preserved in the model.

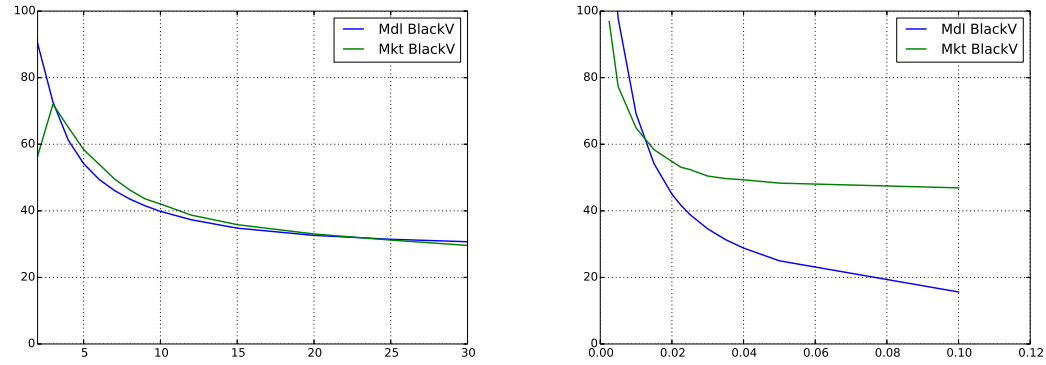

Figure 4.17: Comparison of HCIR model and market Black volatilities for 6-month 1.5% caps case over maturities from 1-year till 30 years (left). 6-month tenor, 5-years maturity caps with strikes from 0.25% to 10% (right)

The reason this happens is that the Black volatilities in the market are practically flat, from 3% strike onwards. This paves the way for either a (shifted) log-normal model, or some other heavy-tailed model. The HW2F model is normal, i.e. assumes normally distributed interest rates. As the rates are low in the current market, a large part of the simulated future rates are negative. Therefore, to replicate the flat Black volatilities, one would need something like an 'increasing normal volatility structure' as in the following figure:

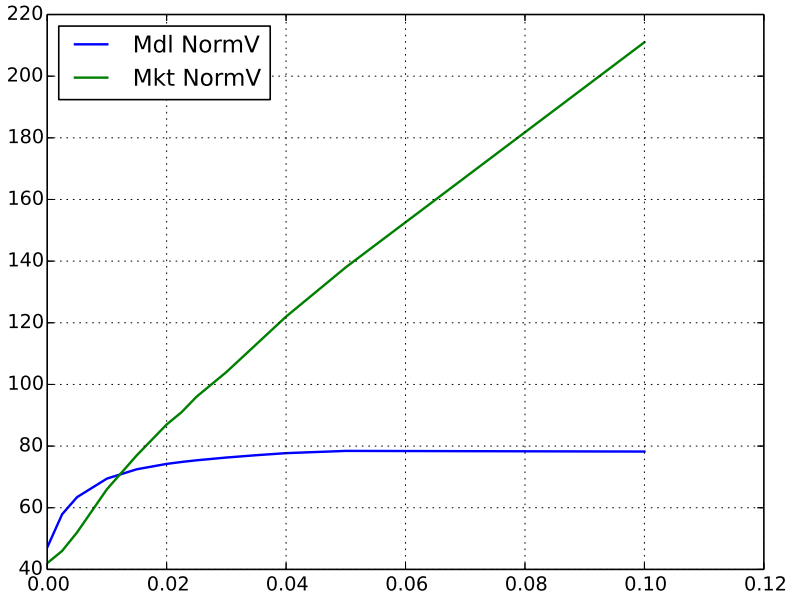

Figure 4.18: Market and HCIR model normal volatilities for 6-month caps with 5-year maturities, ranging from 0.25% to 10% in terms of strike.

In table 4.2 we give example cap values for HW2F-CIR model, HW2F model, Black model and Bachelier (normal) model. We set the volatilities for Black and Bachelier models as constant but aligned to match the market cap values around the 1.5% strike. From the table results we can see the following differences in the model results:

- The difference between full HW2F-CIR model and HW2F (no CIR) is minor, which means that the fitted CIR model has a small impact on the 6-month Cap values and the major PV part is carried by the HW2F component. The CIR model yields a small heavy-tail addition on the right side of the histogram.
- The HW2F model implies a normal distribution of rates, therefore the result is similar to the Bachelier result with constant volatility.

- On the other hand, the log-normal (Black) model has a heavy tail in the distribution, which gives much larger cap values for higher strikes, such as $4, 5, 10\%$.

Model	Vol	0%	0.25%	0.5%	1%	1.5%	2%	2.25%	2.5%	3%	3.5%	4%	5%	10%
HW2F-CIR	-	465	385	318	211	135	82	63	48	26	14	7	1	0
HW2F	-	462	381	314	208	132	80	62	46	25	13	6	1	0
Black	55%	444	338	263	181	135	106	95	86	71	60	51	39	14
Bachelier	0.73%	495	411	336	217	135	80	61	45	24	12	5	0	0

Table 4.2: Table of sample 6-month Caps prices for different strikes.

We confirm the above observations in forward-rate histograms for all four models shown in Figures 4.19 and 4.20. To sum up, while the HW2F model gives enough flexibility to fit the term-structure of the volatility, we do not have many degrees of freedom to fit the smile. While this can be done to some extent to minimise the cap replication errors over some chosen strike (or all ATM levels), the other strikes would remain under/over-priced.

The market volatilities, as shown in Figure 4.17, when plotted against the strikes in log-normal form, are much flatter than the normal volatilities. This is the main reason why fitting HW or HCIR models, who assume normally distributed rates as in Figure 4.18 is difficult.

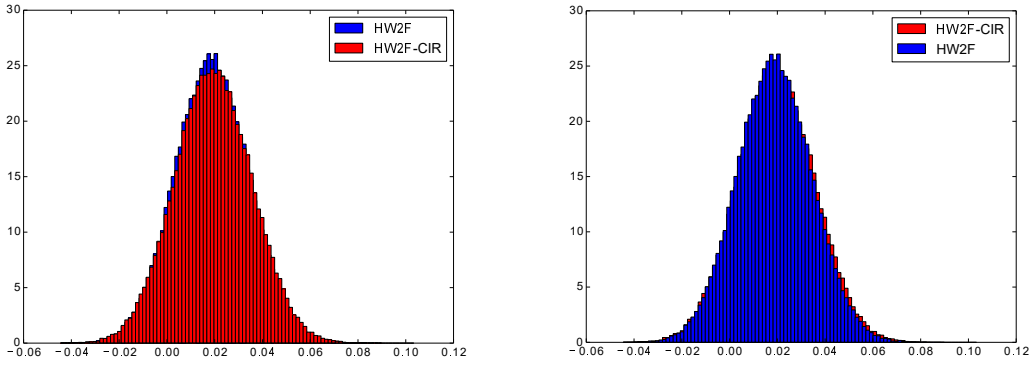

Figure 4.19: Forward rate distribution comparison from HW2F-CIR, HW2F models. We show the distribution of $F(T, S)$ values, where $T = 4.5, S = 5$-years

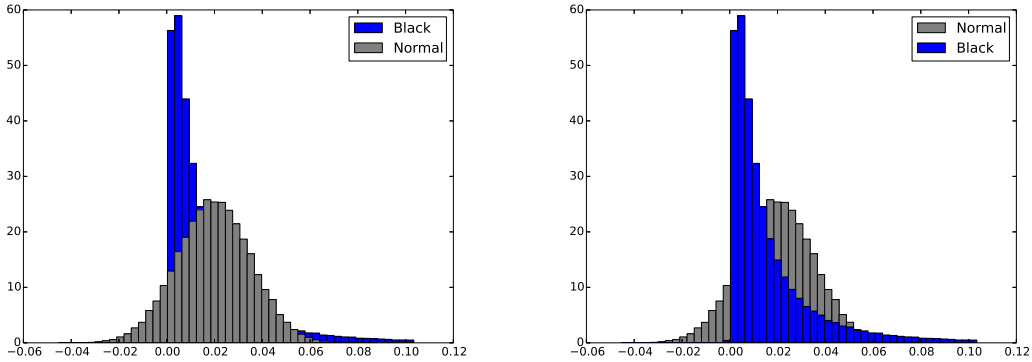

Figure 4.20: Forward rate distribution comparison from Black and Bachelier models. We show the distribution of $F(T, S)$ values, where $T = 4.5, S = 5$-years

4.5 Calibration of HCIR in historical high-basis scenarios

In this section, we seek to investigate how well the HWCIR model calibrates and performs under different market conditions. To do this we picked three historical dates, namely:

- November 30, 2011 (large basis)
- November 30, 2012 (small basis)
- November 30, 2013 (small basis)

and calibrated the model to 3-month forwards and caps, and also 6-month forwards. We implied the 6-month caps from the model.

4.5.1 High-Basis Spread Case, USD Market

In the following sets of figures 4.21,4.22,4.23 we show the market vs model cap and forward fits. The figures are organised in reverse chronological order, first one for data from 2013, then from 2012 and the last one from 2011. The following figures show that:

- The 3% HCIR caps can be repriced well when compared to market (Black) caps.
- The fit of market forwards is best in the 2013 dataset and worst in 2011.

  The cause of a bad fit is the substantially different OIS forward and LIBOR-forward curve structure, or 'hump'. The HCIR model introduces a gap between LIBOR and OIS forward curves of a smooth functional form and cannot properly represent the 'dip' at $10 - 12$-year OIS forward points, which we have in the dataset.
- The implied 6-month caps behave differently on different dates:
  - The 6-month cap value is close to 3-month on 22-Nov-2013, as CIR $\sigma = 15\%$

– The 6-month caps have increasingly greater value than 3M on 30-Nov-2012, as CIR $\sigma = 51\%$

– The 6-month caps have greater with constant distance on 30-Nov-2011, as CIR $\sigma = 12\%$

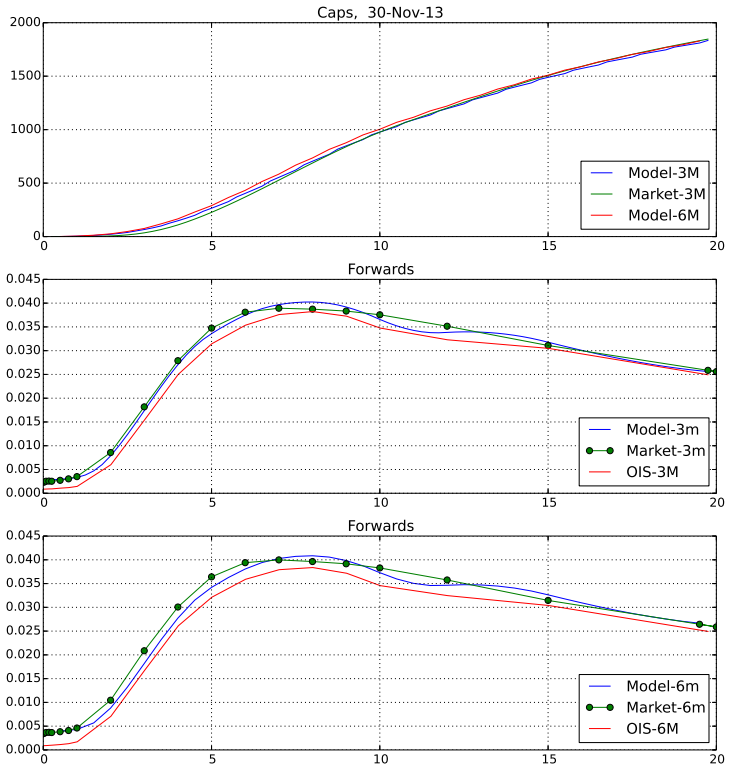

Figure 4.21: HCIR model calibrated to 3 and 6-month USD forwards and 3-month USD caps. The 6-month caps are the resulting extrapolation. Data taken from Reuters Eikon, 30-Nov-2013

Maturity (years)	1	2	3	4	5	6	7	8	9	10	12	15	20
Market (bp)	< 1	2	20	81	192	334	494	660	822	968	1209	1532	1916
Model (bp)	1	9	38	103	211	346	499	656	809	949	1184	1497	1880
Vega Chg. (%)	0	0	47	23	12	6	3	2	1	0	0	0	0

Table 4.3: 30-Nov-13 USD 3-month market and HCIR model cap price (USD) comparison table.

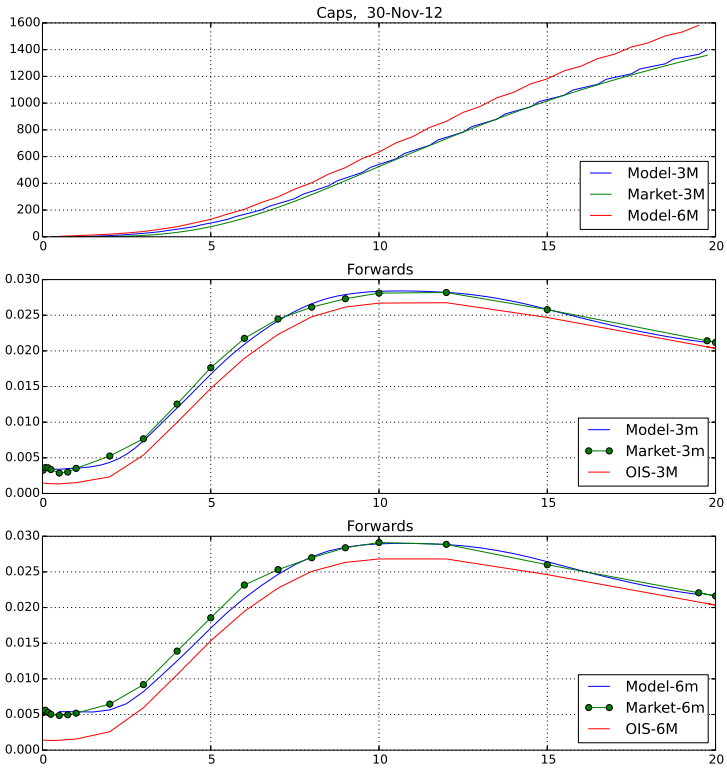

Figure 4.22: HCIR model calibrated to 3 and 6-month USD forwards and 3-month USD Caps. The 6-month caps are the result of extrapolation using the model. Data taken from Reuters Eikon, 30-Nov-2012

Maturity	1	2	3	4	5	6	7	8	9	10	12	15	20
Market (bp)	< 1	2	7	26	63	120	194	283	382	485	691	979	1358
Model (bp)	< 1	3	13	37	78	138	215	304	401	502	703	985	1366
Vega Chg. (%)	0	0	0	27	16	10	6	4	2	1	0	0	1

Table 4.4: 30-Nov-12 USD 3-month market and model cap present value comparison table. The Black-vega change (%) is the change in volatility needed to adjust for the difference between the market and model.

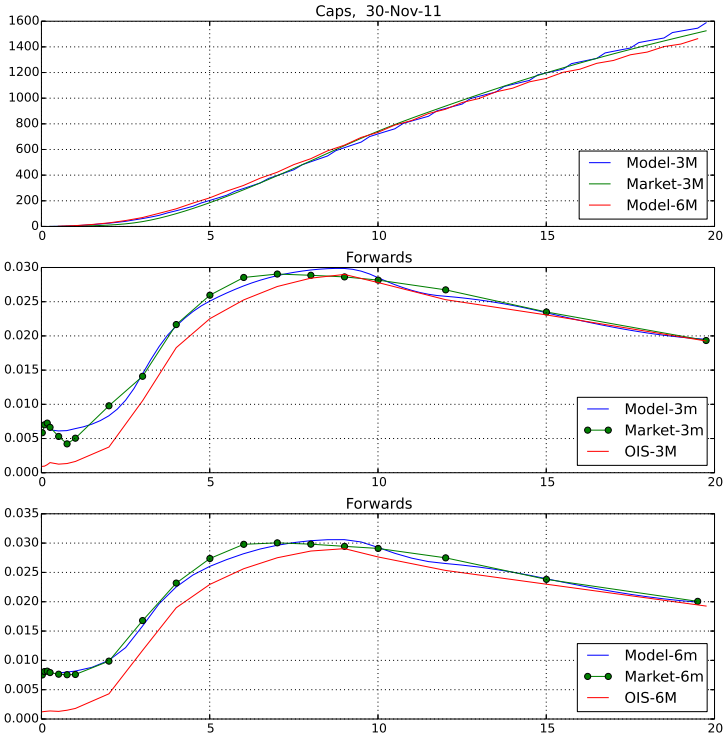

Figure 4.23: HWCIR model calibrated to 3 and 6-month USD forwards and 3-month USD caps. The 6-months Caps are the result of extrapolation using the model. Data taken from Reuters Eikon, 30-Nov-2011

Maturity	1	2	3	4	5	6	7	8	9	10	12	15	20
Market (bp)	< 1	5	22	73	152	248	356	472	591	709	911	1180	1534
Model (bp)	2	17	48	104	183	277	381	491	603	714	913	1182	1549
Vega Chg. (%)	0	0	31	15	6	3	1	0	0	-1	0	0	1

Table 4.5: 30-Nov-11 USD 3-month market and model PV Cap comparison table. The black-vega change (%) is the change in volatility needed to adjust for the difference between the market and model.

4.5.2 High-Basis Spread Case, EUR Market

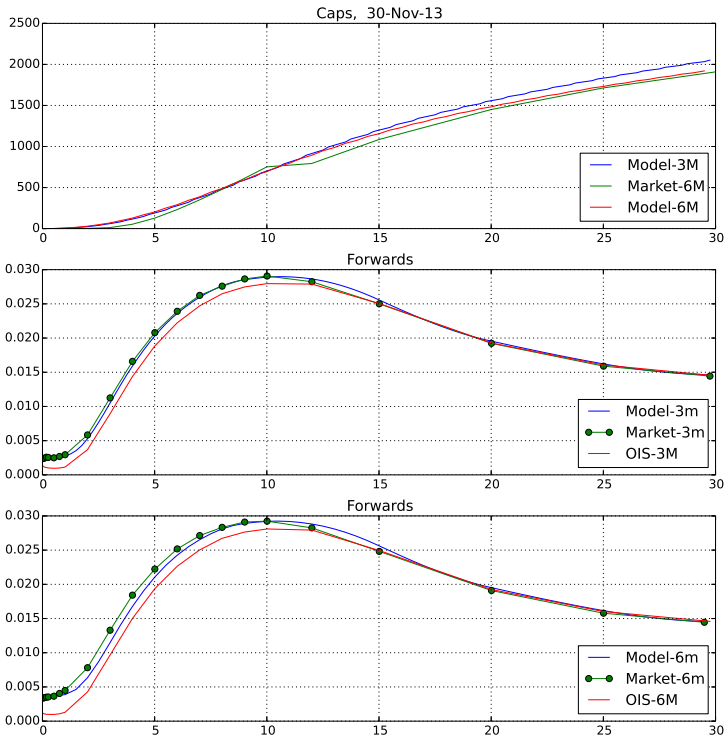

Figure 4.24: HCIR model calibrated to 3 and 6-month EUR forwards and 6-month EUR caps. The 3-month caps are the result of extrapolation using the model. Data taken from Reuters Eikon, 30-Nov-2013

Maturity	1	1	2	3	4	5	6	7	8	9	10	12	15	20	25	30
Market (bp)	0	0	1	11	52	127	231	349	476	611	752	793	1085	1450	1713	1909
Model (bp)	1	6	16	47	98	167	250	343	443	547	650	852	1123	1460	1713	1920
Vega Chg. (%)	0	165	131	102	52	22	6	-1	-5	-7	-9	3	1	0	0	0

Table 4.6: 30-Nov-13 EUR 6-month market and model cap present value comparison table. The Black-vega change (%) is the change in volatility needed to adjust for the difference between the market and model.

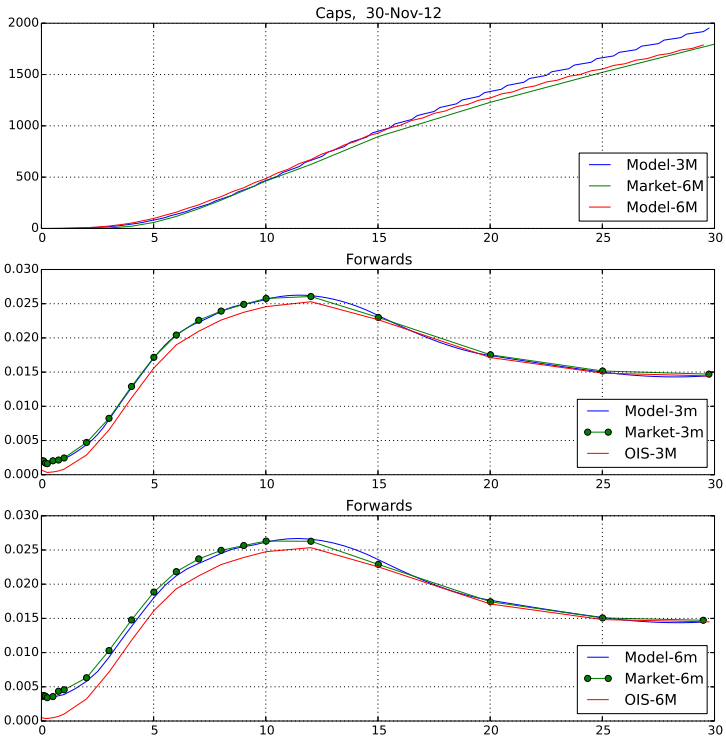

Figure 4.25: HCIR model calibrated to 3 and 6-month EUR forwards and 6-month EUR caps. The 3-month caps are the result of extrapolation using the model. Data taken from Reuters Eikon, 30-Nov-2012

Maturity	1	1	2	3	4	5	6	7	8	9	10	12	15	20	25	30
Market (bp)	0	0	1	4	21	58	116	191	275	366	461	623	894	1228	1521	1795
Model (bp)	0	1	3	14	36	74	128	196	272	357	446	632	899	1249	1536	1788
Vega Chg. (%)	0	10	23	36	20	9	4	1	0	-1	-1	0	0	0	0	0

Table 4.7: 30-Nov-12 EUR 6-month market and model cap present value comparison table. The Black-vega change (%) is the change in volatility needed to adjust for the difference between the market and model.

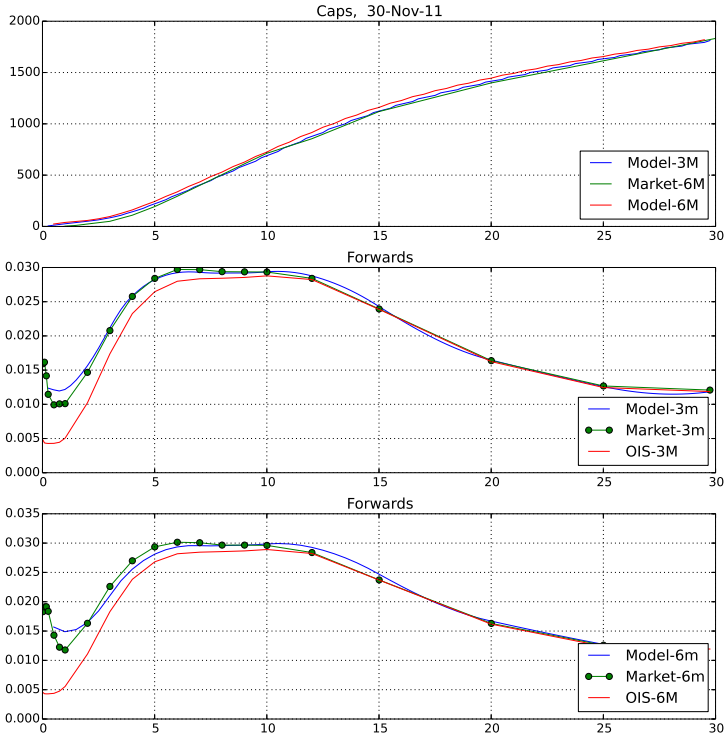

Figure 4.26: HCIR model calibrated to 3 and 6-month EUR forwards and 6-month EUR caps. The 3-month caps are the resulting extrapolation. Data taken from Reuters Eikon, 30-Nov-2011

Maturity	1	1	2	3	4	5	6	7	8	9	10	12	15	20	25	30
Market (bp)	2	10	23	49	109	193	293	399	504	609	712	854	1119	1398	1614	1832
Model (bp)	23	38	48	74	127	203	292	388	486	583	681	875	1130	1426	1641	1819
Vega Chg. (%)	0	135	49	19	7	2	0	-1	-1	-2	-2	1	0	0	0	0

Table 4.8: 30-Nov-11 EUR 6-month market and model cap present value comparison table. The Black-vega change (%) is the change in volatility needed to adjust for the difference between the market and model.

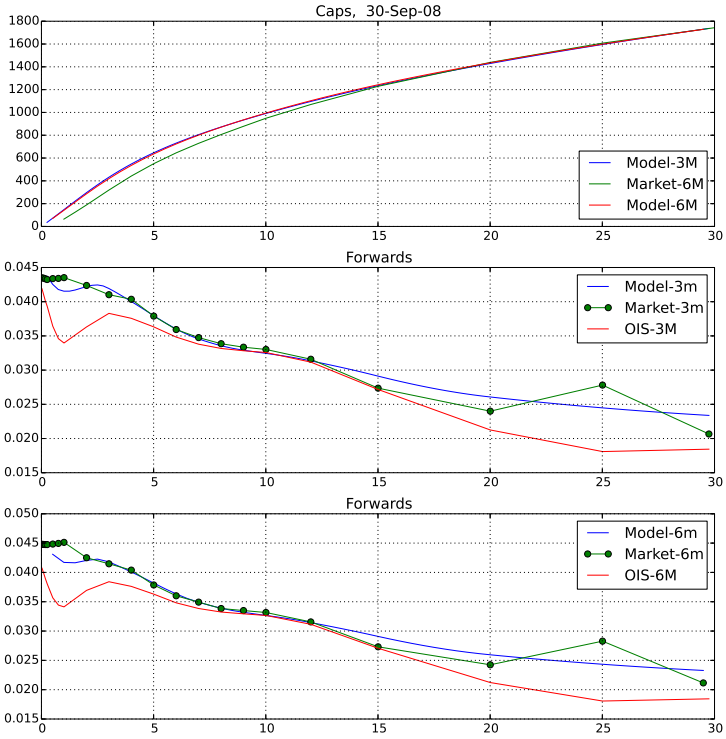

Figure 4.27: HCIR model calibrated to 3 and 6-month EUR forwards and 6-month EUR caps. The 3-month caps are the result of extrapolation using the model. Data taken from Reuters Eikon, 30-Sep-2008

Maturity	1	1	2	3	4	5	6	7	8	9	10	12	15	20	25	30
Market (bp)	64	124	187	318	441	550	645	728	805	877	948	1069	1228	1438	1607	1742
Model (bp)	69	141	213	353	478	587	680	762	836	903	964	1076	1220	1417	1583	1728
Vega Chg. (%)	0	47	27	14	9	6	4	3	2	1	0	0	0	0	0	0

Table 4.9: 30-Sep-2008 EUR 6-month market and model cap present value comparison table. The Black-vega change (%) is the change in volatility needed to adjust for the difference between the market and model.

4.5.3 Cap Pricing with Negative Rates

For the last, and one of the most important tests, we look into HCIR model ability to calibrate and price caps in negative interest rate environment. In the following figures 4.28 and 4.29 we show the forward-curves fit for 30-April-2015 dataset and the cap-volatility fits for all fixings, when the calibration was performed with 6-month ATM caps. Here we also provide the multi-curve cap volatilities in Figure 4.30, but do not test against displaced-diffusion volatilities as standard LMM model does not work for negative rates. The HCIR model is especially useful in the post-credit crisis interest rate markets, where rates are often negative.

The forward rate fit has errors up to 5bp - starting forward point does not match, and there are possible interpolation artefacts in multiple other places. The 6-month cap volatilities, on the other hand, do have a good (< 3bp) fit, except for first three points: 6-month,1 and 1.5-year which differ a lot but are mainly influenced by the mismatch in very-short end forward rates. We provide detail volatility surfaces in Appendix D.2.4.

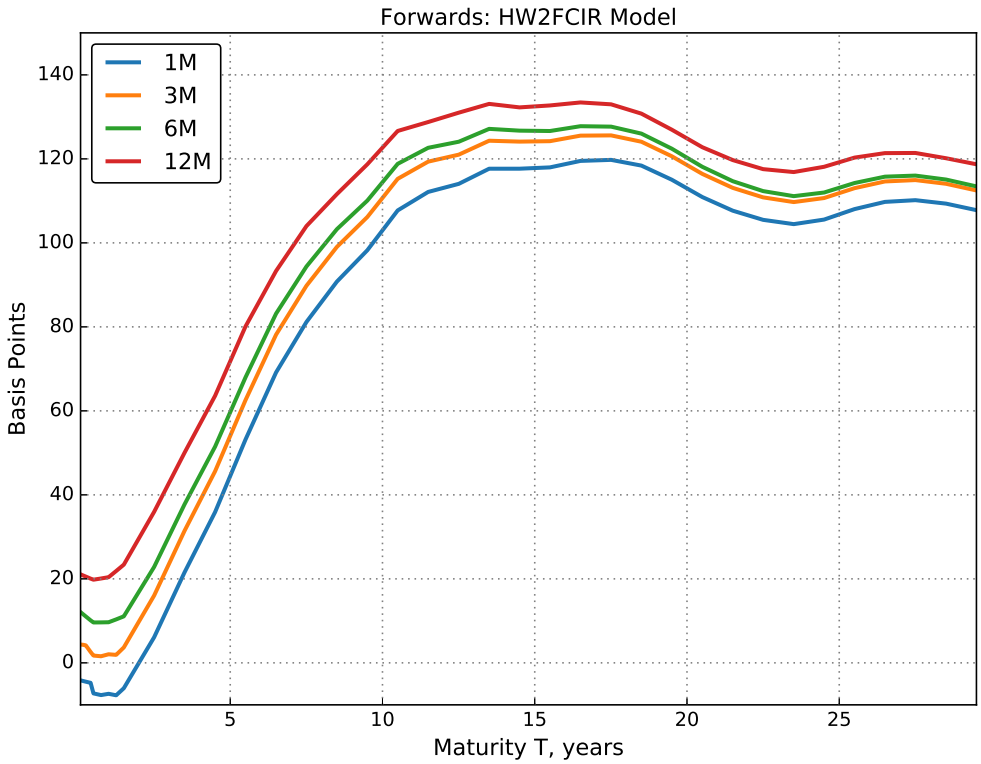

Figure 4.28: HCIR Forwards for 30-Apr-2015

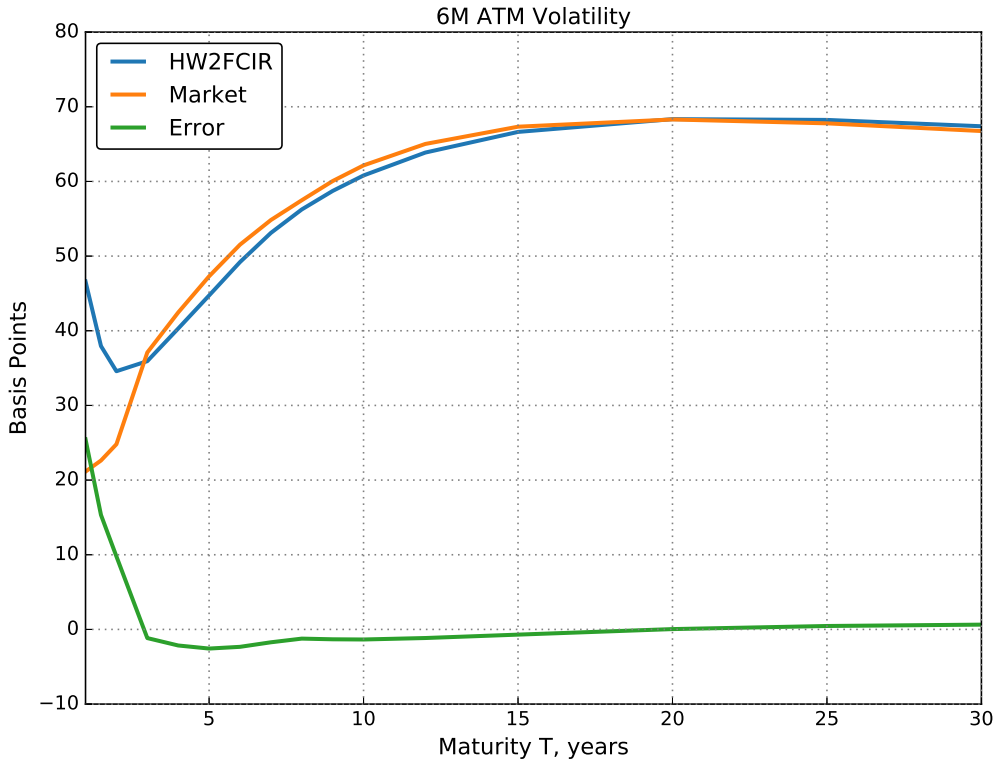

Figure 4.29: HCIR and market 6-month ATM cap volatilities. Data from 30-Apr-2015.

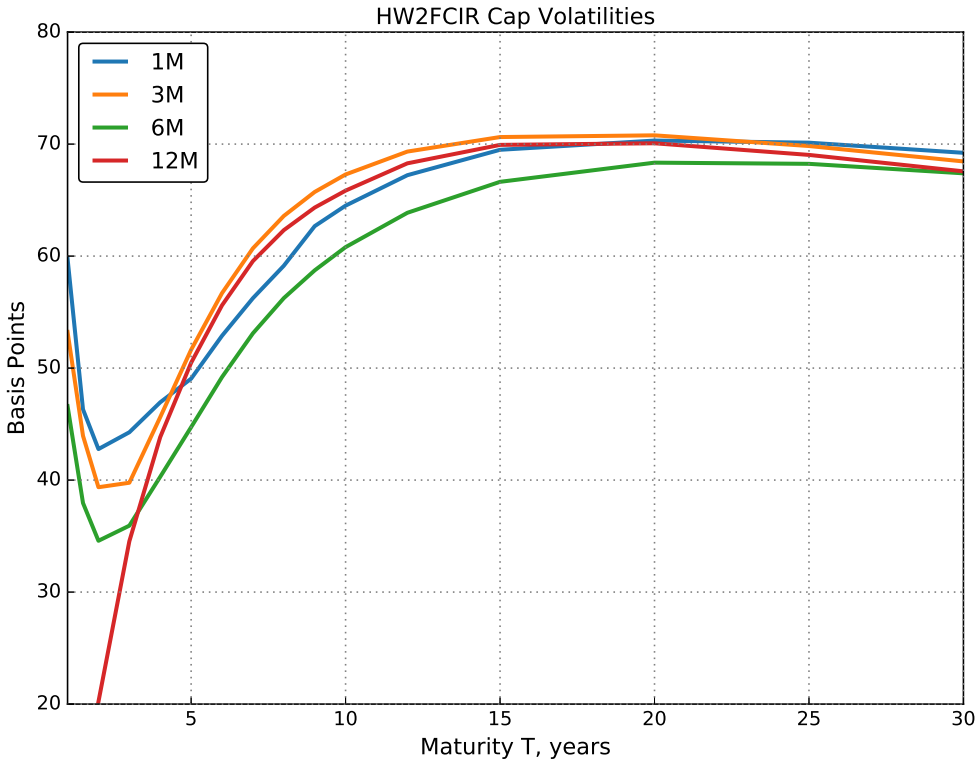

Figure 4.30: Multi-curve 1,3,6,12-month HCIR ATM cap volatilities. Data from 30-Apr-2015.

4.5.4 Conclusion

The Hybrid Hull-White-CIR model (Savickas, 2015) is a novel stochastic basis model within the short-rate framework. We have shown that a 5-curve (including OIS and 1, 3, 6, 12-month LIBOR curves) model can be semi-analytically calibrated to liquid, existing market yield curves and cap volatilities and afterwards, using the fully-parametrized model we have re-priced the market caps.

Our analysis shows that the HCIR model works best when the market forward LIBOR-OIS spread has a smooth structure. Some irregularities are present in the model-to-market forward fit. In our test cases, we had errors of 5bp in many forwards and larger errors with the few starting points of the LIBOR-OIS spreads, where they reached 20bp. In our tests, we were able to match the market caps with few bp error in volatility, when the maturity of the cap is $>= 3$-years. The HCIR model, as well as HW2F model, could not replicate the very low (20bp) market volatilities in the very short-term end of the volatility curve and

potentially needs a piece-wise constant volatility construct. The model-to-market volatility mismatch is even larger if HW1F model is used for OIS modelling, which was the main reason for performing most of calibrations and research on the HW2F-CIR Hybrid model.

We can conclude from our tests that the HCIR model can be calibrated to single-strike caps and used for extrapolation and pricing of caps on illiquid tenors. We have benchmarked the HCIR model against a displaced-diffusion volatility extrapolation technique and shown that the resulting HCIR volatilities are in line with current market-standard techniques. What is more, the HCIR model does not require parameter calibration with exotic derivatives or historical data like the DD approach and therefore is a more robust technique for illiquid cap pricing.

Overall, the HCIR model is a "clean" short-rate mathematical model with some limitations on the market data it can fit. There are, however, workarounds for some of them in practice. For instance, short-maturity caps should be fitted much better using piecewise constant volatility $\sigma(t)$, but this would complicate the valuation formulas. Then, the leftover error in LIBOR-OIS fitting with CIR model can be 'adjusted' by adding a time-dependent term-structure factor $\psi_c(t)$, like in the CIR++ model (Brigo and Mercurio, 2006). However, this adjustment would make the model less mathematically consistent and harder to calibrate.

Chapter 5

Hybrid Model for CVA Valuation

5.1 Introduction

Another important application of the HCIR model with a stochastic basis is the counterparty valuation adjustments (CVA) valuation. CVA charge is included in every over-the-counter trade and if two parties do not agree on the outstanding CVA value, this would lead to trade disputes and missed opportunities as discussed in Chapter 1. Additionally, as CVA is a default-risk measure, using a more elaborate model which includes stochastic basis and potential correlation between the basis would improve the performance of the risk-management strategies.

In this chapter, we outline the setup and experimental results, where we price CVA for a portfolio of a single interest rate swap using the hybrid HW2F-CIR model. First, we introduce the basics of CVA valuation given some stochastic model for the drivers of portfolio value and probability of default. Then, we evaluate CVA under the hybrid model and compare the result to a benchmark, pure HW2F model.

In the first experiment, we assess the situation when the default probability is not correlated with the size of LIBOR-OIS spread, and in the second one, we impose correlation between the CIR state variable, driving the size of LIBOR-OIS spread and the counterparty default probability.

5.2 CVA with short rate models.

To estimate the credit value adjustment for a single derivative or a portfolio position, we have to compute the expected losses L at time-zero:

$$\text{CVA} = \mathbb{E}^Q[L*] = (1-R)\int_0^T \mathbb{E}^Q\left[D(0,t)(L(t))^+\lambda(t)\right]dt, \tag{5.1}$$

where R is the recovery fraction, $D(0,t)$ is the stochastic discount factor, $(L(t))^+$ is the positive net present value of underlying portfolio at time t and $\lambda(t)$ is the instantaneous default probability.

To obtain a fair CVA comparison of all models we calibrate them to market forwards and caps, obtaining risk-neutral estimations of their term-structure and volatility parameters as done in section 4.3 therefore our CVA pricing scheme works fully under risk-neutral pricing measure. We see our approach as a better option, as the alternative of using historical parameters for each of the model would yield incomparable CVA results. For every model, we estimate CVA as:

$$\text{CVA} = \mathbb{E}^Q[L*] = (1-R)\int_0^T \mathbb{E}^Q\left[D(0,t)(L(t))^+\lambda(t)\right]dt, \tag{5.2}$$

$$= (1-R)\int_0^T P_{\text{OIS}}(0,t)\mathbb{E}^{Q_t}\left[(L(t))^+\right]\lambda(t)dt, \tag{5.3}$$

$$\text{CVA} \approx (1-R)\sum_{i=1}^{N} P_{\text{OIS}}(0,T_i)\mathbb{E}^{Q_{T_i}}\left[(L(T_i))^+\right](\text{SP}(T_i)-\text{SP}(T_{i-1}))\,dt. \tag{5.4}$$

Here we price CVA under forward Q_T-measure, and the hazard rate function $\lambda(t)$ has a deterministic hazard rate. The approximation in (5.4) uses survival probability

$$\text{SP}(T) = \mathbb{P}\left[\tau \geq T\right] = \exp\left(-\int_T^\infty \lambda(t)dt\right). \tag{5.5}$$

where τ is the time of default.

Here we also introduce the debt value adjustment (DVA), which is the price of default to the counterparty, if the first party defaults. In the following we will assume that the default risks for both counterparties are equivalent, but the portfolio value only contributes

to DVA, when it is negative $(L(T_i))^- = -L(T_i)$ if $L(T_i) < 0$ else 0.

$$\text{DVA} \approx (1-R)\sum_{i=1}^{N} P_{\text{OIS}}(0,T_i)\mathbb{E}^{Q_{T_i}}\left[(L(T_i))^-\right](\text{SP}(T_i)-\text{SP}(T_{i-1}))\,dt. \tag{5.6}$$

5.2.1 Portfolio Drivers

We want to estimate CVA in HCIR and the benchmark model for the following products:

1. Fixed-floating LIBOR swaps,
2. OIS-LIBOR swaps,
3. Interest rate caps.

As given in (5.1), to assess CVA value of any portfolio $L(t)$ we need to know the stochastic discounting factor $D(0,t)$, which is driven by OIS rate (HW2F or HW1F) model and the recovery fraction R, which we assume to be constant at 0%. This assumes that upon default there is no leftover value from companies assets to cover even part of its liabilities on this portfolio. This is a simplified assumption as modelling the recovery value is a research field by itself.

Then, we value the stochastic time-dependent expected positive exposure $E(t) = (L(t))^+$ under HCIR model using scenario generation

$$E(t) = (L(t))^+ = (L(t,x(t),y(t),z(t)))^+, \tag{5.7}$$

where L is the portfolio value function, dependent on HW2F model state variables $x(t), y(t)$ and the CIR model state variable $z(t)$

In CVA valuation we shall directly use the survival function $\text{SP}(t)$ and distinguish two cases for our use:

1. First, we define a simple, deterministic survival function, for our example CVA computation, where $\text{SP}(T = T_0 = 0) = 1$ and $\text{SP}(T > T_N = 30) = 0$.
   - We choose it to be linear: $\text{SP}(T_i) - \text{SP}(T_{i-1}) = \frac{T_i - T_{i-1}}{T_N - T_0}$.
   - Thus, if we space our time-snapshots T_i every-year, every measured interval carries a deterministic $\frac{1}{30}$ weight for default in (5.4).
2. For the second case, we want to add some randomness in the default rate and ability to correlate it with the CIR state variable $z(t)$.
   - We set the default weight $D_{(i-1,i)} = \text{SP}(T_i) - \text{SP}(T_{i-1})$ for each period i as a

uniformly-distributed random number:

$$D_{(i-1,i)} \sim 2 \left[\frac{T_i - T_{i-1}}{T_N - T_0} \right] \mathcal{U}. \tag{5.8}$$

where $\mathcal{U}$ is the standard uniform random variable over period $[0, 1]$.

- The average of the default weight above is the same as in deterministic case, but with added randomness. The portfolio still expires at $T = 30$ (years).

The deterministic D will be used in most of the following tests. The second case is interesting when the default weight D is related/correlated with the size of the basis spread via a Gaussian copula and we can investigate the impact of such wrong-way risk, as discussed in section 5.4.

The simulation (in both cases) is carried out by function (5.2) by simulating random paths for HCIR state variables $x(t), y(t), c(t)$. Pricing of the defined portfolio containing a single interest rate swap was done following the guidelines in (Savickas et al., 2014). We valued the portfolio at discrete time-points T_i and applied the default weight D. This approach gives an approximate CVA value for our portfolio, but if we do use enough time-points in the simulation, the overall result should be close to the true value.

5.2.2 CVA Setup under HCIR and Benchmark

To fairly compare CVA values with our hybrid HW2F-CIR model, we need a similar, short-rate based standard model or at least a normal-distribution based model to use in these tests. To our knowledge, the following options are available:

- HW2F model for OIS with added constant basis spread for the basis.
- HW2F model for τ-forward LIBOR curve. We could calibrate this model to cap data, using OIS discounting and treating the LIBOR forward curve as independent of the OIS curve.

While the second option offers more flexibility, it does not fit out purpose as we cannot evaluate CVA on IRS if not all tenors have traded caps. On the other hand, the first option with fixed basis spread is a viable option.

As shown in Appendix C.2, the simple HW1F model the discount bond price is expressed as:

$$P(t,T) = \frac{P^M(0,T)}{P^M(0,t)} e^{-B(t,T)x(t)} \cdot \exp\left\{ -B(t,T)\frac{\sigma^2}{2a^2}\left(1-e^{-at}\right)^2 - B(t,T)^2\frac{\sigma^2}{4a}\left(1-e^{-2at}\right)\right\}, \quad (5.9)$$

and the HW2F price is also expressed similarly:

$$P(t,T) = \frac{P^M(0,T)}{P^M(0,t)} \cdot \exp\left[-B_x(t,T)x(t) - B_y(t,T)y(t)\right] \exp\left\{ -\frac{1}{2}(V(0,T) - V(0,t) + V(t,T))\right\}. \quad (5.10)$$

Using either of these models, we can calibrate them to the term-structure of 6-month forwards and 6-month ATM caps using analytical formulas as in Appendix C.4. Then, by leaving σ_i and a_i parameters the same, but switching the term-structure element $\frac{P^M(0,T)}{P^M(0,t)}$ to a different LIBOR curve, e.g. 3, 1 or 12-month - we can simulate the state variable $x(t)$ and price forwards on any of 1, 3, 6, 12-month LIBOR or OIS curves or price caps using the standard HW formulae.

5.3 CVA for Multi-Curve IRS

In this section, we calibrate the single-curve HW1F, HW2F and hybrid, 2-curve HW2F-CIR models to 6-month LIBOR forward curves and 4% 6-month caps with maturities ranging from 1-year to 30-years. The parameters obtained for each model is shown in Table E.1.

First we have made the CVA/DVA valuations for a single ATM ($K = 2.6839\%$) 30-year 6-month swap, resulting in very close estimates, within 10 EUR for a $10'000$ EUR ATM swap, with guaranteed default within 30-years. An alternative way of assessing the value of CVA is by computing the CVA impact as a change in the fixed rate of the underlying swap. For this particular swap, every 1bp change in the swap fixed leg leads to the CVA value change of 5EUR. As shown in Table 5.1 the CVA adjustment when moving from HW2F to HCIR model decreases by 18 EUR, which is approximately 3.5bp move on the fixed leg of the swap. This leads to a conclusion that in a small basis-spread environment, without wrong-way risk, there may be little need for explicit spread model.

The figures 5.1 and 5.2 show the means and the variances of the simulated IRS value

across time for all the chosen models. They demonstrate that the swap mark-to-market (MtM) simulation means for HW1F and HW2F match perfectly, the HCIR is slightly higher, as a result of CIR model smoothing over LIBOR-OIS forward spreads. Nevertheless, the swap mark-to-market variance over time is smallest under HCIR model, followed by HW2F model with fixed basis. Under HW1F model, the swap variance is of different shape as we are missing the second stochastic driver for OIS, hence the different shape in volatility.

While the difference between HCIR and HW2F model CVA/DVA values is small, valuing CVA as well as DVA with HCIR model leads to a smaller, cheaper CVA charge as the spread in HCIR model has small volatility. Then, one should keep in mind that HW1F and HW2F models yield rather different variance profiles, therefore it is expected that they would be different and in this case, the CVA and DVA values in HW2F model are smaller.

Model	CVA	DVA	Swap MtM (t=0)
HCIR	608	359	-6
HW2F	618	374	0
HW1F	626	384	0

Table 5.1: CVA, DVA and swap MtM values in Euros for and ATM swap with fixed rate of 2.6839%

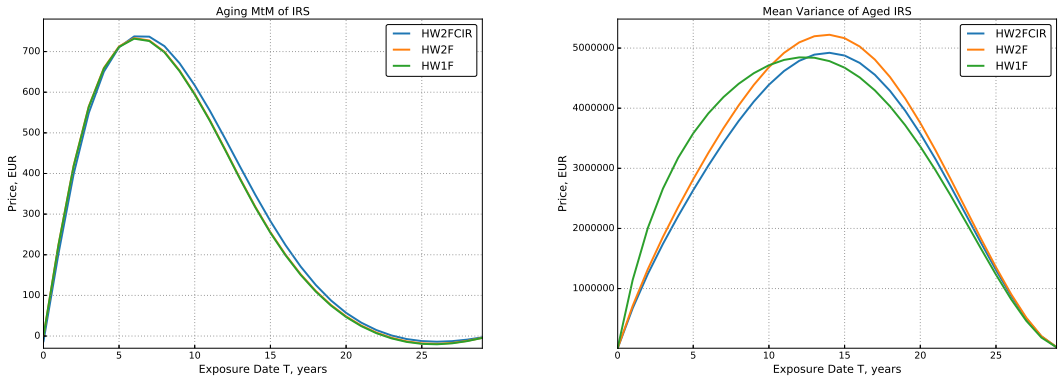

Figure 5.1: Means and variances of the simulated IRS swap with fixed maturity under HCIR and HW-models as a function of the exposure date T. All models calibrated to 22-Nov-2013 dataset.

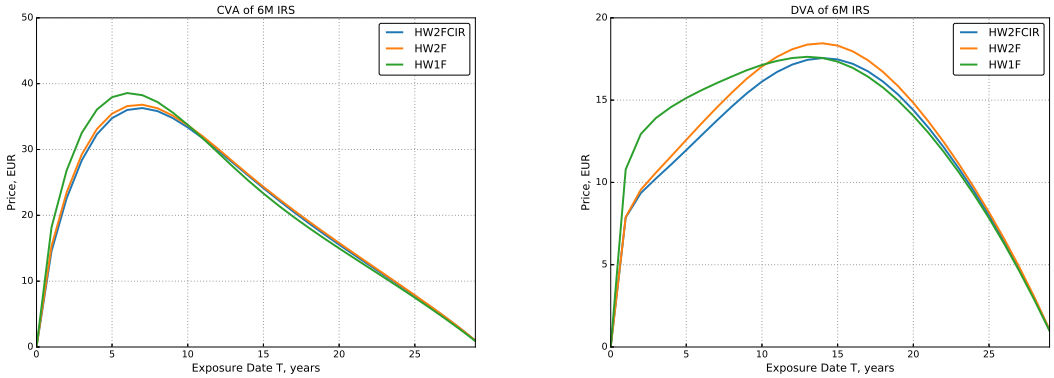

Figure 5.2: CVA and DVA exposure profiles of an 6M ATM IRS with HCIR and Hull-White models as a function of the exposure date T. All models calibrated to 22-Nov-2013 dataset.

5.3.1 Multi-Curve CVA Estimates

As HCIR model allows pricing of swaps on any tenor with stochastic basis, we have calibrated an HCIR model with a CIR_x component for every LOIS spread: 1, 3, 6, 12-month to the forward curves and 6-month 4% caps. Then, we have produced a CVA/DVA table for each of the models, with different tenor 30-year ATM swaps in the portfolios. The results in Table 5.3 show that:

- The HCIR model yields lower CVA/DVA values than the pure HW ones. The differences in CVA values are as high as 30 EUR, or and adjustment of 6bp on the fixed leg (estimated numerically).
- With increasing tenor length, CVA/DVA values decrease indicating decreasing underlying portfolio volatility.

Tenor	ρ	σ	θ	k	c_0
1M	-3.14%	0.115%	1.17e-5	5.67%	0.11%
3M	-3.64%	0.10%	1.14e-5	4.93%	0.27%
6M	-1.8%	0.12%	0.82e-4	9.22%	0.41%
12M	-2.05%	0.35%	0.017%	7.9%	0.54%

Table 5.2: CIR-parameter table for every tenor. HCIR model was calibrated to 4% caps from 22-Nov-2013.

		CVA			DVA		
Tenor	ATM(%)	HCIR	HW2F	HW1F	HCIR	HW2F	HW1F
1M	2.49%	660	690	707	334	352	370
3M	2.59%	636	658	671	342	363	378
6M	2.68%	608	618	626	359	374	384
12M	2.83%	554	562	559	363	381	380

Table 5.3: CVA/DVA table for multi-curve IRS. The HCIR model was calibrated to 4% caps from 22-Nov-2013. The given values show CVA/DVA in EUR values for a respective tenor IRS's with 30-year maturities.

5.3.2 Large-Basis Scenarios

To test the model performance under different market scenarios, e.g. large, increasing and decreasing basis spread cases, we generated a number synthetic datasets with flat, linearly-increasing and curved-decreasing LOIS spreads, the latter resulting in a large CIR volatility $\sigma = 10\%$.

Flat Gap

We introduce a flat 200bp LIBOR-OIS spread into the dataset instead of the market forwards, leaving cap volatility curve unchanged. The Figure 5.3 shows the forward curve and volatility data. We have calibrated the HW1F, HW2F and HCIR models to the scenario dataset obtaining the parameter set given in Table 5.4 and calculated the CVA/DVA on a 6-month ATM swap.

The resulting simulated swaps have identical means in all models, as well as volatilities as shown in Figure 5.4. Hence, the CVA/DVA figures, in this case, are also identical, we have obtained CVA values within simulation error margin, namely of 678 and 679 EUR for CVA and 362 and 363 EUR for DVA, for HW2F and HCIR models respectively. The HW1F model displayed somewhat smaller volatility of exposure and CVA, DVA values of 654 and 335 EUR.

ρ	σ	θ	k	c_0
-0.23%	1.2%	1.96%	59.5%	23%

Table 5.4: CIR parameters in flat high-basis case for 6-month LIBOR forward curve.

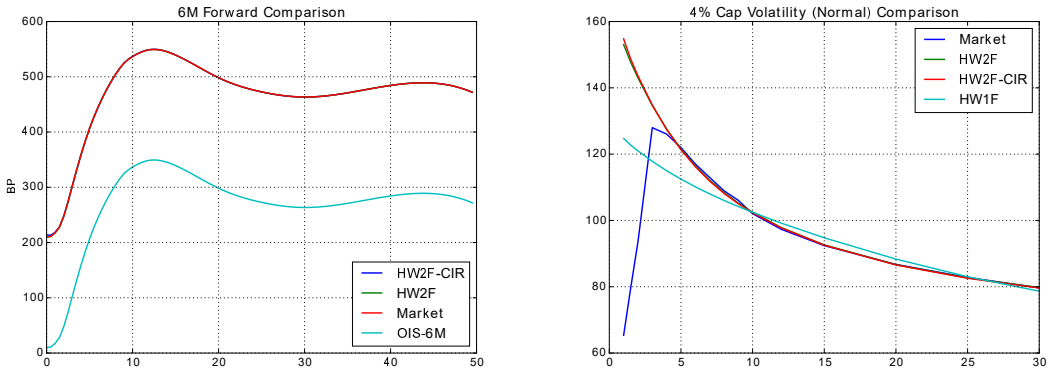

Figure 5.3: Forward rates and (normal) cap volatilities for a high, flat-basis scenario.

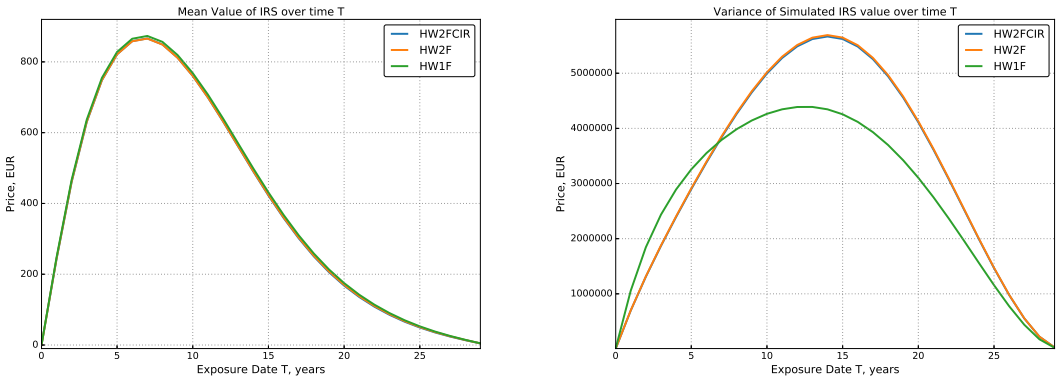

Figure 5.4: Means and variances of the simulated IRS swap under HCIR and HW-models using synthetic forward curve with flat LIBOR-OIS spread and market 4% cap volatilities from 22-Nov-2013. On the X-axis we have the exposure date T.

Increasing Gap

In the second synthetic setup, we introduce a linearly increasing LIBOR-OIS gap from 0 up to 200 basis points (at 30-year forward point) as shown in Figure 5.5. The fitted CIR model has a very low starting short-rate c_0 and large long-term mean θ. As shown in table 5.5, the CIR volatility is small and the mean-reversion speed k is small as well.

The market cap volatility fits for HCIR and HW2F models are practically identical. As a consequence, HCIR model has CVA/DVA of $862/215$ EUR, and HW2F has $865/217$ EUR. Figure 5.6 demonstrates that the HCIR model yields slightly lower portfolio volatility, as the CIR model is close to constant.

ρ	σ	θ	k	c_0
-1.35%	0.12%	48.6%	0.14%	005%

Table 5.5: CIR parameters in increasing high-basis case for 6-month LIBOR curve

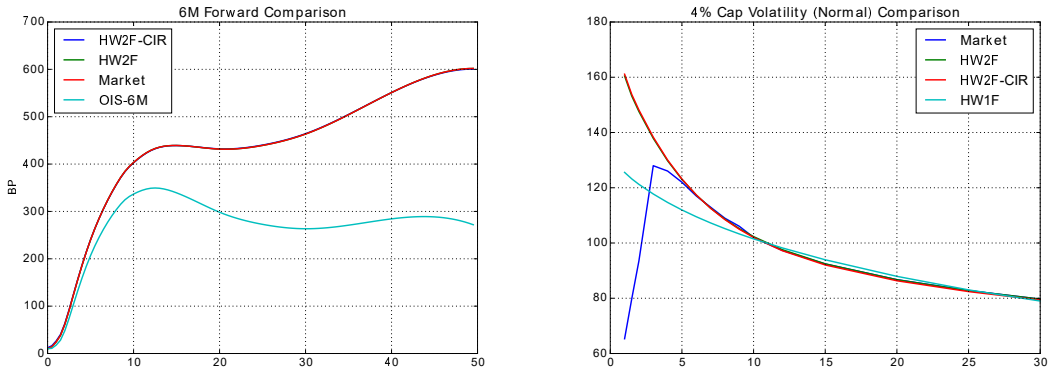

Figure 5.5: Forward rates and (normal) cap volatilities for a high, increasing-basis scenario.

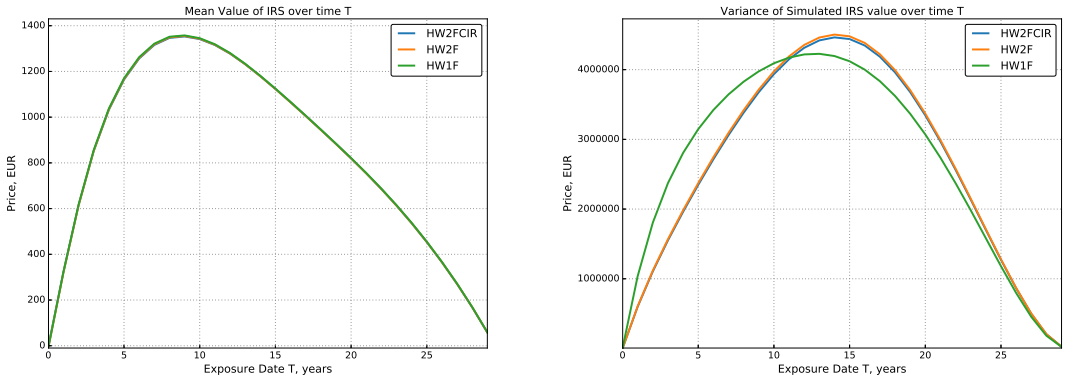

Figure 5.6: Means and variances of the simulated IRS swap under HCIR and HW-models using synthetic forward curve with linearly increasing LIBOR-OIS spread and market 4% cap volatilities from 22-Nov-2013. On the X-axis we have the exposure date T.

Curved-Decreasing Case

In the last case, we produced a decreasing basis-spread scenario with a highly curved short-term forward curve as shown in Figure 5.7, which could be a result of a liquidity squeeze: short term unsecured loans sold at a very high premium above OIS rates, while long-term LIBOR loans have a constant credit-risk premium above OIS. The resulting CIR model parameters are given in Table 5.6. In the case of liquidity squeeze scenario, the CIR volatility

becomes high, even 10%, but the mean reversion speed $k = 100\%$ is also high, due to the positive rate restrictions on the CIR model.

The resulting CVA figures in Table 5.7 show some differences in the models, the HCIR model yields overall larger CVA and DVA figures for the same swap, as our basis spread is now quite volatile $\sigma = 10\%$. The EUR impact of changing from HW2F to HCIR model is 34 EUR, this (approximately) translates to $\approx$ 7bp adjustment on the fixed swap leg.

ρ	σ	θ	k	c_0
0%	10%	0.51%	100%	4.12%

Table 5.6: CIR parameters in curved basis spread case for 6-month LIBOR curve.

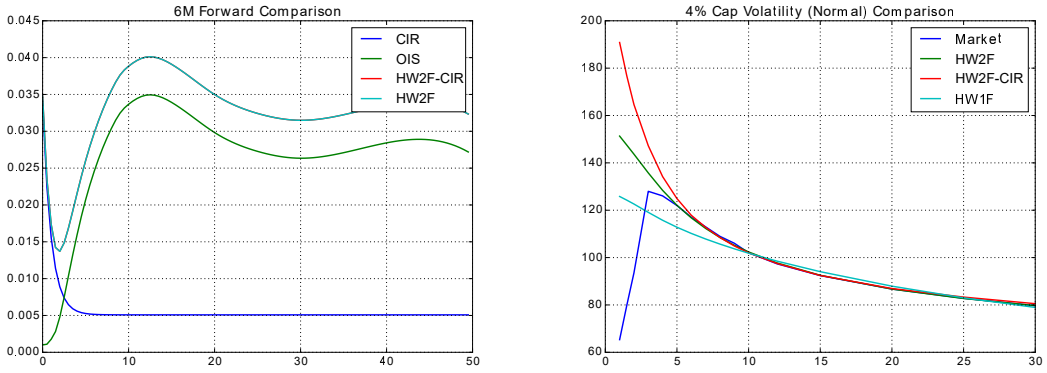

Figure 5.7: Forward rates and (normal) cap volatilities for a high, increasing-basis scenario.

Model	CVA	DVA	Swap MtM
HCIR	658	420	0
HW2F	624	386	0
HW1F	620	384	0

Table 5.7: CVA, DVA and swap MtM EUR values at time $t = 0$ for an ATM swap with fixed rate of 2.6839%

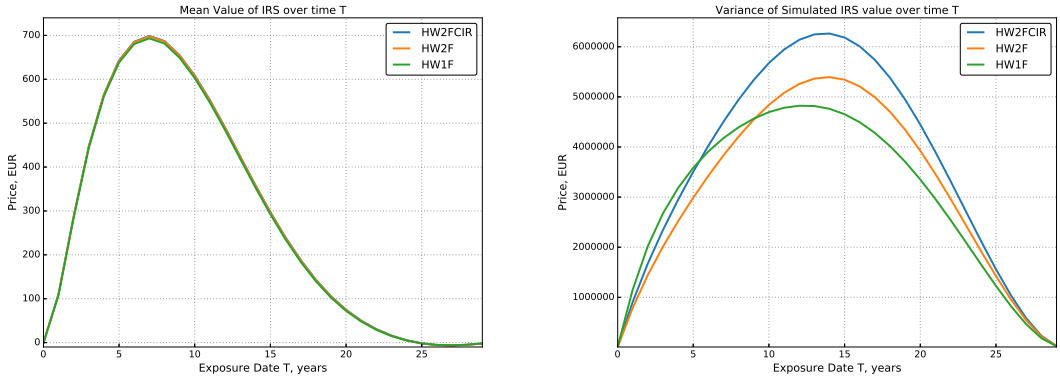

Figure 5.8: Means and variances of the simulated IRS swap under HCIR and HW-models using synthetic forward curve with curved-decreasing LIBOR-OIS spread and market 4% cap volatilities from 22-Nov-2013. On the X-axis we have the exposure date t.

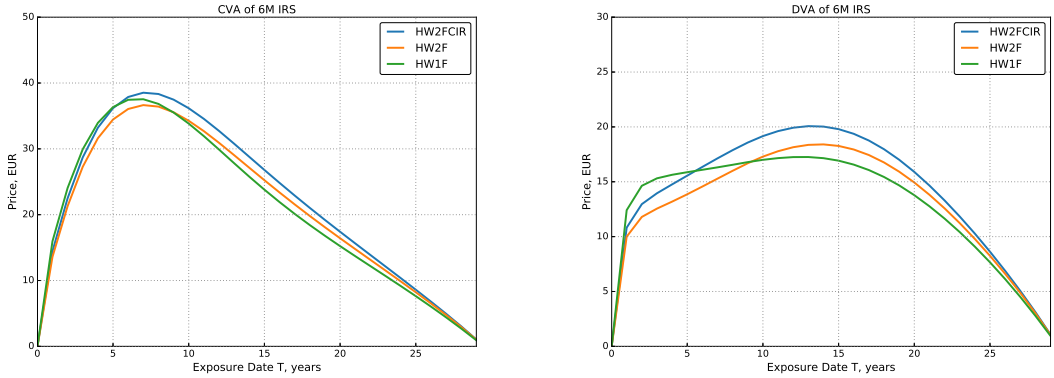

Figure 5.9: CVA and DVA profiles for IRS under HCIR and HW2F models using synthetic forward curve with curved-decreasing LIBOR-OIS spread and market 4% cap volatilities from 22-Nov-2013.

The results from LIBOR-OIS swap and interest rate cap CVA estimation resulted in similar conclusions and are discussed in Appendices E.2 and E.3.

5.4 Wrong-Way Risk in LOIS

The last example considered is the wrong-way risk (WWR) model for CVA on an IRS portfolio. In general, we can manipulate three types of wrong-way risks, namely correlation between counterparty default and:

1. Exposure size (standard WWR)
2. OIS rates (w.r.t risk-free rates)
3. LIBOR-OIS spread (w.r.t. credit-liquidity premium)

Standard 2-Factor Hull-White model only allows to model WWR with respect to the first two factors. Having an explicit LOIS model allows us to include the 3rd risk. To set up wrong-way risk in CVA in a simple way, we impose correlation between the default probability and LIBOR-OIS spread. For this case the CVA pricing formula becomes:

$$\text{CVA} \approx \sum_{i=1}^{N} \mathbb{E}^{Q} \left[P(0,T_i)(L(T_i))^{+}(D(T_{i-1},T_i)) \right], \tag{5.11}$$

where D is the stochastic default weight.

5.4.1 WWR Methodology

To impose wrong-way risk, or correlation, between the LOIS spread and the default we will impose correlation between CIR spread-state variable $c(t)$ and the default weight $D(t)$ via a Gaussian copula. We will also assume that the default weight is not correlated with the Hull-White state variables $x(t), y(t)$. The latter correlation is a viable option to explore, but it is out of scope from this report.

As mentioned previously, the CIR (spread model) state variable $c(t)$ is distributed with non-central chi-squared distribution and the default weight D for every time period (T_{i-1}, T_i) is uniformly distributed over $[0, 6.66\%]$ interval, with a mean of 3.33%.

We constructed a Gaussian copula (Charpentier et al., 2007) correlating $c(t)$ state variable with the default weight D, as follows.

The conditional density function (CDF) of the spread process $c(t)$ shall be called $\mathcal{F}$. For a given sample $X \in \mathcal{F}$, we convert this to uniformly distributed $\mathcal{U}[0,1]$ random sample $\hat{X}$ by evaluating the CDF

$$\hat{X} = \mathcal{F}(X)$$

and, consequently convert to normally distributed sample by using inverse normal CDF

Φ^{-1}

$$\tilde{X} = \Phi^{-1}(\hat{X}).$$

Then, we draw another independent normally distributed sample $\tilde{Z} \in \mathcal{N}$, and derive the sample

$$\hat{Z} = \rho \cdot \tilde{X} + \sqrt{1-\rho^2} \cdot \tilde{Z}$$

which has normal marginal distribution, but is correlated with $\tilde{X}$ by correlation rate ρ.

Finally, we convert the latter sample to uniformly distributed $Z = \Phi(\hat{Z})$. We end up with samples $X \in \mathcal{F}$ and $Z \in \mathcal{U}$ with their respective marginal distributions, but correlated with Gaussian copula with correlation ρ. The latter two samples together with samples for HW2F state variables $x(t), y(t)$ are enough to evaluate CVA for a given IRS portfolio $L(t)$.

5.4.2 WWR for IRS

We shall demonstrate the impact of the correlation ρ parameter on CVA/DVA values for an interest rate swap in three cases of potential WWR correlation $\rho = 0\%$, 100% and -100% and two forward curve cases:

1. Market data from 22-Nov-2013,
2. Synthetic high-basis scenario: curved basis (high vol of $c(t)$).

The table 5.8 shows, the LIBOR-OIS WWR correlation impact on overall CVA is negligible if we use the market dataset with small LOIS basis spreads. On the other hand, in the synthetic high-volatility dataset, the WWR effect is visible, but not very large. As the sensitivity of CVA to changes in the fixed leg are $5EUR/$bp, the WWR impact, in this case, is less than 2bp, the CVA value increases with increasing positive correlation between the CIR state variable $c(t)$ and the uniformly-distributed default probability CDP(t). Equivalent, but opposite, effect is observed in the DVA impact, table 5.9: DVA values decrease with increasing positive correlation ρ, and increase with high-negative correlation.

We have chosen the test correlation values to be very large, as a change in LIBOR-OIS spread is tightly linked to changes in liquidity and credit situation in the interbank lending markets, hence a change in LOIS spread should be well reflected in the default probability (weight) of a banking counterparty.

For this chapter, we skip the WWR assessment for LOIS swaps as well as caps, because the impact on them would be even smaller for the same reasons outlined in the previ-

ous section. To conclude, The WWR impact is visible on interest rate swaps but is not very large even in high-volatility spread (liquidity squeeze) situations. This is highly affected by the chosen CIR model for the spread, as this square-root process is stable and even with high initial volatility quickly converges to a long-term mean spread.

CVA Values:	$\rho = -100\%$	$\rho = 0\%$	$\rho = 100\%$
Market Data	609	609	609
High-Vol sc.	649	660	668

Table 5.8: CVA values under wrong-way risk with different correlation levels between CIR-state $c(t)$ and the CDP(t)

DVA Values:	$\rho = -100\%$	$\rho = 0\%$	$\rho = 100\%$
Market Data	358	359	360
High-Vol sc.	426	420	414

Table 5.9: DVA values under wrong-way risk with different correlation levels between CIR-state $c(t)$ and the CDP(t)

To obtain a benchmark, for the WWR case when LOIS spread is correlated with the default probability, we can compare the latter with CVA with WWR case, when the correlation is between the overall exposure (NPV(t)) and the default weight. This way we can have a comparative view how much impact can LOIS-default correlation have in comparison with more common way of assessing WWR in CVA.

The WWR, correlation between exposure and default, impact on CVA/DVA values is quite large, an increase/decrease by 350 and 400 EUR, alternatively this would mean up to 80bp adjustment on the fixed leg of the ATM swap. This means that when CIR model is used for the LOIS spread - the imposed WWR between the default rate and the LOIS spread has a much smaller impact on CVA than full WWR model, where correlation is set up between exposure and default.

CVA Values:	$\rho = -100\%$	$\rho = 0\%$	$\rho = 100\%$
Market Data	249	609	968
High-Vol sc.	265	659	1052

Table 5.10: CVA values under wrong-way risk with different correlation levels between exposure size NPV(t) and the CDP(t)

DVA Values:	$\rho = -100\%$	$\rho = 0\%$	$\rho = 100\%$
Market Data	643	359	78
High-Vol sc.	753	420	87

Table 5.11: DVA values under wrong-way risk with different correlation levels between exposure size NPV(t) and the CDP(t)

5.5 Conclusions

In this experiment, we have constructed a simple CVA valuation engine, where the portfolio contains only a single interest rate swap, the credit risk is determined by simplified model with a (random) default rate. We have compared the CVA and DVA charges for the IRS when the underlying LIBOR and OIS rates are driven by either HCIR or simple HW2F model with constant basis spread.

We have performed comparative analysis between the two models using market data as well as synthetic data to investigate the realistic and limiting cases. Overall, our results show that the impact on CVA of choosing a hybrid model with stochastic basis over constant spread HW2F is small, as the LIBOR-OIS spreads are rather small in general and CIR model used for its dynamics does not carry a lot of volatility.

This result has some broader implications. Even if the CIR-spread model is one of the simplest analytic stochastic basis models, the fact that WWR with stochastic basis is very close to the CVA value with deterministic basis shows that many simplified models without the stochastic component can be close to the “advanced” model in the current small-basis environment and can be safe to use, without adding unnecessary complexity into CVA computation.

Chapter 6

Conclusions and Future Work

This chapter presents an overview of the work described in this thesis on modelling stochastic basis with two different branches and discusses possible future directions of this research. In Chapter 3 we have analysed and extended a conceptually unique LIBOR panel model, which uses the mechanics of daily LIBOR quotations and changes in the set of banks in the LIBOR panel as the driver for LIBOR-FRA spreads. In Chapter 4 we introduced a novel hybrid short-rate model for joint modelling of multi-tenor LIBOR rates and volatilities, able to re-price a much larger set of traded and illiquid derivatives than the latter model while keeping explicit links to credit and liquidity risks.

6.1 The Extended Panel Model

The LIBOR panel model does not belong to any of the popular classes of financial stochastic interest rate models, like the LIBOR market models or short-rate models. Nevertheless, it offers a unique insight into the problem of joint modelling of FRA rates together with OIS and spot-LIBOR rates. In our work, we have replicated the original results of Morini (2009) and showed that the use of the credit-liquidity volatility proxy, as in the original article, is very limited. What is more, to correct for the lack of external volatility parameters we changed the formulation of the problem and constructed FRA-implied volatility, as often done in the options markets. In the implied-volatility framework, using global calibration methods we were able to jointly re-price all available FRA rates at once using a single set of parameters, leaving less than a 20bp error in repricing.

In our dataset, the bid-ask spreads of most of FRA contracts were well within the 5bp margin, therefore the panel model, in its standard formulation, was not flexible enough to

re-price all instruments within required tolerance. We performed an empirical investigation into the assumptions of the panel model and noted that the assumed log-normal Brownian motion does not hold for the historical LIBOR-OIS spreads. The closest distribution to match the empirical data was the Student-T distribution, but the latter is known to yield non-analytic option prices and other difficulties in pricing. Therefore we chose to use a mixture of Gaussians as the approximating distribution for the stochastic LIBOR-OIS spreads with one Gaussian controlling small micro-movements of the spread and the other one responsible for the occasional large swings in the LIBOR-OIS spread. Using this assumption we obtained a known, analytic uncertain parameter model for options pricing. By calibrating the extended panel model to series of traded FRA contracts we were able to minimise the replication error to less than 5bp in 95% of historical dates. The latter result shows that the extended panel model can be used to price FRAs and detect mispricings in the market.

Moreover, we performed empirical parameter analysis of the extended panel model. The full model is described by 3 parameters: volatilities σ_1, σ_2 and weight parameter λ. We calibrated the model to a set of FRAs for every trading day in our dataset, obtaining three time-series of parameters. We found the levels of volatilities as the weight of the large volatility σ_2, indicating large swings in credit risk, coinciding with the major credit crisis and post-crisis events, reflecting the interest rate market turbulences. As a result, this model can be used by risk managers to observe and anticipate large changes in the interbank lending markets using liquidly traded contracts like the FRAs.

6.2 HCIR model

The hybrid HW2F-CIR model is a very promising, straightforward short-rate model for risk-management purposes. It has a number of original and very important features:

1. Is a short-rate model suitable for low-dimensional simulation of portfolio exposure.
2. Allows for analytic calibration to market OIS, IRS and semi-analytic to ATM (or any fixed strike) caps.
3. Allows calibration to multiple tenors of LIBOR-OIS spreads and pricing of caps on illiquid tenors.
4. And allows simulating IRS, cap exposures on different tenors for CVA valuation.

6.2.1 Calibration

The model can be calibrated to a single-day of market data, yield curves and a series of market caps. In the calibration, the information about OIS term-structure goes into the (base) HW2F model, the LOIS spread term-structure is fitted to CIR fixed parameters and the cap volatility information is fed into both: Hull-White volatility and mean reversion, as well as CIR parameters. Hence, the fitting is done jointly to forward rates and market cap volatilities.

We have successfully calibrated the model to market data on 22-Nov-2013. However, we note that in this global-calibration exercise, multiple local minima exist in the error function and the optimizer can fall into one, ignoring the absolute global solution (see example in Appendix E.4). To avoid this, we propose to calibrate a simple Hull-White model with constant-basis spread assumption to market curves and caps and then use these Hull-White volatility and mean-reversion parameters as a starting point for full HCIR model calibration.

We further note that the model requires a smooth, convergent term-structure of the forward rates and cap volatilities. Any irregularities could disrupt the calibration (see Appendix 4.5). In the current formulation of the model, there may be cases where the calibration is not successful.

6.2.2 Cap Pricing

We have performed a number of tests with the HCIR model, including illiquid cap pricing and comparison to market data, exposure and CVA valuation with HCIR model and benchmarking against pure HW1F and HW2F models. Our analysis has shown that calibration to market forward curves works within 5bp error for HCIR models [1], with exception of the first few IRS points - the difference is up to 20bp, does not fit well as the market LOIS spread increases too fast for the HCIR model. Then, the calibration of HW2F-CIR model to market caps for a single-strike works well, within a 1bp volatility error for maturities > 3 years. The shorter maturity volatilities are hard to match: the 2-year vol is 5bp higher in the model, the 1-year market volatility is too low to be represented by HW2F or HCIR models. The HW1F model is not flexible enough to price a single multi-maturity series of

[1] The ICAP bid-ask spreads are around 5bp for market FRAs and IRS.

market caps and falls behind both previous models. What is more, as the HCIR model is based on HW and CIR models, however, the hybrid model has a very small volatility smile and cannot be used reliably for smile extrapolation.

6.2.3 CVA Impact Evaluation

In our tests for CVA and exposure assessment, we have benchmarked the HCIR model versus the fixed-basis HW1F and HW2F models in market and synthetic-data situations. We have found that the HW2F and HCIR models show comparable IRS exposure profiles and CVA values in market-data tests, with differences around 2bp on an IRS fixed rate adjustment. The HW1F model results in overall higher volatility and higher CVA/DVA values for ATM swaps than the other two models. Whenever the LOIS spread is small or the calibrated CIR model has low-volatility and the HCIR and HW2F models give very close results. The main difference between the models arises in synthetic situation of rapidly decreasing LOIS spread term-structure. This happens in a liquidity squeeze when short-term unsecured borrowing is very expensive when compared to collateralized lending (using OIS rates). In this case the HCIR model yields higher CVA/DVA values than HW2F model by even 7bp change on fixed leg.

Comparison of exposures for LOIS swap as well as caps did now show any changes in CVA/DVA figures, as these derivatives stay in or out-of the money throughout the lifetime of the derivative, depending on the form of the forward curve, and therefore yield matching CVA/DVA mean exposures. The 95%-quantiles of HW2F and HCIR models are slightly different, as the HCIR model in high-volatility spread case has much larger short-term volatility. A full analysis is included in Appendix E. We have also tested the WWR situation, when LOIS spread (or CIR state variable $c(t)$) is correlated with the conditional default probability $CDP(t)$. In high-vol spread environment the CVA/DVA values are inflated/deflated when $\rho = 100\%$ and $\rho = -100\%$ by up to 3bp on fixed IRS leg, which is very small when compared to the adjustment from exposure-default correlation.

6.3 Future Research Directions

Overall, in this work we have outlined a few drawbacks of the hybrid HCIR model. One of the biggest issues is the lack of flexibility when fitting the volatility smile. As we observed from our results, the major part of the volatility is driven by the base Hull-White model,

therefore changing it to a model which incorporates the volatility skew/smile, such as the Cheyette displaced diffusion stochastic volatility (DDSV) model (Hoorens, 2011) could resolve this issue. On the other hand, as the pricing and calibration of DDSV model to bonds and caps is non-analytic, a hybrid DDSV-CIR model could be very computationally expensive, especially for CVA purpose.

Also, we found that the very short term caps cannot be reliably priced by the HCIR model, as the market volatility is too low for the HW2F and CIR models to replicate at the same time as high 5-year cap volatility. This issue could be solved by using a piecewise-constant volatility functions $\sigma_x(t), \sigma_y(t)$ for the Hull-White process. However, this leads to changes in the semi-analytic pricing formulas.

Finally, we have shown the potential impact of HCIR model on CVA and demonstrated an example of wrong-way risk scenario. This was done in a rather simple credit-default model, where we only imposed correlation between the hazard rate and LOIS spread size. It may be interesting to extend this to a full model with default events as well as more sophisticated default risk model.

Appendix A

Basis Consistent Replication of the FRA rate

A very important observation was made by Morini (2009) that the 6-month and 12-month FRA gap can be 'bridged' using a different set of market derivatives - the basis swaps (2.21). This observation yields a model-free way to express the value of a market-traded FRA in terms of OIS and LIBOR rates. In the following we give a generalized version of the proof for basis consistent replication for FRA contracts of any tenor.

We can compute the price of a basis swap (2.21) as the expectation of the LIBOR-linked payments, discounted with the risk-free rate:

$$B(0;T,S;Z) = \mathbb{E}_Q[D(0,T)L_M(0,T)\tau(T) + D(0,S)\tau(S-T)L_M(T,S) - D(0,S)\tau(S)(L_M(0,S)-Z)] \quad \text{(A.1)}$$

with Z being the fixed basis spread in the contract.
The appropriate risk-free discounting rate for basis swaps is the OIS rate, as these contracts (just like FRAs) are collateralized. Therefore:

$$B(0;T,S;Z) = \mathbb{E}_0[D(0,S)\tau(S-T)L_M(T,S)] - P_{OIS}(0,S)\tilde{K}(Z) \quad \text{(A.2)}$$

where $L_M(T,S)$ is a market forward-LIBOR loan, P_{OIS} is the OIS discount bond and

$$\tilde{K}(Z) = (S(L_M(0,S) - Z)) - \frac{P_{OIS}(0,T)}{P_{OIS}(0,S)} T L_M(0,T) \tag{A.3}$$

$$= (\frac{1}{P_L(0,S)} - 1) - SZ - \frac{P_{OIS}(0,T)}{P_{OIS}(0,S)}(\frac{1}{P_L(0,T)} - 1) \tag{A.4}$$

$$= \frac{1}{P_L(0,S)}(\frac{P_L(0,T)}{P_L(0,S)} - \frac{P_{OIS}(0,T)}{P_{OIS}(0,S)}) + (\frac{P_{OIS}(0,T)}{P_{OIS}(0,S)} - 1 - SZ) \tag{A.5}$$

$$= \frac{1}{P_L(0,S)}(F_{Std}(0;T,S)\tau(T,S) - E_{Std}(0;T,S)\tau(T,S)) + E_{Std}(0;T,S)\tau(T,S) - SZ \tag{A.6}$$

$$= \tau(T,S)\left[\frac{1}{P_L(0,T)}\left(F_{Std}(0;T,S) - E_{Std}(0;T,S)\right) + E_{Std}(0;T,S) - \frac{S}{\tau(T,S)}Z\right] \tag{A.7}$$

where F_{Std} and E_{Std} are standard replications (2.11) of, respectively, LIBOR and OIS forwards.

Now, if we compare the basis swap price (A.2) and the FRA value:

$$FRA(0,T,S;K) = \mathbb{E}_0\left[D(0,S)(S-T)(L(T,S) - K)\right] \tag{A.8}$$

$$= \mathbb{E}_0\left[D(0,S)(S-T)L(T,S)\right] - P_{OIS}(0,S)(S-T)K \tag{A.9}$$

We see that by setting $K = \tilde{K}(Z)/\tau(T,S)$, then the basis swap and FRA values coincide. Hence the FRA equilibrium rate, when the FRA market value is zero, can be written as:

$$F_B(0;T,S) = E_{Std}(0;T,S) + \frac{1}{P_L(0,T)}\left(F_{Std}(0;T,S) - E_{Std}(0;T,S)\right) - \frac{S}{\tau(T,S)}B_M(0;T,S) \tag{A.10}$$

where $B_M(0;T,S)$ is the market par basis swap spread.

Appendix B

Multi-Curve Pricing Schemes and Tables

The following two flowcharts explain the pre- and post- crisis methods of stripping market interest rate curves and volatilities.

In Figure B.1 we show the classic OIS, LIBOR curves and LIBOR volatility bootstrapping framework. In this setup one obtains the OIS and LIBOR interest rates from their respective swaps, choosing the most liquid derivatives if multiple are available. For example, to strip the LIBOR curve one would use spot LIBOR curve up to 1-year, then the 6-month FRA rates up to 5 years and then IRS rates. If one used another tenor, like 3-month swap rates, the final result would be unchanged as there were no significant basis spreads between 6 and 3-month forward rates.

The same, separate, bootstrapping procedure applied for credit default probability curves obtained from CDS spreads. The forward LIBOR volatilities were obtained by using already stripped unique LIBOR curve and current, most liquid market caps.

In Figure B.2 we show the modern, post-crisis curve bootstrapping setup. While CDS and OIS stripping is left unchanged, now we have to strip a forward-LIBOR curve from every tenor (1,3,6,12)-month FRA's and IRS's. Additionally, the OIS and spot-LIBOR curve affects each of these bootstrap procedures and also affects the, now tenor-dependent, LIBOR-volatility bootstrapping procedure.

The volatility bootstrapping is now exceptionally hard as only one tenor caps are liquid per currency, e.g. 6-months in Euro, 3-months in US dollar. The latter means that the volatilities for other-tenor LIBOR forwards are not known due to lack of market data and have to be implied by a model. Such situations before the credit crash only happened when dealing with exotic derivatives. Now the vanilla derivatives obtained the features of exotics.

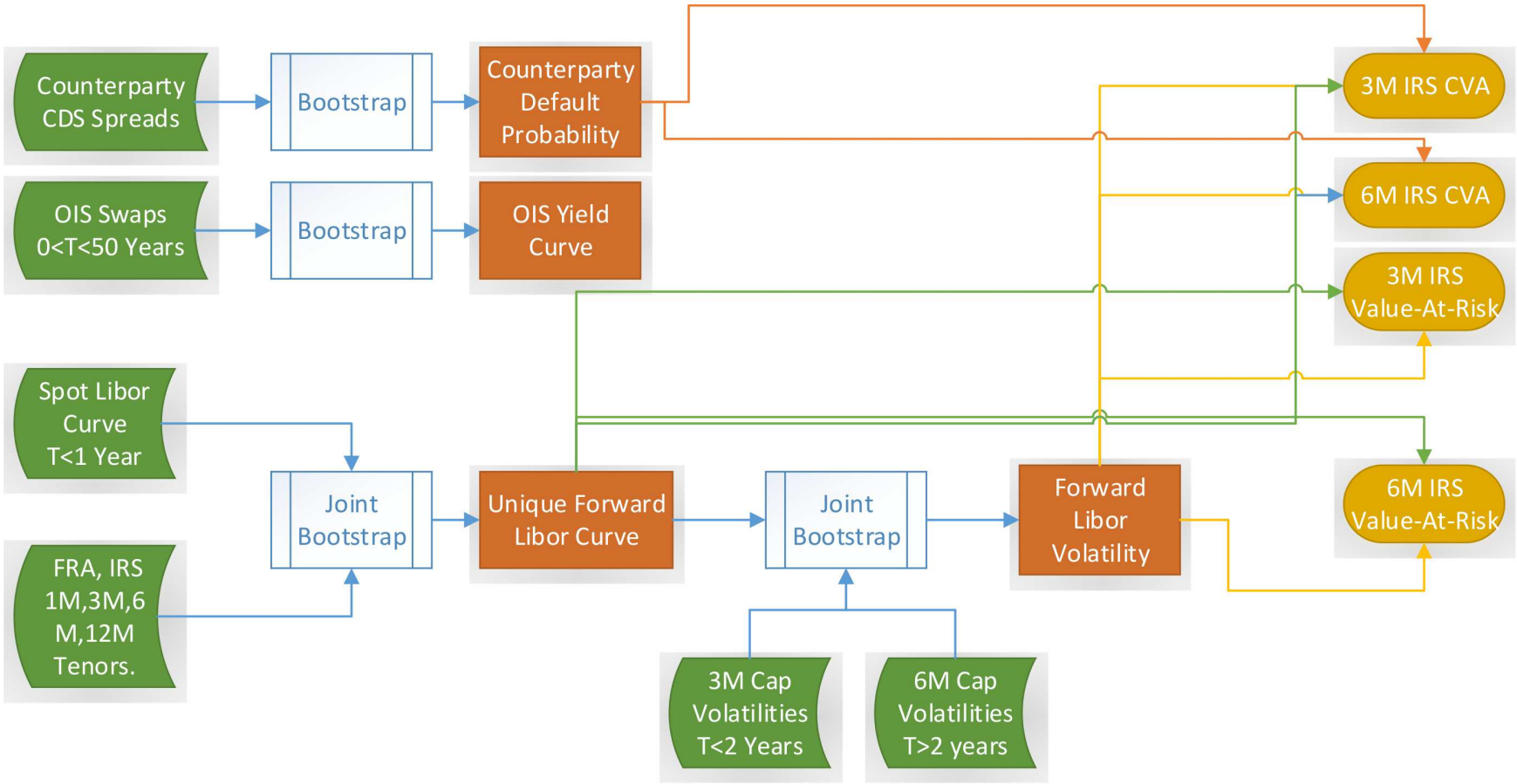

Figure B.1: Old OIS discounting framework

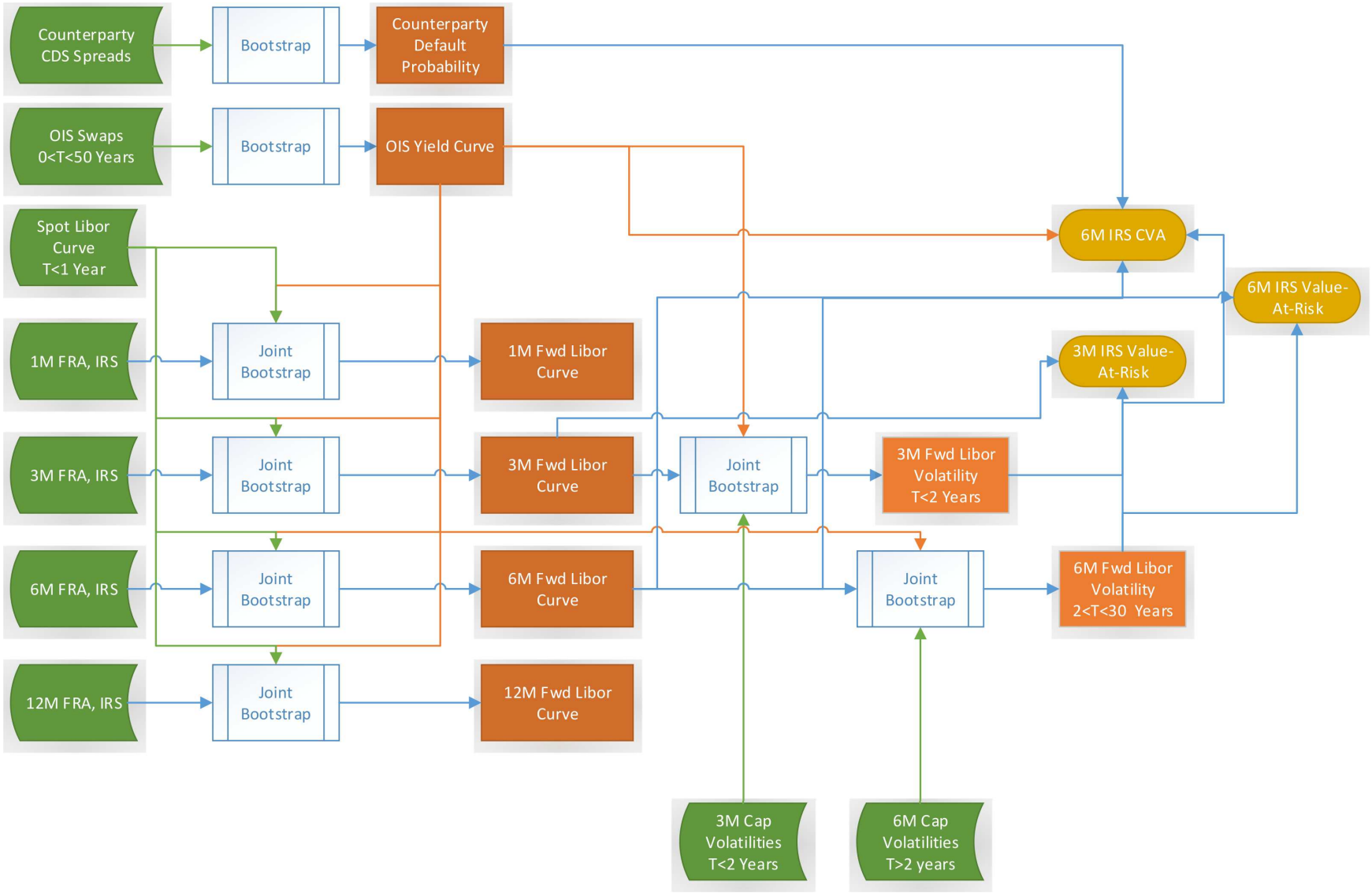

Figure B.2: New OIS discounting framework

B.1 Table of Common Multi-Curve Modelling Approaches

As the basis spread modelling problem is new, there is no industry-wide standard way of approaching it, but there have been multiple proposals for multi-curve interest rate models. In this section, we briefly outline them and discuss pros and cons.

Author	Method	Strengths	Weaknesses
(Kienitz, 2013)	Volatility transformation by treating LIBOR as displaced diffusion over OIS forward rate.	Extrapolate ATM-Option volatilities across tenors; Allows to superimpose SABR parameters to transfer caplet volatility smile.	Not a stochastic-spread model, a way of filling up LIBOR-vol surface
(Mercurio, 2010)	Extended Multi-Curve LIBOR Model	Exact calibration to available curves and option products	Distinct volatility surfaces for every tenor τ, lack of data for calibration of volatilities, correlations, etc. Impossible to calibrate OIS volatility to market instruments.
(Morini, 2009)	(Extended) LIBOR as and Option	It can price FRA contracts using spot-LIBOR, OIS curves and credit-liquidity volatility data. Good historical fit for tested FRAs	Difficult to use beyond 1-year maturity due to lack of spot-LIBOR curve and lack of credit proxies. caplet pricing may be unrealistic in high FRA-OIS basis scenarios (spread volatility is too high)
(Crépey et al., 2012)	Levy-Hull-White model for default-able LIBOR	Analytic valuation of FRAs and Swaps can reproduce historical LIBOR-OIS spreads. Semi-Analytic valuation of caps and Swaptions; The jump model for LIBOR rates can be used well for xVA calculations.	Non-analytic pricing with characteristic functions; Unclear if Swaps, caps can be repriced at market rate simultaneously.
(Bianchetti, 2010)	Two short rates for OIS and forward Curves, as in FX analogy	Consistent, known model, simple pricing	Quanto Terms, negative LIBOR-OIS basis spreads are possible, published calibrations show unusable fits for swaptions.
(Kenyon, 2010)	Two short-rate setup for OIS and LIBOR-OIS basis	Consistently reprices market Swaps and FRAs. There are multiple choices for short-rate models involved, the author demonstrates setup with Vasicek models.	It loses pricing simplicity, volatility calibration requires illiquid cap data.

Table B.1: Table of popular multi-curve pricing models.

Appendix C

Appendix: More Theoretical Definitions and Derivations

In this appendix we include the definitions for bond pricing under CIR and 1-or-2 factor Hull-White models. Then, we give the derivations for bond option and caplet pricing in two-curve framework and when the underlying is a k-scaled zero coupon bond.

C.1 The CIR Model

The Cox, Ingersoll and Ross (CIR) model (Brigo and Mercurio, 2006) is the first model to use the square-root diffusion term in the short rate diffusion SDE:

$$dc(t) = \kappa[\theta - c(t)]dt + \sigma_c\sqrt{c(t)dW(t)}, c(0) = c_0 \tag{C.1}$$

where $c_0, \kappa, \theta, \sigma_c$ are constants. A condition

$$2k\theta > \sigma^2 \tag{C.2}$$

has to be imposed to guarantee the positivity of the short-rate $c(t)$.

The CIR model yields non-Gaussian dynamics for the short-rate, in particular the $c(t)$ has the density of a non-central Chi-squared distribution (Brigo and Mercurio, 2006), with:

$$\mathbb{E}\left[c(t)|\mathcal{F}_u\right] = c(u)e^{-\kappa(t-u)} + \theta\left(1 - e^{-\kappa(t-u)}\right) \tag{C.3}$$

$$\mathbb{V}\left[c(t)|\mathcal{F}_u\right] = c(u)\frac{\sigma^2}{\kappa}\left(e^{-\kappa(t-u)} - e^{-2\kappa(t-u)}\right) + \theta\frac{\sigma^2}{2\kappa}\left(1 - e^{-\kappa(t-u)}\right)^2 \tag{C.4}$$

Nevertheless, the price at time t of a zero-coupon bond with maturity T can be obtained in

an analytic, affine form:

$$P_c(t,T) = A_c(t,T)e^{-B_c(t,T)c(t)}, \tag{C.5}$$

where

$$A_c(t,T) = \left[\frac{2h\exp\{(\kappa+h)(T-t)/2\}}{2h+(\kappa+h)(\exp\{(T-t)h\}-1)}\right]^{\frac{2\kappa\theta}{\sigma^2}}, \tag{C.6}$$

$$B_c(t,T) = \frac{2(\exp\{(T-t)h\}-1)}{2h+(\kappa+h)(\exp\{(T-t)h\}-1)}, \tag{C.7}$$

$$h = \sqrt{\kappa^2+2\sigma^2}. \tag{C.8}$$

For pricing of European call options on zero-coupon bonds we first need to change the CIR SDE (4.1) from risk-neutral Q to future time T-forward measure Q^T (Brigo and Mercurio, 2006):

$$dc(t) = \left[\kappa\theta - (\kappa + B(t,T)\sigma^2)c(t)\right]dt + \sigma\sqrt{c(t)}dW^T(t) \tag{C.9}$$

Under Q^T the distribution of the short rate $c(t)$, conditional on $c(u), u \leq t \leq T$, is given by:

$$p_c^T(t)(x) = q(t,u)p_{\chi^2(\nu,\delta(t,u))}(q(t,u)x) \tag{C.10}$$

$$q(t,u) = 2\left[\rho(t-u) + \psi + B_c(t,T)\right] \tag{C.11}$$

where $p_{\chi^2(\nu,\lambda)}$ is a non-central chi-squared density with ν degrees of freedom and non-centrality parameter λ.

$$\delta(t,u) = \frac{4\rho(t-u)^2c(u)e^{h(t-u)}}{q(t,u)} \tag{C.12}$$

$$\rho(t-u) = \frac{2h}{\sigma^2(\exp\{h(t-u)\}-1)} \tag{C.13}$$

$$\psi = (\kappa+h)/\sigma^2 \tag{C.14}$$

C.2 Pricing under two-curve HW models

Pricing of zero coupon bond options in two-curve framework using the Hull-White short rate model is slightly different than in the single-curve framework. We give the details for zero bond option and interest rate caplet pricing under (scaled) HW1F and HW2F model versions. The scaling parameter k is needed in the HCIR model and should be assumed to

be zero in the simplified case.

C.2.1 Pricing under scaled HW1F-K Model

The solution to scaled Hull-White $(1+k)$ zero-coupon bond price in two-curve framework is derived as

$$P^k(t,T) = \mathbb{E}^Q\left[e^{-(1+k)\int_t^T r(u)du}|\mathcal{F}_t\right], \tag{C.15}$$

where $r(t)$ is the short rate under HW1F model (Brigo and Mercurio, 2006) with constant volatility $\sigma(t) = \sigma$. The interior argument of the latter expectation can be rewritten using

$$\int_t^T r(u)du = \int_t^T \phi(u) + x(u)du, \tag{C.16}$$

$$\int_t^T x(u)du = \frac{1-e^{-a(T-t)}}{a}x(t) + \frac{\sigma}{a}\int_t^T \left[1-e^{-a(T-u)}\right]dW(u), \tag{C.17}$$

$$\phi(u) = f^M(0,u) + \frac{\sigma^2}{2a^2}(1-e^{-au})^2, \tag{C.18}$$

where the expected value of the integral

$$\mathbb{E}\left[\int_t^T x(u)du|\mathcal{F}_t\right] = \frac{1-e^{-a(T-t)}}{a}x(t), \tag{C.19}$$

and the variance is

$$V(t,T) = \mathbb{V}\left[\int_t^T x(u)du|\mathcal{F}_t\right] = \frac{\sigma^2}{a^2}\left[T-t+\frac{2}{a}e^{-a(T-t)} - \frac{1}{2a}e^{-2a(T-t)} - \frac{3}{2a}\right]. \tag{C.20}$$

Using the above, the bond price can be split up as:

$$P(t,T) = \left[e^{-(1+k)\int_t^T \phi(u)du}\right]\mathbb{E}^Q\left[e^{-(1+k)\int_t^T x(u)du}|\mathcal{F}_t\right] \tag{C.21}$$

as $\phi(t)$ is a deterministic function. Now, with $k=0$, we have the simple OIS zero-coupon bond and it is calibrated to the OIS discount curve, hence at time $t=0$

$$P^{k=0}(0,T) = P^M(0,T),\ \forall T \geq 0, \tag{C.22}$$

which holds if and only if

$$e^{-\int_t^T \phi(u)du} = \frac{P^M(0,T)}{P^M(0,t)}\exp\{-1/2\left[V(0,T)-V(0,t)\right]\}. \tag{C.23}$$

We summarize all the steps into a formula for bond price when $k = 0$:

$$\begin{aligned} P^{k=0}(t,T) &= \mathbb{E}^Q\left[e^{-\int_t^T r(u)du}|\mathcal{F}_t\right] \\ &= \frac{P^M(0,T)}{P^M(0,t)}\exp\{-1/2\left[V(0,T)-V(0,t)\right]\}\mathbb{E}^Q\left[e^{\int_t^T x(u)du}|\mathcal{F}_t\right] \\ &= \frac{P^M(0,T)}{P^M(0,t)}e^{-1/2[V(0,T)-V(0,t)]}e^{\frac{1-e^{-a(T-t)}}{a}x(t)+\frac{1}{2}V^2(t,T)}, \end{aligned}$$

because $\int_t^T x(u)du$ is normally distributed random variable with mean $\frac{1-e^{-a(T-t)}}{a}x(t)$ and variance $V^2(t,T)$. Respectively, if we were to scale the bond by $1+k$, we would obtain

$$\begin{aligned} P^k(t,T) &= \mathbb{E}^Q\left[e^{-(1+k)\int_t^T r(u)du}|\mathcal{F}_t\right] = \left[e^{-\int_t^T \phi(u)du}\right]^{(1+k)}\mathbb{E}^Q\left[e^{-(1+k)\int_t^T x(u)du}|\mathcal{F}_t\right] \\ &= \frac{P^M(0,T)}{P^M(0,t)}^{(1+k)}\exp\left[-\frac{1}{2}(1+k)\left[V(0,T)-V(0,t)\right]\right] \\ &\exp\left[(1+k)\frac{1-e^{-a(T-t)}}{a}x(t)+\frac{1}{2}(1+k)^2V^2(t,T)\right], \end{aligned}$$

as the mean of $\int_t^T x(u)du$ scales by $(1+k)$ and the variance scales by $(1+k)^2$. This leads to the final result where the k-scaled zero coupon bond price, under 1-factor Hull-White model

$$\begin{aligned} P^k_{HW}(t,T) = &\left[\frac{P^M(0,T)}{P^M(0,t)}\right]^{(1+k)}\exp[-(1+k)B(t,T)x(t)] \\ &\cdot\exp\left[\frac{(1+k)}{2}\left(V(0,t)-V(0,T)+(1+k)V(t,T)\right)\right], \quad x(0)=0. \end{aligned}$$

C.2.2 Option Price Derivation: HW1F-K

To price a zero-coupon bond (ZCB) option of the $k-$scaled bond, we can use an analytic formula:

$$ZBP_{HWK}(t,T,S,X) = P_{ois}(t,T)(X\Phi(-h+\hat{\Sigma}(t,T,S)) - \hat{P}^k_{HW}(T,S)\Phi(-h)), \quad \text{(C.24)}$$

where

$$h = \frac{\ln\frac{\hat{P}^k_{HW}(T,S)}{X}}{\bar{\Sigma}(t,T,S)} + \frac{\bar{\Sigma}(t,T,S)}{2}, \quad \text{(C.25)}$$

$$\bar{\Sigma}(t,T,S)^2 = (1+k)^2\left(\frac{\sigma^2}{2a^3}\left[1-e^{-a(S-T)}\right]^2\left[1-e^{-2a(T-t)}\right]\right), \quad \text{(C.26)}$$

$$\hat{P}^k_{HW}(T,S) = \mathbb{E}^{Q_T}\left[P^k_{HW}(T,S)\right]. \quad \text{(C.27)}$$

To prove this, we start by defining the ZCB-call option. This is an European call option with exercise date T on a bond with maturity S

$$ZBC(t,T,S,X) = \mathbb{E}^{Q}\left[e^{-\int_t^T r(u)du}(P_{HW}^k(T,S)-X)^+|\mathcal{F}_t\right]. \tag{C.28}$$

Via change-of-numeraire technique we change the measure to OIS T-forward measure, obtaining

$$ZBC(t,T,S,X) = P_{OIS}(t,T)\mathbb{E}^{Q_T}\left[(P_{HW}^k(T,S)-X)^+|\mathcal{F}_t\right] \tag{C.29}$$

Now, since the value of the future k-Bond is

$$P_{HW}^k(T,S) = \left[\frac{P_{OIS}(0,S)}{P_{OIS}(0,T)}\right]^{(1+k)} e^{-(1+k)B_a(T,S)x(T)} e^{\left[\frac{(1+k)}{2}(V(0,T)-V(0,S)+(1+k)V(T,S))\right]},$$
$$B_a(T,S) = \frac{1}{a}\left(1-e^{-a(S-T)}\right),$$

where $x(T)$ is a normally distributed random variable under the Q_T-measure. In turn, the zero-coupon-bond $P_{HW}^k(T,S)$ is log-normal random variable with mean and variance

$$\mu := \mathbb{E}^{\mathbb{Q}_T}\left[\log P_{HW}^k(T,S)|\mathcal{F}_t\right] = (1+k)\log\left[\frac{P_{OIS}(0,S)}{P_{OIS}(0,T)}\right] - (1+k)B_a(T,S)\mathbb{E}^{\mathbb{Q}_T}[x(T)] \tag{C.30}$$
$$+\frac{(1+k)}{2}\left(V(0,T)-V(0,S)+(1+k)V(T,S)\right),$$

$$V^2 := \mathbb{V}^{\mathcal{Q}_T}\left[\log P_{HW}^k(T,S)|\mathcal{F}_t\right] = \frac{\sigma^2}{2a}\left[1-e^{-2a(T-t)}\right](-(1+k)B_a(T,S))^2. \tag{C.31}$$

The expected call payoff with strike X is computed as

$$\int_{-\infty}^{+\infty}\frac{1}{\sqrt{2\pi}V}(e^z-X)^+e^{-\frac{1}{2}\frac{(z-\mu)^2}{V^2}}dz \tag{C.32}$$
$$= X\Phi(-d_2) - e^{\mu+\frac{1}{2}V^2}\Phi(-d_1), \tag{C.33}$$
$$d_1 = (\mu - \ln X + V^2)/V, \tag{C.34}$$
$$d_2 = d1 - V. \tag{C.35}$$

We discount the payoff at the time of option expiration T with OIS bonds obtaining the final result:

$$ZBP(t,T,S,X) = P_{OIS}(t,T)\left[e^{\mu+\frac{1}{2}V^2}\Phi(d_1) - X\Phi(d_2)\right] \tag{C.36}$$

C.2.3 Caplet Pricing with HW1F-K

Definition C.1. *1 To price a caplet which pays out the difference between LIBOR rate $L(T,S)$ and strike K scaled by day-count fraction $\tau = (S-T)$, we need to compute*

$$Cplt(t,T,S,K) = \mathbb{E}^Q\left[e^{-\int_t^S r(u)du}\tau(L(T,S)-K)^+|\mathcal{F}_t\right] \tag{C.37}$$

$$= P_{OIS}(t,S)\mathbb{E}^{Q_S}\left[\tau(L(T,S)-K)^+|F_t\right] \tag{C.38}$$

$$= P_{OIS}(t,S)\mathbb{E}^{Q_S}\left[\tau\left(\frac{1}{\tau}\left(\frac{1}{P_L(T,S)}-1\right)-K\right)^+|\mathcal{F}_t\right] \tag{C.39}$$

$$= P_{OIS}(t,S)\mathbb{E}^{Q_S}\left[\left(\frac{1}{P_L(T,S)}-(1+\tau K)\right)^+|\mathcal{F}_t\right]. \tag{C.40}$$

While in classic, single-curve setting this could be changed to T-forward measure and made into a zero-coupon bond put option on $P_L(T,S)$ with strike $X = 1/(1+\tau K)$, in our case the discount factor inside the expectation is the OIS discount, $P_{OIS}(T,S)! = P_L(T,S)$ and we cannot use this relationship.

However, the zero-bond is a log-normally distributed random variable, and its inversion is also a log-normally distributed r.v.

$$P_L(T,S) \approx \exp(\mathcal{N}(\mu,V^2)) \implies \frac{1}{P_L(T,S)} \approx \exp(\mathcal{N}(-\mu,V^2)), \tag{C.41}$$

therefore our caplet can be priced as a ZCB-call option on inverted $\frac{1}{P_L(T,S)}$. Let $X = (1+\tau K)$ and $\hat{P}(T,S) = \frac{1}{P_L(T,S)}$, then

$$Cplt(t,T,S,K) = P_{OIS}(t,S)\mathbb{E}^{Q_S}\left[(\hat{P}(T,S)-(1+\tau K))^+\right] \tag{C.42}$$

$$= ZBC(t,T,S,X) = P_{OIS}(t,S)\left[e^{-\mu+\frac{1}{2}V^2}\Phi(d_1)-X\Phi(d_2)\right], \tag{C.43}$$

$$d_1 = (-\mu-\ln X+V^2)/V, \tag{C.44}$$

$$d_2 = d_1 - V, \tag{C.45}$$

where

$$\mu = \mathbb{E}^{Q_S}\left[\log P(T,S)\right] \tag{C.46}$$

$$= (1+k)\log\left[\frac{P_{OIS}(0,S)}{P_{OIS}(0,S)}\right] - (1+k)B_a(T,S)\mathbb{E}^{Q_S}[x(T)], \tag{C.47}$$

$$V^2 = \mathbb{V}^{Q_S}\left[\log P(T,S)\right] \tag{C.48}$$

$$= \frac{\sigma^2}{2a}\left[1-e^{-2a(T-t)}\right](-(1+k)B_a(T,S))^2 \tag{C.49}$$

are the mean and variance of $\log \hat{P}(T,S)$ under the Q_S-measure.

C.3 Pricing under scaled HW2F-K Model

This section includes the derivations of bond and option prices under the K-scaled 2-factor Hull-White model.

C.3.1 2-Curve Option Pricing with HW2F

Standard single-curve bond and option valuation formulas for the Hull-White model are given in (Brigo and Mercurio, 2006). However, if we were to consider 2-curve framework with OIS-discounting for a LIBOR bond option, the formulas for zero-bond calls and puts become more involved. First, we assume that the LIBOR-forward rates are $\mathbb{Q}^S = \mathbb{Q}^S_D$-martingales for OIS curve D as $L(t;T,S) = \mathbb{E}^{\mathbb{Q}_S}\left[L(T,S)|\mathcal{F}_t\right]$

Lemma. C.3.1. *The zero-bond options, put and call, under two-curve Hull-White framework can be priced with*

$$ZBP_{HW2F}(t,T,S,X) = P_{ois}(t,T)\left(X\Phi\left(-h+\Sigma(t,T,S)\right) - P_{HW2F}(t;T,S)\Phi(-h)\right) \tag{C.50}$$

$$ZBC_{HW2F}(t,T,S,X) = P_{ois}(t,T)\left(P_{HW2F}(t;T,S)\Phi(h) - X\Phi(h-\Sigma(t,T,S))\right) \tag{C.51}$$

where

$$h = \frac{\ln\frac{P_{HW2F}(t;T,S)}{X}}{\Sigma(t,T,S)} + \frac{\Sigma(t,T,S)}{2} \tag{C.52}$$

and Σ defined as

$$\Sigma(t,T,S)^2 = \frac{\sigma_x^2}{2a_x^3}\left[1-e^{-a_x(S-T)}\right]^2\left[1-e^{-2a_x(T-t)}\right]+\frac{\sigma_y^2}{2a_y^3}\left[1-e^{-a_y(S-T)}\right]^2\left[1-e^{-2a_y(T-t)}\right]$$
$$+2\rho\frac{\sigma_x\sigma_y}{a_xa_y(a_x+a_y)}\left[1-e^{-a_x(S-T)}\right]\left[1-e^{-a_y(S-T)}\right]\left[1-e^{-(a_x+a_y)(T-t)}\right]. \quad \text{(C.53)}$$

Lemma. C.3.2. *A single caplet on a LIBOR payment, with strike K expiring at time T and maturing at time S price, must be valued under Q^S-forward measure:*

$$\begin{aligned} Cplt(t,T,S,K) &= \mathbb{E}^{\mathbb{Q}}\left[e^{-\int_t^S r_{OIS}(u)du}\tau(L(T,S)-K)^+\middle|\mathcal{F}_t\right] \quad \text{(C.54)}\\ &= P_{OIS}(t,S)\mathbb{E}^{\mathbb{Q}_S}\left[\tau(L(T,S)-K)^+|\mathcal{F}_t\right]\\ &= P_{OIS}(t,S)\mathbb{E}^{\mathbb{Q}_S}\left[\left(\frac{1}{P_L(T,S)}-(1+\tau K)\right)^+\middle|\mathcal{F}_t\right] \end{aligned}$$

where $\tau = (S-T)$ is a year fraction. The bond $P_L(T,S)$ under $\mathbb{E}^{\mathbb{Q}_S}$ is distributed log-normally $\mathcal{LN}(\mu,V_p)$ for $V_p = \Sigma(t,T,S)$ and

$$\mu = \mathbb{E}^{\mathbb{Q}_S}\left[\ln P_L(T,S)|\mathcal{F}_t\right] = \ln\frac{P^M(0,S)}{P^M(0,T)}+\frac{1}{2}\left[V(T,S)-V(0,S)+V(0,T)\right]$$
$$-B_a(T,S)\mathbb{E}^{\mathbb{Q}_S}[x(T)|\mathcal{F}_t]-B_b(T,S)\mathbb{E}^{\mathbb{Q}_S}[y(T)|\mathcal{F}_t], \quad \text{(C.55)}$$

and $\mathbb{E}^{\mathbb{Q}_S}[x(T)|\mathcal{F}_t], \mathbb{E}^{\mathbb{Q}_S}[y(T)|\mathcal{F}_t]$ are given in (Brigo and Mercurio, 2006)

Lemma. C.3.3. *The inverted bond $\hat{P}(T,S) = \frac{1}{P_L(T,S)}$ follows log-normal distribution $\mathcal{LN}(-\mu,V_p)$, therefore we can analytically price caplet under $\mathbb{E}^{\mathbb{Q}_S}$ measure as:*

$$\begin{aligned} Cplt(t,T,S,K) &= P_{OIS}(t,S)\mathbb{E}^{\mathbb{Q}_S}\left[\left(\hat{P}_L(T,S)-X\right)^+\middle|\mathcal{F}_t\right]\\ &= P_{OIS}(t,S)\left[e^{-\mu+\frac{1}{2}V_p^2}\Phi(d)-X\Phi(d-V_p)\right] \quad \text{(C.56)} \end{aligned}$$

where $X = (1+(S-T)K)$, $d = (-\mu-\ln X+V_p^2)/V_p$

C.3.2 Bond Price Derivation: HW2F-K

In the hybrid HCIR model we use a scaled HW2F bonds, their pricing can be done by light modification of the standard formulas.

Lemma. C.3.4. *The zero-coupon bond price under the k-scaled 2-factor HW model is*

derived similarly as above:

$$P^k_{HW2F}(t,T) = \mathbb{E}^Q\left[e^{-(1+k)\int_t^T r(u)du}\right] \tag{C.57}$$

where $r(t)$ is the short rate under HW2F model (Brigo and Mercurio, 2006). We continue, by noting that

$$\int_t^T r(u)du = \int_t^T \phi(u) + x(u) + y(u)du, \tag{C.58}$$

$$\begin{aligned}\mathbb{E}\left[\int_t^T x(u)+y(u)du\right] &= \frac{1-e^{-a(T-t)}}{a}x(t) + \frac{1-e^{-b(T-t)}}{b}y(t)\\ &:= B_a(t,T)x(t) + B_b(t,T)y(t),\end{aligned} \tag{C.59}$$

$$\begin{aligned}V_{HW2F}(t,T) &= \mathbb{V}\left[\int_t^T x(u)+y(u)du\right]\\ &= \frac{\sigma^2}{a^2}\left[T-t+\frac{2}{a}e^{-a(T-t)} - \frac{1}{2a}e^{-2a(T-t)} - \frac{3}{2a}\right]\\ &+ \frac{\eta^2}{b^2}\left[T-t+\frac{2}{b}e^{-b(T-t)} - \frac{1}{2b}e^{-2b(T-t)} - \frac{3}{2b}\right]\\ &+ 2\rho\frac{\sigma\eta}{ab}\left[T-t+\frac{e^{-a(T-t)}-1}{a} + \frac{e^{-b(T-t)}-1}{b} + \frac{e^{-(a+b)(T-t)}-1}{a+b}\right],\end{aligned} \tag{C.60}$$

we set:

$$\phi(u) = f^M(0,u) + \frac{\sigma^2}{2a^2}(1-e^{-au})^2 + \frac{\sigma^2}{2b^2}(1-e^{-bu})^2 + \rho\frac{\sigma\eta}{ab}(1-e^{-au})(1-e^{-bu}) \tag{C.61}$$

as we calibrate the model to market OIS zero-coupon bond prices when $k = 0$. Following the narrative of the HW1F-K bond price derivation, we obtain the HW2F-K bond price:

$$\begin{aligned}P^k_{HW2F}(t,T) = \mathbb{E}^Q\left[e^{-(1+k)\int_t^T r(u)du}\right] &= \left[e^{-\int_t^T \phi(u)du}\right]^{(1+k)}\left[e^{-(1+k)\int_t^T x(u)+y(u)du}\right]\\ &= \frac{P^M(0,T)}{P^M(0,t)}^{(1+k)} \exp\left[-\frac{1}{2}(1+k)\left[V_{HW2F}(0,T) - V_{HW2F}(0,t)\right]\right]\\ &\exp\left[(1+k)\frac{1-e^{-a(T-t)}}{a}x(t) + (1+k)\frac{1-e^{-b(T-t)}}{b}y(t) + \frac{1}{2}(1+k)^2V^2_{HW2F}(t,T)\right],\end{aligned} \tag{C.62}$$

which leads to the final result:

$$P^k_{HW2F}(t,T) = \left[\frac{P_{OIS}(0,T)}{P_{OIS}(0,t)}\right]^{(1+k)} \exp[-(1+k)B_a(t,T)x(t)] \exp[-(1+k)B_b(t,T)y(t)] \\ \exp\left[\frac{(1+k)}{2}\left(V_{HW2F}(0,t) - V_{HW2F}(0,T) + (1+k)V_{HW2F}(t,T)\right)\right] \tag{C.63}$$

C.3.3 Option Pricing with HW2F-K

Similarly to the 1-factor case the k-scaled zero-bond option price can be computed analytically:

$$ZBP_{HW2FK}(t,T,S,X) = P_{ois}(t,T)\left(\hat{P}^k_{HW2F}(t;T,S)\Phi(h) - X\Phi(h-\hat{\Sigma}(t,T,S))\right) \tag{C.64}$$

where

$$h = \frac{\ln\frac{\hat{P}^k_{HW2F}(t;T,S)}{X}}{\hat{\Sigma}(t,T,S)} + \frac{\hat{\Sigma}(t,T,S)}{2} \tag{C.65}$$

$$\hat{\Sigma}(t,T,S)^2 = (1+k)^2\Sigma(t,T,S)^2 \tag{C.66}$$

$$\hat{P}^k_{HW2F}(t;T,S) = \mathbb{E}^{Q_T}[P^k_{HW2F}(T,S)|\mathcal{F}_t] \tag{C.67}$$

and $\Sigma(t,T,S)$ is given in (C.53)

Lemma. C.3.5. *Pricing caplets under HW2F model requires the use of $\mathbb{Q}^S$-forward measure:*

$$Cplt_{HW2F}(t,T,S,K) = P_{OIS}(t,S)\mathbb{E}^{\mathbb{Q}_S}\left[(S-T)\left(L(T,S)-K\right)^+\middle|\mathcal{F}_t\right] \\ = P_{OIS}(t,S)\mathbb{E}^{\mathbb{Q}_S}\left[\left(\frac{1}{P^k_{HW2F}(T,S)} - X\right)^+\middle|\mathcal{F}_t\right] \tag{C.68}$$

we can apply the same inverted-bond valuation methodology as in (C.56) *obtaining*

$$Cplt_{HW2F}(t,T,S,K) = P_{OIS}(t,S)\left[\left(e^{-\mu+\frac{1}{2}\hat{V}^2}\Phi(d) - \hat{X}\Phi(d-\hat{V})\right)\right] \tag{C.69}$$

where

$$d = (-\mu - \ln \hat{X} + \hat{V}^2)/\hat{V}$$
$$\hat{X} = (1 + (S - T)K)$$
$$\mu = \mathbb{E}^{\mathbb{Q}_S}[\ln P^k_{HW2F}(T, S)|\mathcal{F}_t]$$
$$\hat{V} = (1 + k)^2 \Sigma(t, T, S)^2$$

and $\Sigma(t, T, S)$ *is defined in* (C.53)*.*

Lemma. C.3.6. *To price an interest rate cap with strike* K *and fixing dates* T_i*, under HW2F model, we only need to sum the caplet values:*

$$Cap(t, \{T_0, ...T_N\}, K) = \sum_{i=1}^{N} Cplt_{HW2F}(t, T_{i-1}, T_i, K) \tag{C.70}$$

C.4 Building Hybrid Hull-White Model

The two-curve hybrid HCIR model can be built in two flavours: using HW1F or HW2F as the base OIS stochastic driver. We derive pricing formulas for both of them.

C.4.1 HW1F + CIR

We define the short-rate process $r(t)$ to be the driver of the instantaneous OIS rates, and the process s_t the driver of the LIBOR-OIS spread as:

$$r(t) = \Psi_1(t) \tag{C.71}$$
$$s(t) = k\Psi_1(t) + \Psi_2(t) \tag{C.72}$$

where Ψ_1 is a short rate from standard HW1F model (Brigo and Mercurio, 2006) and Ψ_2 is the CIR model short rate 4.1 and k is the correlation-dependence level between the risk-free OIS rate and the LIBOR-OIS spread. In this setup, the OIS rates are normally distributed and can be negative. Then, while $\Psi_2(t)$, the CIR process, is positive, due to explicit involvement of $HW1F$ process, the spread $s(t)$ can get negative.

This additive model yields a couple of convenient results. First, the risk-free OIS zero-coupon-bond prices are determined as in standard textbook extended Hull-White model (Brigo and Mercurio, 2006)

$$P_{OIS}(t, T) = P_{HW}(t, T) \tag{C.73}$$

Second, pricing of risky LIBOR-bond becomes:

$$
\begin{aligned}
P_L(t,T) &= E^Q\left[exp\left(-\int_t^T (r(u)+s(u))du\right)\right] \\
&= E^Q\left[exp\left(-\int_t^T (\Psi_1(u)+k\Psi_1(u)+\Psi_2(u))du\right)\Big|\mathcal{F}_t\right] && \text{(C.74)} \\
&= E^Q\left[exp\left(-\int_t^T (1+k)\Psi_1(u)du\right)exp\left(-\int_t^T \Psi_2(u)du\right)\Big|\mathcal{F}_t\right] && \text{(C.75)} \\
&= E^Q\left[exp\left(-\int_t^T (1+k)\Psi_1(u)du\right)\Big|\mathcal{F}_t\right]P_{CIR}(t,T) && \text{(C.76)}
\end{aligned}
$$

The left expectation becomes a modified version of the Hull-White bond price as given in (C.30).

Lemma. C.4.1. *To price a LIBOR-based zero-coupon bond option with expiry T and maturity S in the hybrid-model (HCIR) setting under the forward Q^T-measure, we let*

$$
\begin{aligned}
ZBC_{HCIR}(t,T,S,X) &= \mathbb{E}^Q\left[e^{-\int_t^T r(u)du}\left(P_L(T,S)-X\right)^+|\mathcal{F}_t\right] && \text{(C.77)} \\
&= P_{OIS}(t,T)\mathbb{E}^{Q_T}\left[(P_L(T,S)-X)^+|\mathcal{F}_t\right] \\
&= P_{OIS}(t,T)\mathbb{E}^{Q_T}\left[(P_{CIR}(T,S)P^k_{HW1F}(T,S)-X)^+|\mathcal{F}_t\right] \\
&= P_{OIS}(t,T)\mathbb{E}^{Q_T}\left[P_{CIR}(T,S)\left(P^k_{HW1F}(T,S)-X/P_{CIR}(T,S)\right)^+|\mathcal{F}_t t\right] \\
&= \mathbb{E}^{Q_T}\left[P_{CIR}(T,S)\mathbb{E}^{Q_T}\left[P_{ois}(t,T)\left(P^k_{HW1F}(T,S)-X/P_{CIR}(T,S)\right)^+|\mathcal{F}_t\right]|\mathcal{F}\right. \\
&= \mathbb{E}^{Q_T}\left[P_{CIR}(T,S)ZBC^k_{HW1F}\left(t,T,S,X/P_{CIR}(T,S)\right)|F_t\right] \\
& && \text{(C.78)}
\end{aligned}
$$

the latter expectation must be evaluated numerically, but is simple to do as we have analytic terminal distribution for CIR-state variable $c(t)$ under our chosen measure and, therefore, the CIR-bond prices at time T, $P_{CIR}(T,S)$.

Lemma. C.4.2. *Pricing caplets under HW1F-CIR (H1FCIR) model also requires, as in the standard hull-white two-curve caplet price the use of $\mathbb{Q}^S$-forward measure (see Appendix*

C.2.3):

$$
\begin{aligned}
Cplt_{H1FCIR}(t,T,S,K) &= P_{OIS}(t,S)\mathbb{E}^{\mathbb{Q}_S}\left[(S-T)\left(L(T,S)-K\right)^{+}\middle|\mathcal{F}_t\right] \\
&= P_{OIS}(t,S)\mathbb{E}^{\mathbb{Q}_S}\left[\left(\frac{1}{P_{CIR}(T,S)P^k_{HW1F}(T,S)}-X\right)^{+}\middle|\mathcal{F}_t\right] \\
&= P_{OIS}(t,S)\mathbb{E}^{\mathbb{Q}_S}\left[\frac{1}{P_{CIR}(T,S)}\left(\frac{1}{P^k_{HW1F}(T,S)}-XP_c(T,S)\right)^{+}\middle|\mathcal{F}_t\right] \quad \text{(C.79)}
\end{aligned}
$$

with $X = 1+(S-T)K$*, we can apply the inverted-bond valuation methodology as in* (C.41) *obtaining*

$$
Cplt_{H1FCIR}(t,T,S,K) = P_{OIS}(t,S)\mathbb{E}^{\mathbb{Q}_S}\left[\frac{1}{P_{CIR}(T,S)}\left(e^{-\mu+\frac{1}{2}\hat{V}^2}\Phi(d)-\hat{X}\Phi(d-\hat{V})\right)\middle|\mathcal{F}_t\right] \quad \text{(C.80)}
$$

where

$$
\begin{aligned}
d &= (-\mu-\ln\hat{X}+\hat{V}^2)/\hat{V} \\
\hat{X} &= P_c(T,S)(1+(S-T)K) \\
\mu &= \mathbb{E}^{\mathbb{Q}_S}[\ln P^k_{HW1F}(T,S)|\mathcal{F}_t] \\
\hat{V} &= \tilde{\Sigma}(t,T,S)^2+
\end{aligned}
$$

This expectation must be evaluated numerically, by integrating over analytically-known distribution of $P_{CIR}(T,S)$ under the $\mathbb{Q}^S$-forward measure.

Lemma. C.4.3. *To price an interest rate cap with strike* K *and fixing dates* T_i*, under HCIR model, we only need to sum the caplet values:*

$$
Cap(t,\{T_0,...T_N\},K) = \sum_{i=1}^{N} Cplt_{HCIR}(t,T_{i-1},T_i,K) \quad \text{(C.81)}
$$

C.4.2 HW2F + CIR

In the three-factor setup, we have used the 2-factor Hull-White model and the CIR model. This combination gives additional degrees of freedom to fit the caplets, especially some

flexibility on the short end of the volatility curve. Our setup stays the same

$$r(t) = \Psi_1(t), \tag{C.82}$$

$$s(t) = k\Psi_1(t) + \Psi_2(t), \tag{C.83}$$

but Ψ_1 is a short rate from standard HW2F model and Ψ_2 is the CIR model short rate.

The zero-coupon bond price can be split into CIR-Bond and K-scaled 2-factor Hull-White $(1+k)$ zero-coupon bond.

$$P_L(t,T) = P_c(t,T)P^k_{HW2F}(t,T), \tag{C.84}$$

and the price for the latter bond is given in (C.62)

Lemma. C.4.4. *Pricing caplets under HCIR model also requires, as in the standard hull-white two-curve caplet price* (C.56)*, the use of $\mathbb{Q}^S$-forward measure:*

$$\begin{aligned} Cplt_{HCIR}(t,T,S,K) &= P_{OIS}(t,S)\mathbb{E}^{\mathbb{Q}_S}\left[(S-T)\left(L(T,S)-K\right)^+ \middle| \mathcal{F}_t\right] \\ &= P_{OIS}(t,S)\mathbb{E}^{\mathbb{Q}_S}\left[\left(\frac{1}{P_c(T,S)P^k_{HW2F}(T,S)} - X\right)^+ \middle| \mathcal{F}_t\right] \\ &= P_{OIS}(t,S)\mathbb{E}^{\mathbb{Q}_S}\left[\frac{1}{P_c(T,S)}\left(\frac{1}{P^k_{HW2F}(T,S)} - XP_c(T,S)\right)^+ \middle| \mathcal{F}_t\right] \end{aligned} \tag{C.85}$$

we can apply the same inverted-bond valuation methodology as in (C.56) *obtaining*

$$Cplt_{HCIR}(t,T,S,K) = P_{OIS}(t,S)\mathbb{E}^{\mathbb{Q}_S}\left[\frac{1}{P_c(T,S)}\left(e^{-\mu+\frac{1}{2}\hat{V}^2}\Phi(d) - \hat{X}\Phi(d-\hat{V})\right)\middle| \mathcal{F}_t\right] \tag{C.86}$$

where

$$\begin{aligned} d &= (-\mu - \ln\hat{X} + \hat{V}^2)/\hat{V} \\ \hat{X} &= P_c(T,S)(1+(S-T)K) \\ \mu &= \mathbb{E}^{\mathbb{Q}_S}[\ln P^k_{HW2F}(T,S)|\mathcal{F}_t] \\ \hat{V} &= (1+k)^2\Sigma(t,T,S)^2 \end{aligned}$$

and $\Sigma(t,T,S)$ is defined in (C.53) *and Φ.*

This expectation must be evaluated numerically, by integrating over analytically-

known distribution of $P_c(T,S)$ under the $\mathbb{Q}^S$-forward measure.

Lemma. C.4.5. *To price an interest rate cap with strike K and fixing dates T_i, under HCIR model, we only need to sum the caplet values:*

$$Cap(t,\{T_0,...T_N\},K) = \sum_{i=1}^{N} Cplt_{HCIR}(t,T_{i-1},T_i,K) \tag{C.87}$$

Appendix D

Appendix: More Cap Pricing and Calibration Results with HCIR

D.1 Scheme for HCIR Model Calibration

The HCIR model in a joint HW-CIR model, which assumes that the LIBOR rates are a sum of OIS rate and tenor-dependent LIBOR-OIS spread. Using the latter assumption, we price LIBOR-bonds and LIBOR-caplets, and both are affected by the Hull-White and the CIR model parameters.

If the LOIS-OIS correlation parameter k as in (4.2) is zero, then the LOIS spread is fully independent of the OIS movements. In this case, the CIR model is calibrated separately to LOIS term-structure, and the HW parameters are fitted to OIS term-structure and, later, to LIBOR-cap volatilities.

On the other hand, if $k \neq 0$, then the LOIS spread is dependent on OIS movements, and therefore the optimal choice of CIR parameters $\sigma_c, \kappa, \theta, c_0$ is dependent on the HW parameters σ_i, a_i, ρ_{HW}, as these influence the LIBOR-bond pricing formula (C.84). This leads to a joint forward and cap present value calibration problem, where we want to find CIR and HW parameter set so that we minimise

$$\min_{\omega\in\Omega}\left[\sum_{i=1}^{N}(Fwd^{M}(t,T_{i-1},T_i)-Fwd^{HCIR}(t,T_{i-1},T_i,\omega))^2*v_i + \sum_{i=1}^{M}(Cap^{M}(t,S_i,K_i)-Cap^{HCIR}(t,S_i,K_i,\omega))^2*w_i\right] \tag{D.1}$$

where S_i's are cap maturities, v_i, w_i are weighting parameters to proportionally weight

errors in forward rates and caps. Thus, if we calibrate the HCIR model to 6-month forwards and 6-month caps, we have 10-parameter calibration, which needs a global solver. Note:

- The CIR_x parameters for 1,3,12-month forward curves can be calibrated after we obtain HW-volatility parameters, as 1,3,12-month LOIS spread parameters do not affect the pricing of 6-month caps.
- In calibration, we minimise the present-value error of caps. We have alternative calibration available to cap volatilities, but this requires PV-to-volatility conversion at every HCIR cap evaluation, which is another root-finding problem. This calibration method is very computationally expensive.

We have attempted multiple calibration methods to get a good fit for the 10-parameter model. Some global methods work well but are very slow, for instance the differential evolution and basin-hopping algorithm (truncated newton root finding with multiple random restarts). In the end, we devised a good, fast calibration scheme for HCIR model:

1. Calibrate HW2F model with constant-basis to liquid 6-month forwards and caps,
2. Use the latter set of parameters as starting point x_0 for HW model in HCIR,
3. Calibrate CIR_{6M} in HCIR to LOIS spreads, obtain x_{CIR},
4. Run a single global-solver (e.g. basin-hopping) run on x_0 and x_{CIR}, obtaining solution ω,
5. We note that this may not be the global optimum, but we found it to be very successful.

D.2 Auxiliary Tables and Figures

Some results were excluded from the main text to improve readability and flow of arguments. We have included all the skipped results and tables in this appendix.

D.2.1 ATM Cap Calibration Parameters, 22-Nov-2013

The obtained parameter set for HCIR calibration with 22-Nov-2013 data, using ATM 6-month cap volatilities is given in the following table.

Model	a_x	σ_x	a_y	σ_y	ρ_{HW}
H1F-CIR	4.05%	0.96%			
H2F-CIR	45.07%	2.07%	12.3%	2.49%	-99.6%

Table D.1: Hull-White model parameters for OIS in the 1 and 2-factor Hybrid HW models.

Model	ρ_{CIR}	σ_c	θ	k	c_0
H1F-CIR: 1M	-2.1%	0.17%	8e-6	18%	0.13%
H1F-CIR: 3M	-3%	5e-5	1e-7	6.85%	0.27%
H1F-CIR: 6M	-1.9%	0.14%	1e-5	9.1%	0.41%
H1F-CIR: 12M	-1.2%	0.14%	1e-5	8.8%	0.5%
H2F-CIR: 1M	-4%	0.06%	1e-4	4.9%	0.13%
H2F-CIR: 3M	-3.4%	0.3%	1e-4	6.1%	0.28%
H2F-CIR: 6M	-2.0%	0.4%	1e-4	9.4%	0.42%
H2F-CIR: 12M	-1.8%	0.35%	1e-4	8.0%	0.54%

Table D.2: CIR model parameters for LOIS spread in the 1 and 2-factor Hybrid HW models .

In the following, we include a table of extrapolated volatilities comparison between the HCIR model and displaced-diffusion approach. We note that the DD results were obtained using simple constant parameters, e.g. LMM forward $\rho = 95\%$ (historically relevant value), and the overall fit can be improved using many degrees of freedom in the model as shown by Andong (2013).

Tenor / MAT	3Y	5Y	7Y	12Y	20Y	30 Y	
1M	61.1	67.4	73.4	78.6	78.6	73.0	66.3
3M	62.6	70.9	76.2	78.5	79.0	74.7	67.8
6M	63.6	71.5	77.3	80.2	81.1	77.0	69.9
12M	67.4	74.6	80.0	82.8	84.0	79.7	71.8

Table D.3: Multi-curve ATM cap volatilities: Calibrated HCIR model extrapolations.

Tenor / MAT	3Y	5Y	7Y	12Y	20Y	30 Y	
1M	41.8	59.5	70.3	77.9	79.3	76.8	71.1
3M	45.9	65.6	74.4	78.7	79.6	77.2	71.0
6M	58.0	73.5	79.0	81.6	80.7	76.6	70.0
12M	70.2	80.5	84.2	85.6	83.5	77.9	70.8

Table D.4: Multi-curve ATM cap volatilities: displaced-diffusion extrapolations, $\rho = 0.95$, DD with this value is closer to HCIR surface.

D.2.2 3% Cap Calibration Parameters, 22-Nov-2013

We show the calibrated HCIR model parameters when calibration was performed by minimising the mean squared errors of cap present values and forward rates. As demonstrated in Table D.5, the HW2F-CIR model has very different HW-parameters than in the ATM case. The HW 2-factor correlation parameter ρ_{HW} is very negative as in the previous case, but because the mean reversion rates a_x, a_y are not as different anymore - we no longer observe the volatility hump at 5-year cap volatility. The CIR-component parameters have stayed similar: the HW-CIR correlation is negative and smaller for longer tenors, θ, k, c_0 within 1% difference from ATM values.

Model	a_x	σ_x	a_y	σ_y	ρ_{HW}
H2F-CIR	4.1 %	2.1 %	9.4 %	3.3 %	-94.5 %

Table D.5: Hull-White model parameters for OIS in the HW2F-CIR model.

Model	ρ_{CIR}	σ_c	θ	k	c_0
H2F-CIR: 1M	-3.8 %	0.3 %	1e-4 %	5.4 %	0.1 %
H2F-CIR: 3M	-3.5 %	0.1 %	1e-4 %	6.0 %	0.3 %
H2F-CIR: 6M	-2.5 %	0.4 %	1e-4 %	8.4 %	0.4 %
H2F-CIR: 12M	-2.6 %	0.3 %	1e-4 %	7.0 %	0.5 %

Table D.6: CIR model parameters for LOIS spread in the HW2F-CIR model. The CIR-correlation is negative to OIS rates and decreases with increasing tenor.

D.2.3 4% caps including illiquid quotes, 22-Nov-2013

In the tables below, we give the resulting PV, normal and Black volatilities from HCIR model calibration to 4% caps and given illiquid quotes in the test case. We have marked the cap values which should be close to the illiquid caps. The differences between the model values for illiquid caps and input data are rather large, few 100's of bp in some cases. Calibration of 6-month 4% caps was also affected by the extra data in the calibration - resulting normal volatilities are 20-30bp larger than the market data.

In this setup, the illiquid 3-month caps were repriced lower than the input data by up to 60bp. The illiquid 12-month caps were repriced higher than market data even by 100-200 bp in present value terms.

T/K	1%	1.5%	2%	2.25%	2.5%	3%	3.5%	**4%**	5%	6%	8%	10%
1Y	12	6	2	1	1	0	0	0	0	0	0	0
1.5Y	32	19	10	7	5	2	1	0	0	0	0	0
2Y	60	38	23	18	13	8	4	2	0	0	0	0
3Y	140	97	66	54	44	28	18	11	4	1	0	0
4Y	256	188	136	115	97	67	46	31	13	5	0	0
5Y	404	309	232	200	172	125	90	63	30	13	2	0
6Y	579	454	350	306	266	200	147	107	54	26	5	0
7Y	774	617	485	428	376	288	217	161	85	42	8	1
8Y	983	794	633	562	498	386	295	223	121	61	13	2
9Y	1201	980	790	706	628	493	381	291	161	84	18	3
10Y	1424	1172	952	854	764	604	472	363	205	108	24	4
12Y	1864	1551	1274	1150	1034	828	654	509	294	159	38	6
15Y	2483	2084	1729	1567	1416	1145	913	718	423	234	58	10
20Y	3313	2795	2331	2118	1919	1559	1249	985	585	325	81	15
25Y	3965	3350	2797	2543	2305	1873	1501	1185	704	391	97	17
30Y	4495	3798	3170	2882	2611	2122	1699	1341	795	440	109	19

Table D.7: Present value surface for 6-month caps. The HCIR model values are given in EUR for caps of notional=10000 and rounded to nearest integer.

T/K	1%	1.5%	2%	2.25%	2.5%	3%	3.5%	4%	5%	6%	8%	10%
1Y	14	6	3	2	1	0	0	0	0	0	0	0
1.5Y	33	19	10	7	5	2	1	0	0	0	0	0
2Y	60	37	22	17	13	7	3	2	0	0	0	0
3Y	136	93	62	50	41	26	16	10	3	1	0	0
4Y	247	180	129	108	***91***	***62***	42	28	11	4	0	0
5Y	392	298	222	191	163	118	83	58	26	11	1	0
6Y	565	440	338	295	256	191	140	100	49	22	3	0
7Y	758	602	472	415	365	278	***208***	***153***	***79***	38	7	0
8Y	965	778	619	550	486	376	287	215	115	57	11	1
9Y	1184	965	777	693	617	484	374	284	157	81	17	2
10Y	1407	1157	940	843	754	596	465	358	***201***	***106***	23	3
12Y	1851	1539	1266	1142	1028	824	652	508	295	160	38	6
15Y	2474	2078	1726	1567	1417	1148	918	724	430	239	60	11
20Y	3313	2800	2340	2129	1931	1574	1265	1003	602	339	87	16
25Y	3976	3366	2817	2565	2329	1900	1530	1214	730	412	106	20
30Y	4515	3823	3200	2915	2646	2159	1738	1379	829	467	120	23

Table D.8: Present value surface for 3-month caps. The HCIR model values are given in EUR for caps of notional=10000 and rounded to nearest integer.

T/K	1%	1.5%	2%	2.25%	2.5%	3%	3.5%	4%	5%	6%	8%	10%
2Y	50	33	21	16	12	7	4	2	0	0	0	0
3Y	134	95	66	55	45	30	20	13	5	2	0	0
4Y	254	191	140	119	101	72	51	35	17	8	1	0
5Y	408	315	240	208	180	133	97	70	36	18	4	0
6Y	587	464	361	317	278	211	158	117	62	32	8	2
7Y	785	630	499	442	390	301	229	173	95	50	13	3
8Y	996	810	649	578	514	401	309	236	132	71	18	4
9Y	1216	997	807	723	645	509	396	304	173	94	24	5
10Y	1440	1189	970	871	781	620	486	377	217	119	31	7
12Y	1881	1568	1291	1166	1050	843	667	521	305	169	44	9
15Y	2496	2098	1741	1579	1427	1155	921	725	430	240	62	13
20Y	3317	2799	2333	2120	1920	1558	1247	983	584	326	84	17
25Y	3960	3345	2789	2534	2295	1863	1490	1174	696	387	98	19
30Y	4480	3783	3152	2864	2592	2102	1679	1321	781	432	108	21

Table D.9: Present value surface for 12-month caps. The HCIR mode values are given in EUR for caps of notional=10000 and rounded to nearest integer.

T/K	1%	1.5%	2%	2.25%	2.5%	3%	3.5%	4%	5%	6%	8%	10%
1Y	163	164	164	165	165	165	166	167	168	169	171	172
1.5Y	158	159	159	159	159	160	160	161	162	163	165	167
2Y	155	155	156	156	156	156	156	157	157	158	161	163
3Y	147	148	148	148	148	148	148	148	148	148	150	152
4Y	140	141	140	140	140	140	140	140	139	139	140	141
5Y	134	134	134	134	134	133	133	133	132	132	132	132
6Y	129	129	129	128	128	128	127	127	126	126	125	125
7Y	124	124	124	123	123	123	122	122	121	120	119	118
8Y	120	120	119	119	119	118	118	117	116	115	114	113
9Y	116	116	115	115	115	114	114	113	112	111	110	109
10Y	113	113	112	112	112	111	110	110	109	107	106	105
12Y	107	107	106	106	106	105	104	104	103	102	100	98
15Y	100	100	100	99	99	98	98	97	96	95	93	91
20Y	91	91	91	91	91	90	90	89	88	87	85	83
25Y	85	85	85	85	84	84	84	83	82	81	79	77
30Y	80	80	80	80	80	79	79	79	78	77	75	73

Table D.10: Normal volatilities surface for 3-month caps. The HCIR model values are given in basis points and rounded to the nearest integer.

T/K	1%	1.5%	2%	2.25%	2.5%	3%	3.5%	4%	5%	6%	8%	10%
1Y	166	169	171	172	173	174	176	177	179	180	181	180
1.5Y	161	163	165	165	166	167	169	170	173	175	179	180
2Y	157	159	160	161	161	162	164	165	167	170	174	177
3Y	149	150	151	151	152	152	153	154	156	158	163	166
4Y	141	142	143	143	143	143	144	144	145	147	151	155
5Y	134	135	135	135	135	135	136	136	136	137	140	143
6Y	128	129	129	129	129	129	129	129	129	129	131	133
7Y	122	123	123	123	123	123	123	123	122	122	123	124
8Y	118	118	118	118	118	118	118	117	117	117	116	117
9Y	113	114	114	114	114	113	113	113	112	112	111	111
10Y	110	110	110	110	110	110	109	109	108	107	106	106
12Y	103	104	104	104	104	103	103	102	101	101	99	98
15Y	96	97	97	97	97	96	96	95	94	93	91	90
20Y	88	88	88	88	88	88	87	87	86	85	83	82
25Y	81	82	82	82	82	82	82	81	80	79	78	76
30Y	76	77	77	77	77	77	77	77	76	75	73	71

Table D.11: Normal volatilities surface for 6-month caps. The HCIR model values are given in basis points and rounded to the nearest integer.

T/K	1%	1.5%	2%	2.25%	2.5%	3%	3.5%	4%	5%	6%	8%	10%
2Y	161	164	167	169	171	174	177	180	185	189	192	192
3Y	151	154	156	157	159	161	163	165	170	175	183	188
4Y	141	144	146	147	148	150	151	153	156	161	169	176
5Y	133	136	138	138	139	140	141	142	145	148	156	163
6Y	126	129	130	131	131	132	133	133	135	138	144	151
7Y	120	122	124	124	124	125	125	126	127	129	134	140
8Y	115	117	118	118	119	119	119	120	120	122	125	130
9Y	110	112	113	113	114	114	114	114	115	115	118	121
10Y	106	108	109	109	109	110	110	110	110	110	111	114
12Y	99	101	102	102	102	102	102	102	102	102	102	103
15Y	91	93	94	94	94	95	94	94	94	93	93	93
20Y	83	84	85	85	86	86	86	86	85	85	84	83
25Y	76	78	79	79	79	79	80	79	79	79	78	77
30Y	71	73	74	74	74	75	75	75	75	74	73	72

Table D.12: Normal volatilities surface for 12-month caps. The HCIR model values are given in basis points and rounded to the nearest integer.

T/K	1%	1.5%	2%	2.25%	2.5%	3%	3.5%	4%	5%	6%	8%	10%
1Y	360	250	199	182	168	147	131	119	101	89	72	61
1.5Y	399	248	192	174	160	138	122	111	94	82	67	57
2Y	466	242	182	164	150	129	114	102	86	75	61	52
3Y	400	195	146	131	119	102	89	80	67	58	47	40
4Y	252	150	114	103	94	80	71	63	53	46	37	32
5Y	184	121	94	85	78	67	59	53	45	39	32	27
6Y	148	102	81	73	67	58	52	47	40	34	28	24
7Y	125	89	71	65	60	52	47	42	36	31	25	22
8Y	110	80	65	59	55	48	43	39	33	29	23	20
9Y	99	73	59	55	51	44	40	36	31	27	22	18
10Y	91	68	55	51	47	42	37	34	29	25	20	17
12Y	79	60	50	46	43	38	34	31	26	23	19	16
15Y	69	53	44	41	38	34	31	28	24	21	17	15
20Y	61	48	40	37	35	31	28	25	22	19	16	14
25Y	58	45	37	35	33	29	26	24	21	18	15	13
30Y	55	43	36	33	31	28	25	23	20	18	15	12

Table D.13: Black volatilities surface for 3-month caps. The HCIR model values are given in basis points and rounded to the nearest integer.

T/K	1%	1.5%	2%	2.25%	2.5%	3%	3.5%	4%	5%	6%	8%	10%
1Y	288	215	177	164	153	136	123	113	97	86	70	59
1.5Y	295	210	170	157	145	128	115	105	91	81	67	57
2Y	302	204	162	149	137	120	108	98	85	75	62	53
3Y	259	170	134	122	112	98	87	79	67	59	49	43
4Y	199	136	108	98	90	78	70	63	54	47	39	34
5Y	158	112	90	82	76	66	59	53	45	40	33	29
6Y	131	96	77	71	65	57	51	46	40	35	29	25
7Y	113	84	68	63	58	51	46	42	35	31	26	22
8Y	100	76	62	57	53	47	42	38	32	29	23	20
9Y	90	69	57	52	49	43	39	35	30	26	22	19
10Y	83	64	53	49	46	40	36	33	28	25	20	17
12Y	73	57	47	44	41	36	33	30	26	23	18	16
15Y	64	50	42	39	37	33	30	27	23	20	17	14
20Y	57	45	38	35	33	30	27	25	21	19	15	13
25Y	53	42	36	33	31	28	25	23	20	18	15	13
30Y	51	40	34	32	30	27	24	22	19	17	14	12

Table D.14: Black volatilities surface for 6-month caps. The HCIR model values are given in basis points and rounded to the nearest integer.

T/K	1%	1.5%	2%	2.25%	2.5%	3%	3.5%	4%	5%	6%	8%	10%
2Y	236	177	147	137	129	116	106	98	87	78	65	55
3Y	201	149	124	114	107	95	86	80	70	63	54	48
4Y	163	122	101	94	87	77	70	64	56	50	43	39
5Y	134	103	85	79	73	65	59	54	47	42	36	33
6Y	114	88	74	68	64	56	51	47	41	36	31	28
7Y	100	78	65	61	57	50	45	42	36	32	28	25
8Y	89	70	59	55	51	46	41	38	33	29	25	22
9Y	81	64	54	50	47	42	38	35	30	27	23	20
10Y	74	60	50	47	44	39	35	33	28	25	21	19
12Y	65	53	45	42	39	35	32	29	25	22	19	16
15Y	57	47	40	37	35	31	29	26	23	20	17	15
20Y	51	42	36	33	31	28	26	24	21	18	15	13
25Y	48	39	33	31	29	27	24	22	20	17	15	13
30Y	46	37	32	30	28	25	23	21	19	17	14	12

Table D.15: Black volatilities surface for 12-month caps. The HCIR model values are given in basis points $1bp = 1e-4$ and rounded to the nearest integer.

D.2.4 ATM Cap Calibration, 30-Apr-2015

In the negative rates calibration case for the 30-Apr-2015 dataset, after calibrating to ATM 6-month caps the H2F-CIR model parameters are as follows:

	a_x	σ_x	a_y	σ_y	ρ_{HW}
HW2F	3.4 %	1.1 %	67.8 %	2.0 %	-99.9 %
	ρ_{CIR}	σ_c	θ	k	c_0
H2F-CIR: 1M	3.1 %	0.5 %	1e-4	25.1 %	0.1 %
H2F-CIR: 3M	1.2 %	0.1 %	1e-4	4.7 %	0.2 %
H2F-CIR: 6M	0.8 %	0.3 %	1e-4	5.4 %	0.3 %
H2F-CIR: 12M	-1.5 %	0.3 %	1e-4	4.4 %	0.4 %

Table D.16: Calibrated multi-curve HCIR model parameters. Data from 30-Apr-2015.

In the following tables we show the 4-curve cap volatility surfaces from calibrated HCIR model:

T(Y)/K(%)	-0.25	0.5	1.5	1	2	3	4	5
1	57	42	41	40	52	80	107	134
1.5	45	34	30	31	41	62	84	105
2	39	31	29	29	34	52	69	87
3	37	35	38	39	41	42	54	68
4	40	41	44	47	49	51	52	57
5	44	46	49	52	54	56	58	59
6	47	50	53	56	58	61	62	63
7	51	53	57	59	61	64	65	66
8	54	56	59	61	63	66	67	68
9	56	58	61	63	65	67	69	70
10	58	60	62	64	66	68	70	70
12	61	62	65	66	68	70	71	72
15	64	65	67	68	69	71	71	72
20	66	67	68	69	70	71	71	71
25	67	67	68	68	69	70	70	70
30	66	66	67	67	68	68	68	68

Table D.17: HCIR normal 6-month cap volatilities surface, data from 30-Apr-2015.

T(Y)/K(%)	-0.25	0.5	1.5	1	2	3	4	5
1	59	55	52	50	51	74	98	122
1.5	43	44	42	40	40	58	77	97
2	40	41	38	37	37	50	67	84
3	43	43	43	44	45	46	54	68
4	46	47	48	50	52	53	55	58
5	47	50	52	55	56	58	60	60
6	51	54	56	58	60	62	64	64
7	54	57	59	61	63	65	66	67
8	57	60	62	64	65	67	68	69
9	61	63	65	66	68	69	70	71
10	63	64	66	68	69	70	71	72
12	66	67	68	69	70	72	72	73
15	68	69	70	71	72	72	73	73
20	69	69	70	71	71	72	72	72
25	69	69	70	70	71	71	71	71
30	68	68	69	69	69	69	69	69

Table D.18: HCIR normal 1-month cap volatilities surface, data from 30-Apr-2015.

T(Y)/K(%)	-0.25	0.5	1.5	1	2	3	4	5
1	61	50	46	44	50	76	101	126
1.5	49	41	38	36	40	60	80	100
2	44	38	35	34	35	51	68	86
3	42	39	40	42	43	44	53	67
4	44	44	46	48	50	52	53	57
5	47	48	51	53	55	57	59	60
6	51	52	55	57	59	61	63	64
7	54	55	58	60	62	64	66	67
8	57	58	61	63	64	66	68	68
9	59	60	62	64	66	68	69	70
10	60	62	64	66	67	69	70	71
12	63	64	66	67	68	70	71	71
15	65	66	67	69	70	71	71	72
20	67	67	68	69	70	70	71	71
25	67	67	68	69	69	69	70	69
30	66	67	67	68	68	68	68	68

Table D.19: HCIR normal 3-month cap volatilities surface, data from 30-Apr-2015.

T(Y)/K(%)	-0.25	0.5	1.5	1	2	3	4	5
2	37	20	19	25	35	54	73	92
3	33	31	34	35	35	41	56	71
4	36	38	42	45	47	48	49	57
5	39	42	47	50	53	55	57	58
6	43	47	51	54	57	60	61	63
7	47	50	54	57	60	63	64	66
8	50	53	57	60	62	65	66	68
9	52	55	58	61	63	66	68	69
10	54	56	60	62	64	67	69	70
12	58	60	63	65	66	69	70	71
15	62	63	65	67	68	70	71	72
20	64	65	66	68	68	70	70	71
25	65	65	66	67	68	69	69	69
30	64	64	65	66	67	67	67	67

Table D.20: HCIR normal 12-month cap volatilities surface, data from 30-Apr-2015.

Appendix E

Appendix: More CVA Results with HCIR

In this appendix, we include additional results for CVA assessment with HCIR model. We also compare the impact of HCIR and benchmark models on CVA for LIBOR-OIS swap products as well as interest rate caps using multiple sets of real and synthetic market data. We conclude that for these mostly one-sided payout products the CVA values are affected very little after including the stochastic LOIS spread in the simulation.

E.1 CVA with HCIR Model Calibration to 4% Caps

Model	a_x	σ_x	a_y	σ_y	ρ_{HW}
HW1F	7.92%	1.29%	-	-	-
HW2F	5.6%	2.3%	12.9%	3.7%	-94%
HCIR	5.6%	2.3%	12.9%	3.8%	-94%
	ρ_{HCIR}	σ	θ	κ	c_0
CIR	-1.8%	0.12%	00082%	9.2%	0.416%

Table E.1: HW1F,HW2F,HCIR model parameters, when calibrated to 4% cap data from 22-Nov-2013.

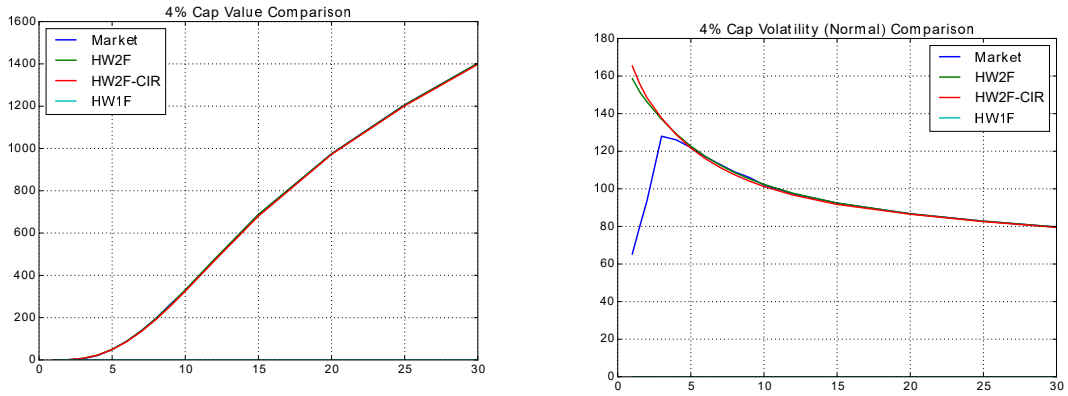

Figure E.1: Market cap present-value (left) and volatility (right) fits using HCIR and HW2F models.

E.2 CVA for LIBOR-OIS Swap

In another case, we wanted to visualise the model impact on the CVA for a pure spread-product like a OIS-to-LIBOR swap. As in the HW2F model, the LOIS spread is constant and in HCIR it is stochastic, this scenario should show a sizeable difference between the two models. We shall consider a 30-year, 6-month LIBOR vs 6-month OIS swap:

$$LOISSwap(t,\mathcal{T},K) = N\cdot\sum_{i=1}^{N} P(t,T_i)(LIBORFwd_{6M}(T_{i-1},T_i) - OISFwd_{6M}(T_{i-1},T_i) - K) \tag{E.1}$$

E.2.1 LOIS Swap with Market Curve Data

The second set of CVA experiments with high-basis scenarios were accomplished with a different product, the LIBOR-OIS swap, where both swap legs are floating, yet one is based on stochastic OIS 6-month forward rates, the other on LIBOR forward rates. First, we have performed the simulations with the HCIR and HW-models calibrated to real market forwards and cap volatilities. In this setup, the LIBOR-OIS spread is small with low-volatility as shown in Table E.1. This results in very small LOIS swap volatility in time, but the volatility of payouts is non-zero in all cases: HCIR, HW2F, HW1F, as with changing state variable $x(t)$ even in constant basis HW-models, the cashflows do vary, simply because

the difference between 6-month LIBOR-bond price and OIS-bond price:

$$P_{6M}(t,T) = A(t,T) \cdot e^{-\alpha_{6M}(t)B(t,T)} e^{-x(t)B_x(t,T)-y(t)B_y(t,T)} \tag{E.2}$$

$$P_{OIS}(t,T) = A(t,T) \cdot e^{-\alpha_{OIS}(t)B(t,T)} e^{-x(t)B_x(t,T)-y(t)B_y(t,T)} \tag{E.3}$$

varies depending on the shared state variables $x(t), y(t)$, where $\alpha_X(t)$ are the deterministic term-structure components (different for 6-month and OIS bonds). The latter is visualized in Figure E.2.

Then, the CVA/DVA values for this case are small and close to each other (around 1bp adjustment on swap strike.):

Model	CVA	DVA	Swap MtM (t=0)
HCIR	0	71	-12
HW2F	0	77	0
HW1F	0	77	0

Table E.2: CVA, DVA values in EUR for and ATM LOIS swap with fixed rate of 0.12847%, $5EUR$ 1bp adjustment on fixed leg

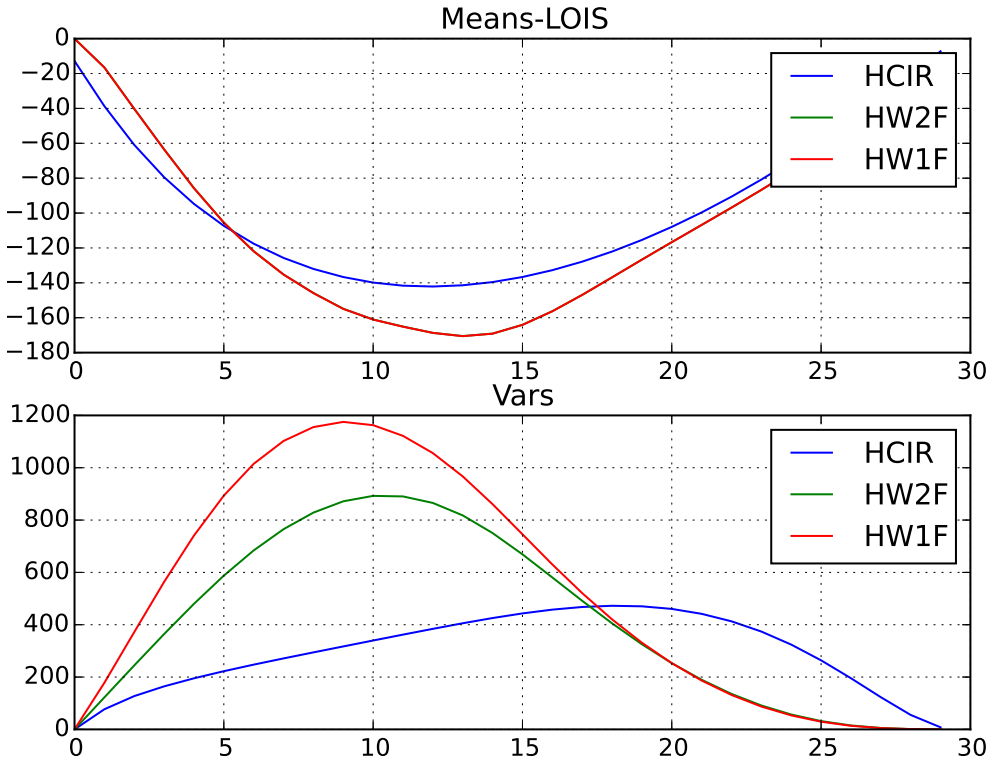

Figure E.2: Means and variances of the simulated LIBOR-OIS swap under HCIR and HW-models. On the X-axis we have the valuation date t.

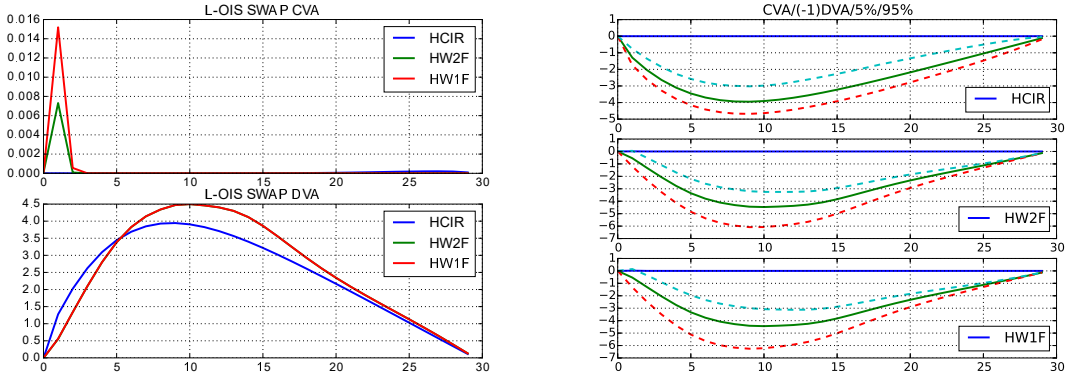

Figure E.3: CVA, DVA profiles (left) of HCIR and HW2F models for LIBOR-OIS swap, and CVA, DVA figures with exposure $5-95\%$ quantiles (right). 22-Nov-2013 market data for forwards and caps.

E.2.2 LOIS Swap with Synthetic Flat-Basis Curve Data

In the second test, we have calibrated the models for synthetic, flat 2% basis spread (over OIS) forward curve and same volatility data.

In this flat-basis scenario, the spread is high but practically constant as shown in Table 5.4, hence the LIBOR-OIS spread does not change much at all, even in HCIR model, and all the variation in simulated swap values comes from HW model for OIS.

Then, the CVA/DVA values for this case are small and with hardly any differences between the models.

Model	CVA	DVA	Swap MtM (t=0)
HCIR	6	6	0.5
HW2F	5	5	0
HW1F	5	5	0

Table E.3: CVA, DVA values for and ATM LOIS swap with fixed rate of 2%

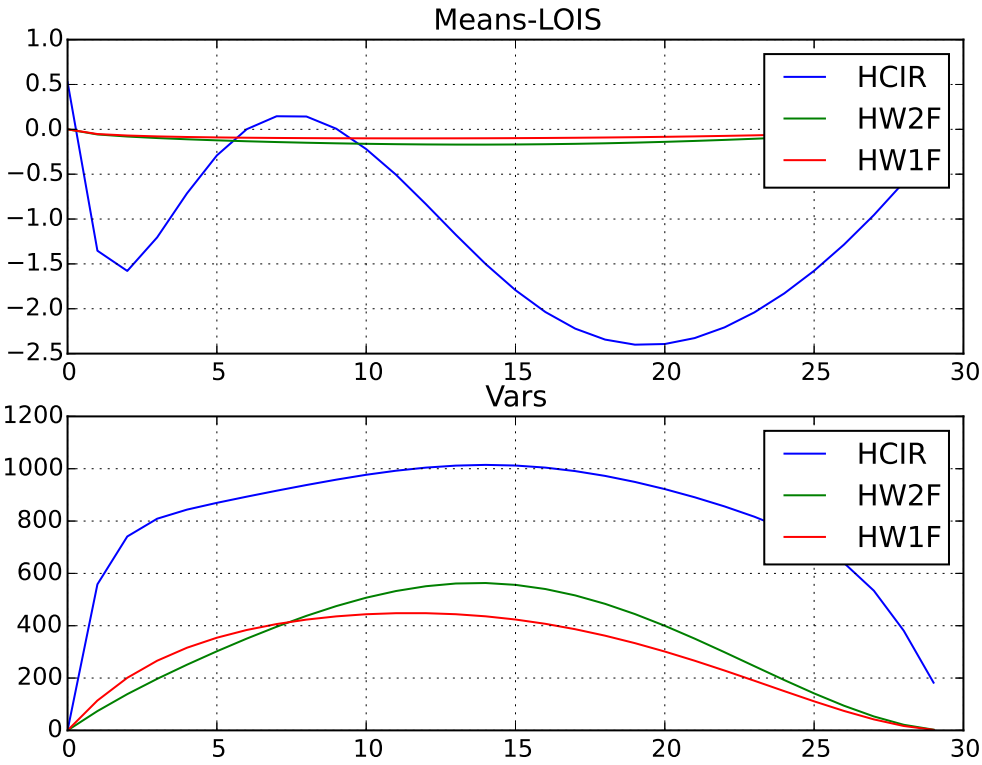

Figure E.4: Means and variances of the simulated LIBOR-OIS swap under HCIR and HW-models. On the X-axis we have the valuation date t.

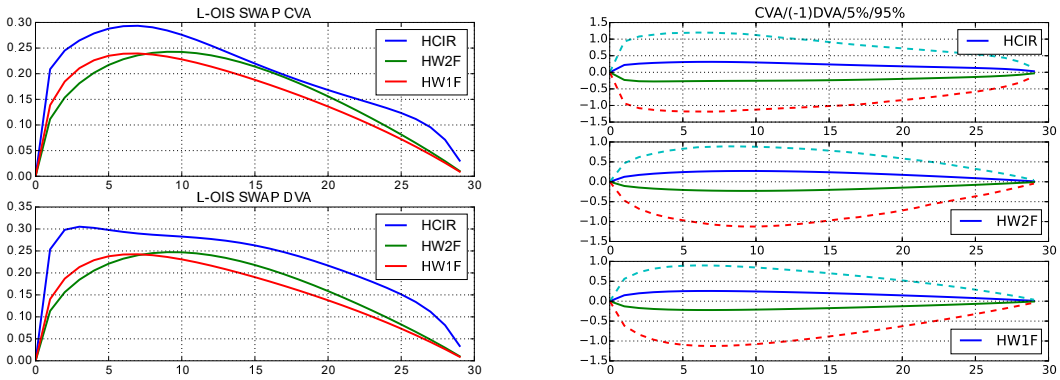

Figure E.5: CVA and DVA profiles (left) of HCIR and HW2F models for LIBOR-OIS swap, and CVA/DVA figures with exposure $5-95\%$ quantiles (right). Synthetic market data: flat basis spread.

E.2.3 LOIS Swap with synthetic Increasing-Basis Curve Data

In the third case of increasing basis, we calibrated the models to OIS curve and synthetic forward curve where the LOIS basis spread increases from 0% to 2% over a 30-year period. The calibrated CIR model is also a nearly deterministic, with low initial short rate and high long-term rate θ. This led to a reasonably small variance of the simulated LOIS swap, and as the mean MtM across time was positive, the CVA values are the same across all models, as DVA are null.

Model	CVA	DVA	Swap MtM (t=0)
HCIR	325.5	0	5
HW2F	326	0	0
HW1F	326	0	0

Table E.4: CVA, DVA values for and ATM LOIS swap with fixed rate of 0.8596%

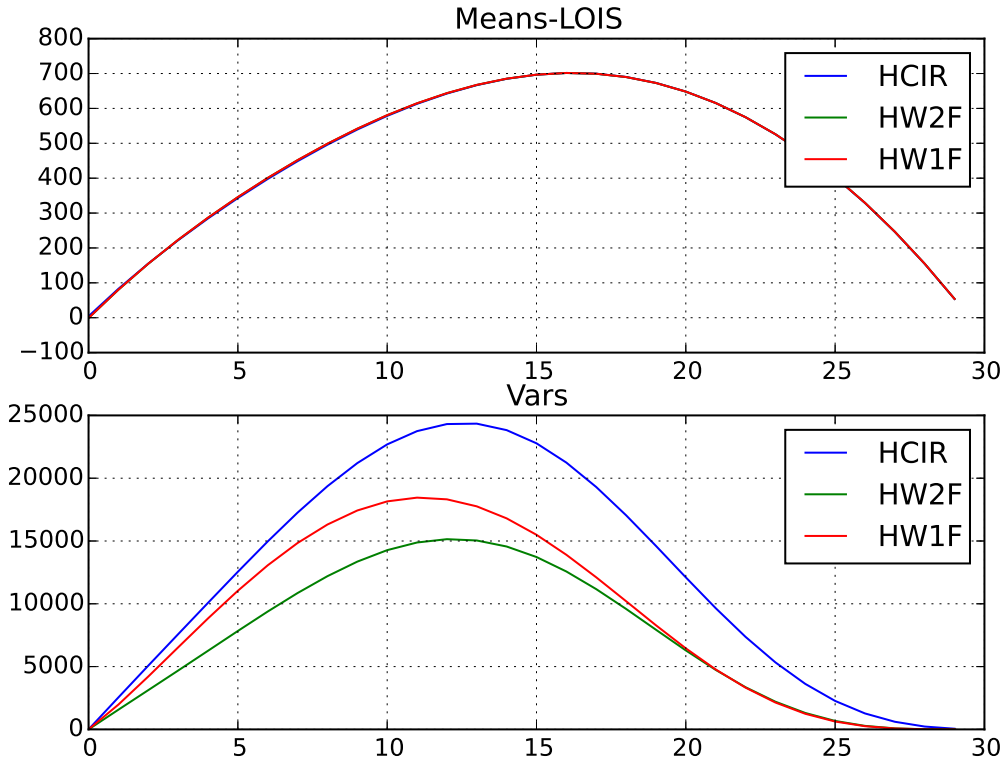

Figure E.6: Means and variances of the simulated LIBOR-OIS swap under HCIR and HW-models. On the X-axis we have the valuation date t.

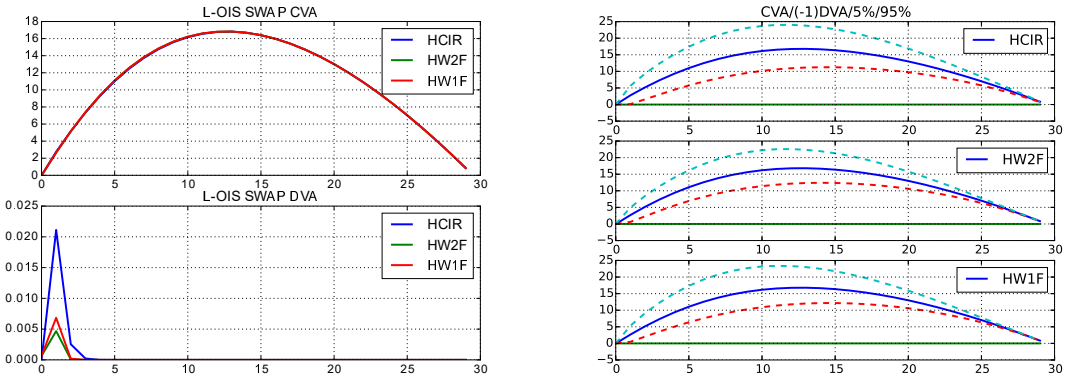

Figure E.7: CVA and DVA profiles (left) of HCIR and HW2F models for LIBOR-OIS swap, and CVA/DVA figures with exposure $5 - 95\%$ quantiles (right). Synthetic market data: increasing basis spread.

E.2.4 LOIS Swap with synthetic High Volatility Basis Curve Data

In the case of high-volatility spread, the HCIR model gains significant swap volatility in comparison to the HW-models, as shown in Figure E.8. Nevertheless, as we are assessing CVA of an ATM-swap, throughout the simulation period, the swap MtM stays mostly negative, also as the spread is volatile, but not very large (50bp in long-term), the CVA/DVA values are very close for HCIR and HW models as shown in the table E.5.

Model	CVA	DVA	Swap MtM (t=0)
HCIR	0	84	0
HW2F	0	83	0
HW1F	0	83	0

Table E.5: CVA, DVA values for and ATM LOIS swap with fixed rate of 0.61745%

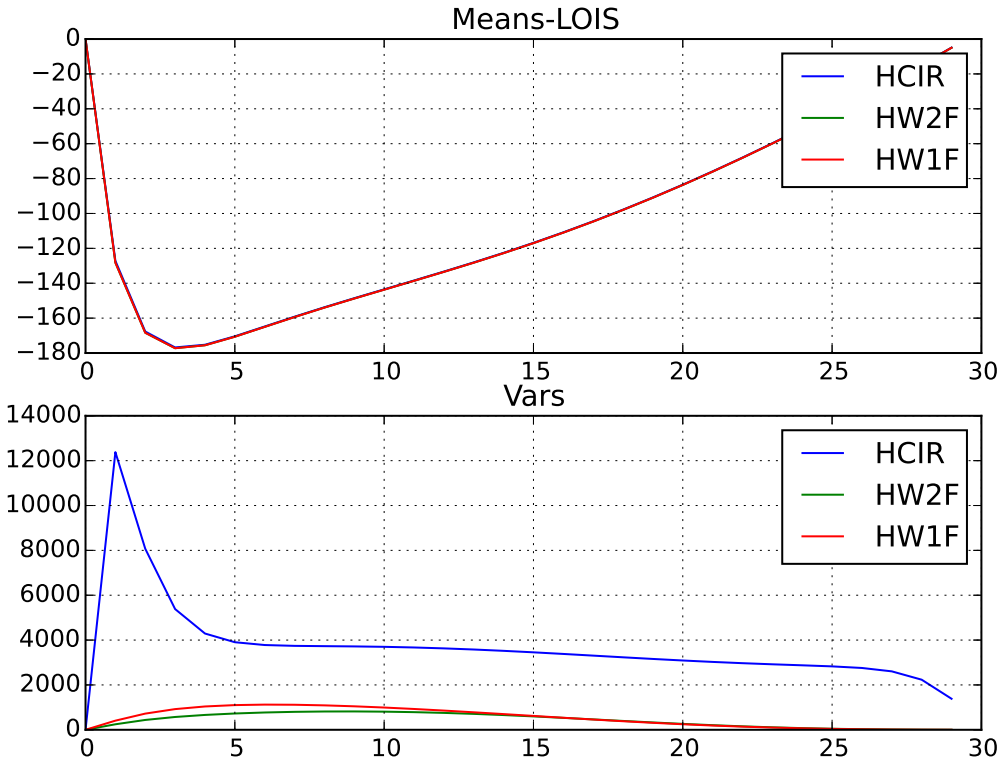

Figure E.8: Means and variances of the simulated LIBOR-OIS swap under HCIR and HW-models. On the X-axis we have the valuation date t.

The main differences in LOIS swap exposures between the HCIR and HW models can only be observed in the $5\&95\%$ quantile levels - the HCIR model has wider exposure

quantiles as demonstrated in Figure E.9.

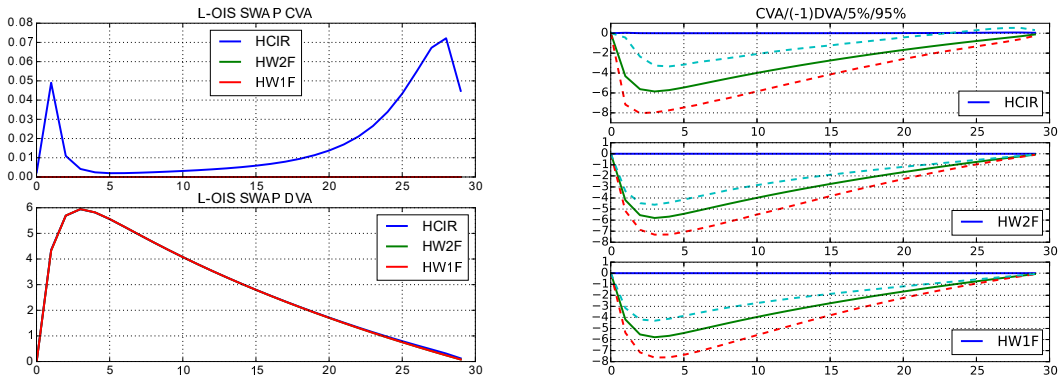

Figure E.9: CVA and DVA profiles (left) of HCIR and HW2F models for LIBOR-OIS swap, and CVA/DVA figures with exposure $5 - 95\%$ quantiles (right). Synthetic market data: curved, high-volatility basis spread.

E.3 CVA for Caps

In this section, we seek to compare the model effects on CVA of caps. The issue with CVA of caps is that because caps are options, their value at any point in time will stay positive and will only contribute to CVA or DVA figures. On top, because the simulation and cap pricing is done via risk-neutral measures, the expected positive exposure (EPE) for a single cap at time T_i, will be exactly:

$$EPE(T_i) = D(0, T_i)Cap(T_i; \cdot)SP(T_{i-1}, T_i) \tag{E.4}$$

which also says that if we calibrate the two HCIR, HW2F models to the same caps, we will obtain the same EPE figures for them. The main difference in CVA/DVA for caps can be observed via the variance of caps over time, as well as 95%-quantile of the exposure profile in Figure E.10.

Model	CVA	DVA
HCIR	2585	0
HW2F	2595	0
HW1F	2582	0

Table E.6: CVA, DVA values in EUR for 30-year 0% 6-month cap. Case with market data from 22 Nov 2013.

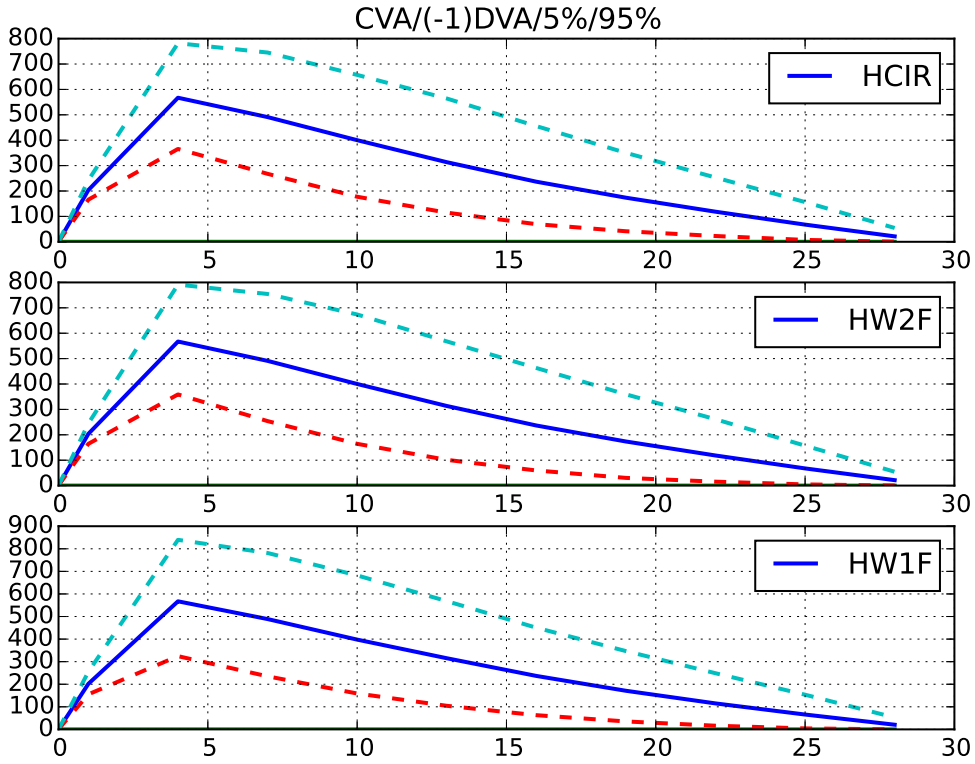

Figure E.10: CVA, DVA and quantile profiles for EUR for 30-year 0% 6-month cap. Case with market data from 22 Nov 2013.

Model	CVA	DVA
HCIR	2940	0
HW2F	2935	0
HW1F	2912	0

Table E.7: CVA, DVA values in EUR for 30-year 0% 6-month cap. Case with synthetic high-vol basis data.

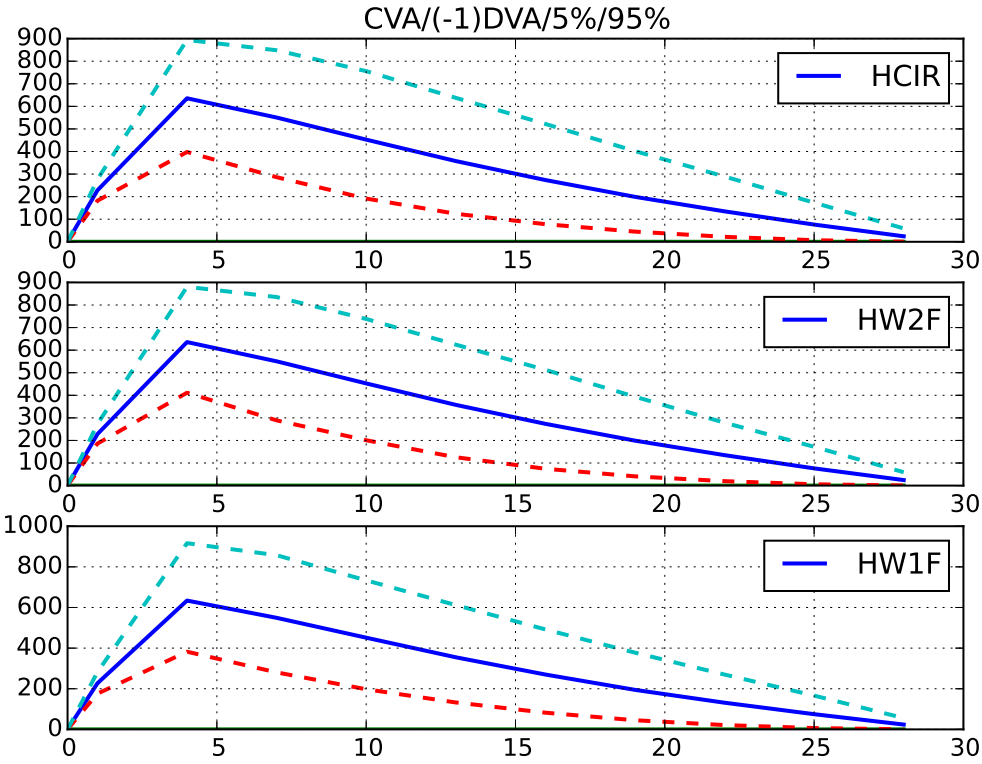

Figure E.11: CVA, DVA and quantile profiles for EUR for 30-year 0% 6-month cap. Case with synthetic high-vol basis data.

E.4 Impact of Local Minima in HW2F and HCIR calibration

We have mentioned before that in the 10-parameter calibration problem, there is a risk of calibrating the HCIR model and obtaining only a locally optimal solution. This section serves as an extensive example of such a situation which we have encountered. The following results can be compared to the main result in section 5.3.

We have calibrated the three models to 6-month 4% EUR caps for the 22-Nov-2013 dataset. The overall cap and forward curve fits are shown in Figure E.13. The HW2F and HCIR models offer the best fit for caps, the HW1F model under-fits the short-term caps. We note that the very-short-term cap volatilities are not very well matched, as we calibrated to PV and these OTM caps carry very little present value in general.

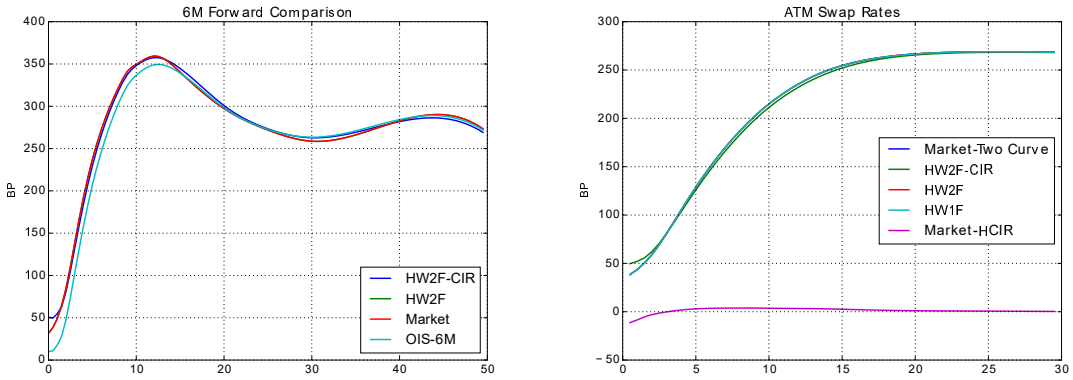

Figure E.12: Calibration to 6-month forward curves on 22-Nov-2013. Demonstration of ATM swap rates for all three models: HW1F, HW2F and HCIR.

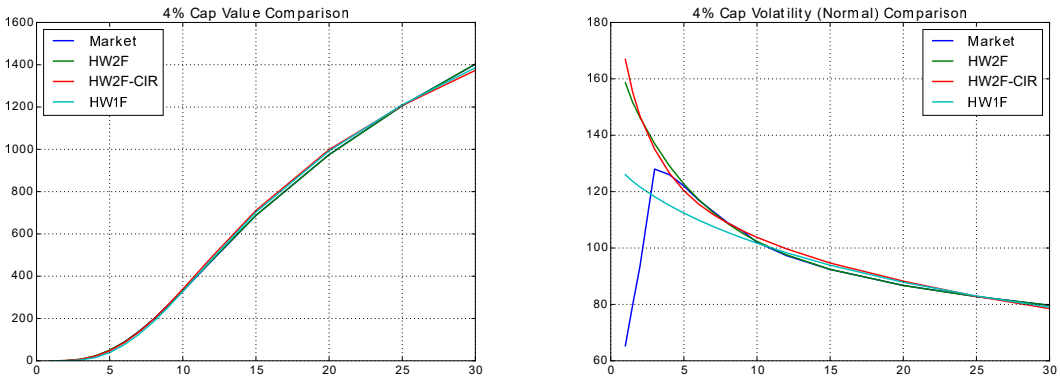

Figure E.13: Calibration to 4% 6-month caps on 22-Nov-2013. Results for market caps for HCIR, HW2F, HW1F models.

We show the calibrated parameters for all three models in the following table. While both HW2F and HCIR models have a very negative correlation between the 2-factors, their mean-reversion and volatility levels remain distinct. The HW1F model has similar levels of volatility and mean reversion as the HW2F model. In all the models we have used OIS-discounting approach for payouts. The same OIS-discounting was used in the calibration to caps phase.

Model	a_x	σ_x	a_y	σ_y	ρ	dCurve
HW2F-CIR	25.69%	4.48%	15.11%	3.74%	-91.2%	OIS
HW2F	5.62%	2.34%	12.9%	3.74%	-943%	OIS
HW1F	7.92%	1.29%				OIS

CIR	ρ_{CIR-HW}	σ	θ	k	c_0
CIR - 6M	-1.5%	0.1%	0005%	9.5%	0.4%

Using the latter sets of parameters, we have estimated the CVA / DVA values for a 30-year 6-month fixed-for-floating swap with ATM 2.6839% strike. The respective CVA / DVA values using uniform hazard rate $\lambda(t) = \frac{1}{30}$, for all models are:

Model	CVA	DVA	Swap MtM (t=0)
HCIR	549	284	-6
HW2F	623	367	0
HW1F	642	377	0

Table E.8: CVA, DVA and swap MtM values for and ATM swap with fixed rate of 2.6839%

We can compare these values with the Table 5.1, which shows that the differences in

CVA resulting from a local minima in cap calibration can be substantial (12bp adjustment on a fixed leg here for HCIR model).

E.4.1 CVA Profiles

Our investigation goes deeper into comparing the full exposure profiles for this swap under the different models. In Figure E.14, we plot for all 4-models:

- CVA Profile of IRS (otherwise the mean discounted positive exposure)
  $P_{OIS}(0,t)\mathbb{E}^{Q_T}\left[(NPV(t))^{+}\right]$
- DVA Profile of IRS (otherwise the mean discounted negative exposure)
  $P_{OIS}(0,t)\mathbb{E}^{Q_T}\left[(NPV(t))^{-}\right]dt$

In the CVA profiles:

- The HW1F model yields the largest CVA value, followed by HW2F model. The difference is not large - the short-term volatility of the HW1F model is larger, while in HW2F this is dampened by the negative correlation effect.
- The HCIR model yields a lower CVA and DVA values than the pure HW models.
- THE HCIR-0 model, which has CIR component set to zero, results in lower CVA on the short end and higher DVA, as our simulated forwards are now slightly smaller.

We foresee the following reasons for the apparent difference between HCIR model and HW2F model:

- The added CIR component has very low 0.1% volatility and a negative correlation to OIS rates. This reduces overall simulated forward and swap volatility
- The HW parameters in HCIR model yield, overall, lower volatility of the forward rates. This is a result of HCIR calibration to the same market 6-month caps.

In Figure E.15 we show the aged MtM of the swap under consideration in all three (four) models. We can observe that while the MtM in main three models goes one-to-one until 5-year gap, a gap in value exists between 10-20 year period, its size goes from 5 to 20bp, and is caused by the imperfect alignment of the forward rates in the HCIR model. The swap MtM of the HCIR-0 model shows the OIS-only swap MtM development over time, and the difference up to the HCIR model MtM is our spread-model component.

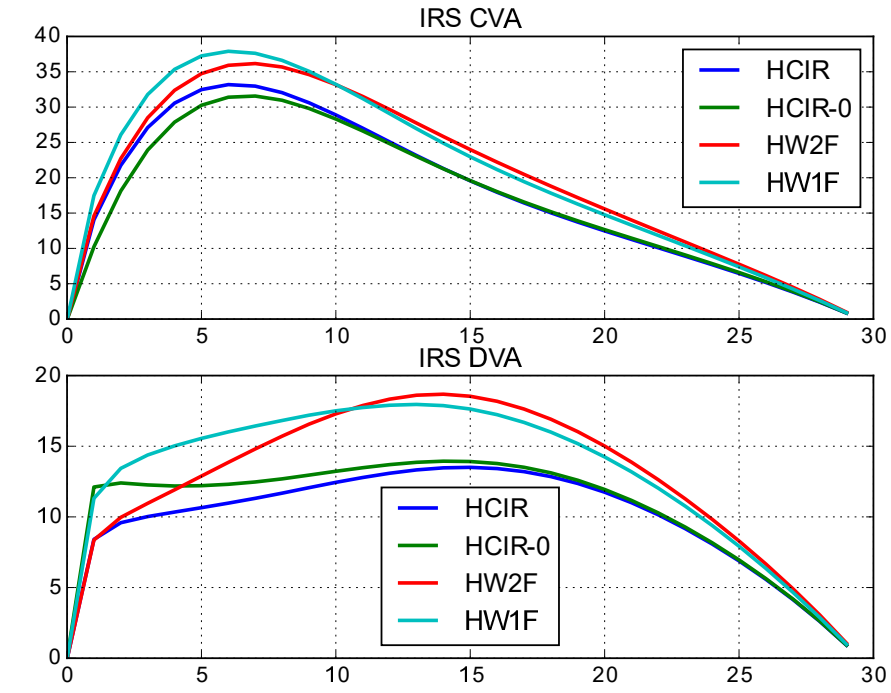

Figure E.14: CVA and DVA for 2.6839% (ATM) IRS with uniform default. Results for all four tested models (HCIR, HCIR0, HW1F, HW2F)

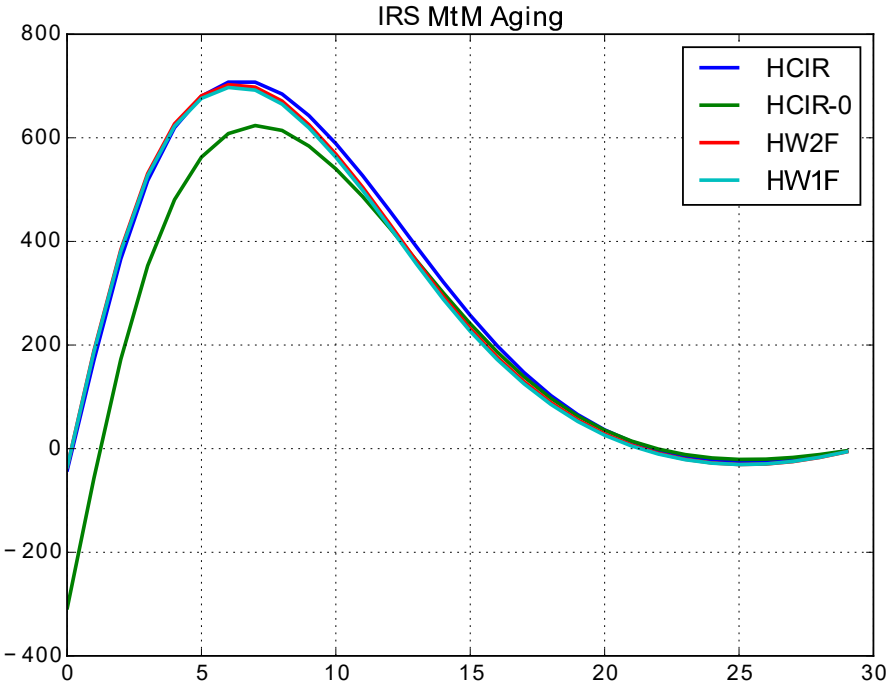

Figure E.15: Aging of the ATM swap within the four IR models.

E.4.2 Non-ATM Swaps

To give more insight into the behaviour of the four models for swap CVA, we have performed equivalent experiments with OTM (0%) and ITM (4%) swaps below. We note, that:

- In OTM swap case (4%) the CVA & DVA is smallest for HCIR model.
  HCIR model reduces CVA by 60bp, DVA by 65pb, but the MtM is also smaller by 12bp. 1F and 2F HW model values are within 10bp.
  We show the results in Figures E.16, E.17
- In ITM swap case (0%) HCIR model reduces CVA by 15bp and DVA by 20bp when compared to HW2F. The swap MtM differs between HCIR and HW2F models by 12bp. This result is rather intuitive, as in this case, we have small payouts depending on the simulated forward rates, as our swap is in the money and we get paid a large fixed rate.
  We show the results in Figures E.18, E.19

Model	CVA	DVA	MtM
HCIR	129.6	1010	-2801
HCIR-0	129.1	1049	-3061
HW2F	189	1074	-2789
HW1F	196	1085	-2789

Table E.9: CVA, DVA and swap MtM values for and OTM swap with fixed rate of 4%

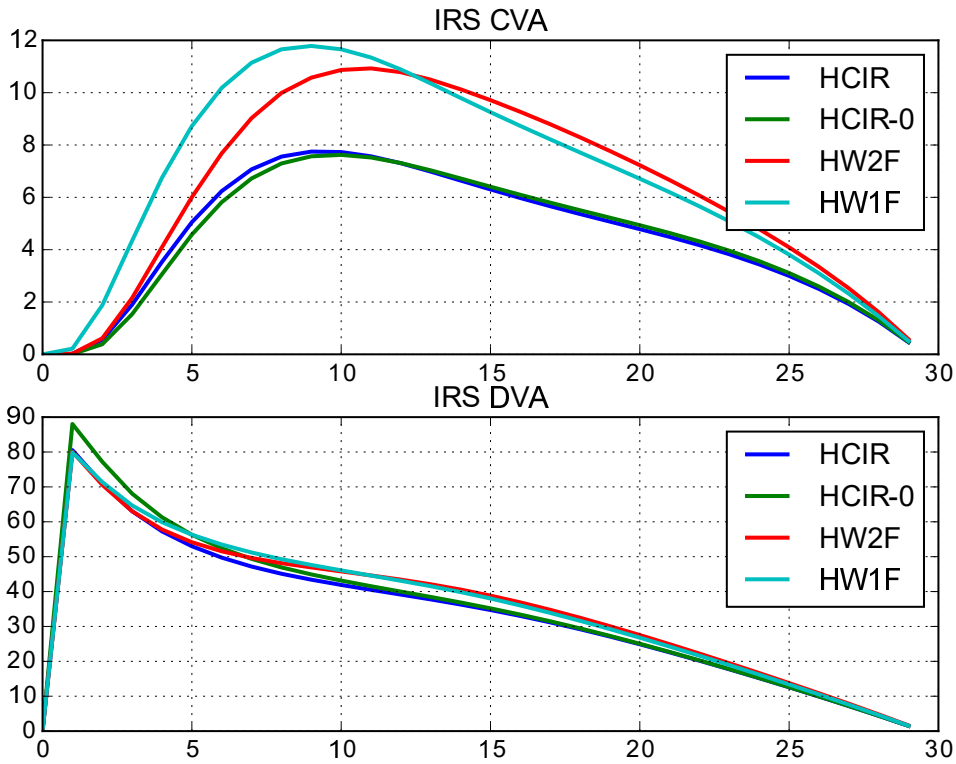

Figure E.16: CVA and DVA for 4% IRS with uniform default. Results for all three tested models (HCIR, HW1F, HW2F)

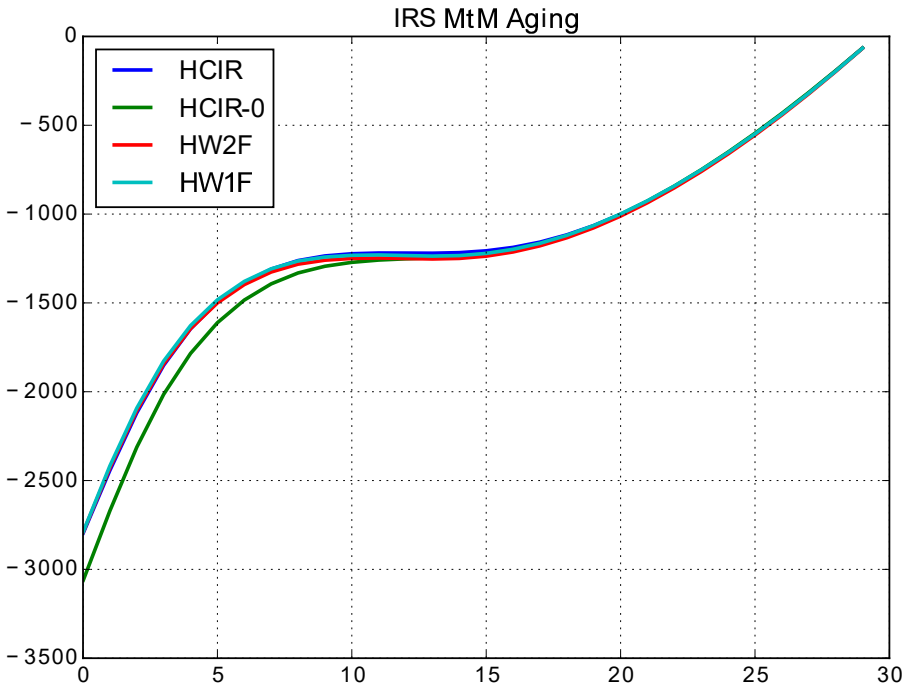

Figure E.17: CVA and DVA for 4% IRS with uniform default. Results for all three tested models (HCIR, HW1F, HW2F)

Model	CVA	DVA	MtM
HCIR	2565	11	5676
HCIR-0	2526	12	5416
HW2F	2580	31	5688
HW1F	2572	25	5688

Table E.10: CVA, DVA and swap MtM values for and ITM swap with fixed rate of 0%

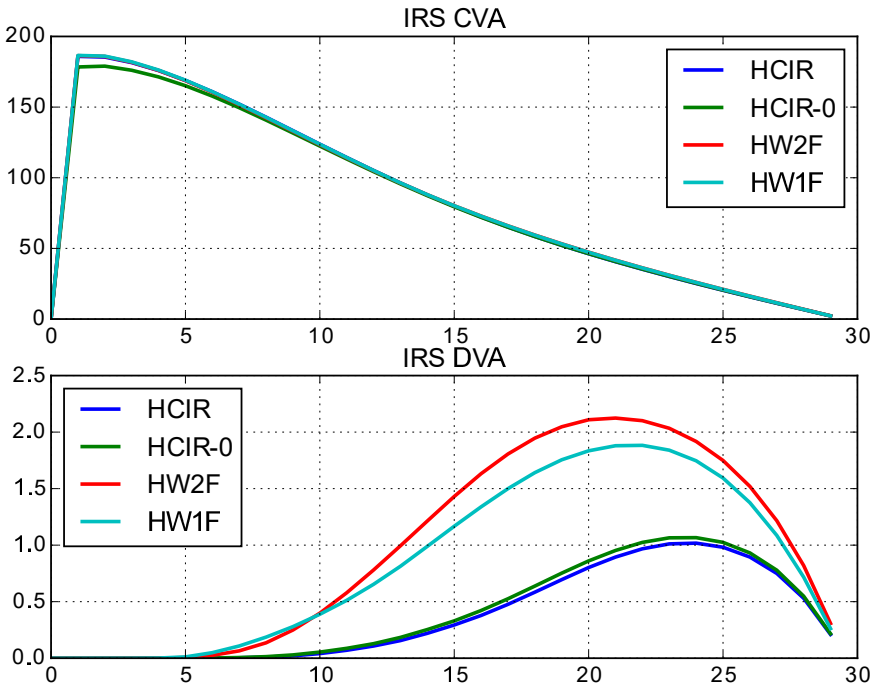

Figure E.18: CVA and DVA for 0% IRS with uniform default. Results for all three tested models (HCIR, HW1F, HW2F)

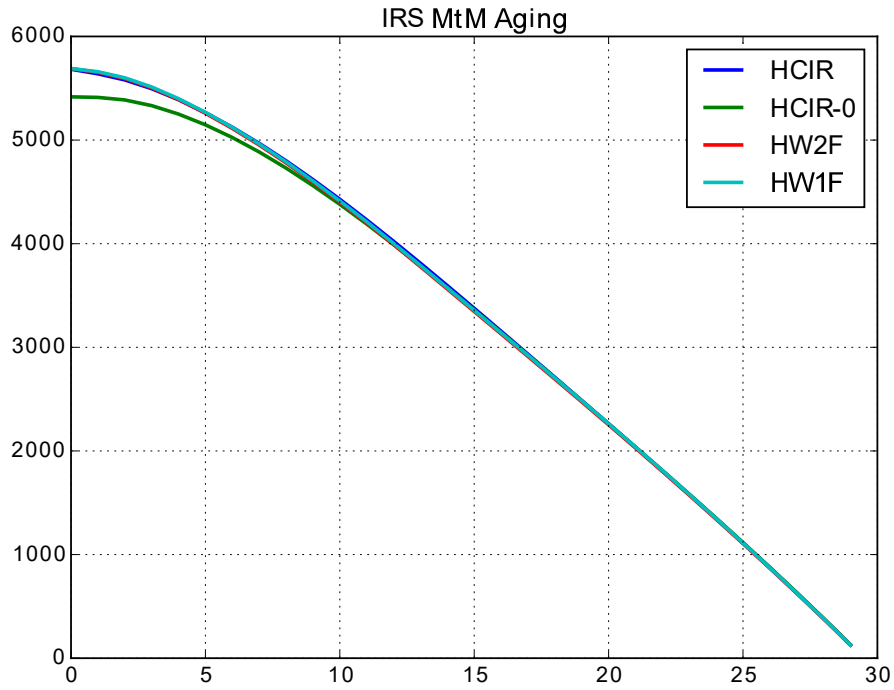

Figure E.19: CVA and DVA for 0% IRS with uniform default. Results for all three tested models (HCIR, HW1F, HW2F)

E.4.3 CVA for Multi-Curve Swaps

In the following, we extend our experiments to multi-curve swaps. Our setup contains CVA valuation in 3 different cases, which can be compared to the main text result in 5.3.1:

- a 30-year 1-month EUR swap, strike = 2.49%
- a 30-year 3-month EUR swap, strike = 2.59%
- a 30-year 12-month EUR swap, strike = 2.83%

In each of the cases, we have calibrated the HCIR model to relevant yield curves to reproduce the $\tau-$month forward rates. The HW2F parameters remain the same as before, as they were calibrated to 6-month EUR caps.

Tenor	ρ	σ	θ	k	c_0
1M	-3.14%	0.115%	1.17e-5	5.67%	0.11%
3M	-3.64%	0.10%	1.14e-5	4.93%	0.27%
6M	-1.65%	0.15%	1.37e-5	9.15%	0.41%
12M	-25%	0.35%	017%	7.9%	0.54%

Then, we estimate CVA and compare the two models:

1. HCIR model, where $\sigma_x, \sigma_y, a_x, a_y, \rho$ were calibrated to 6-month caps, and CIR parameters $\rho_k, \sigma, \theta, k, c_0$ to relevant τ-month basis-spread curves.
2. HW2F/1F model, where $\sigma_x, \sigma_y, a_x, a_y, \rho$ were calibrated to 6-month caps and the term-structure $\theta(t)$ is changed depending on $\tau-$month forward curve.

Tenor	ATM(%)	HCIR:CVA	HW2F:CVA	HW1F:CVA	HCIR:DVA	HW2F:DVA	HW1F:DVA
1M	2.49%	611	697	724	269	345	364
3M	2.59%	579	664	687	272	357	372
6M	2.68%	549	623	642	284	367	377
12M	2.83%	485	566	573	283	375	373

Note for the swaps below, a 1bp change in the fixed rate, yields 5 EUR change in CVA value. Hence the CVA adjustment on the fixed leg is of the order of 100bp. While the basis spreads increase when going from 1-month swap to 12-month swap, the overall floating leg volatility decreases and results in decreasing CVA (by 20bp on fixed leg) and slightly increased DVA (by 3bp on fixed leg) for HCIR model.

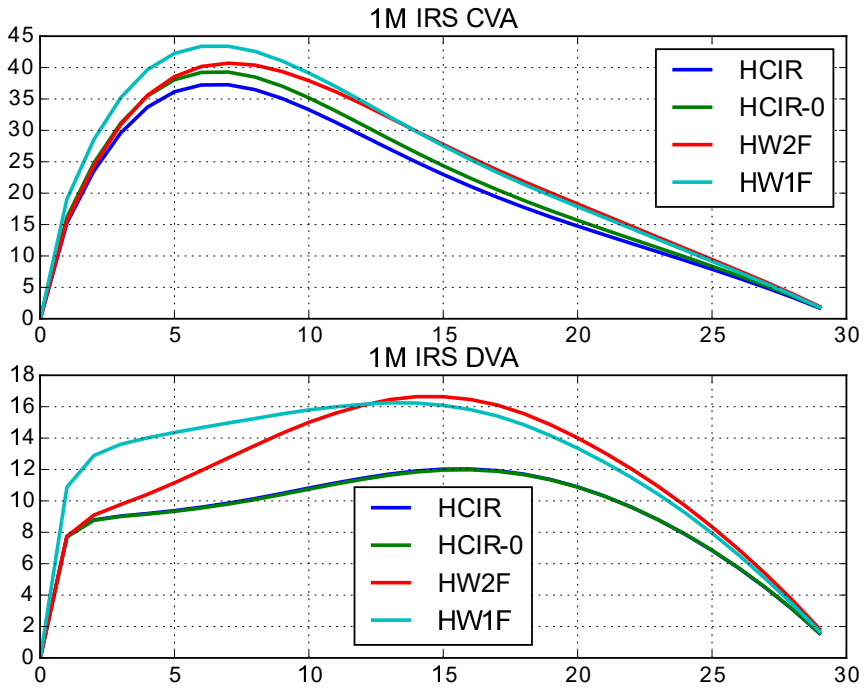

Figure E.20: CVA and DVA for 30-year ATM 1-month swap. Results for all three models (HCIR, HW1F, HW2F)

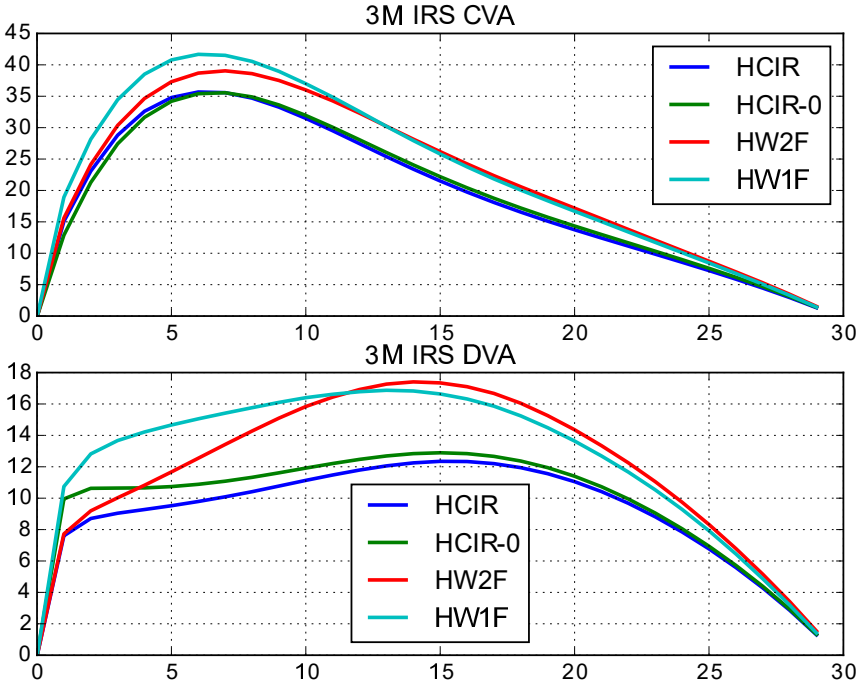

Figure E.21: CVA and DVA for 30-year ATM 3-month swap. Results for all three models (HCIR, HW1F, HW2F)

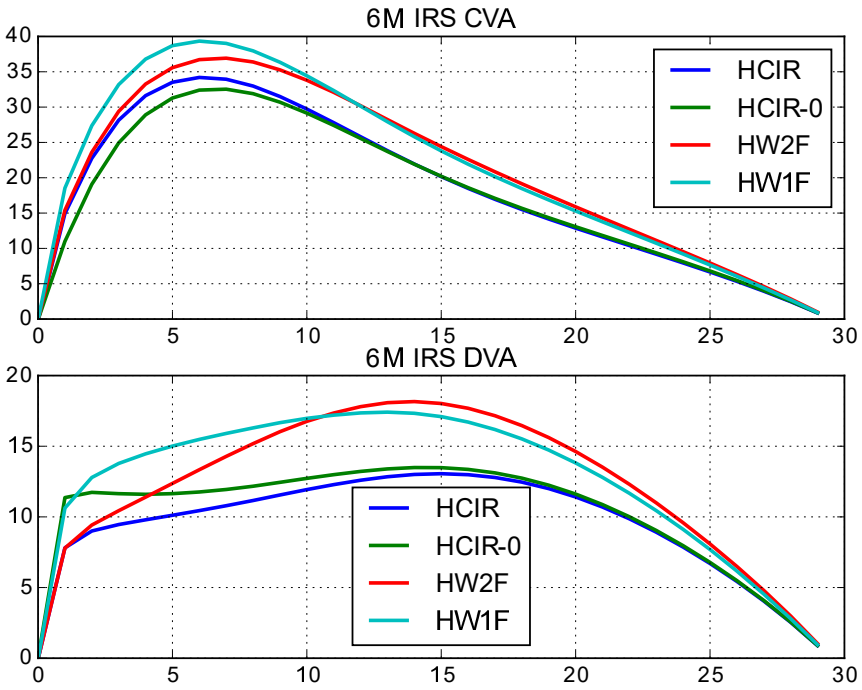

Figure E.22: CVA and DVA for 30-year ATM 6-month swap. Results for all three models (HCIR, HW1F, HW2F)

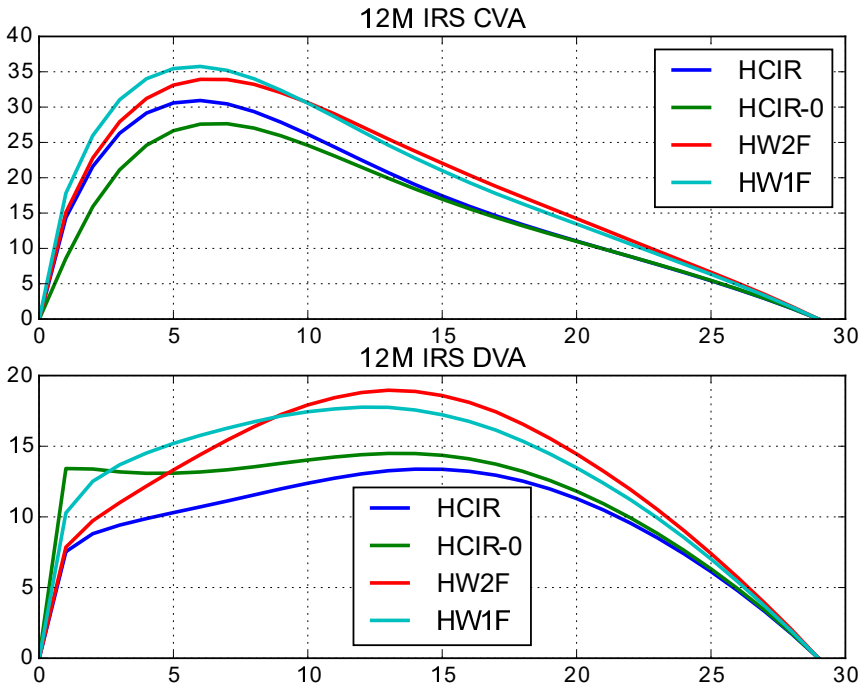

Figure E.23: CVA and DVA for 30-year ATM 12-month swap. Results for all three models (HCIR, HW1F, HW2F)

References

Alexander, C. (2004). Normal mixture diffusion with uncertain volatility: Modelling short- and long-term smile effects. *Journal of Banking & Finance*, 28(12):2957–2980.

Ametrano, F. M. and Bianchetti, M. (2013). Everything you always wanted to know about multiple interest rate curve bootstrapping but were afraid to ask. *SSRN 2219548*.

Andong, W. (2013). *Modern Pricing of Caps*. Master thesis, University of Amsterdam.

Bhar, R. and Nikolova, B. (2013). Measuring the interconnectedness of financial institutions. *Economic Systems*, 37(1):17–29.

Bianchetti, M. (2010). Two curves, one price. *Risk*, (August):74–80.

Bianchetti, M. (2012). The Zeeman effect in finance: libor spectroscopy and basis risk management. *SSRN 1951578*.

BIS (2010). Basel III: A global regulatory framework for more resilient banks and banking systems. *Basel Committee on Banking Supervision, Basel*, 2010(June).

Bormetti, G., Brigo, D., Francischello, M., and Pallavicini, A. (2015). Impact of multiple curve dynamics in credit valuation adjustments under collateralization. *SSRN 2638229*.

Bozdogan, H. (1987). Model selection and Akaike information criterion (AIC) - the general-theory and its analytical extensions. *Psychometrika*, 52(3):345–370.

Brent, R. (1971). An algorithm with guaranteed convergence for finding a zero of a function. *The Computer Journal*, 14.4:422–425.

Brigo, D. and Mercurio, F. (2002). Lognormal-mixture dynamics and calibration to market volatility smiles. *International Journal of Theoretical and Applied Finance*, 05(04):427–446.

Brigo, D. and Mercurio, F. (2006). *Interest Rate Models - Theory and Practice with Smile, Inflation and Credit*. Springer.

Brigo, D. and Pallavicini, A. (2013). CCPs, central clearing, CSA, credit collateral and funding costs valuation FAQ: re-hypothecation, CVA, closeout, netting, WWR, gap-risk, initial and variation margins, multiple discount curves, FVA. *SSRN 2361697*.

Cassidy, D., Hamp, M., and Ouyed, R. (2010). Pricing European options with a log Student's t-distribution: A Gosset formula. *Physica A: Statistical Mechanics and its Applications*, 389.24:5736–5748.

Charpentier, A., Fermanian, J.-D., and Scaillet, O. (2007). The estimation of copulas: theory and practice. In *Copulas: From Theory to Applications in Finance*, pages 35–62. Risk Books.

Chibane, M. and Sheldon, G. (2009). Building curves on a good basis. *SSRN 1394267*.

Crépey, S. and Douady, R. (2012). The whys of the LOIS: Credit risk and refinancing rate volatility. *SSRN 2118354*.

Crépey, S. and Douady, R. (2013). LOIS: credit and liquidity. *Risk Magazine*, (June):78–82.

Crepey, S., Grbac, Z., Ngor, N., and Skovmand, D. (2013). A Levy HJM multiple-curve model with application to CVA computation. *Quantitative Finance*, 15(3):401–419.

Crépey, S., Grbac, Z., and Nguyen, H. N. (2012). A multiple-curve HJM model of interbank risk. *Mathematics and Financial Economics*, 6(3):155–190.

Cui, J., In, F., and Maharaj, E. A. (2016). What drives the Libor-OIS spread? Evidence from five major currency Libor-OIS spreads. *International Review of Economics & Finance*, 45:358–375.

Das, S. and Suganthan, P. N. (2011). Differential evolution: A survey of the state-of-the-art. *IEEE Transactions on Evolutionary Computation*, 15(1):4–31.

Dawson, P., Blake, D., G Cairns, A. J., Dowd, K., and Dawson David Blake Andrew G Cairns Kevin Dowd, P. J. (2007). Options on normal underlyings. *Centre for Risk & Insurance Studies*, (CRIS Discussion Paper Series 2007).

Eisenschmidt, J. and Tapking, J. (2009). Liquidity risk premia in unsecured interbank money markets. *ECB Working Paper Series*, (1025).

Elliott, L. (2012). China's collapse 'will bring economic crisis to climax in 2012'. Technical report.

Filipović, D., Hughston, L. P., and Macrina, A. (2012). Conditional density models for asset pricing. *International Journal of Theoretical and Applied Finance*, 15(01).

Filipovic, D. and Trolle, A. (2013). The term structure of interbank risk. *Journal of Financial Economics*, 109(3):707–733.

Grbac, Z., Papapantoleon, A., Schoenmakers, J., and Skovmand, D. (2015). Affine LIBOR models with multiple curves: theory, examples and calibration. *SIAM Journal on Financial Mathematics*, 6(1):984–1025.

Gupta, S. (2005). *Financial Derivatives: Theory, concepts and problems*. Prentice-Hall of India.

Heider, F., Hoerova, M., and Holthausen, C. (2009). Liquidity hoarding and interbanking market spreads. The role of counterparty risk. *ECB Working Paper Series*, (1126).

Hoorens, B. (2011). *On the Cheyette short rate model with stochastic volatility*. Master thesis, Delft University of Technology.

Hull, J. and White, A. (2016). *Multi-curve modelling using trees*, pages 171–189. Springer International Publishing.

Intercontinental Exchange (2014). ICE Libor Panel.

Joshi, M. S. and Rebonato, R. (2003). A displaced-diffusion stochastic volatility LIBOR market model: motivation, definition and implementation. *Quantitative Finance*, 3(6):458–469.

Kenyon, C. (2010). Short-rate pricing after the liquidity and credit shocks: including the basis. *SSRN 1558429*.

Kenyon, C. and Stamm, R. (2012). *Discounting, Libor, CVA and funding: interest rate and credit pricing*. Palgrave Macmillan.

Kienitz, J. (2013). Transforming volatility - multi curve cap and swaption volatilities. *SSRN 30617*.

Kitwiwattanachai, C. (2012). The stochastic recovery rate in CDS: Empirical test and model. *SSRN 2136116*.

Kraemer, M. and Gill, F. (2012). Credit FAQ: Factors Behind Our Rating Actions On Eurozone Sovereign Governments. *Available at: http://www.nacionalre.es/pdf/variousratingsactions.pdf*.

Li, M. and Mercurio, F. (2016). The basis goes stochastic : A jump-diffusion model for financial risk applications. *SSRN 2827769*.

Massey, F. J. (1951). The Kolmogorov-Smirnov Test for goodness of fit. *Journal of the American Statistical Association*, 46(253):68–78.

Mauro F. Guillén (2012). The global economic & financial crisis: A timeline. Technical report, The Lauder Institute, Wharton, University of Pennsylvania.

Mercurio, F. (2009). Interest rates and the credit crunch: New formulas and market models. *SSRN 1332205*.

Mercurio, F. (2010). A LIBOR market model with stochastic basis. *SSRN 1583081*.

Mercurio, F. and Morini, M. (2007). No-Arbitrage dynamics for a tractable SABR term structure Libor model. *Analysis*, (March):1–21.

Michaud, F. and Upper, C. (2008). What drives interbank rates? Evidence from the Libor panel. *BIS Quarterly Review*, (March):47–58.

Moreni, N. and Pallavicini, A. (2014). Parsimonious HJM modelling for multiple yield-curve dynamics. *Quantitative Finance*, 14(2):199–210.

Moreni, N. and Pallavicini, A. (2015). FX Modelling in collateralized markets: foreign measures, basis curves, and pricing formulae. *SSRN 2646516*.

Morini, M. (2009). Solving the puzzle in the interest rate market (Part 1 & 2). *SSRN 1506046*.

Morini, M. and Brigo, D. (2008). Arbitrage-free pricing of credit index options: The no-armageddon pricing measure and the role of correlation after the subprime crisis. *arXiv:0812.4156*.

Morino, L. and Ruggaldier, W. (2014). On multicurve models for the term structure. *arXiv:1401.5431*.

Pallavicini, A. and Tarenghi, M. (2010). Interest-rate modeling with multiple yield curves. *SSRN 1629688*.

Poskitt, R. and Waller, B. (2011). Do liquidity or credit effects explain the behavior of the BKBM-LIBOR differential? *Pacific Basin Finance Journal*, 19(2):173–193.

Savickas, V. (2013). Deep dive into basis spreads and FRA replication problem. In *Quantitative Methods in Finance*.

Savickas, V. (2015). Hybrid short-rate model for Libor-OIS. In *IMA Mathematics in Finance*.

Savickas, V., Hari, N., Wood, T., and Kandhai, D. (2014). Super fast greeks : An application to counterparty valuation adjustments. *Wilmott Magazine*, (69):76–81.

Wales, D. and Doye, J. P. K. (1997). Global optimization by basin-hopping and the lowest energy structures of Lennard-Jones clusters containing up to 110 atoms. *Journal of Physical Chemistry A*, 101:5111–5116.

West, G. (2005). Calibration of the SABR model in illiquid markets. *Applied Mathematical Finance*, 12(4):371–385.